Efficient Radio Resource Management For Future Generation Heterogeneous Wireless Networks

BY

Mary Abosede Adedoyin

A thesis submitted for the degree of

Doctor of Philosophy

in the Department of Electrical Engineering,

Faculty of Engineering and the Built Environment, University of Cape Town

September 2017

Supervisor: A/Professor Olabisi Emmanuel Falowo

As the candidate's supervisor, I have approved this dissertation for submission.

Supervisor: A/Professor Olabisi Emmanuel Falowo

Sign: _____

Date: 15 September 2017

Declaration

I hereby declare that: (1) the above thesis is my own unaided work, both in conception and execution, and that apart from the normal guidance of my supervisor, I have received no assistance apart from that stated below; (2) except as stated below, neither the substance nor any part of the thesis, has been submitted in the past, or is being, or is to be submitted for a degree in the University, or any other University.

I am now presenting the thesis for examination for the Degree of PhD in Electrical Engineering. I also grant the University free license to reproduce the above thesis in whole or in part, for the purpose of research.

Mary Abosede Adedoyin	15 September 2017
Name	Date

Dedication

To my darling husband; Pastor Adedoyin Segun Emmanuel Adedoyin and our wonderful children: Miss Deborah Ebunoluwa Adedoyin and Master David Erioluwa Adedoyin.

Acknowledgements

First of all, I appreciate Almighty God the creator, for the gift of life, ability, and strength to complete this thesis. I would like to specially thank my supervisor, A/Prof. Olabisi E. Falowo for his consistent support, excellent guidance, and usual encouragement throughout my PhD studies. Also, I am thankful to the Head of Centre of Excellence in Broadband Networks and Applications, Mr. Neco Ventura for his moral and financial support and all the academic staff in the Centre - A/Prof. Mqhele Dlodlo, A/Prof. Daniel O'Hagan and Ms. Joyce Mwangama as well as all my colleagues in the communications research group at the University of Cape Town for their comments and useful suggestions during various presentations.

I also acknowledge the management of University of Cape Town for given me the Incoming International Student Award, the Centre of Excellence at University of Cape Town and the National Research Foundation (NRF), South Africa for the provision of research grants that have helped me to sustain myself and attend conferences during the course of my studies.

Furthermore, my sincere appreciation is extended to the members of the Deeper Life Bible Church, Western Cape Province, Cape Town, South Africa for their prayers and encouragement. I would also like to thank the Head of Department - Prof. Edward Boje

and the entire staff members of the department of Electrical Engineering, in particular, Mrs Kehinde Awodele, Ms Nicole Moodley, Ms Carol Koonin, Ms Janine Buxey, Mr. Matthew Van Der Westhuizen and Ms Josephine. Likewise, I would like to say thank you to the members of staff, Postgraduate Funding Office, University of Cape Town. In addition, I appreciate the management, Lagos State University, Nigeria for giving me study leave to pursue this programme as well as the members of staff, Lagos State University, Nigeria who have morally and financially contributed in one way or the other in the course of this work. I can not include your names due to the limitation of space. A big thank you to everyone.

Moreover, a very special thank you to my family for their unwavering support, prayer, and sacrifice during my PhD studies. In particular, I would like to thank my lovely husband, Pastor Adedoyin Segun Emmanuel Adedoyin, for his prayers and support throughout this PhD journey, and our wonderful children, Deborah Ebunoluwa Adedoyin and David Erioluwa Adedoyin. My beloved uncles and their wives; Pastor David Adekoyejo and Mrs. Kehinde Bamigbowu as well as Pastor Clement and Mrs. Funmilayo Ogunsina. My dear sister and her husband, Mr. Kunle and Mrs. Aramide Obikoya. My precious cousin and her husband, Mr. Beloved and Mrs. Titilope Olaniyi. My caring in-laws, Mrs. Florence Odogiyon, Mr. and Mrs. Yinka Olaniyi, Mr. and Mrs. Olatunji, Mr. and Mrs. Philip Odogiyon, Mr. David and Mrs. Rhoda Kehinde, Mr. Caleb Odogiyon and Mr. Gabriel Odogiyon.

Finally, I remember and acknowledge my late parents, Mr. Manipekun and Mrs. Dorcas Adebisi Otegbeye.

Contents

Abstract

The heterogeneous deployment of small cells (e.g., femtocells) in the coverage area of the traditional macrocells is a cost-efficient solution to provide network capacity, indoor coverage and green communications towards sustainable environments in the future fifth generation (5G) wireless networks. However, the unplanned and ultra-dense deployment of femtocells with their uncoordinated operations will result in technical challenges such as severe interference, a significant increase in total energy consumption, unfairness in radio resource sharing and inadequate quality of service provisioning. Therefore, there is a need to develop efficient radio resource management algorithms that will address the above-mentioned technical challenges.

The aim of this thesis is to develop and evaluate new efficient radio resource management algorithms that will be implemented in cognitive radio enabled femtocells to guarantee the economical sustainability of broadband wireless communications and users' quality of service in terms of throughput and fairness. Cognitive Radio (CR) technology with the Dynamic Spectrum Access (DSA) and stochastic process are the key technologies utilized in this research to increase the spectrum efficiency and energy efficiency at limited interference. This thesis essentially investigates three research issues relating to the efficient radio resource management: Firstly, a self-organizing radio resource management algorithm for radio resource allocation and interference management is proposed. The algorithm considers the effect of imperfect spectrum sensing in detecting the available transmission opportunities to maximize the throughput of femtocell users while keeping interference below pre-determined thresholds and ensuring fairness in radio resource sharing among users. Secondly, the

effect of maximizing the energy efficiency and the spectrum efficiency individually on radio resource management is investigated. Then, an energy-efficient radio resource management algorithm and a spectrum-efficient radio resource management algorithm are proposed for green communication, to improve the probabilities of spectrum access and further increase the network capacity for sustainable environments. Also, a joint maximization of the energy efficiency and spectrum efficiency of the overall networks is considered since joint optimization of energy efficiency and spectrum efficiency is one of the goals of 5G wireless networks. Unfortunately, maximizing the energy efficiency results in low performance of the spectrum efficiency and vice versa. Therefore, there is an investigation on how to balance the trade-off that arises when maximizing both the energy efficiency and the spectrum efficiency simultaneously. Hence, a joint energy efficiency and spectrum efficiency trade-off algorithm is proposed for radio resource allocation in ultra-dense heterogeneous networks based on orthogonal frequency division multiple access. Lastly, a joint radio resource allocation with adaptive modulation and coding scheme is proposed to minimize the total transmit power across femtocells by considering the location and the service requirements of each user in the network.

The performance of the proposed algorithms is evaluated by simulation and numerical analysis to demonstrate the impact of ultra-dense deployment of femtocells on the macrocell networks. The results show that the proposed algorithms offer improved performance in terms of throughput, fairness, power control, spectrum efficiency and energy efficiency. Also, the proposed algorithms display excellent performance in dynamic wireless environments.

List of Abbreviations

3GPP	Third Generation Partnership Project
4G	Fourth Generation
5G	Fifth Generation
AMC	Adaptive and Modulation Coding
AWGN	Additive White Gaussian Noise
BE	Best Effort
BER	Bit-Error-Rate
BnB	Branch and Bound
BPSK	Binary Phase Shift Keying
BS	Base Station
C	Constraint
CA	Carrier Aggregation
CAC	Call Admission Control
CAGR	Compound Annual Growth Rate
CAPEX	Capital Expenditure
CCC	Common Control Channel
CFN	Cognitive Femtocell Network
CN	Core Network
CQI	Channel Quality Indicator
CR	Cognitive radio
CRRM	Cognitive Radio Resource management
CSG	Closed Subscriber Group
CSI	Channel State Information
DL	Downlink
D2D	Device-to-Device
DSA	Dynamic Spectrum Access
DSL	Digital Subscriber Line
E2E	End-to-End
EE	Energy Efficiency
EE-SET	Energy Efficiency and Spectrum Efficiency Trade-off
eNB	evolve Node-B
EPA	Equal Power Allocation
EPC	Evolved Packet Core

E-UTRAN	Evolved Universal Terrestrial Radio Access network
FAP	Femto Access Point
FAP-GW	Femto Access Point Gateway
FD	Full Duplexing
FDD	Frequency Division Duplexing
FGWNs	Future Generation Wireless Networks
FSMM	Finite State Markov Model
FTP	File Transfer Protocol
FUE	Femtocell User Equipment
GA	Genetic Algorithm
Gbps	Giga bits per second
GHz	Giga Hertz
HeNB	Home evolve Node-B
HetNet	Heterogeneous Network
HSDPA	High-Speed Data Packet Access
HWNs	Heterogeneous Wireless Networks
ICI	Inter Cell Interference
IEEE	Institute of Electrical and Electronic Engineers
IoT	Internet of Things
IP	Internet Protocol
IPsec	Internet Protocol Security
J	Joule
JRRA	Joint Radio Resource Allocation
LDD	Lagrangian Dual Decomposition
LTE	Long Term Evolution
LTE-A	Long Term Evolution-Advanced
M2M	Machine-to-Machine
MAC	Medium Access Control
MATLAB	Matrix Laboratory
Max	Maximum
MBS	Macro Base Station
MCS	Modulation and Coding Scheme
MHz	Mega Hertz
MIMO	Multiple Input Multiple Output
Min	Minimum
MINLP	Mixed Integer Non-Linear Programming
MILP	Mixed Integer Linear Programming
MME	Mobility Management Entity
mmWave	Millimetre Wave
NE	Nash Equilibrium
NP	Non-deterministic Polynomial time
NRT	Non-Real Time
NSGA	Non-dominated Sorting Genetic Algorithm

OFDM	Orthogonal Frequency Division Multiplexing
OFDMA	Orthogonal Frequency Division Multiple Access
OOB	Out-of-Band
OPEX	Operating Expenditure
PAPR	Peak to Average Power Ratio
PHY	Physical
PRB	Physical Resource Block
PU	Primary User
QAM	Quadrature Amplitude Modulation
QoE	Quality of Experience
QoS	Quality of Service
QPSK	Quadrature Phase Shift Keying
RAN	Radio Access Network
RATs	Radio Access Technologies
RB	Radio Block
RF	Radio Frequency
RLC	Radio Link Control
RNC	Radio Network Controller
RRA	Radio Resource Allocation
RRAO	Radio Resource Allocation Optimization
RRM	Radio Resource Management
RT	Real Time
SAE	System Architecture Evolution
SC-OFDMA	Single Carrier Orthogonal Frequency Multiple Access
SE	Spectrum Efficiency
Se GW	Security Gateway
S-GW	Serving Gate Way
SINR	Signal-to-Interference-plus-Noise Ratio
SNR	Signal-to-Noise Ratio
SOHO	Small Office/Home Office
SON	Self Organized Network
SORRM	Self-Organizing Radio Resource Management
SQP	Sequential Quadratic Programming
SU	Secondary User
TDD	Time Division Duplexing
TTI	Transmission Time Interval
UE	User Equipment
UL	Uplink
UMTS	Universal Mobile Telecommunications System
VoIP	Voice over Internet Protocol
WiFi	Wireless Fidelity
WiMAX	Worldwide Interoperability for Microwave Access
WLANs	Wireless Local Area Networks
WMAN	Wireless Metropolitan Area Networks

List of Tables

List of Figures

List of Publications

The complete list of the publications associated with the contributions of this thesis is presented as follows:

- **Journal papers**

  [J.1] Mary Adedoyin, and Olabisi Falowo, "QoS-Aware Radio Resource Allocation for 5G Ultra-Dense Heterogeneous Network," *Computer Networks Journal*, Manuscript Number: COMNET-D-17-856. (Submitted).

  [J.2] Mary Adedoyin, and Olabisi Falowo, "Joint Radio Resource Management with Adaptive Modulation and Coding Scheme for Ultra-Dense Networks with QoS Guarantees," *Journal of Network and Computer Applications*, Manuscript Number: JNCA-D-17-01015 (Submitted).

  [J.3] Mary Adedoyin, and Olabisi Falowo, "QoS-Based Joint Optimization of EE and SE for 5G Ultra-Dense Heterogeneous Network," *to be submitted to IEEE Transaction on Vehicular Technology.*

- **Conference Papers**

[C.1] Mary Adedoyin, and Olabisi Falowo, "QoS-Aware Radio Resource Allocation for Ultra-Dense Heterogeneous Networks," *28th Annual IEEE International Symposium on Personal, Indoor and Mobile Radio Communications* (PIMRC 2017), 08-13 Oct., 2017 Montreal, Canada, pp. 1-7, (**Best Paper Award**).

[C.2] Mary Adedoyin, and Olabisi Falowo, "QoS-Aware Radio Resource Allocation for Green Wireless Communication in 5G Networks," *in Proc. Southern Africa Telecommunication Networks and Applications Conference (SATNAC)*, 3-10 Sept. 2017, Freedom of the Seas Cruise Liner, Barcelona, Spain, pp. 86-91, (**Best Paper Award**).

[C.3] Mary Adedoyin, and Olabisi Falowo, "QoS-based Radio Resource Management for 5G Ultra-Dense Heterogeneous Networks," *in Proc.* 26^{th} *European Conference on Networks and Communications (EUCNC), Oulu, Finland*, 12-15 Jun. 2017, pp. 1-6.

[C.4] Mary Adedoyin, and Olabisi Falowo, "Joint Optimization of Energy Efficiency and Spectrum Efficiency in 5G Ultra-Dense Networks," *in Proc.* 26^{th} *European Conference on Networks and Communications (EUCNC), Oulu, Finland*, 12-15 Jun. 2017, pp. 1-6.

[C.5] Mary Adedoyin, and Olabisi Falowo, "An Energy-Efficient Radio Resource Allocation Algorithm for Heterogeneous Wireless Networks," *in Proc. IEEE PIMRC, Valencia, Spain*, 4-7 Sept. 2016, pp. 1-6.

[C.6] Mary Adedoyin, and Olabisi Falowo, "Joint Energy-Efficiency and Spectrum-Efficiency Trade-off for Radio Resource Allocation in Heterogeneous Wireless networks," *in Proc. SATNAC, Fancourt, George, South Africa*, Sept. 2016, pp. 56-61.

[C.7] Mary Adedoyin, and Olabisi Falowo, "Self-Organizing Radio Resource Management for Next Generation Heterogeneous Wireless Networks," *in Proc. IEEE ICC, 23-27 Kuala Lumpur, Malaysia*, May 2016, pp. 1-6.

[C.8] Mary Adedoyin, and Olabisi Falowo, "Hybrid-Based Radio Resource Allocation for Future Generation Heterogeneous Networks," *in Proc. SATNAC, Hermanus, South Africa*, Sept. 2015, pp. 75-80.

- **Poster and Work-in-Progress Papers**

[P.1] Mary Adedoyin, and Olabisi Falowo, "Efficient Radio Resource Management for Future Generation Heterogeneous Wireless Networks," *in Proc. of the Poster Booklet, Faculty of Engineering and the Built Environment, University of Cape Town Research Expo, Cape Town, South Africa*, May. 2016, pp. 1-2.

[W.1] Mary Adedoyin, and Olabisi Falowo, "Self-Organizing Radio Resource Management for Next Generation Heterogeneous Wireless Networks," *in Proc. of SATNAC, Hermanus, South Africa*, Sept. 2015, pp. 1-2.

Chapter 1

Introduction

1.1 Research Background

In wireless communications, providing coverage for indoor users is challenging due to path loss, shadowing and multipath fading that weaken the signal received by the users from the conventional macrocells. In this situation, a distant macrocell does not provide the users with the best quality-of-service (QoS) for multimedia applications such as Voice over Internet Protocol (VoIP), online gaming, video streaming and internet surfing, that are in high demands by indoor users. The suitable approach of tackling this problem is to reduce the distance between an indoor user and a macrocell [1]-[3].

Furthermore, the demand for higher data rates in wireless networks is unrelenting. According to a recent report by Cisco in [4], the global mobile data traffic will increase at a compound annual growth rate (CAGR) of 46% between 2016 and 2021 reaching 48.3 exabytes per month by 2021. In fact, only video traffic will account for 82% of the total

traffic by 2021. This will lead to traffic explosion, which is mainly due to the advent of tablets, smartphones, and laptops with mobile broadband. Moreover, research findings on wireless usage reveal that more than 70% of data traffic and 50% of voice traffic happen indoors [1]. Similarly, in the near future, indoor/hotspot traffic may approach 90% [5]. Also, the report presented in [6] indicates that the future wireless communication systems will have to accommodate about 100 billion connected devices. Additionally, the newly emerging applications such as machine-to-machine (M2M) communication, Internet of Things (IoT), device-to-device (D2D) communication, wearable and financial technologies [7] will be essentially deployed in the indoor environments and would require broadband connectivity. Consequently, this predicted traffic explosion and ever increasing users' demand for bandwidth intensive applications necessitate the deployment of efficient and economical solutions in the indoor environments. Recently, there has been a paradigm shift in the cellular network infrastructure deployment, which is moving away from the conventional high-power tower-mounted base station (homogeneous network) deployments towards heterogeneous network (HetNet) deployments to provide efficient and cost-effective solutions for indoor users in the fifth generation (5G) wireless networks [8], [10] .

HetNets are defined as multiple networks with different radio access technologies (RATs). HetNet is one of the strategies of the future 5G wireless networks to improve capacity, coverage, and to ensure green communications in indoor and hotspots environments. Also, HetNets can significantly improve the overall spectrum efficiency and energy efficiency through a full spatial resource reuse [11]. Integrating small cells into the traditional macrocells results in HetNets [12]. Examples of small cells are microcells, picocells,

femtocells, and distributed antenna systems (remote radio heads), which are differentiated by their physical sizes, transmit powers/coverage areas, propagation characteristics and backhaul [8] [9].

In this thesis, the focus is on HetNets comprising macrocells and femtocells. In the future 5G wireless network, the heterogeneous deployment of ultra-dense femtocells overlaying the coverage area of conventional macrocells has been referred to as a promising solution by researchers and telecommunication industry to improve indoor coverage, enhance network capacity and facilitate green communications towards sustainable environments [8]-[12]. A typical example of HetNets consisting of a macrocell and femtocells is depicted in Fig. 1.1. The biggest "dashed" circle represents the coverage area of the macrocell while the smaller "dashed" circles represent the coverage area of the femtocells. The macrocell communicates with its associated users while each femtocell also communicates with its attached users.

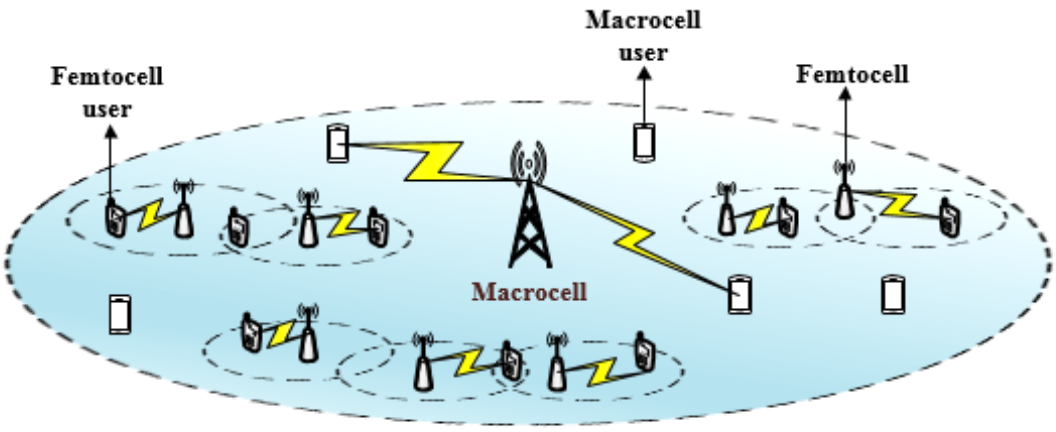

Figure 1.1: Heterogeneous wireless networks.

1.2 Overview of Femtocell Technology

This section presents a brief description of femtocells, types of access modes in femtocells, spectrum assignment techniques in femtocells, the benefits of deploying femtocells and the challenges of deploying femtocells.

1.2.1 Description of Femtocell

A femtocell is defined as "a low-power (10-100mW), short-range (10-30m) and low-cost wireless access point that operates in licensed spectrum to connect standard mobile devices to a mobile operator's network using residential digital subscriber line (DSL), cable broadband connections or wireless. It is installed inside buildings such as residential and small office/home office (SOHO) in a random manner to boost signal reception [1], [2]. Femtocells are designed to operate on the plug and play features. Also, femtocells are installed in indoor environments by the end users like wireless fidelity (WiFi) routers and provide almost all the macrocell functionalities to the end users [13]. Technically, a femtocell is referred to as femto access point (FAP) [14]. A femtocell can communicate with each associated femtocell user equipment (FUE) such as a laptop, personal computer, or smartphone. Fig. 1.2 illustrates the connection of a femtocell through DSL modem or broadband router to a mobile operator's network. Different FUEs can connect to a femtocell to use different services such as voice and data services.

Femtocells are designed to use the same physical layer technology as macrocells. Moreover, femtocells have been standardised in the third generation partnership project (3GPP) Release 8, where femtocells are called Home evolved Node-B (HeNB) in long term

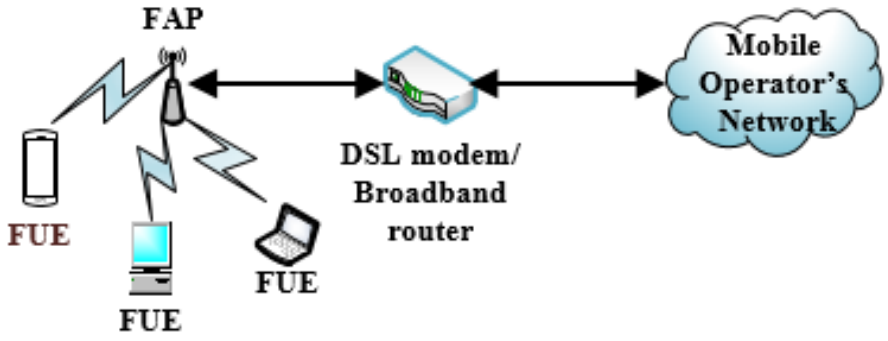

Figure 1.2: FUEs connected through an FAP to a mobile operator's network.

evolution (LTE) systems [13], [15]. Also, the 3GPP has come up with the enhanced version of LTE standard termed long term evolution-advanced (LTE-A) standard to support the heterogeneous deployment of femtocells within the service area of macrocells [12].

1.2.2 Types of Access Modes in Femtocells

Femtocells operate in three different access modes namely; closed access, open access, and hybrid access modes [16], [17] as shown in Fig. 1.3.

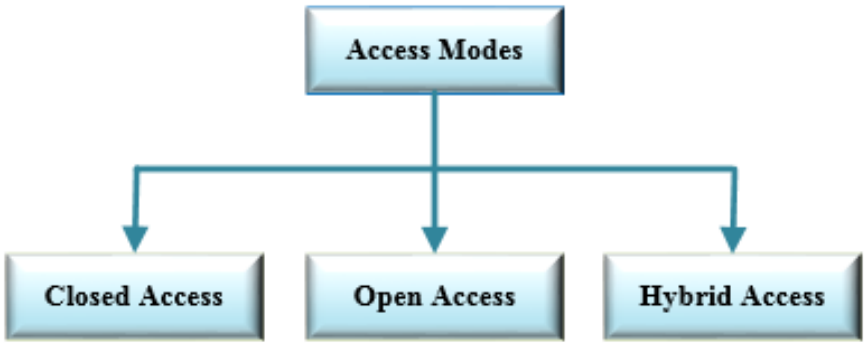

Figure 1.3: Types of access modes.

1.2.2.1 Closed Access Mode

In the closed access mode, only the registered users are authorised to access the femtocell. These users are referred to as closed subscriber group (CSG). This access mode offers exclusive service to femtocell users in the CSG but the performance can be affected if there are nearby macrocell users that cause severe interference. This is a typical user-deployed scenario.

1.2.2.2 Open Access Mode

In the open access mode, all nearby users can have access to an FAP. This type of access mode offers the highest level of network capacity but QoS degradation occurs when the number of unregistered nearby macrocell users increases rapidly or when they are running bandwidth-consuming applications. Also, this type of access mode is typically deployed by mobile operators, where femtocells with open access are deployed in public regions.

1.2.2.3 Hybrid Access Mode

The hybrid access mode is the trade-off between the closed and the open access modes. A limited amount of resources is available to all nearby users but a certain amount of resources is reserved for the subscribed users in CSG. Hybrid access mode offers differentiable services to the registered femtocell users and nearby unregistered macrocell users that are in the coverage area of the femtocell. In [18] and [19], the authors have shown that hybrid access mode based schemes outperform either closed access mode or open access mode based schemes.

1.2.3 Spectrum Assignment Techniques in Femtocells

Femtocells are overlaid within the macrocells in a two-tier heterogeneous network. Therefore, allocating spectrum resources between femtocells and macrocells is a very important issue. There are three possible strategies as shown in Fig. 1.4 for spectrum resource assignment in femtocell: dedicated-channel assignment, partial-channel-sharing assignment, and co-channel assignment [20], [21].

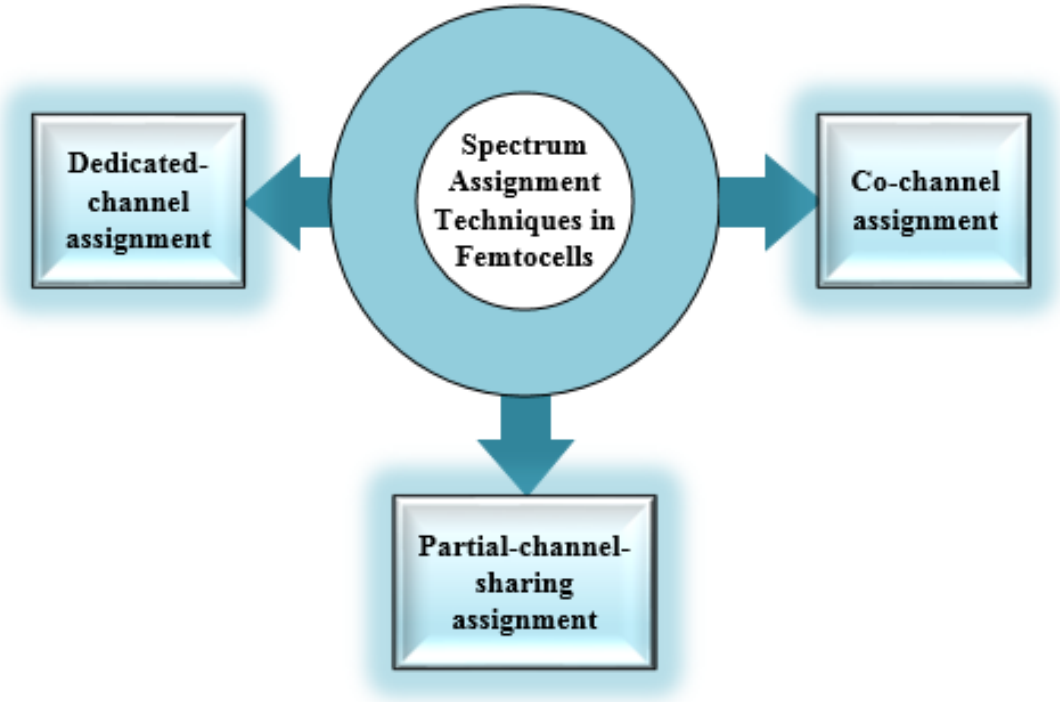

Figure 1.4: Spectrum assignment techniques in femtocells.

- Dedicated-channel assignment: Femtocells and macrocells utilise different frequency bands in the dedicated-channel assignment. This assignment is a simple solution to avoid mutual interference between the two tiers, but the spectral usage is inefficient

due to bandwidth segmentation. Hence, a dedicated-channel assignment is infeasible for the ultra-dense deployment of femtocells [20], [21].

- Partial-channel-sharing assignment: The overall bandwidth is segmented into two parts in the partial-channel-sharing assignment. One part is exclusively assigned to macrocell users, and the other part is shared by macrocells and femtocells. Macrocell users benefit from ubiquitous coverage on an exclusive carrier frequency and partial coverage (outside the femtocell coverage) on sharing carrier frequency. This assignment is efficient without causing much bandwidth loss and mutual interference, but a portion of the spectrum and high-cost carrier-aggregation-capable terminals are required [20], [21].

- Co-channel assignment: In this assignment, spectral usage is high because both femtocells and macrocells share the same frequency bands without bandwidth segmentation but severe interference occurs. This low-cost and backward-compatible strategy does not rely on high spectrum availability and carrier aggregation support at terminals [20], [21]. The co-channel assignment is preferred to the dedicated-channel assignment and the partial-channel-sharing assignment by wireless network operators since the licensed spectrum is costly and scarce.

1.2.4 Benefits of Deploying Femtocell

The benefits of deploying femtocell include better indoor coverage, higher capacity, enhanced macrocell reliability and traffic offloading, longer battery life, seamless connectivity, and

improved QoS. Additionally, there is a significant reduction in both the operating expenditure (OPEX) and capital expenditure (CAPEX) [1], [2], [11]-[14]. These benefits are summarised below:

- **Better indoor coverage:** The deployment of femtocells in indoor environments would cover the coverage holes of macrocells due to the close proximity of the transmitters (FAPs) and receivers (FUEs).

- **Higher capacity**: The deployment of femtocells in indoor environments would improve the network capacity because femtocells transmit at lower power, thereby reducing interference and achieving a higher signal-to-interference-plus-noise ratio (SINR). Hence, more users are grouped into an area operating on the same spectrum.

- **Enhanced macrocell reliability:** The traffic congestion on macrocells would reduce by offloading the indoor traffic to femtocells, thus making macrocells more reliable. Also, the deployment of femtocells would improve the overall network performance and service quality by offloading the indoor traffic from the conventional macrocells.

- **Longer system battery life:** A lower transmission power is required in femtocells, which increases the life span of the system battery.

- **Seamless connectivity:** A femtocell has the capability to perform handover to a nearby macrocell. Therefore, there is an unbroken service even if a femtocell user leaves the coverage area of the serving femtocell.

- **Improved QoS:** Offloading users from macrocells to femtocells enhances the satisfaction level of users since a femtocell serves a small number of indoor users, each user can receive more resources leading to improved QoS.

- **Reduced OPEX and CAPEX:** A large portion of OPEX and CAPEX is attributed to site acquisition, energy bills, installation and maintenance of cell tower and backhaul in macrocells. The deployment of femtocells reduces the infrastructure, maintenance and operating costs of the mobile operators.

1.2.5 Challenges of Deploying Femtocell

In the literature, a number of challenges of deploying femtocells have been identified. Examples are

- **Interference problems:** The deployment of femtocells in the coverage area of macrocells will cause unwanted signals to the nearby macro user equipment (MUEs) or FUEs when femtocells are communicating with their attached UEs. Also, the deployment of a large number of femtocells in an unplanned fashion will introduce interference.

- **High frequency of handovers:** The small range of femtocells can cause frequent handovers, which may introduce frequent service disruption to a user that is moving away from the coverage area of a femtocell and entering into the coverage area of another nearby femtocell or macrocell.

- **Backhauling of femtocells:** A femtocells is connected to a core network through the backhaul, which comprise copper, fibre, microwave, and satellite links. These backhauls can limit the performance of femtocells because they are limited in terms of capacity and also very expensive.

- **Radio resource management:** Radio resource is limited and scarce. Therefore, there is need for effective radio resource management among femtocell users as well as macrocell users to ensure excellent network performance.

1.3 Overview of Cognitive Radio Technology

Coginitive radio (CR) is one of the enabling technologies in the future wireless network to address the challenges of deploying femtocells. CR is an intelligent technology that addresses the problem of spectrum scarcity [22]-[25]. The major idea of CR is to intelligently identify and allocate unutilised or underutilised spectrum known as a spectrum hole to an opportunistic user. The main functions of CR include spectrum sensing, spectrum decision, spectrum sharing and spectrum mobility [26]-[28]. There are other capabilities of CR, which include interference coordination, load balancing, coverage, and capacity optimisation [28]. Fig. 1.5 shows the dynamic spectrum access in power, frequency, and time domains.

In CR architecture, there are two kinds of networks: the primary and secondary networks. The primary network is the existing network infrastructure, which operates at some frequency bands known as licensed bands. The elements of the primary network are the primary user (PU) and primary base station. On the other hand, the secondary network is a network

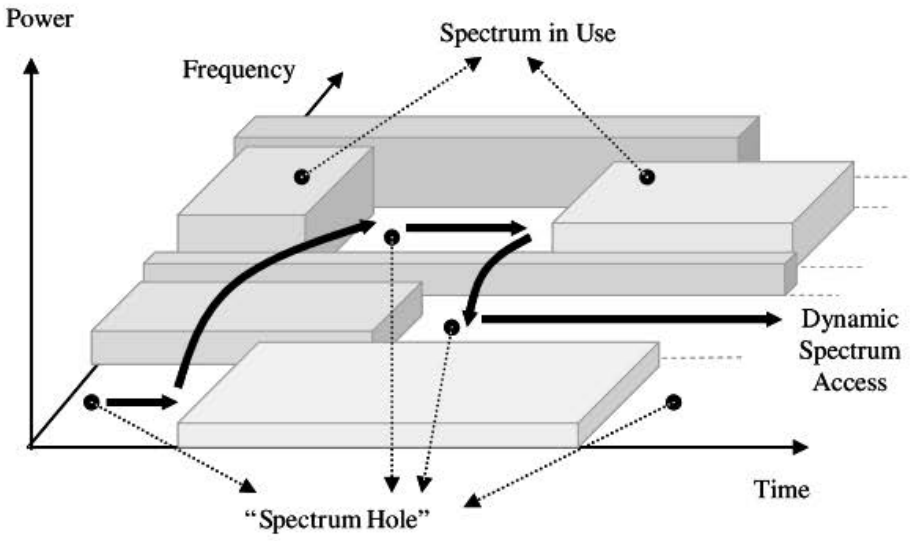

Figure 1.5: Dynamic spectrum access in power, frequency, and time domains [24].

infrastructure, which does not own any licensed band. The elements of the secondary network are the secondary user (SU) and secondary base station. The SUs are also known as opportunistic users. In the context of the heterogeneous networks comprising macrocells and femtocells, a macrocell network is regarded as a primary network and a femtocell network as a secondary network [12].

The CR technology enables a femtocell to sense its radio environment, identify and allocate radio resources in frequency, time, and power domains, which are not occupied by the macrocell users in the network. There are different types of sensing method in cognitive femtocell, which are matched filter, cyclostationary feature detection, waveform detection, wavelet detection and co-operative sensing [23].

1.3.1 Cognitive Radio-Enabled Femtocell

A cognitive radio-enabled femtocell has a reasoning ability and can use experiences to make decisions without necessarily acquiring information all the time from the network. This reduces the amount of signalling overhead associated with data transmission. Also, it can detect the spectrum holes of a macrocell network and learn from the previous experience in order to dynamically adjust its transmission parameters such as power, frequency, and modulation to access the vacant spectrum. Thus, unlicensed FUEs can be allowed to use the licensed spectrum, as long as it does not interfere with any of the macrocell UEs (MUEs) in the band [24]. In HetNets consisting of macrocells and femtocells, macrocells are the primary base stations and the associated users (MUEs) are the primary users, while femtocells are the secondary base stations and the attached users (FUEs) are the secondary users. Integrating cognitive functionalities into femtocell has a great potential to enhance the macrocell's energy efficiency and spectrum efficiency. In cognitive femtocell networks, the femtocell in the network performs spectrum sensing with the cooperation of its associated FUEs. It is very important to state that, the terms CR-enabled femtocell, CR-enabled FAP, cognitive femtocell, and cognitive FAP are used interchangeably throughout this thesis to mean the same concept.

1.4 Research Motivation

There will be a co-existence of several radio access technologies in the future wireless communication systems such as Wireless Local Area Networks (WLANs), Universal Mobile

Telecommunications System (UMTS), Worldwide Interoperability for Microwave Access (WiMAX), LTE, LTE-Advance, and femtocells to meet the traffic explosion and the demand of end users for broadband services [22]. Femtocells are one of the recent technological achievements, which began to draw the attention of telecommunication industry and research community in early 2008 [1], [22]. Femtocells have been regarded as a vital part of 5G systems by the 3GPP forum to achieve the peak data rate requirement of 1 Gbps for users in indoor environments [21]. However, in order to fully exploit the benefits offered by deploying femtocells, the mobile operators must take special care to address the technical issues that may arise due to the ultra-dense deployment of femtocells overlaid on the macrocells. Also, the overall QoS of each user connected to the conventional macrocell should not be adversely affected or degraded by the deployment of femtocells.

Moreover, femtocells are randomly deployed by the end users, which can be switched on and off or relocated by the end users at any time. Therefore, the number as well as locations of femtocells, continuously change in the coverage of macrocells. Consequently, this renders the typical centralised design schemes and network planning unfeasible. Hence, femtocells need to be intelligent enough to autonomously integrate into already existing radio access network (RAN). Additionally, femtocells should be able to self-configure and self-optimise without causing any performance degradation to the existing macrocell systems. Thus, there is a strong motivation to incorporate cognitive radio capabilities into femtocells. For example, since there will be an ultra-dense deployment of femtocells in an unplanned manner, a centralised-scheduling technique will not be able to provide the required level of energy efficiency (EE), spectrum efficiency (SE) and QoS. The effective solution will be to

integrate cognitive radio (CR) functionalities into femtocell, which will make it to be aware of its radio frequency (RF) environment.

1.5 Problem Statement

The heterogeneous deployment of ultra-dense femtocells in the coverage area of the traditional macrocells in an unplanned manner will result in serious technical challenges such as cross-tier interference (interference between macrocells and femtocells) and co-tier interference (interference between neighbouring femtocells), inefficient utilisation of radio resource, a significant increase in energy consumption, unfairness in sharing radio resource, inadequacy in the provision of QoS and network complexity. These technical problems need to be resolved before the performance gain of the ultra-dense deployment of femtocells can be achieved. Therefore, this thesis provides efficient radio resource management (RRM) algorithms for cognitive radio-enabled femtocells deployed within the geographical location of macrocells to address the above-mentioned technical challenges.

1.6 Research Questions

The current distributed radio resource management (RRM) algorithms developed for femtocells have not fully addressed the technical problems, which may arise due to the heterogeneous deployment of ultra-dense femtocells in an unplanned fashion overlaying the coverage region of macrocells. Therefore, to fully tackle the technical challenges, the following are the research questions addressed in this research.

1. How can intelligent allocation of radio resources (subchannel and power) minimise cross-tier and co-tier interferences, ensure fairness in the sharing of radio resources and provide an adequate level of QoS in the HetNet?

2. How can the QoS be improved on while considering the joint optimisation of energy efficiency and spectrum efficiency without a significant complexity increase in allocating radio resources to a user?

3. How can joint radio resource allocation (RRA) with adaptive modulation and coding scheme (MCS) minimise cross-tier and co-tier interferences, ensure fairness and provide an adequate level of QoS in the HetNets?

1.7 Hypothesis/Research Objectives

1.7.1 Hypothesis

In a fully distributed network architecture, introducing intelligent radio resource management mechanisms into the access network can mitigate interference, ensure fairness in radio resource sharing, increase the energy efficiency and spectrum efficiency and hence, guarantee an adequate level of QoS using 3GPP standard parameters. This provides flexible and scalable solutions that efficiently manage the radio resources in HetNets to offer excellent services for indoor users.

1.7.2 Research Objectives

The objectives of this research are:

- To review the existing literature and discuss how advances in technology provide a basis for this research. The review also recognises the existing techniques used for comparison purposes to determine the performance improvement of the proposed algorithms.

- To develop intelligent RRM algorithms: These algorithms protect femtocell users from interfering with macrocell users, ensure fairness in radio resource allocation among users, maximise energy efficiency and spectrum efficiency and also improve the QoS of users.

- To implement the proposed algorithms: The intelligent algorithms for radio resource allocation between macrocells and femtocells are implemented in MATLAB software package.

- To evaluate the performance of the proposed algorithms: The performance of the algorithms is evaluated to determine the improvement in QoS of users that are admitted into the two-tier networks for real-time (RT), non-real time (NRT) and best effort services.

- To compare the proposed algorithms with the related existing algorithms: The performance improvement of the proposed algorithms over the existing state-of-the-art RRM algorithms is also investigated. These previously existing algorithms are also implemented in MATLAB software environment.

- To investigate the trade-off analysis on the proposed algorithms: Further investigations are also conducted to determine how the proposed algorithms perform under different wireless network performance metrics and how the performance compares to that of existing algorithms under these metrics.

1.8 Research Methodology

In this research, there are two types of methodology approach, which are theoretical analysis and system-level simulations adopted to solve the research questions outlined in Section 1.6 and achieve the objectives presented in Section 1.7.2. Firstly, a solid foundation on the research topic was established through a comprehensive literature review. The sources used in conducting the literature review research were textbooks, journals, workshop papers, international and local conference papers, standardised technical specifications and other related materials accessible on the Internet. The theoretical foundation was very essential in order to know the limitations of the state-of-art RRM algorithms in the literature and how to formulate the novel contributions presented in this thesis. Furthermore, the comprehensive review was needed to establish the system models that would be implemented in the simulator used in this research. The simulation parameters used in this thesis are based on the 3GPP standards [15], [29]. In this thesis, simulations are used with mathematical models to validate the proposed RRM algorithms and for comparison with the existing RRM schemes.

The RRM schemes proposed in this thesis have been implemented in MATLAB simulation software package. CPLEX software is also used to solve the mixed integer linear problems in this thesis [30]. Moreover, the performance evaluation of the proposed RRM algorithms in

this thesis is based on the analysis of the simulation results. Also, the simulation scenarios for different objectives are simulated several times to have a reliable statistical confidence. The MATLAB simulator is flexible in the sense that each snapshot can have different time durations in line with the research objectives.

1.9 Research Scope

The main focus of this research is to develop efficient radio resource management algorithms to mitigate interference, ensure fairness, maximise EE and SE, and guarantee users' QoS requirements in heterogeneous wireless networks consisting of macrocells and cognitive femtocells. The work presented in this thesis concentrates on downlink transmissions of femtocells with hybrid access mode. Also, femtocells work in co-channel operation with macrocells and it is assumed in this thesis that both systems belong to the same mobile operator and have orthogonal frequency division multiple access (OFDMA), such as in long term evolution-advanced. There are two main reasons for choosing to study the downlink transmission direction in this thesis, which are detailed as follows:

- Firstly, in the mobile communication research community, it is generally assumed that most of the data traffic in wireless networks is transmitted from a base station to a mobile user (forward link). This is because the data generation of multimedia services is extremely asymmetric.

- Secondly, in the downlink, the OFDMA technology is basically used. OFDMA is the enabling physical layer technology of femtocells. Recently, the LTE-A system uses the

single carrier frequency division multiple access (SC-FDMA) technology for the uplink, because of the advantage of presenting a peak to average power ratio (PAPR) lower than the OFDMA case. Hence, this has highly benefited the mobile terminal in terms of costs and transmit power efficiency [15].

Moreover, the evaluations of the proposed schemes are carried out using MATLAB simulation software. In addition, mobility management is not considered since indoor scenario with limited range is the main focus of this thesis.

1.10 Thesis Novel Contributions

This thesis addresses the technical challenges in HetNets consisting of macrocell and femtocell networks. It provides novel RRM algorithms with the special focus on self-organisation, joint optimisation of EE and SE, and joint radio resource allocation with adaptive and modulation (AMC) scheme. Fig. 1.6 highlights the main contributions of the new efficient radio resource management algorithms in this thesis. The complete structure of the efficient radio resource management algorithms presented in this thesis can be summarised as follows:

1.10.1 Self-Organising Radio Resource Management Algorithm

In this task, a novel self-organising radio resource management for optimal subchannel and power allocation is researched in order to solve the throughput maximisation problem. The self-organising component of the developed algorithm enables a cognitive femtocell to sense its radio environment with the cooperation of its attached UEs, takes decision based on the

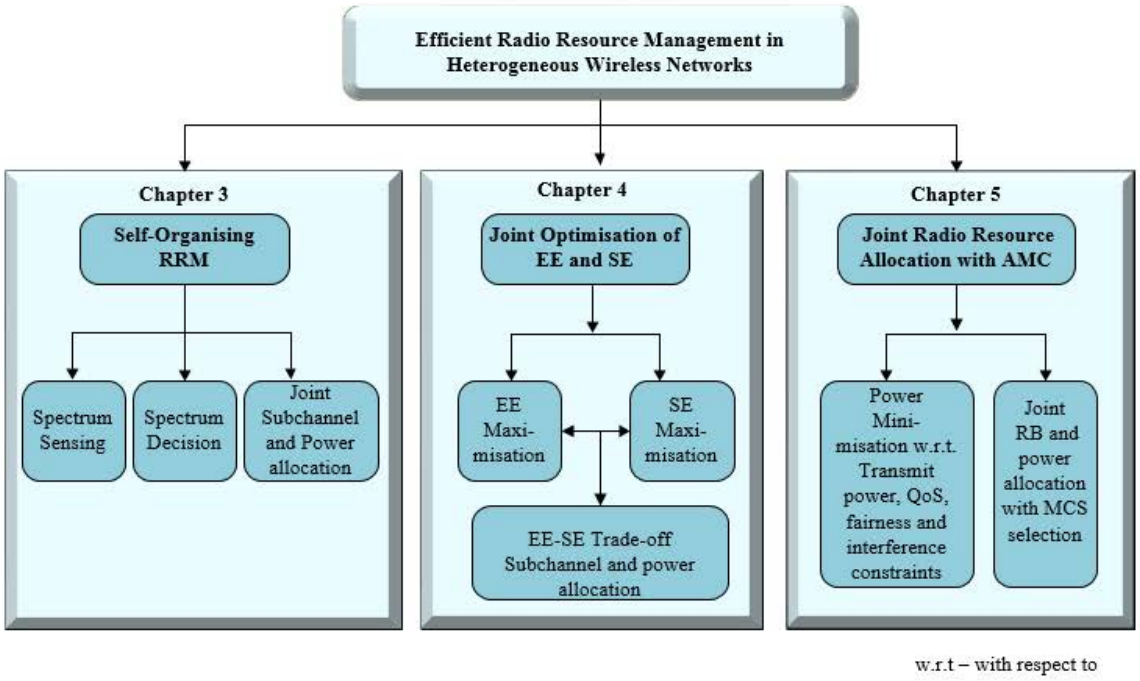

Figure 1.6: Complete structure of research contributions.

information collected during the sensing of the environment and then performs radio resource allocation in a distributed manner. The algorithm is integrated into the physical (PHY) and media access control (MAC) layers of cognitive femtocells to enable reliable communications between LTE-A based macrocell and cognitive femtocell as shown in Fig. 1.7.

The following are the main features of the self-organising radio resource management (SORRM) algorithm:

- **Spectrum Sensing:** Here, a cognitive femtocell cooperates with its associated user equipment to make observations of the RF spectrum and captures the relevant information to determine and detect which of the subchannels of the macrocell network are occupied and which ones are vacant. The vacant subchannels can be used by the cognitive femtocell network. At this stage, there is a consideration for imperfect

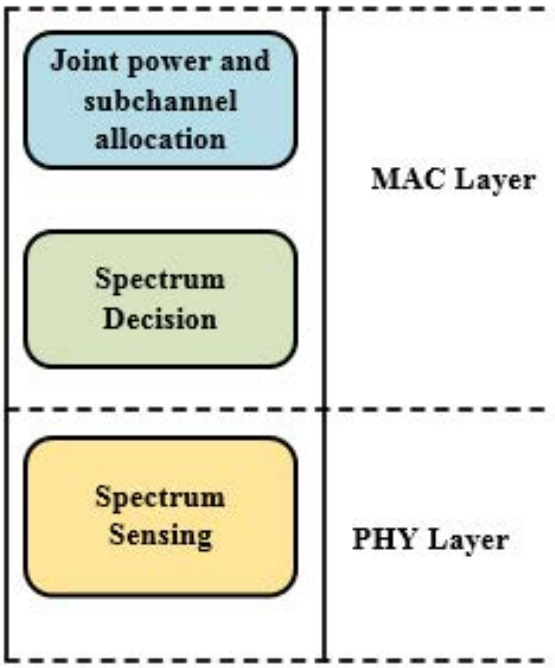

Figure 1.7: Functional design of SORRM.

spectrum sensing (spectrum sensing error) such as mis-detection error and false-alarm error.

- **Spectrum Decision:** The cognitive femtocell decides on the best spectrum band to be allocated to each attached user equipment among the vacant bands according to the QoS requirements of the requested services based on the information that is gathered from the spectrum sensing phase and spectrum availability.

- **Joint Radio Resource Allocation:** Based on the spectrum decision results, the cognitive femtocell has the ability to jointly allocate subchannel and corresponding power to its associated users depending on the QoS requirements of the requested

service using SORRM algorithm. Therefore, the algorithm can effectively improve the throughput of users in the network, ensure fairness in radio resource sharing, mitigate cross-tier and co-tier interference.

1.10.2 Joint Energy Efficiency and Spectrum Efficiency Trade-off based Radio Resource Allocation Algorithm

The 5G systems need to target trade-off analysis and joint optimisation of energy efficiency and spectrum efficiency in the development of RRA algorithms. Therefore, three different algorithms are proposed for comparison purpose, which are energy-efficient RRA algorithm, spectrum-efficient RRA algorithm with a special interest on the energy efficiency and spectrum efficiency trade-off (EE-SET) based RRA (EE-SET RRA) algorithm for optimal subchannel and power allocation to resolve the aspect of joint energy efficiency and spectrum efficiency maximisation problem. The following are the main features of the EE-SET radio resource allocation algorithm:

- **Energy Efficiency and Spectrum Efficiency Trade-off Determination:** The EE-SE trade-off is determined based on the normalisation factor. The normalisation factor ensures that both the energy efficiency and spectrum efficiency are on the same scale.

- **Radio Resource Allocation:** Based on the results of energy efficiency and spectrum efficiency trade-off, the cognitive femtocell allocates subchannel and corresponding power to its associated users using the EE-SET radio resource allocation algorithm.

Therefore, the algorithms can efficiently increase both the energy efficiency and spectrum efficiency of the HetNets.

1.10.3 Joint Radio Resource Allocation with Adaptive Modulation and Coding Scheme

The development of a joint radio resource allocation with adaptive modulation and coding scheme (JRRA-AMC) for the ultra-dense HetNets is crucial to mitigate interference, ensure fairness and provide an adequate level of QoS. This certainly leads to a flexible and intelligent RRM scheme. The following are the major features of the JRRA-AMC algorithm:

- **Power Control:** The optimisation algorithm that intelligently controls the transmit power of a cognitive femtocell is proposed to minimise the total transmit power consumed in the overall network.

- **Power Update:** Based on the power control results, the algorithm periodically updates the power configuration depending on the user's service requirement and location.

- **Radio Resource Allocation:** Based on the power updates results, the cognitive femtocell has the ability to allocate resource block (RB), corresponding power and modulation and coding scheme (MCS) to its associated users using the JRRA-AMC algorithm. Therefore, the algorithms can efficiently minimise the total transmit power consumed in the overall HetNet.

1.11 Thesis Organisation

This thesis mainly addresses the aforementioned technical challenges of ultra-dense and unplanned femtocell deployments in the coverage region of macrocells in 5G wireless systems. Moreover, the work presented in this thesis is organised into six chapters as shown in Fig. 1.8.

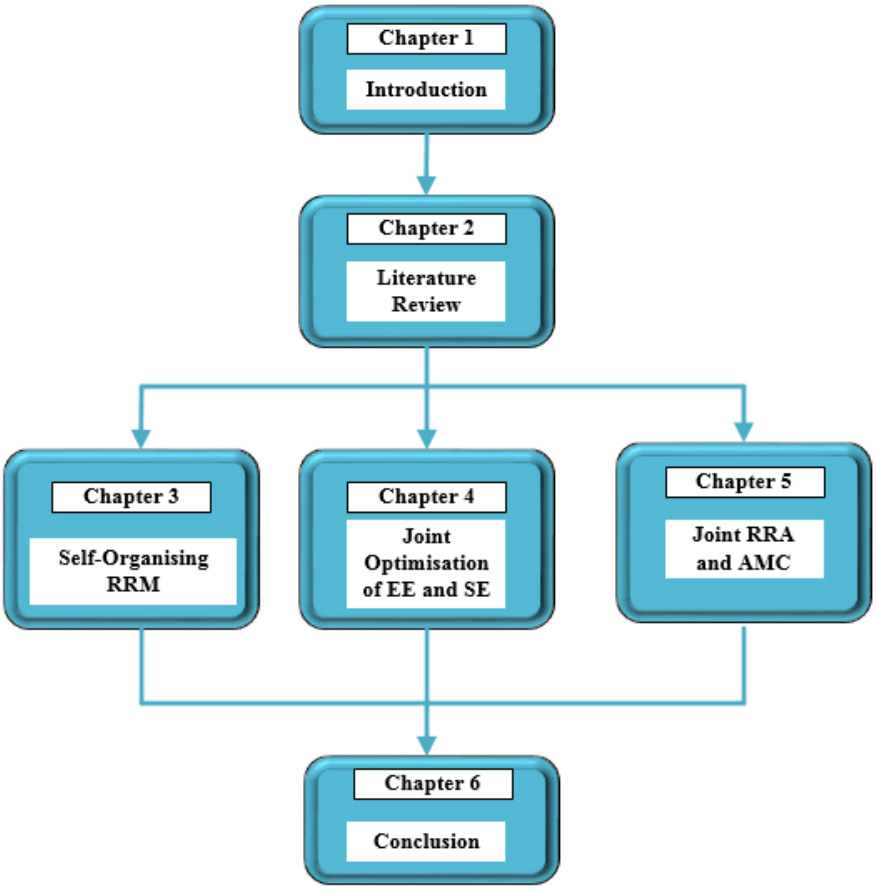

Figure 1.8: Complete thesis organisation.

Chapter 1 introduces the thesis background and the overview of femtocell technology. Also, research motivation, problem statement, research questions, hypothesis and the objectives of the research are presented. In addition, the methodology adopted in this

research, research scope and the novel contributions in this thesis are provided. The research objectives of this thesis are stated according to the performance requirements in 5G wireless networks. Moreover, chapters 3-5 start with a brief introduction that provides an overview of each particular chapter, highlights the main contributions and its organisation. There are also sections such as related work, the summary of notations, system model, problem formulation and proposed algorithm. Also, in each of these chapters, technical solutions are evaluated using system-level simulations and compared to the related existing works in the literature. At the end of each chapter, a brief conclusion is presented. The rest of the thesis is organised as follows:

Chapter 2 gives the detailed background and overview of radio resource management in 5G heterogeneous wireless networks. The subjects discussed in this chapter include the evolution of 5G wireless networks, HetNets and its architecture, radio resources in the OFDMA-based system, technical issues in HetNets, RRM techniques in HetNets and some optimisation tools found in the literature that can be used in solving RRM problems.

Chapter 3 presents the proposed SORRM algorithm. The algorithm considers the effect of imperfect spectrum sensing in detecting the available transmission opportunities to maximise the throughput of femtocell user while keeping interference below pre-determined thresholds and ensuring fairness in radio resource sharing. The performance of the proposed algorithm is compared with existing methods. Comparative performance evaluations are carried out through intensive simulation in MATLAB. Available information and 3GPP standard specifications are used as input for the simulation scenarios. The simulation outputs are used to assess the effectiveness of the proposed algorithm. The results

presented in this chapter have been published in the proceedings of the Southern Africa Telecommunications and Network Applications Conference (SATNAC 2015) and the IEEE International Conference on Communications (IEEE ICC 2016). Part of the results have also been accepted for presentation in the proceedings of IEEE Conference on Personal Indoor and Mobile Radio Communication (IEEE PIMRC 2017). In addition, the presented results have also been submitted for publication in the Computer Networks Journal.

Chapter 4 describes the effect of maximising the energy efficiency and the spectrum efficiency individually on radio resource allocation. Then, an energy-efficient radio resource allocation algorithm is proposed for green communication to improve the probabilities of spectrum access and further increase the network capacity for sustainable environments. Also, a spectrum-efficient radio resource allocation algorithm is proposed to increase efficient utilization of radio resources in the network. Moreover, a joint maximisation of the energy efficiency and spectrum efficiency of the overall network is considered since joint optimisation of energy efficiency and spectrum efficiency is one of the goals of 5G. Although, maximising the energy efficiency results in low performance of the spectrum efficiency and vice versa. Therefore, there is an investigation on how to balance the trade-off that arises when maximising both the energy efficiency and the spectrum efficiency simultaneously. Hence, an energy efficiency and spectrum efficiency trade-off algorithm is proposed for radio resource allocation in ultra-dense heterogeneous networks based on orthogonal frequency division multiple access. The results presented in this chapter have been published in the proceedings of the IEEE Conference on Personal Indoor and Mobile Radio Communication (IEEE PIMRC 2016), the Southern Africa Telecommunications and Network Applications Conference

(SATNAC 2016) and the European Conference on Networks and Communications (EUCNC 2017). Moreover, the presented results will also be submitted for publication in the IEEE Transaction on Vehicular Technology.

Chapter 5 presents a joint radio resource allocation with adaptive modulation and coding algorithm to minimise the total transmit power across femtocells by considering the location and the service requirements of each user in the network. The simulation results are presented to show the performance and efficiency of the proposed scheme. The results presented in this chapter have been published in the proceedings of the European Conference on Networks and Communications (EUCNC 2017) and the Southern Africa Telecommunications and Network Applications Conference (SATNAC 2017). Additionally, the presented results have been submitted for publication in the Journal of Network and Computer Applications.

Chapter 6 gives the summary of this thesis, the main conclusions and a discussion of a number of possible areas for future research.

Chapter 2

Radio Resource Management for Future 5G Heterogeneous Wireless Networks: Background and Overview

2.1 Introduction

This chapter gives a review on the published research works related to 5G and radio resource management for heterogeneous wireless networks. The deployment of low-power nodes such as femtocells within the macrocell's coverage area is one of the main features of the future 5G networks [31]-[33]. In this context, femtocell network has been proposed to enhance system capacity and improve indoor coverage in a distributed manner. The deployment of ultra-dense femtocells on the coverage area of the traditional cellular networks in an unplanned manner can seriously degrade the performance of the heterogeneous networks (HetNets)

due to the resultant technical issues involved. To overcome such issues, network operators must utilise efficient radio resource management (RRM) techniques [34]. RRM algorithms are essential in these heterogeneous networks (HetNets) to ensure efficient utilisation of the radio resources of the air interface of a given cellular network. The RRM algorithms are also responsible for acceptable fairness in the sharing of radio resources among users, optimisation of energy efficiency (EE) and spectral efficiency (SE) as well as adequate provision of QoS for different users in a network.

The rest of this chapter is organised as follows: An overview of the evolution of 5G wireless networks is given in Section 2.2, followed by a review of heterogeneous networks in Section 2.3. Section 2.4 presents various standardisation for heterogeneous networks. In Section 2.5, the radio resources that are managed in OFDMA based system are explained. Section 2.6 provides detailed explanations on the technical issues in heterogeneous networks. In Section 2.7, a comprehensive review of RRM techniques in HeNets is given. Additionally, the functions of RRM algorithm and different approaches to designing RRM algorithms found in the literature are described. Optimisation tools used in solving the RRM problems are explained in Section 2.8. In Section 2.9, a concluding remark is presented.

2.2 Evolution of 5G Wireless Networks

The issue of exponential growth of mobile data traffic in an unprecedented manner according to the Cisco reports in [4] is putting more pressure on mobile network operators, who are facing continuously increasing demand for network capacity, higher data rates, energy efficiency and spectrum efficiency. On the other hand, the current 4G networks have

reached the theoretical limits and therefore, are not adequate to accommodate the above challenges [35]. Thus, a new generation of mobile communications, the fifth generation (5G) becomes indispensable. Unlike in the current fourth generation (4G), 5G will be a paradigm shift, which will include extreme base station and device densities, ultra-high carrier frequencies with massive bandwidths, and unprecedented number of antennas [36]. The schematic diagram of 5G wireless networks is shown in Fig. 2.1.

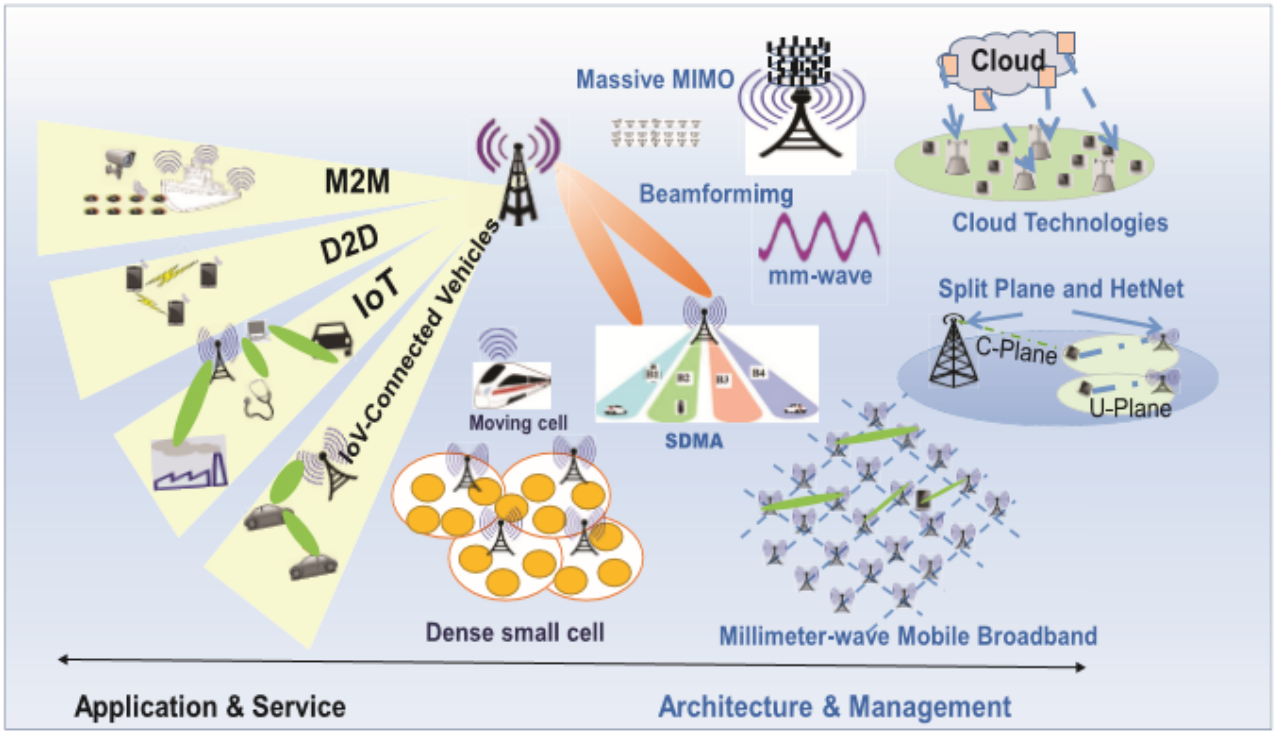

Figure 2.1: Schematic diagram of next generation 5G wireless networks [7].

Currently, the interest of the mobile industry and research community is now motivated towards the 5G evolution of the wireless broadband systems to satisfy the ever-increasing demands of the end users. It is widely assumed that 5G wireless networks must address eight

challenges that are not efficiently addressed by the current 4G i.e. higher data rate, lower end-to-end (E2E) latency, massive device connectivity, a higher battery life of systems, reduced cost, reduced energy consumption, ultra-high reliability for consistent quality of experience (QoE) provisioning [37], [38]. The ubiquitous goal of the future 5G mobile broadband systems is to achieve up to 100 times higher user data rates (1 to 10 Gb/s in dense urban areas) while supporting 100 times more connected devices. Moreover, to facilitate the vision of the future Internet, E2E latency will need to be less than 1 ms, while energy efficiency and spectrum efficiency will be 10 times higher [37]-[39].

2.2.1 Requirements of 5G Wireless Networks

Blending the different research initiatives by industries and academia, eight major requirements [5], [7], [36], [40] of next generation 5G systems are identified as shown in Fig. 2.2:

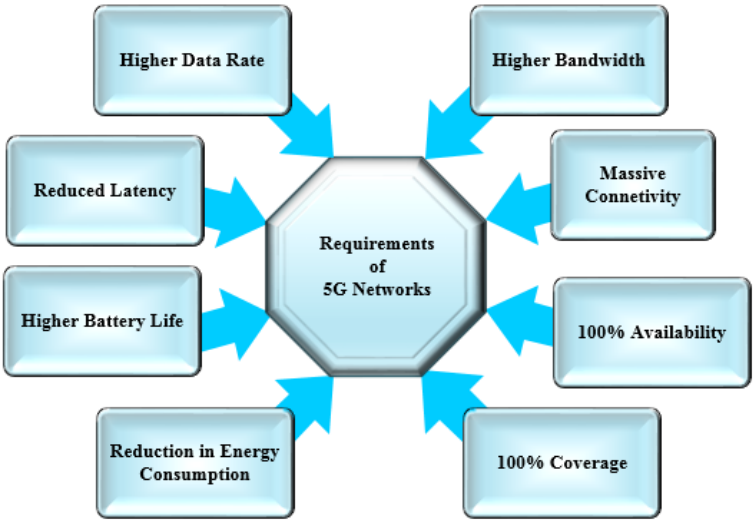

Figure 2.2: Requirements of 5G wireless networks.

- **Higher Data Rate:** $1 \sim 10$ Gbps data rates in real networks is required in 5G wireless networks. This amounts to 10 times increase from conventional long term evolution (LTE) network's theoretical peak data rate of 150 Mbps [7], [40].

- **Reduced Latency**: Lower latency of less than 1 ms latency is required in 5G wireless networks. This amount to 10 times reduction from the 10 ms round trip time in 4G wireless networks.

- **Higher Battery Life**: 5G wireless systems should have a higher battery life to support the emerging applications compared to the existing 4G systems.

- **Higher Bandwidth in Unit Area:** This is needed to enable a large number of connected devices with higher bandwidths for longer durations in a specific area [7], [40].

- **Massive Number of Connected Devices:** To realise the vision of IoT, M2M, and D2D communications, emerging 5G networks need to provide connectivity to millions of devices [7], [36], [40].

- **100% Network Availability:** 5G envisions that network should practically be always available everywhere, everytime [5], [7].

- **100% Coverage for Ubiquitous Connectivity**: 5G wireless networks need to ensure complete coverage irrespective of users' locations [7].

- **Reduction in Energy Usage:** Reduction in power consumption by devices is fundamentally important in the emerging 5G wireless networks. Development of green

technology is already being considered by standardisation bodies. This is going to be even more crucial with higher data rates and massive connectivity of 5G wireless networks [7], [36], [40].

2.2.2 Advanced Cellular Technologies in 5G

The evolution of wireless and cellular mobile network has experienced successive changes over the years, resulting in different generations of wireless networks. The emergence of each generation introduces new wireless technologies and services. Current research trends have shown that aggregation of technologies can achieve the goals of 5G. Moreover, there are three major advanced wireless technologies that have been identified in 5G [35]. The technologies are massive multiple-input multiple-output (massive MIMO), millimetre wave (mmWave), and network densification

Similarly, as noticed by Martin Cooper, the celebrated pioneer of cellular communications, the increase in wireless system capacity can be attributed to three major factors (in increasing order of impact): improvement in the link efficiency, enhancement in the use of radio spectrum, and an increase in the number of wireless infrastructure nodes. Therefore, these three factors continue to be the prevailing drivers of wireless capacity increase today [42]. For a simple visualisation of the key factors governing the performance of a cellular system, the following equation based on the Shannon capacity of an additive white Gaussian noise (AWGN) channel is considered. The upper bound on the achievable throughput τ of a user

in a cellular system is expressed as follows [35], [42]:

$$\tau \leq C = m\left(\frac{B}{u}\right)\log_2\left(1 + \frac{S}{I+N}\right). \tag{2.1}$$

In Equation (2.1), the spatial multiplexing factor m is the number of spatial streams between a base station and its associated user equipment (UE), B denotes the base station signal bandwidth, while the load factor u represents the number of users connected to the given base station. S is the signal power, while I is the interference power and N represents the noise power at the receiver. Spatial multiplexing factor can be increased by engaging a massive antennas system at the base station and UE (massive MIMO). As for the signal bandwidth, the additional spectrum can be used in order to increase the capacity (mmWave). On the other hand, the load factor u can be reduced through cell splitting, which involves deploying a larger number of base stations (network densification) [43], and making sure that user traffic is distributed as evenly as possible among all the base stations [35], [42].

The traditional cellular architecture uses an outdoor base station placed at the centre of a cell communicating with its associated mobile users, no matter whether they stay indoor or outdoor. For indoor users communicating with the outdoor base station, the signals suffer from high path loss, shadowing and multipath fading, which significantly decrease data rate, energy efficiency and spectral efficiency. This is illustrated in Fig. 2.3, where d represents the distance between the transmit and receive antennas. P_t and P_r denote the transmitted and received power respectively.

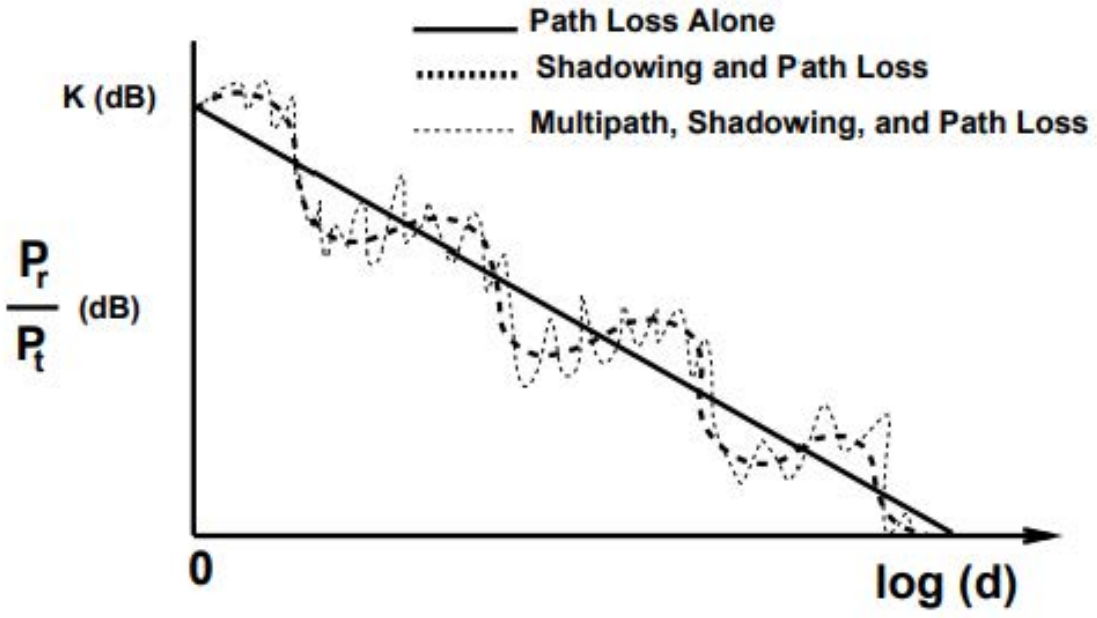

Figure 2.3: Pathloss, shadowing and multipath against distance [44].

One of the key concepts of designing the 5G cellular architecture is to separate outdoor and indoor scenarios so that propagation loss can somehow be avoided [45]. This will be assisted by massive MIMO, mmWave, and network densification technologies. These three technologies are summarised as follows:

2.2.2.1 Massive MIMO Systems

Massive MIMO is a type of multiuser MIMO in which the number of antennas at the base station is more than the number of devices per signaling resource as demonstrated in Fig. 2.4. This concept allows for orders of magnitude improvement in energy efficiency and spectral efficiency using relatively simple (linear) processing [45]-[48]. The benefits of massive MIMO systems are identified in [49] as follows:

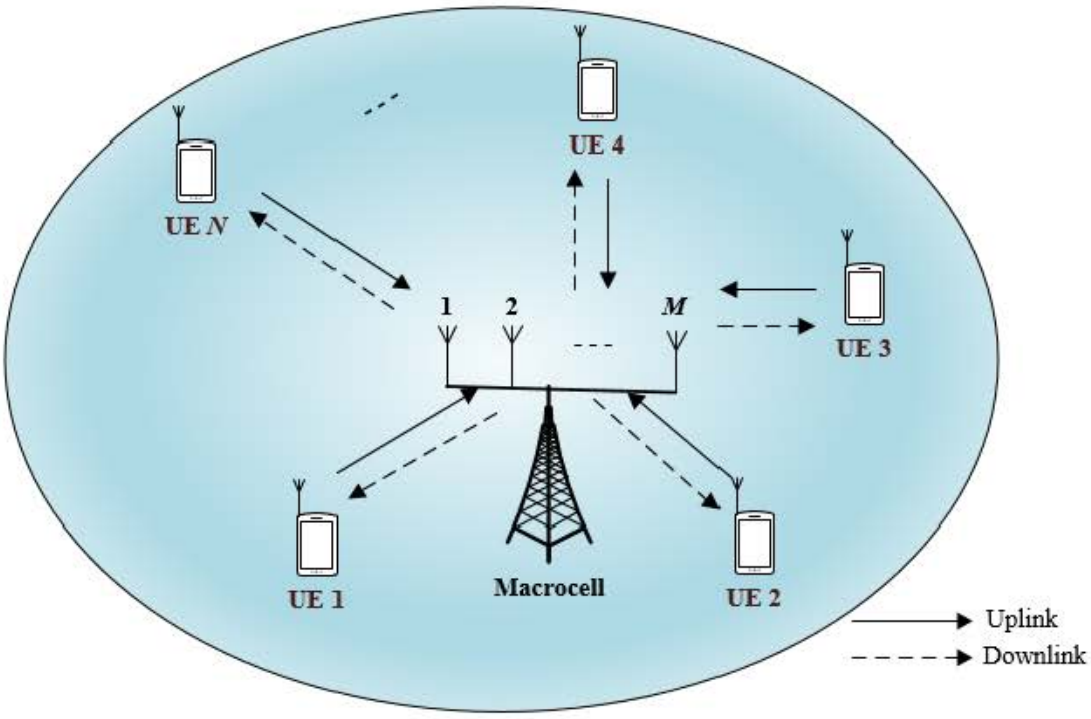

Figure 2.4: Massive MIMO technology: a multi-user MIMO technology where N UEs are serviced by a base station with $M \gg N$ antennas.

- The massive MIMO systems are based on phase-coherent but computationally very simple signal processing occurs from all the antennas at the base station.

- The increment of the capacity is at least 10 times, resulting from the aggressive spatial multiplexing, while the radiated energy efficiency is about the order of 100 times. The dependence of transmitted power for each user from the number of antennas increment in the case of perfect and estimated channel state information is considered in [50].

- The massive MIMO systems can be designed using inexpensive, low-power components, i.e., instead of expensive ultra-linear amplifiers, hundreds of low-cost milli-Watt amplifiers can be implemented.

- These systems enable remarkably reduction of latency using the minimum of large numbers and beamforming.

- Each subcarrier in the massive MIMO systems has the same channel gain, which means that the whole bandwidth can be dedicated to each channel. In that way, multiple access layer is simplified.

- These systems offer a lot of possibilities to eliminate harmful signals.

Recently, research trends in the massive MIMO systems have to be pointed out and solved before incorporating massive MIMO in the future cellular architecture [51]. For example, a large amount of channel state information (CSI) will be required in beamforming, which is not convenient for the downlink transmission. That is the reason why the massive MIMO is not feasible in the frequency division duplexing (FDD), but can be applicable in the time division duplexing (TDD) domain. As an alternative solution, limited feedback can be used [52]. In addition, massive MIMO suffers from pilot contamination and thermal noise produced by neighbouring cells [49].

2.2.2.2 Millimeter Wave Technology

Mobile communication systems today mainly use sub-3 GHz spectrum. However, as the traffic demands grow, this band is becoming increasingly crowded, while a vast amount

of spectrum in the 3-300 GHz range remains unutilised. A logical way of increasing the throughput will be through bandwidth expansion. Traditionally, due to the high propagation loss and lack of cost-effective components, among other reasons, mmWave spectrum has mostly been utilised for outdoor point-to-point backhaul links or for carrying high resolution multimedia streams for short-range applications, but not for cellular access links. Recently, the possible utilisation of this spectrum in mobile systems is introduced in [53]. After deep analysis of propagation characteristics, it was concluded that the mmWave technology can potentially provide the bandwidth required for mobile broadband applications for the next few decades and beyond. The application of mmWave beam steered fibre wireless systems for 5G indoor coverage, in terms of network architectures, key enabling devices and fibre-wireless links is presented in [54]. In [55], 28 GHz and 38 GHz frequencies are extensively studied to understand their propagation characteristics in different environments, paving the way for their use in 5G systems.

Moreover, the two principal features of the mmWave technology are identified as massive bandwidth, enabling ultra-high coverage throughput as well as very small wavelengths leading to a large number of antennas in a particular area. On the other hand, the major challenges for mmWave communications are larger path loss (especially with non-line-of-sight propagation (NLOS)), absorption/blocking of a signal by different objects in a particular environment, and very low transmission power in the current amplifiers. In this situation, large antenna arrays driven by smart beam selection algorithms have been recommended to combat signal attenuation. An approach for the implementation of mmWave technology in cellular architecture is proposed in [53]. In order to improve coverage, mmWave base stations

need to be deployed with higher density than MBSs. In general, approximately the same site-to-site distance as microcell or picocell deployment in an urban environment has been recommended. Also, transmission is based on narrow beams that suppress the interference from neighboring mmWave base stations and extend the link range by allowing substantial overlapping of cells. Unlike cellular systems that partition the geographic area into cells with each cell served by one or more base stations, the mmWave base stations form a grid with a large number of nodes to which a UE can attach. The mmWave grid eliminates the problem of poor link quality at the cell edge that is inherent in traditional cellular systems and enables high-quality equal grade of service regardless of the location of a UE. With the high density of mmWave base stations, the cost to connect every base station via a wired infrastructure can be very high. One solution to mitigate the cost (and expedite the deployment) is to allow some mmWave base stations to connect to the backhaul via other mmWave base stations.

Furthermore, due to large beamforming gains, the mmWave inter-base station backhaul link can be deployed in the same frequency as the mmWave access link. Cost-effective and low-latency solutions for wireless backhaul will be essential for supporting the envisaged densification in high capacity 5G networks. In [56], an initial analysis and solution framework for supporting an inband, point-to-multipoint, mmWave backhaul and non-line-of-sight are presented. In additionn, it is shown that an in-band solution is feasible at mmWave frequencies for tolerable losses in access capacities assuming modest hardware capabilities.

2.2.2.3 Network Densification

Prof. Webb investigated and analysed the different techniques used to enhance network capacity from the year 1950 to 2000 [43], [57]. According to his report, the wireless capacity has increased around a 10^6 fold in five decades. The breakdown of these wireless capacity gains is as follows: 15× enhancement was achieved from a wider spectrum, 5× enhancement from better medium access control (MAC) and modulation techniques, 5× enhancement by developing better coding techniques, and an astonishing 2700× enhancement through network densification. According to this data, it seems obvious that a 1000× enhancement, which is one of the visions of 5G wireless networks, is achievable in network performance. Therefore, network densification through ultra-dense heterogeneous deployments is the most attractive approach, and today's networks are moving in this direction. Currently, reduction of the cell size is one of the solutions available to mobile operators for the growing data rate demands.

On the other side, coverage is improved by deploying indoor small cells under the assumption of serving overflow traffic from macrocells when required in indoor. Data and control signals are allowed to be tunneled via the Internet owing to some changes in the access network architecture. In such a way, small cells are enabled to be deployed anywhere with the Internet. The downlink throughput performance of a network with small cells relative to a macrocell-only deployment noticed in a dense urban simulation environment is illustrated in Fig. 2.5, based on the research conducted in [42]. The performance evaluation is carried out for different small cell penetrations. It can be seen that 1000× gain is noticed with 20% penetration while serving 200 UEs per macrocell. Furthermore, to

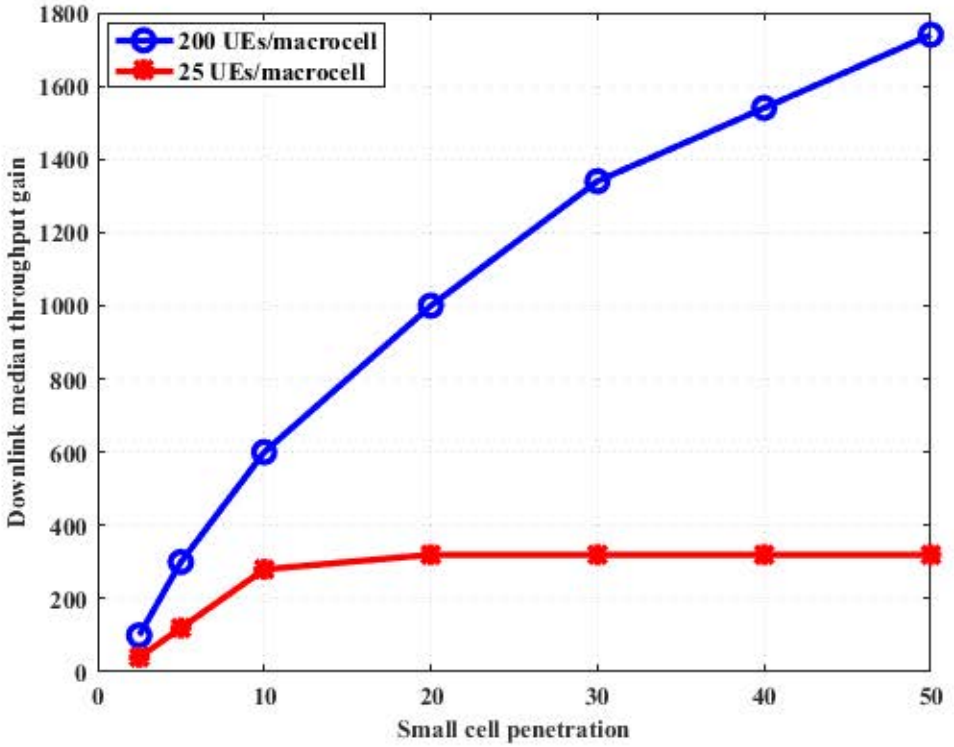

Figure 2.5: Performance gains of small cell deployments relative to a macrocell deployment [42].

provide a convenient coverage as well as improved energy efficiency and spectrum efficiency, heterogeneous networks can be considered as a promising solution [8], [10], [58]. This is also demonstrated by the research conducted in [59], where 144 small cell deployments in the coverage area of a macrocell gives 1000× capacity gains.

Thus, the heterogeneous network consisting of macrocells and small cells is presented as a new network paradigm evolution to the 5G wireless systems. In order to meet the exponentially increasing traffic demands, mobile operators are already changing their networks from the classical macrocell-only networks to the heterogeneous network, in which small cells reuse the spectrum and provide most of the capacity while macrocells provide an umbrella coverage for mobile UEs [60].

2.3 Review of Heterogeneous Networks

A promising solution for the future generation wireless networks (FGWNs) to cope with the demands for better coverage and higher data rates is the deployment of heterogeneous network, which consists of smaller, cheaper and less energy consuming base stations such as femtocells and the traditional macrocells. An HetNet is a network comprising infrastructure elements with several wireless access technologies, each of them having several capabilities, operating functionalities, constraints, and has already drawn substantial attention in the wireless industry and research community over the last few years [8], [60]. The deployment of femtocells brings the UEs nearer to the base station, therefore, HetNets can boost spatial radio resource reuse and enhance network coverage, thus allowing the users to achieve better data rates with lower energy consumption while maintaining an unbroken connectivity and seamless mobility of cellular networks [61].

The basic components of HetNet are UEs, base stations/access points (APs), and a core network (CN), with base stations and APs serving as the communication bridges for UEs [62]. A review of interference management, radio resource allocation, self-organisation, and research associated with different parts of HetNets, including deployments, system models, as well as key performance metrics are presented in [11]. The aspect of self-configuration and self-optimisation for HetHet is considered in [63]. In [20], an overview of the topology and different deployment options for HetNets, including the 3GPP LTE air interface, spectrum allocation options, and network nodes, is presented, along with the state-of-the-art enabling mechanisms for heterogeneous deployments. Moreover, significant progress in related fields by the 3GPP is presented, which includes radio frequency (RF)

requirements, backhaul, network architecture, security, and new features that will enable the heterogeneous deployment of femtocells.

2.3.1 Heterogeneous Networks Architecture

In the 3GPP LTE-Advanced standard, heterogeneous deployment has been defined as a cost-effective means to significantly enhance capacity, where performance gains can be achieved through increasing node density with low-power nodes, such as femtocells [29], [64]. Fig. 2.6

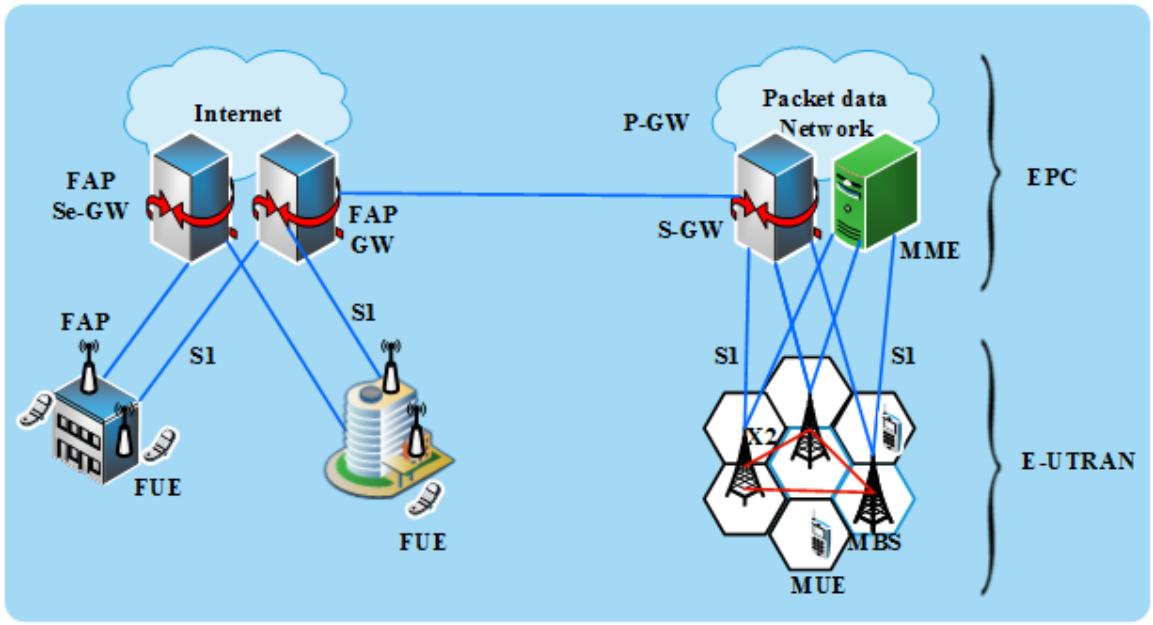

Figure 2.6: Heterogeneous architecture networks.

presents a system architecture, which consists of both macrocell and femtocell networks. The high-level system architecture for this two-tier network is in alignment with the current 3GPP LTE-Advanced standards [65]-[68] and IEEE Mobile WiMAX Release 2 systems [69]-[71]. The core network is referred to as the evolved packet core (EPC), which is divided into the serving-gateway (S-GW), the mobility management entity (MME) and the packet data

network gateway (P-GW). The S-GW is responsible for routing and forwarding user data packets, while also acting as the mobility anchor during inter-base station and inter-radio access technology (RAT) handovers. Also, S-GW can manage and store UE contexts. The MME is concerned with radio bearer management, where a radio bearer is a logical channel or a data flow established between a macrocell and a UE [72]. it allocates IP address to UEs and enforces QoS. Also, the connection management between LTE-A and other 3GPP technologies are handled by the MME. Additionally, the functions of MME includes user mobility management, tracking of idle mode UEs, bearer activation/deactivation process, paging procedure, ciphering/integrity protection, security management, user authentication, and roaming. The P-GW acts as the channel between the EPC and other IP networks such as the Internet.

The radio access network is referred to as the evolved-universal terrestrial radio access network (E-UTRAN), which consists of user equipment and base stations. The EPC and E-UTRAN are connected through the S1 interface between the S-GW and macrocells. Regarding the macrocell network, various macrocells provide multimedia services to UEs in their coverage regions. Each macrocell manages uplink and downlink transmissions among UEs. It also performs RRM functions and controls signalling in the E-UTRAN for radio access. It can be seen in Fig. 2.6 that these macrocells are connected to each other using the X2 interface for direct signalling. The connection allows the macrocells to exchange information that is related to inter-cell interference (ICI) coordination and mobility management. For the femtocell network, an FAP deployed in a building must connect to an FAP Gateway (FAP GW) to reach the mobile network through an Internet fixed broadband

connection, such as digital subscriber line (DSL), optic fibre or cable. Generally, for secure communications, the connection between the FAP and its gateway passes through an FAP Security Gateway (FAP Se-GW). The FAP Se-GW provides IP Security (IPsec) channels for the FAPs, which is also responsible for their authorisation and authentication. The IPsec channel connects each FAP to the FAP gateway (FAP GW) and other functional entities in the network. The FAP GW serves as an accumulator to aggregate the traffic of a large number of FAPs to the core network. FAP GW supports some specific RRM functionalities, such as interference management, admission control, and handover control [73].

In the physical layer of LTE-A systems, OFDMA is adopted as the enabling technology. The channel bandwidth is divided into small orthogonal physical resource blocks (PRBs) [68]. The PRB is the smallest unit of radio resource that can be allocated to UEs. Each PRB comprises twelve consecutive subcarriers as well as seven orthogonal frequency division multiplexing symbols in which each PRB occupies a spectrum of 180kHz and takes a time slot of 0.5ms. With this OFDMA technology, there is a significant reduction in the impact of frequency selective fading as a result of dividing the channel bandwidth into smaller frequency bands, with each exhibiting flat fading. Fig. 2.7 explains the LTE-A frame structure. Conversely, the LTE-A uplink uses the single carrier frequency division multiple access (SC-FDMA). The major reason for using the SC-FDMA in the uplink is to reduce the peak-to-average power ratio of UEs, consequently, reducing the power consumption of UEs. On the other hand, in the downlink, the OFDMA allows the UE to be allocated several PRBs from any part of the channel bandwidth. In LTE-A systems, a radio frame comprises 10 subframes with each consisting of two-time slots of 0.5ms. Therefore, an LTE-A subframe

has a duration of 1ms, which is one transmission time interval (TTI) and an LTE/LTE-A radio frame lasts for 10ms [12], [68].

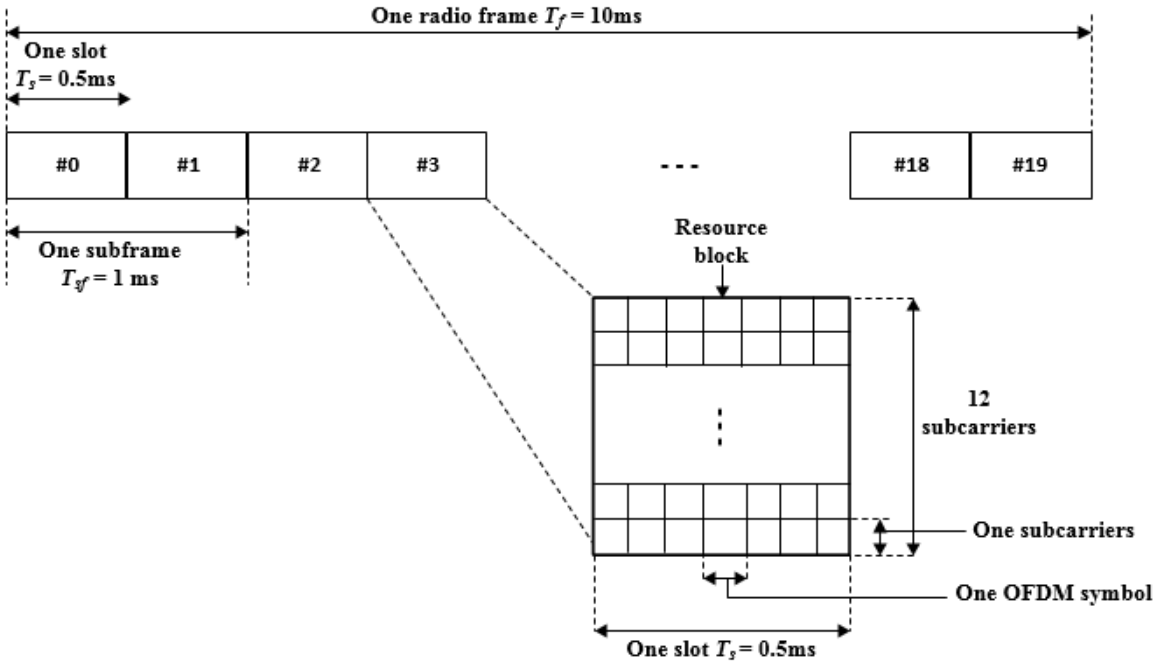

Figure 2.7: LTE-A frame structure.

2.4 Standardisation

Recently, HetNets have drawn the attention of standardisation bodies, which results in standards such as IEEE 802.16 wireless metropolitan area networks (WMANs) and 3GPP LTE-Advanced [74]. In 3GPP Release 10, different tasks for HetNets have been established to study interference coordination and mobility management of femtocells, and wireless local area network (LAN) offload. Moreover, in 3GPP Release 11, a self-organising network (SON) for HetNets has been recommended in the technical specifications and requirement and the

corresponding tasks have been clearly specified [75]. Subsequently, 3GPP Release 12 has included tasks with a focus on additional improvement for interference management and joint operation with carrier aggregation in HetNets, and there are also activities concerning carrier aggregation (CA), coordinated multi-point (CoMP) operation and reception with non-ideal backhaul, interference suppression and cancellation [76]. Additionally, a new study group has been formed on heterogeneous networks for IEEE 802.16 WMAN, where the network architectures, key characteristics, use cases, requirements, and backhaul improvements, and the simulation modelling methodologies are considered [77]. Hence, 5G will incorporate various recent technological innovations in order to achieve the best performance. Moreover, it is expected that LTE-Advanced will continue to evolve, as an integral part of 5G technologies, in a backward compatible manner to maximise the benefit from the massive economies of scale established around the 3GPP LTE/LTE-Advanced ecosystem from Release 8 to Release 12 [64], [77].

2.5 Radio Resources in OFDMA-based System

There are various radio resources that need to be efficiently allocated among the users in an OFDMA-based system [73]. These radio resources are summarised as follows:

- Transmission power: The transmit power in a subchannel can be adjusted to further increase the spectral efficiency due to the frequency-selective attenuation of the wireless channel. The capacity can be maximised provided more transmit power is applied to the frequency areas with a low attenuation relative to the other frequencies. Moreover,

as different subchannels experience different types of fading and transmit a different number of bits, the transmit power must be allocated accordingly.

- Subchannel: The frequency domain adaptation achieves higher performance gains especially in situations where the channel varies extensively over the system bandwidth. Therefore, frequency domain adaptation becomes increasingly very crucial with an increasing system bandwidth. The OFDM transmission supports such frequency-domain scheduling through the dynamic allocation of different sets of subchannels for transmission to different UEs.

- Time slot / frame: Time slot/frame can also be allocated in an OFDMA-based system. A substantial increase in spectral efficiency has been attributed to exploiting channel variations in the time domain through channel dependent scheduling. Similarly, multiplexing can also be performed in the time domain of OFDM-based systems, provided that it occurs at a multiple of the symbol rate or at the OFDM symbol rate.

- Modulation and Coding Scheme (MCS): The transmitter can send higher data rates over the subchannels using the adaptive modulation and coding (AMC), with better channel conditions to simultaneously ensure an acceptable bit error rate (BER) in all subchannels and improve the throughput of the system. The MCS used for each subchannel can also be changed at a multiple of the OFDM symbol rate. The dynamic modification of the MCS is generally referred to as link adaptation.

2.6 Technical Issues in Heterogeneous Networks

The use of HetNets has the potential to provide both the required coverage and increase the data rates of the end users. However, there are technical issues that arise due to the deployment of ultra-dense femtocells in an uncoordinated manner as stated in Section 1.5. These are summarised below:

2.6.1 Interference Management

Due to the deployment of femtocells, the cellular architecture changes and now it consists of two layers. The first layer is the conventional macrocell network while the second layer is the femtocell network. In heterogeneous networks, co-channel deployment of multiple layers of network introduces interference. Generally, there are two types of interference associated with the co-channel deployment of heterogeneous networks (HetNets) comprising macrocells and femtocells, which are cross-tier interference and co-tier interference. Cross-tier interference occurs between femtocells and macrocells and their respective UEs when they share the same set of frequency bands. Co-tier interference occurs among femtocells and their respective UEs when neighbouring femtocells reuse the same set of frequency bands [13]. Fig. 2.8 illustrates different classes of interference in HetNets. Uplink co-tier interference is caused by surrounding, co-located FUEs creating interference to nearby FAPs. Downlink co-tier interference is caused by the FAP transmissions interfering with neighbouring FUEs [78]. Uplink cross-tier interference occurs when an FUE acts as a source of interference to a macrocell. Downlink cross-tier interference is caused by an FAP transmitting close to an

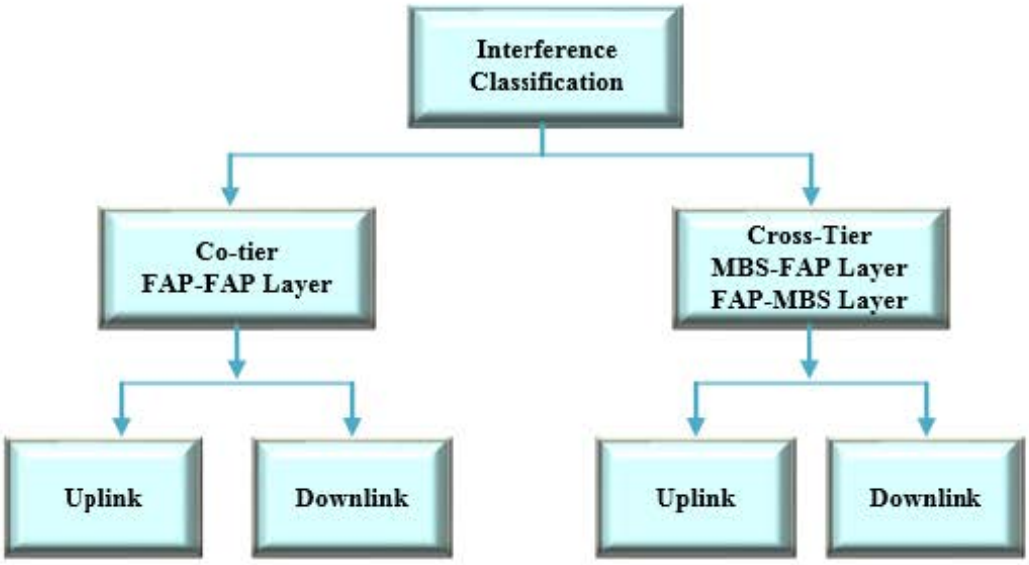

Figure 2.8: Interference classification.

MUE. Employing effective measures to avoid interference issues are the major key to the successful deployment of ultra-dense femtocells.

The possible different types of interference scenarios in two-layer networks are explained in Fig. 2.9. In scenario 1, downlink cross-tier interference occurs between an FAP and a nearby MUE, while the FAP is communicating with its attached FUE. Downlink is the channel from a base station to a user equipment. In scenario 2, uplink cross-tier interference occurs between an FUE and a neighbouring MBS, while the FUE is communicating with its serving FAP. Uplink is the channel from a user equipment to a base station. In scenario 3, downlink cross-tier interference occurs between an MBS and a nearby FUE, while the MBS is communicating with its attached MUE. In scenario 4, uplink cross-tier interference occurs between an MUE and neighbouring FAP, while the MUE is communicating with

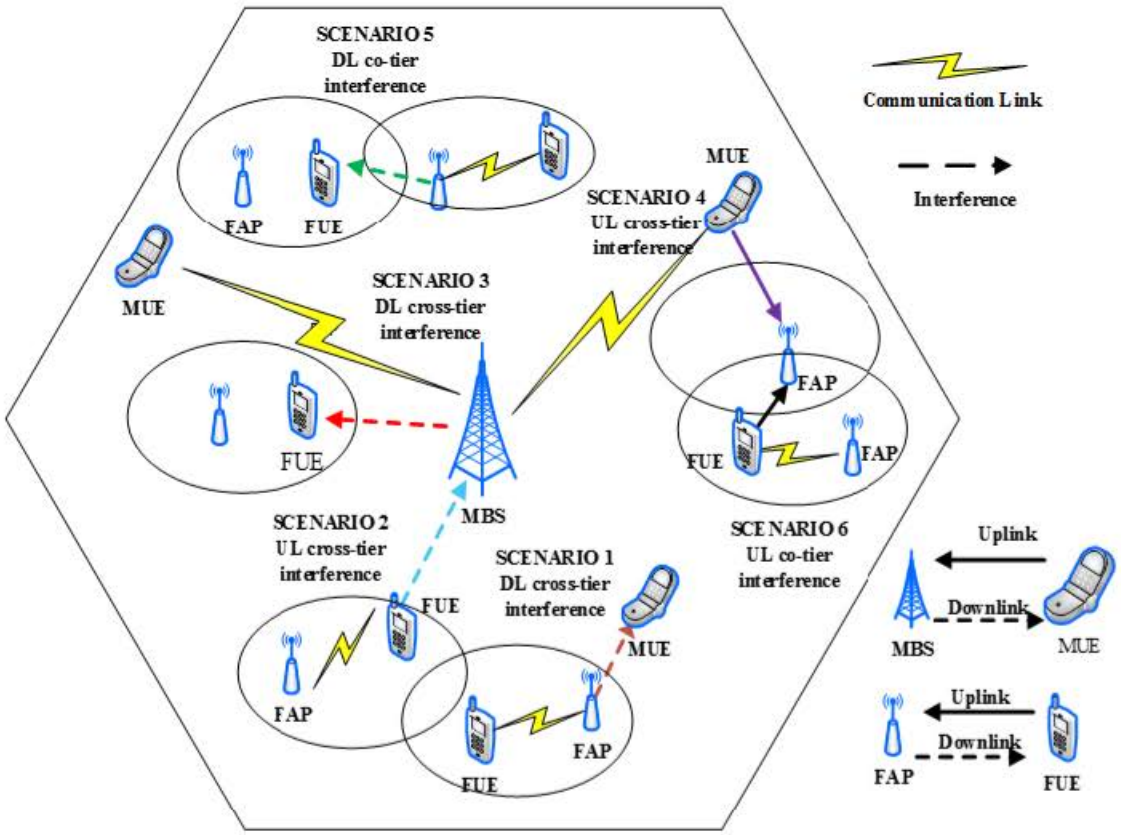

Figure 2.9: Interference scenarios in heterogeneous networks.

its serving MBS. In scenario 5, downlink co-tier interference occurs between an FAP and a nearby FUE, while the FAP is communicating with its associated FUE. In scenario 6, uplink co-tier interference occurs between an FUE and a neighbouring FAP, while the FUE is communicating with its serving FAP. Table 3.2 gives a summary of the interference scenarios in HetNets. It shows the link direction, the types of interference, the aggressor (source of interference) and the victim of interference in each scenario as illustrated in Fig. 2.9.

A comprehensive survey for interference management in cognitive femtocells was presented in [23]. Different methods such as power control [79]-[81], interference cancellation

Table 2.1: Interference scenarios in heterogeneous networks.

Scenario	Direction	Interference	Aggressor	Victim
1	Downlink	Cross-tier	FAP	MUE
2	Uplink	Cross-tier	FUE	MBS
3	Downlink	Cross-tier	MBS	FUE
4	Uplink	Cross-tier	MUE	FAP
5	Downlink	Co-tier	FAP	FUE
6	Uplink	Co-tier	FUE	FAP

[82], an adaptive FAP access scheme [83], and spectrum allocation [84], [85] have been extensively investigated to address the interference management problem in two-tier femtocell networks.

2.6.2 Spectrum Efficiency

The spectrum obtainable by any mobile operator is limited compared to the growing capacity for 5G wireless networks. Spectrum bands are conventionally allocated to base stations and UEs by a centralised radio network controller (RNC). In a femtocell network, this approach will not be applicable because of the random deployment of femtocells. Hence, distributed intelligent algorithms and architectures are required for efficient radio resource management. Dynamic spectrum access (DSA) of cognitive radio (CR) technology is a promising approach to simplify spectrum management and to improve spectrum efficiency in femtocell networks [22]. Radio resource allocation technique has been proposed in [86] to improve spectrum efficiency in LTE-A HetNets.

2.6.3 Energy Efficiency

Green communication is becoming very important in the future wireless networks. In a typical wireless cellular network, only the radio access part accounts for more than 70% of the total energy consumption [87]. It can be anticipated that the energy issue will be more serious in femtocell networks because a large number of femtocells are densely deployed. Hence, increasing the energy efficiency of femtocell radio networks is very crucial. In [88], the authors have proposed two energy-efficient power-allocation schemes for heterogeneous networks to increase the energy efficiency of the networks. In [89], the problem of energy efficiency in cellular heterogeneous networks is investigated using radio resource and power management combined with the base station ON/OFF switching. The objective is to minimise the total power consumption of the network while satisfying the quality-of-service requirements of each connected user. The case of co-existing macrocell BS, small cell BSs, and private femtocell access points (FAPs) is considered. Moreover, three different network scenarios are investigated, depending on the status of the FAPs, i.e., HetNets without FAPs, HetNets with closed FAPs, and HetNets with hybrid FAPs. A unified framework is proposed to simultaneously allocate spectrum resources to users in an energy-efficient manner and switch off redundant small cell BSs.

2.6.4 Fairness

Fairness is related to the amount of achievable throughput in a heterogeneous network. An efficient RRM algorithm is necessary to prevent a user with a favourable channel from greedily utilizing the whole radio resource and ensure at least minimum radio resource is allocated

to each user in the network. Also, the efficiency of radio resource sharing increases when deploying femtocell within macrocell networks. Moreover, efficient radio resource sharing is very important in such a two-tier network. In fact, fairness in radio resource sharing is not unique to only femtocell networks but is also applicable to macrocell networks. Since the number of femtocells would be much higher than the number of macrocells, this kind of radio resource allocation requires an efficient and fair radio resource utilisation. There are different metrics defined for fairness in wireless networks. Examples of such metrics include Jain's index, temporal fairness and utilitarian fairness. A survey of fairness in wireless networks has been presented in [90]. An example of fairness application can be found in [91], and [92].

2.6.5 Quality-of-Service

Quality-of-service management for wireless networks is a set of standards and mechanisms for ensuring high-quality performance for all applications or services. The objective of QoS management is to ensure sufficient bandwidth, control latency, jitter and reduce data loss. QoS can be managed if the number of UEs served by an FAP is small so that available radio resource would be adequate to satisfy the QoS requirements of each UE. An efficient RRM algorithm must be designed to satisfy each user QoS requirements for real time (RT), non-real time (NRT) and best effort services. Also, dynamic spectrum nature of cognitive femtocell may require good channel conditions with interference coordination, which means that in the case of dead zone coverage such as indoors, QoS cannot be guaranteed due to the variations in channel conditions. Hence, efficient radio resource management will be

necessary to address this challenge. In [93]-[95], QoS has been taken into consideration in the design of the proposed radio resource management schemes.

2.6.6 Network Complexity

Network management is another challenge in the femtocell architecture. On the one hand, the heterogeneous architecture requires complex algorithms to manage radio resources. However, the management information brings heavy overheads, which reduces network performance. A localised self-organising network management strategy is potentially an effective approach to address the challenge of network complexity. An example of low complexity algorithm is presented in [93], and [96]. Therefore, efficient RRM algorithms with self-organisation capabilities are required to tackle this challenge in the future 5G wireless networks.

For successful rollouts and commercial operations, these technical issues need to be jointly addressed to improve energy efficiency and spectrum efficiency, using the techniques of the interference coordination and cancelation and radio resource allocation optimisation (RRAO). Furthermore, the cognitive radio-based RRM and self-organising network (SON) are very important to jointly allocate and manage the scarce radio resources to mitigate interference and achieve good QoS for UEs [11], [63].

2.7 RRM Algorithms in Heterogeneous Networks

An RRM algorithm can be described as a series of tasks that control the amount of radio resources such as power, frequency or time that should be allocated to each user in a

wireless network to either maximise or minimise some network performance metrics [97]. RRM algorithm ensures optimal utilisation of the available radio resources and interference mitigation based on the QoS requirements of each user and channel information. Efficient RRM algorithms are very important to provide substantial gains in capacity, coverage, and QoS for OFDMA-based broadband wireless networks. Also, in a commercial wireless network, enhanced coverage, capacity, and QoS represent better investment return costs and better services. For the end users, this should provide enhanced services, higher fairness and better QoS levels with ubiquitous availability at possibly reduced prices. Therefore, it is of the utmost importance to study novel methods to optimise RRM algorithms that deal with the radio resources in OFDMA-based heterogeneous networks.

2.7.1 Classification of RRM Algorithms

There are three classifications of RRM algorithms considering the processing requirements, which are centralised, semi-distributed and fully-distributed [12], [97].

- In the centralised method, each network has a central entity, which executes RRM functions. This central entity needs global knowledge of the channel state information (CSI) and interference for all base stations and UEs in the network. Then, it gathers information from the serving base stations. The central entity assigns the required amount of radio resources to each UE in the network, depending on the information obtained. This method can yield optimal RRA for cellular networks, but the amount of signaling may be very high. Therefore, centralised methods are only feasible for

small-sized femtocell networks. An example of a centralised algorithm can be found in [98].

- In the semi-distributed method, a central entity performs specific global RRM functions, such as the collection of information about traffic and channel, while local RRM functions, like packet scheduling, are distributed to macrocells and femtocells. The RRM algorithms require a limited global knowledge of network link conditions. This approach could be suitable for moderately large networks. Also, in the semi-distributed approach, the RRM algorithm provides each radio resource-allocating node the ability to allocate radio resources based on local channel conditions. The authors in [99] adopt the semi-distributed approach in the design of radio resource allocation algorithm for a dense femtocell deployment.

- In the fully-distributed RRM schemes, a central entity is not required. Both macrocells and femtocells determine the radio resource allocation policies among the associated MUEs and FUEs by themselves. This method is attractive because of its low signaling overhead and low implementation complexity. This approach is more appropriate for large-sized femtocell networks [12], [97]. A fully distributed algorithm is developed in [100] for power allocation in heterogeneous networks.

2.7.2 Functions of RRM

RRM algorithms have different functions such as packet scheduling, link adaptation, radio resource allocation among macrocells and small cells, radio admission control, and handover management [12], [14], [101], which are summarised as follows:

2.7.2.1 Packet Scheduling:

Packet scheduling is one of the major RRM functions at the medium access control (MAC) layer of LTE-A systems. It performs PRB allocation among UEs with the objective of maximising the cell throughput and spectral efficiency. The decision regarding scheduling is based on the channel quality indicator (CQI), the QoS requirement of each UE, or channel state information (CSI) of the UEs, and the interference level. Hence, in heterogeneous networks, packet scheduling algorithms can be incorporated into femtocells to allocate PRBs to their connected UEs. The most common scheduling algorithms are the following:

- Round-robin scheduler: This scheduler is fairness conscious and user-centric, which allocates the same amount of PRB to UEs in turn. Traditional round-robin scheduler does not guarantee an adequate level of QoS since, it neither utilises the queue state nor exploits the channel variability in the scheduling policy, thus sacrificing the inherent achievable network capacity and multi-user diversity [90], [92], [97].

- Max-SINR scheduler: This scheduler is a network-centric scheduler and it is the best in terms of total capacity maximisation at the expense of fairness, as it fully exploits multi-user diversity inherent in the network [97].

- Proportional-fair scheduler: This scheduler offers an intermediate solution that realises the multi-user diversity gains while retaining fairness across UEs. At any transmit node, this scheduler assigns a subchannel to the UE that maximises the ratio of its achievable rate on that subchannel to its exponentially weighted average rate [90], [97].

- Opportunistic scheduler: Opportunistic schedulers take into account information such as the channel quality in terms of QoS metrics that allows the scheduler to find the proper transmission resources for each user. It allocates radio resources based on the flow of QoS. A survey of opportunistic scheduling in wireless communication is presented in [102]

2.7.2.2 Link Adaptation

Link adaptation is another crucial RRM function in the MAC layer to realise higher user throughput performance with a given target block error rate (BLER) [103]. This approach is also regarded as bit loading [104]. It uses the frequency and time diversities in order to assign the most appropriate modulation and coding scheme to each subchannel according to its signal-to-noise ratio (SINR) threshold. The functions of link adaptation include transmission power control and adaptive modulation and coding (AMC). In AMC, a higher order modulation and coding scheme is allocated to UEs with good channel quality. The transmission power coordination typically works jointly with AMC to enhance cell throughput.

2.7.2.3 Joint Subcarrier and Power Allocation

Joint subcarrier and power allocation takes place at the MAC layer and allocation is performed among UEs according to the location of the base station and its attached UEs [103]. The objective is to maximise cell throughput while considering the QoS requirements of each user, channel quality indicator of UEs and interference levels [14]. For instance, in Fig. 2.10, there are two FAPs, FAP1 and FAP 2, serving two UEs each.

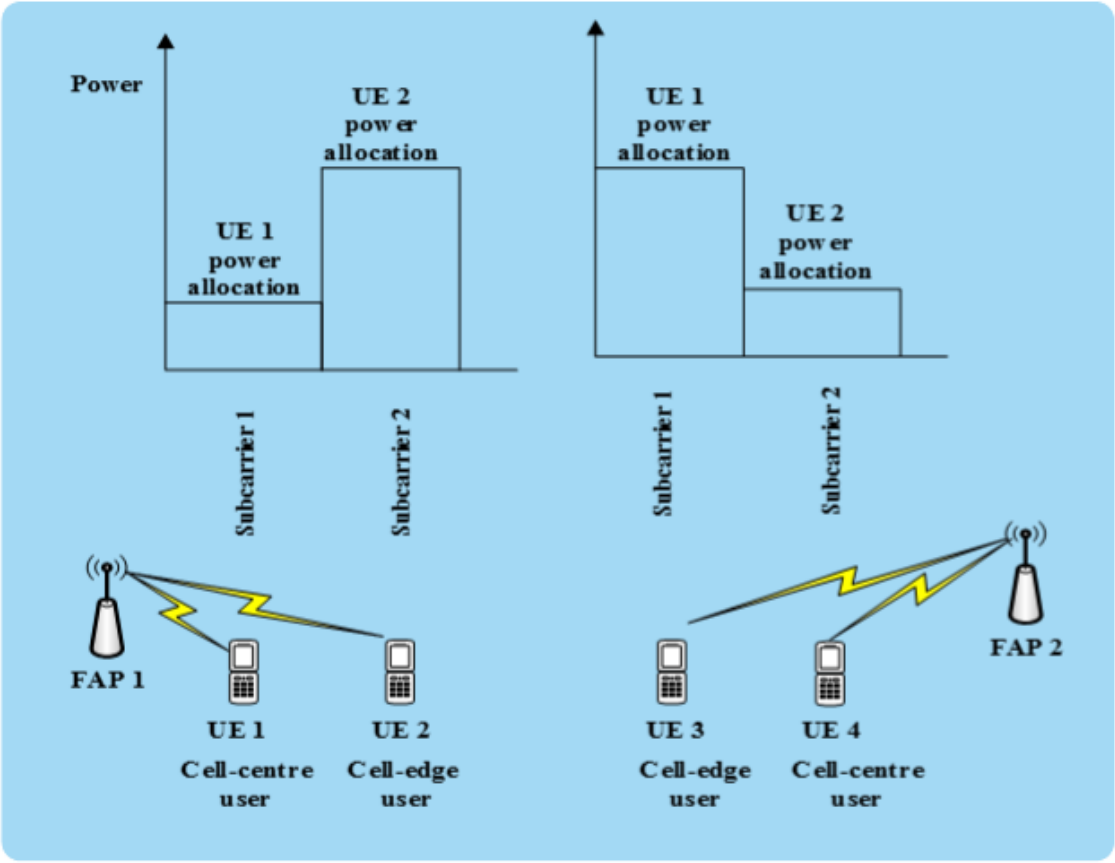

Figure 2.10: Subcarrier and power allocation [103]

FAP 1 is serving UE 1 and UE 2, while FAP 2 is serving UE 3 and UE 4. UE 1 and UE 4 are cell-centre users because they are closer to their serving FAPs. UE 2 and UE 3 are cell-edge users because they are far away from their serving FAPs. More power can be allocated to

the cell-edge users (UE 2 and UE 3), while less power can be allocated to the cell-centre users (UE 1 and UE 4). Subcarrier 1 can be allocated simultaneously to UE1 and UE 3 while subcarrier 2 can be allocated simultaneously to UE 2 and UE 4 to avoid interference.

2.7.2.4 Radio Admission Control and Handover Management

The radio admission control entity can be found at the radio resource control entity in Layer 3 of the LTE-A protocol stack, which decides whether a new user request should be accepted. The decision is made based on the QoS requirements of the requesting user and the availability of radio resources [12]. In order to admit a user into a network, the available radio resources must be enough to satisfy the QoS requirements of all users. Decision making can also be based on whether the user is a new user coming from the cell itself or a handover user from a neighbouring cell. Handover management is concerned with user mobility and it is performed at the radio resource control (RRC) layer.

2.7.3 Existing RRM Algorithms in Heterogeneous Networks

There are different approaches that can be adopted in the design of RRM algorithms such as radius reduction and frequency scheduling [105], graph theory [86], [106], frequency reuse [107], [108], game theory [95], [109], femtocell clustering [14], [110], learning [111], [112], power minimisation approach [103] and the CR approach [18], [31]. A survey of different approaches can be found in [12]. In this thesis, we concentrate on CR approach based on self-organisation capabilities. A survey of self-organisation in future cellular networks is presented in [113]. The RRM problem in the CR-based femtocell networks has been investigated in

the literature [18], [31], [115]-[119]. The CR technology is an emerging technology that plays an important role in improving the efficiency of spectrum access in femtocell networks [21] as stated in Section 1.4. The cognitive capabilities can further enhance the wireless resource utilisation, spectrum efficiency, and interference mitigation by interference sensing, efficient spectrum sensing, and adaptive transmission [120]. Therefore, femtocell combined with CR can further enhance the system performance [121], [122].

The authors in [18] address the problem of downlink resource scheduling and power allocation for hybrid access femtocells. The proposed algorithm falls into the category of the fully distributed (decentralised) scheme. They introduced a refund mechanism by giving incentive to FAPs to serve MUEs suffering from low SINR to enhance overall performance. The goal of the work is to guarantee QoS for users while allowing spectrum sharing between MBS and the underlying FAPs. In the work, it is assumed that the unknown MBS-MUE wireless channel undergoes Rayleigh fading and, can be modelled by Markov processes. Also, two basic and simple models are considered: 1st order autoregressive (AR) channel model; and the finite state Markov model (FSMM). They employ the methods of dynamic programming and Hungarian algorithm to solve the formulated optimisation problem.

The study in [31] proposes a co-channel interference management technique for downlink transmission in macrocell-femtocell networks based on macrocell user tracking. The work considers multipath channel model. A new method is proposed for robust spectrum sharing, performed by the co-channel femtocell in order to become aware of the current and future scheduling opportunities. The femtocell, in addition to listening to the macrocell downlink signal and sensing the uplink signal to discover spectrum opportunities, is enabled to receive

the nearby macrocell users' uplink signal and to predict future resource preferences using the channel-dependent scheduling process in LTE. It is demonstrated that macrocell users can exist with a femtocell in co-channel deployment as long as the femtocell enhances its cognitive capabilities by predicting the macrocell user's future resources. Enhanced sensing and detection by prediction is required for improved performance when the macrocell is heavily loaded. The QoS at the femtocell user's side and the overhead at the femtocell radio link control (RLC) sublayer are also presented. Furthermore, it is demonstrated that femtocells are able to avoid utilising the subcarriers that have been allocated to the victim macrocell user.

The dynamic spectrum allocation for the downlink OFDMA-based hybrid access cognitive femtocell networks is studied in [114]. Perfect spectrum sensing is assumed in this study. Also, the OFDMA-based downlink transmission is considered. In the proposed method, the MBS allocates a portion of subchannels to a femtocell to spur the femtocell to serve the macrocell users (MUs). Then, the femtocell allocates the subchannels and power to maximise the femtocell network utility, whereas the throughput of the served MUs is guaranteed. Moreover, a sum-utility maximisation problem is formulated for resource allocation and the dual decomposition method is adopted to derive the optimal solution.

Furthermore, it is noted that cognitive femtocells working jointly with OFDMA can further improve cellular capacity, coverage and offload traffic from the existing macrocells through radio resource allocation and interference mitigation. In [115], the authors propose a radio resource allocation technique for OFDMA-based cognitive femtocells. The target of

the algorithm is to maximise the total capacity of all femtocell users under certain QoS and cotier/cross-tier interference constraints with imperfect channel sensing.

In [116], the radio resource allocation problem in a two-tier OFDMA-based heterogeneous cellular network is studied, where the femtocells with closed access strategy are equipped with the cognitive radio (CR) functionalities to sense the radio environment so that they can share subchannels with the macrocells without generating excessive interference to the macrocell users, which are in the coverage of the femtocells. The problem is formulated as an optimisation problem and solved using barrier and Newton methods.

A distributed resource allocation that consists of subchannel- and power-level allocation in the uplink of the two-tier cognitive femtocell network (CFN) comprising a conventional macrocell and multiple femtocells using underlay spectrum access is proposed in [117]. The distributed radio resource allocation problem is addressed via an optimisation problem, in which they maximise the uplink sum rate under constraints of cross-tier and co-tier interference while maintaining the average delay requirement for cognitive femtocell users.

Apart from the SE maximisation, there has also been a growing interest for joint EE and SE for femtocell networks due to the rising energy cost and increasing environmental awareness. Some works have considered joint EE and SE such as [123]-[126]. In [123], the joint power and channel allocation problem in two-tier OFDMA femtocell networks is investigated based on a multi objective approach with consideration for energy efficiency, spectral efficiency, and power consumption. A non-dominated sorting genetic algorithm (NSGA-II) is used to solve the formuated multi objective optimisation problem. The authors in [124] explore the potential cooperation gains through a cooperative bargaining game to

address the issues relating to mitigating interference and saving energy, thus improving both energy efficiency and spectrum efficiency. The current optimization and trade-offs of energy efficiency and spectrum efficiency are investigated, and the basics of cooperative game theory are introduced. Moreover, two applications are studied for the cases of dedicated and co-channel deployment including cooperative relay with spectrum leasing and cooperative capacity offload. Furthermore, in [125] the performance analysis of two-tier femtocell networks with partially open channels are conducted. A Markov chain is developed to model the channel access in the femtocell network and the performance metrics is derived in terms of the blocking probabilities. Based on the obtained stationary state probabilities by the developed Markov chain models, spectrum and energy efficiency is analysed under different scenarios including number of femtocells in a macrocell network, average number of users, and number of open channels in a femtocell. Also, the authors in [126] provide an analytical framework for evaluating energy efficiency and spectrum efficiency for heterogeneous cellular networks.

2.8 Optimisation Tools for Solving RRM Problems

There are various objectives of RRM schemes such as enhanced coverage, better capacity, lower energy consumption (green radio), higher fairness, better utilisation of the radio resources and improved QoS. Most of the RRM techniques can be formulated as RRA optimisation problems, with an objective function that must be maximised or minimised and optimisation constraints that correspond to physical limitations in the network. Also, some of these optimisation problems can be multi-objective optimisation. Multi-objective

optimisation is the optimisation problem that involves more than one objective function to be optimised simultaneously and it is concerned with the minimisation/maximisation of a vector of objectives subjects to a number of inequality and/or equality constraints. The procedure for the formulation of different optimisation problems can be summarised into four basic steps as follows [127]:

- **A clear statement of each user's requirements in the network:** It is very important to account for the requirements of all users in the formulation of a problem. This will guide the decisions to be made and the choice of metrics by which such decisions are measured. Decisions need to be made in order to satisfy the requirements of all users while considering conditions such as channel quality indicator and interference levels.

- **Identification of the decision variables:** Once the requirements of all users have been identified, the next step is to identify the variables that measure the amounts of radio resource to be given to each user. This can be set as threshold values.

- **Definition of the objective function:** Once the demand of all users and the decision variables have been identified, the next step is to define the objective function of the RRA problem. An example of an objective function includes throughput maximisation and power minimisation.

- **Inclusion and definition of a set of constraints:** The constraints need to be specified in order for the optimisation model to find the optimal operating rules which reflect the restrictions in the network.

Furthermore, in order to solve these RRA problems, different optimisation tools can be employed. Some of these optimisation tools are more suitable than the others. The choice of any optimisation tools depends on some factors such as the formulation of the optimisation problem itself, the nature of the variables involved, the possibility of linearisation of the objective function and the possibility of relaxation of the optimisation constraints. Moreover, for the same RRM problems, different optimisation formulations lead to different RRA policies. When it is very difficult to find the optimal solution of an optimisation problem, some sub-optimal methods can be adopted. some of the most common methods found in the literature are listed below:

- **Relaxation of constraints:** The concept of this method is to relax some of the constraints in order to make the problem easy to provide a solution. An example is to relax the integer constraint on the subchannel assignments so that each subchannel can be allocated to multiple different UEs at the same time. Therefore, the optimisation problems can be transformed into linear programming (LP) problems, which can be solved easily and efficiently. However, it must be noted that after solving the relaxed problem, the relaxed solution has to be re-evaluated because only the integer solutions are feasible from the network's point of view [73]. The authors in [115] use the approach of relaxation of constraints to make the formulated problem tractable.

- **Problem splitting:** This method uses the idea of "divide to conquer", i.e. splitting the complex problem into two or more simpler sub-problems so that a sub-optimal solution close enough or an approximation to the optimal solution can be found. This

approach is commonly used in the RRA schemes. This method is used in [116] to split the formulated problem into two so that it can be easy to solve.

A great variety of optimisation tools exists in the literature for solving RRM problems. These optimisation tools are based on several approaches. A brief description of some common optimisation tools is presented below:

- **Convex optimisation:** This approach is one of the most common tools used to develop RRM algorithms for the heterogeneous networks. Convex optimisation is a specific class of mathematical optimisation problems such as semidefinite programs and second-order cone programs. The convexity makes an optimization problem easier to solve, and first-order conditions are sufficient conditions for optimality. The main advantage of convex optimisation is that the optimisation problem can be solved, efficiently, and very reliably using interior-point methods or other special methods for convex optimisation. Also, the associated dual problem often has an interesting interpretation in terms of the original problem, and leads to an efficient or distributed method for solving it. For instance, the Lagrangian's dual decomposition method, which is a classical tool for nonlinear optimisation problems with constraints, was utilised in [115] to solve the formulated RRM problem.

- **The Simplex approach:** This is an efficient tool for solving an important class of optimisation problems known as linear programming (LP), in which the objective function and all constraints are linear. In [103], LP was applied in a multi-cell system

in order to solve a linear programming problem that minimizes the total transmit power of the network while guaranteeing the QoS of the users.

- **The Sequential Quadratic Programming (SQP)**: This optimisation tool is used to solve non linear constrained optimisation problems. It has attracted much attention in designing efficient RRA schemes. The authors in [128] adopt this tool to design an RRA policy with the aim of bit rate maximisation using power allocation algorithms.

- **Utility Theory:** This theory offers the flexible means to formulate quantitatively the relationship between the user experience and various network performance metrics. Utility functions are able to capture the satisfaction level of users for a given radio resource assignment [129], [130]. This theory has been used extensively in the field of economics but has been drawing the attention of researchers in the area of wireless and communication networks recently.

- **Branch and Bound (BnB):** This optimisation tool is developed for solving combinatorial optimisation problems. The BnB method combines a list of all possible solutions by means of "branches", and the process of "pruning" some of them. The BnB technique is not an approximating procedure but it is a deterministic optimisation approach that finds the optimal solution. In [131], a BnB method was applied in a heterogeneous network to solve the power minimisation problem.

- **Heuristics:** This is an experience-based technique for solving an optimisation problem, which is used to find sub-optimal solutions very close to the optimal solution

with lower complexity than other traditional combinatorial optimisation techniques. It has been extensively used by many works in the literature such as [132].

- **Probabilistic optimisation:** An example of this approach is stochastic programming, which has been used in [133], [134] to solve an optimisation proplem. A survey of stochastic geometry models was discussed in [20] for single-tier and multi-tier cognitive cellular networks, where a taxonomy model was presented [10]. Also, this class of optimisation tool comprises genetic algorithm (GA). GA is a well-known stochastic search method based on the Charles Darwin's theory of natural selection. GA, unlike other conventional methods of optimisation (such as random search, enumerative schemes, and gradient-based method) is an effective tool for solving combinatorial optimisation problems. GA is effective because of its capability to utilise favourable features of previous solutions and successively generate better solutions. Moreover, another advantage of GA is that it is not compulsory to know if the objective function is differentiable or continuous, and it is very easy to implement. An example of the application of GA can be found in [123], [135].

- **The Hungarian method:** This is a traditional tool for solving allocation problems. The allocation problem is formulated as an optimisation to minimise the total costs when a cost matrix is defined [136]. Some works have employed the Hungarian method as an optimisation tool in the development of an RRM scheme, such as the work in [137].

In this thesis, convex optimisation is used to solve the formulated optimisation problems presented in chapters 3 and 4. The proof of convexity of the formulated problems is established based on [138]. In chapter 5, the formulated optimization problem is reformulated using a reformulated-linearisation technique that is based on BnB optimization tool.

2.9 Conclusion

The evolution of the cellular and wireless networks is leading to 5G wireless networks. The basic requirements of 5G wireless systems are described. Also, the most common advanced cellular technologies in 5G are presented. A brief review of heterogeneous networks and its network architecture are given. The activities of the standardisation such as LTE-A are described. Additionally, the radio resources to be allocated in the OFDMA-based system have been presented. There are several technical challenges, which must be addressed by the wireless network operators in order to make the femtocell able to have a positive impact on the end users in terms of improving the energy efficiency, spectrum efficiency, fairness and QoS performance. These major challenges have been described to enable a clear view of the main requirements of the 5G wireless technology. From a technical viewpoint, the main focus of this thesis is to design and implement RRM algorithms for improving cognitive femtocell coexistence in two tier heterogeneous networks. Therefore, some existing RRM algorithms have been presented. Furthermore, The classifications and functions of RRM algorithms have been described as well as some common optimisation tools found in the literature for solving the RRM problems.

Chapter 3

Self-Organising Radio Resource Management for Future Generation Heterogeneous Wireless Networks

3.1 Introduction

Future generation heterogeneous wireless networks will consist of ultra-dense small cell deployments. Recently, it has been revealed that the existing heterogeneous networks (HetNets) comprising indoor small cells such as femtocells overlaying the conventional macrocells will not be able to satisfy the upcoming traffic demands in the next few years [43], [139]. Therefore, the ultra-dense heterogeneous network (ultra-dense HetNet), which is one of the key techniques to address the traffic explosion and meet the users' various demands,

has been referred to by mobile operators and research community as an efficient and cost-effective solution for providing indoor coverage and network capacity by 2020 [36], [140]-[143]. Fig. 3.1 shows how the conventional homogeneous networks evolved to the existing HetNets, and in turn to the future ultra-dense HetNets. However, the unplanned and ultra-dense deployment of femtocells that adopt co-channel radio resource assignment may lead to severe interference problem, unfairness in resource sharing and throughput degradation considering different users with heterogeneous services, if radio resources are not efficiently managed. Hence, efficient radio resource management (RRM) techniques with self-organising capabilities are crucial to autonomously mitigate cross-tier and co-tier interference, ensure fairness in resource sharing among users and guarantee an adequate level of QoS for both macrocell and femtocell users in the network.

Figure 3.1: The evolution of networks.

3.1.1 Related Work

The self-organising network (SON) is proposed to achieve the potential high performance gain in ultra-dense HetNets [144]. Recently, cognitive radio (CR) technology is integrated into femtocells to improve the efficiency of spectrum access and mitigate interference in the 5G wireless networks. CR enabled femtocells have capabilities to perform self-organisation roles

such as sensing the radio environment, making decisions based on the sensed information, and then, intelligently allocating the radio resources [23], [31],[115]. There are some existing works in the literature solving the problems of interference mitigation and radio resource allocation (RRA), which is based on cognitive radio technology such as [109], and [115] in HetNets. The authors in [109] study the subchannel allocation problem for hybrid/underlay cognitive femtocell networks in order to enhance the performance of the networks. The subchannel allocation problem is formulated as a coalition formulation game among users and solved based on the concept of a recursive core. In [115], the authors propose a dynamic RRA for a cognitive femtocell that adopts the hybrid access mode. The algorithm is based on a centralised orthogonal frequency division multiple access (OFDMA) HetNet architecture to maximise the throughput of femtocell users. The RRA problem is formulated as a sum-utility maximisation problem and solved using the dual decomposition method. In these works, perfect spectrum sensing is assumed, which is difficult to achieve as a result of rapid changes in the radio environments.

In addition, some works have studied joint subchannel and power allocation for cognitive femtocell networks using power control based approach [145], [146], adaptive management based method [147], reinforcement learning based technique [148], and game theory approach [149] but the aspect of user satisfaction needs further investigation. Moreover, some RRM algorithms have considered RRA for user's satisfaction in ultra-dense HetNets [150]-[152]. In [150], the authors study the downlink RRA to improve user experience in ultra-dense small cell networks based on multi-dimensional heterogeneities in terms of spectrum, cells, and user requirements and propose a concurrent best response iterative algorithm that can guarantee

the convergence to Nash equilibrium. The aspect of user-centric QoS-aware interference coordination is investigated in [151] for ultra-dense cellular networks to guarantee the desired signal quality for each user by avoiding the major inter-cell interference (ICI) and allocate resource with priorities to each user according to its QoS requirements. In [152], the authors propose a novel scheme for dynamic RRA for a cluster of heavily overlapped small cells to avoid interference. In all these algorithms, the aspect of incorporating self-organising capability based on CR technology has not been considered. Some authors such as in [115], and [153] considered imperfect spectrum sensing in cognitive femtocell networks to mitigate interference and enhance throughput of femtocell users but these works cannot be directly applied to network with massive femtocells because the authors assume co-tier interference to be negligible, while the aspect of users with different QoS requirements has not been considered.

3.1.2 Contributions and Organisation

Different from the existing works, in this chapter, a self-organising radio resource management (SORRM) algorithm for ultra-dense femtocell deployments based on CR technology is proposed. The proposed SORRM algorithm put into consideration imperfect spectrum sensing and users with heterogeneous services during the downlink transmission. The objective is to maximise the overall throughput of femtocell users by considering the location and the service requirement of each user in the network. The location of each user is assumed to be within the current cell. Also, the effect of shadowing, path loss, multipath fading on

the received signal is considered. The contributions of this chapter can be summarised as follows:

- The throughput maximisation problem for joint RRA (subchannel and power) in the downlink of an OFDMA-based HetNet is formulated as an optimisation problem subject to the constraints of maximum transmit power, QoS requirement, fairness, cross-tier and co-tier interference.

- The formulated optimisation problem belongs to the class of mixed integer non-linear programming (MINLP), which is non-deterministic polynomial-time (NP)-hard. However, in order to find the optimal solution, the Lagrangian dual decomposition (LDD) method is employed to get an approximately optimal solution.

- Based on the obtained solution, an RRM algorithm termed self-organising radio resource management (SORRM) algorithm is proposed. The algorithm has the potential of mitigating the cross-tier and co-tier interference and providing adequate QoS to femtocell users in terms of throughput and fairness in sharing radio resource in the 5G wireless networks.

- The convergence of the proposed algorithm to a near optimal value is demonstrated through extensive simulations.

The rest of this chapter is organised as follows: Section 3.2 presents the list of important notations used in this chapter. Section 3.3 discusses the system model such as signal-to-interference-plus-noise ratio (SINR), achievable rate and interference model. In Section 3.4, the optimisation problem formulation for joint power and subchannel allocation is described.

Section 3.5 presents the solution to the formulated problem for throughput maximisation. In Section 3.6, the proposed self-organising radio resource management algorithm and its computational complexity are described. Section 3.7 discusses the obtained simulation results. Finally, Section 3.8 concludes this chapter.

3.2 Notations

The list of notations presented in Table 3.1 consists of the most relevant notations used in this chapter.

3.3 System Model

In this chapter, the OFDMA-based downlink communication of an HetNet is considered. Let $S_n = \{1, 2, ...N\}$, and $\mathcal{U} = \{1, 2, ...U\}$ represent the set of all femto access points (FAPs) and femtocell user equipment (FUEs) respectively. N is the total number of cognitive FAPs, which are randomly and ultra-densely deployed in the coverage area of a macro base station (MBS) named M. U is the total number of FUEs in the network. $\mathcal{J} = \{1, 2, ...J\}$ denotes the set of all macro user equipment (MUEs), where J is the total number of MUEs served by the MBS in the network. Also, a cognitive FAP n serves a total number of U_n FUEs in the network. Fig. 3.2 illustrates the heterogeneous deployment of ultra-dense FAPs overlaid on a traditional MBS. The bigger circle represents the coverage area of the MBS while each smaller circle represents the coverage area of each FAP in the network. Also, each FAP adopts a co-channel resource assignment. It is assumed that both the MBS and cognitive

Table 3.1: Summary of notations I.

Symbol	Description
N	Total number of cognitive FAPs
J	Total number of MUEs
U	Total number of FUEs
U_1	Total number of Real-time FUEs
U_2	Total number of Non-real-time and best effort FUEs
S_n	Set of all FAPs
$\mathcal{U}$	Set of all FUEs
$\mathcal{U}_\mathcal{A}$	Set of real-time FUEs
$\mathcal{U}_\mathcal{B}$	Set of non-real-time and best effort FUEs
$\gamma_{n,u,k}$	Signal-to-interference-plus-noise ratio of the received signal of an FUE from an FAP
$h^{FF}_{n,u,k}$	Channel gain between an FAP and its attached FUE
$h^{MF}_{M,j,u,k}$	Channel gain from an MBS servicing an MUE
β	Signal-to-noise ratio gap for an uncoded quadrature amplitude modulation
σ^2	Additive white Gaussian noise (AWGN)
$p^M_{j,k}$	Transmit power of an MBS M servicing an MUE j on subchannel k.
$p_{n,u,k}$	Required transmit power of an FAP n to an FUE u on subchannel k
$p_{z,w,k}$	Transmit power applied by an FAP $z \neq n$ to an FUE $w \neq u$ on subchannel k
$h^{FF}_{n,u,w,k}$	Channel gain between FAP n serving FUE u to a nearby FUE w on subchannel k
$R_{n,u,k}$	Achievable transmission rate of an FUE u attached to an FAP n on subchannel k
$I^{MF}_{n,u,k,q}$	The sum of OOB interference power introduced into an MUE's subchannel
$I^{FF}_{n,u,k,q}$	The sum of OOB interference power introduced into a nearby FUE's subchannel
$g^{MF}_{n,u,k,q}$	The power gain from an FAP to an MUE's subchannel
$g^{FF}_{n,u,k,q}$	The power gain from an FAP to an FUE's subchannel
$\tilde{I}^{MF}_{n,u,k}$	Downlink cross-tier interference due to OOB emissions
$\tilde{I}^{FF}_{n,u,k}$	Downlink co-tier interference due to OOB emissions
$\varphi(f)$	Power spectrum density of the OFDM signal on subchannel k
Pr^{fa}_k	Probability of false alarm error
Pr^{md}_k	Probability of mis-detection error
Pr^{j}_k	Probability of MUE j's occupation in a subchannel k
$\mathcal{K}_o$	Set of occupied subchannels
$\mathcal{K}_v$	Set of vacant subchannels

FAPs belong to the same wireless system such as long term evolution-advanced (LTE-A), where the frame structures of both are the same. The OFDMA system has a total bandwidth of B, which is divided into K subchannels. The channel model for each subchannel consists of pathloss and frequency flat Rayleigh fading. Each FAP performs a cooperative spectrum

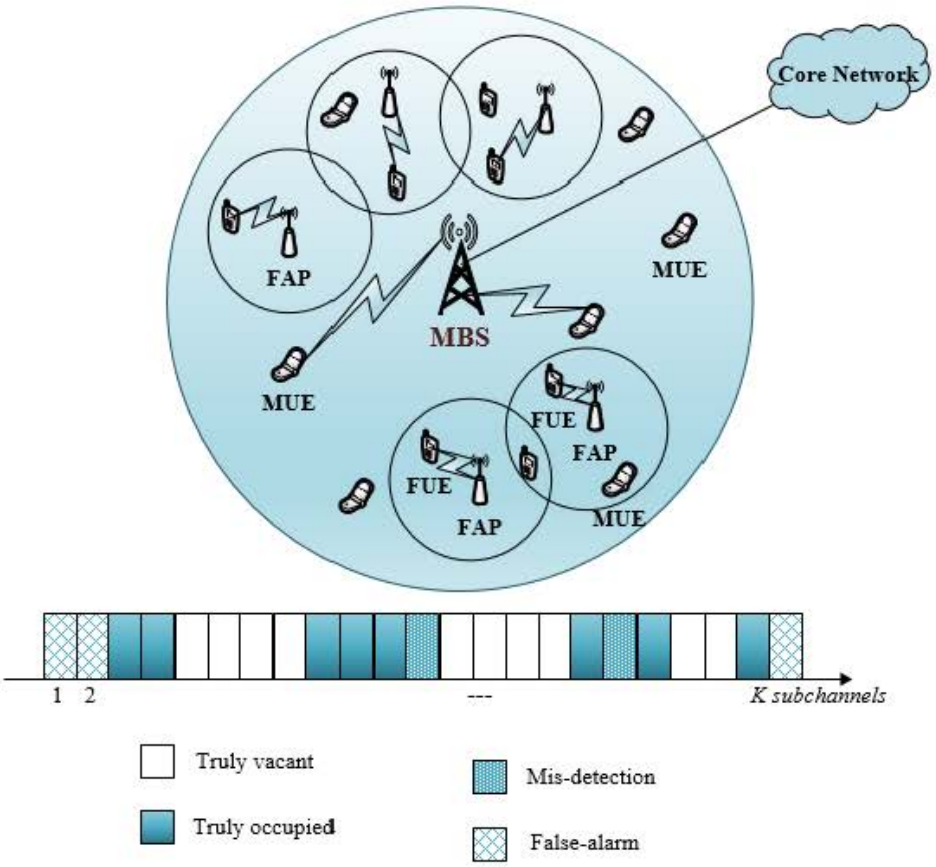

Figure 3.2: The heterogeneous deployment of ultra-dense FAPs overlaying the coverage of an MBS.

sensing with its affiliated FUEs to determine if a subchannel is occupied or vacant by the method of energy detection of CR technology.

The OFDMA system is assumed to support three service types, which are real-time (RT), non-real-time (NRT) and best effort (BE) [154]. There are U_1 RT FUEs with minimum rate requirements as well as U_2 NRT FUEs and BE FUEs with a proportional rate constraint. Let $\mathcal{U}_{\mathcal{A}} = \{1, 2, ...U_1\}$ represents the set of RT FUEs, while $\mathcal{U}_{\mathcal{B}} = \{1, 2, ...U_2\}$ denotes the set of NRT and BE FUEs.

3.3.1 Signal-to-Interference-plus-Noise Ratio

The signal-to-interference-plus-noise ratio $\gamma_{n,u,k}$ of the received signal of an FUE u from an FAP n on subchannel k is given as:

$$\gamma_{n,u,k} = \frac{p_{n,u,k} h^{FF}_{n,u,k}}{\beta\left(p^{M}_{j,k} h^{MF}_{M,j,u,k} + \sum\limits_{z=1,z\neq n}^{N} \sum\limits_{w=1}^{U} p_{z,w,k} h^{FF}_{n,u,w,k} + \sigma^2\right)}, \tag{3.1}$$

where $\beta = \frac{-ln(5BER)}{1.5}$ is the signal-to-noise ratio (SNR) gap for an uncoded quadrature amplitude modulation (QAM) [116] and BER is a given bit error rate for FUE u attached to an FAP n on subchannel k. $h^{FF}_{n,u,k}$ is the channel gain between an FAP n and its attached FUE u on subchannel k. Let I_M and I_F represent the $p^{M}_{j,k} h^{MF}_{M,j,u,k}$ and $\sum\limits_{z=1,z\neq n}^{N} \sum\limits_{w=1}^{U} p_{z,w,k} h^{FF}_{n,u,w,k}$ respectively, where $p^{M}_{j,k} h^{MF}_{M,j,u,k}$ and $\sum\limits_{z=1,z\neq n}^{N} \sum\limits_{w=1}^{U} p_{z,w,k} h^{FF}_{n,u,w,k}$ are the interference caused by the MBS and the FAPs respectively. $p^{M}_{j,k}$ is the transmit power of an MBS M servicing an MUE j on subchannel k. $h^{MF}_{M,j,u,k}$ is the channel gain from an MBS M servicing MUE j to a nearby FUE u on subchannel k. $p_{z,w,k}$ is the unwanted transmit power applied by another FAP $z \neq n$ to a nearby FUE $w \neq u$ on subchannel k. $h^{FF}_{n,u,w,k}$ is the channel gain between FAP n serving FUE u to a nearby FUE w on subchannel k. σ^2 denotes the additive white Gaussian noise (AWGN) power.

3.3.2 Achievable Transmission Rate

The achievable transmission rate (throughput) $R_{n,u,k}$ of an FUE u attached to an FAP n on subchannel k according to Shannon's law is given as:

$$R_{n,u,k} = W log_2(1 + \gamma_{n,u,k}), \tag{3.2}$$

where $p_{n,u,k}$ is the required transmit power of an FUE u in an FAP n on subchannel k. $W = \frac{B}{K}$ is the bandwidth of each subchannel. $\gamma_{n,u,k}$ is obtained from Equation (3.1).

3.3.3 Interference Model

The co-existence of macrocell and femtocell networks results in cross-tier and co-tier interference, which can also be attributed to out-of-band (OOB) emissions and imperfect spectrum sensing [115].

3.3.3.1 Out-of-band (OOB) Emissions

The OOB emissions occur as a result of power leakage in the sidelobes of an orthogonal frequency division multiplexing (OFDM) signals. The sum of OOB interference power $I^{MF}_{n,u,k,q}$ introduced into a given subchannel q, which is occupied by an MUE, as a result of FUE u transmitting on subchannel k with unit transmit power is given as:

$$I^{MF}_{n,u,k,q} = \int_{f^c_q - \frac{B}{2K} + f^c_k}^{f^c_q + \frac{B}{2K} + f^c_k} g^{MF}_{n,u,k,q} \; \varphi(f) df, \tag{3.3}$$

where $g^{MF}_{n,u,k,q}$ represents the power gain from an FAP n serving an FUE u on subchannel k to an MUE on subchannel q. $\varphi(f) = \frac{1}{T}\left(\frac{sin\pi(f-f_k^c)T}{\pi(f-f_k^c)T}\right)^2$ is the power spectrum density (PSD) of the OFDM signal, where f, f_q^c and f_k^c are the starting frequency, centre frequencies of subchannels q and k respectively. T is the duration of an OFDM symbol.

Similarly, an FUE u belonging to an nth femtocell transmitting on subchannel k may cause interference to a nearby FUE on subchannel q. The interference caused by this signal is expressed as:

$$I^{FF}_{n,u,k,q} = \int_{f_q^c-\frac{B}{2K}+f_k^c}^{f_q^c+\frac{B}{2K}+f_k^c} g^{FF}_{n,u,k,q}\ \varphi(f)df, \tag{3.4}$$

where $I^{FF}_{n,u,k,q}$ is the co-tier interference due to OOB emissions, $g^{FF}_{n,u,k,q}$ is the power gain between an nth FAP and an FUE u to a nearby FUE on subchannel q.

3.3.3.2 Imperfect Spectrum Sensing

Imperfect spectrum sensing occurs when an FAP fails to sense the weak signals that are below the spectrum sensing thresholds. This makes an FAP to identify a subchannel as vacant when it is actually occupied in its actual state. This is known as mis-detection error and it leads to co-channel interference. On the other hand, an FAP may sense that a subchannel is occupied, whereas, in its actual state, it is vacant. This is known as false-alarm error. This type of error does not increase the interference level, but it leads to lost opportunities for transmission of an FAP. This error can decrease the overall femtocell network throughput.

Let $\mathcal{O}_k$ represent the hypothesis that a subchannel k is occupied in its actual state, while $\mathcal{V}_k$ denotes the hypothesis that the subchannel k is vacant in its actual state. Let $\tilde{\mathcal{O}}_k$

and $\tilde{\mathcal{V}}_k$ represent the sensing result of an FAP as being occupied and vacant respectively. Denote $\mathcal{K}_o$ and $\mathcal{K}_v$ as the sets of occupied and vacant subchannels respectively. Let Pr_k^{md} and Pr_k^{fa}, Pr_k^j denote the probabilities of mis-detection error, false alarm error, and MUE j's occupation in a subchannel k respectively. There are four possible events for spectrum sensing as summarised in Table 3.2, which are:

1. subchannel k is occupied in its actual state ($\mathcal{O}_k$), and the decision by an FAP for subchannel k is occupied ($\tilde{\mathcal{O}}_k$).

2. subchannel k is occupied in its actual state ($\mathcal{O}_k$) and the decision by an FAP for subchannel k is vacant ($\tilde{\mathcal{V}}_k$).

3. subchannel k is vacant in its actual state ($\mathcal{V}_k$), and the decision by an FAP for subchannel k is occupied ($\tilde{\mathcal{O}}_k$).

4. subchannel k is vacant in its actual state ($\mathcal{V}_k$), and the decision by an FAP for subchannel k is vacant ($\tilde{\mathcal{V}}_k$).

The first and the fourth events are accurately sensed. The second and the third events are mis-detection and false alarm respectively. The conditional probabilities of all events are detailed as follows:

(a) **Event 1:** $\Pr_{k,1}$ is the probability that subchannel $k \in \mathcal{K}_o$ is occupied in its actual state by an MUE j ($\mathcal{O}_k$) *given that* the sensing result of a cognitive FAP is occupied ($\tilde{\mathcal{O}}_k$), which can be expressed as:

$$Pr_{k,1} = Pr(\mathcal{O}_k \mid \tilde{\mathcal{O}}_k), \tag{3.5}$$

Table 3.2: Conditional probability information from imperfect spectrum sensing

Event	**Actual state**	**Sensing result**	**Probability Information**
1	Occupied $\mathcal{O}_k$	Occupied $\tilde{\mathcal{O}}_k$	$P_{n,1} = P\{(\mathcal{O}_k) \mid (\tilde{\mathcal{O}}_k)\}$
2	Occupied $\mathcal{O}_k$	Vacant $\tilde{\mathcal{V}}_k$	$P_{n,2} = P\{(\mathcal{O}_k) \mid (\tilde{\mathcal{V}}_k)\}$
3	Vacant $\mathcal{V}_k$	Occupied $\tilde{\mathcal{O}}_k$	$P_{n,3} = P\{(\mathcal{V}_k) \mid (\tilde{\mathcal{O}}_k)\}$
4	Vacant $\mathcal{V}_k$	Vacant $\tilde{\mathcal{V}}_k$	$P_{n,4} = P\{(\mathcal{V}_k) \mid (\tilde{\mathcal{V}}_k)\}$

$$Pr_{k,1} = \frac{Pr(\tilde{\mathcal{O}}_k \mid \mathcal{O}_k)Pr(\mathcal{O}_k)}{Pr(\tilde{\mathcal{O}}_k \mid \mathcal{O}_k)Pr(\mathcal{O}_k) + Pr(\tilde{\mathcal{O}}_k \mid \mathcal{V}_k)Pr(\mathcal{V}_k)}, \tag{3.6}$$

$$Pr_{k,1} = \frac{(1 - Pr_k^{md})Pr_k^j}{(1 - Pr_k^{md})Pr_k^j + Pr_k^{fa}(1 - Pr_k^j)}. \tag{3.7}$$

(b) **Event 2:** $\Pr_{k,2}$ is the probability that subchannel $k \in \mathcal{K}_v$ is actually occupied by an MUE j ($\mathcal{O}_k$) *given that* the sensing result of an FAP is vacant ($\tilde{\mathcal{V}}_k$).

$$Pr_{k,2} = Pr(\mathcal{O}_k \mid \tilde{\mathcal{V}}_k), \tag{3.8}$$

$$Pr_{k,2} = \frac{Pr(\tilde{\mathcal{V}}_k \mid \mathcal{O}_k)Pr(\mathcal{O}_k)}{Pr(\tilde{\mathcal{V}}_k \mid \mathcal{O}_k)Pr(\mathcal{O}_k) + Pr(\tilde{\mathcal{V}}_k \mid \mathcal{V}_k)Pr(\mathcal{V}_k)}, \tag{3.9}$$

$$Pr_{k,2} = \frac{Pr_k^{md}Pr_k^p}{Pr_k^{md}Pr_k^j + (1 - Pr_k^{fa})(1 - Pr_k^j)}. \tag{3.10}$$

(c) **Event 3:** $\Pr_{k,3}$ is the probability that subchannel $k \in \mathcal{K}_o$ is vacant in its actual state ($\mathcal{V}_k$) *given that* the sensing result of a cognitive FAP is occupied ($\tilde{\mathcal{O}}_k$).

$$Pr_{k,3} = Pr(\mathcal{V}_k \mid \tilde{\mathcal{O}}_k), \tag{3.11}$$

$$Pr_{k,3} = \frac{Pr(\tilde{\mathcal{O}}_k \mid \mathcal{V}_k)Pr(\mathcal{V}_k)}{Pr(\tilde{\mathcal{O}}_k \mid \mathcal{V}_k)Pr(\mathcal{V}_k) + Pr(\tilde{\mathcal{O}}_k \mid \mathcal{O}_k)Pr(\mathcal{O}_k)}, \tag{3.12}$$

$$Pr_{k,3} = \frac{Pr_k^{fa}(1 - Pr_k^{j})}{Pr_k^{fa}(1 - Pr_k^{p}) + (1 - Pr_k^{md})(Pr_k^{j})}. \tag{3.13}$$

(d) **Event 4:** $\Pr_{k,4}$ is the probability that subchannel $k \in \mathcal{K}_v$ is vacant in its actual state ($\mathcal{V}_k$) given that the sensing result of an FAP is vacant ($\tilde{\mathcal{V}}_k$).

$$Pr_{k,4} = Pr(\mathcal{V}_k \mid \tilde{\mathcal{V}}_k), \tag{3.14}$$

$$Pr_{k,4} = \frac{Pr(\tilde{\mathcal{V}}_k \mid \mathcal{V}_k)Pr(\mathcal{V}_k)}{Pr(\tilde{\mathcal{V}}_k \mid \mathcal{V}_k)Pr(\mathcal{V}_k) + Pr(\tilde{\mathcal{V}}_k \mid \mathcal{O}_k)Pr(\mathcal{O}_k)}, \tag{3.15}$$

$$Pr_{k,4} = \frac{(1 - Pr_k^{fa})(1 - Pr_k^{j})}{(1 - Pr_k^{fa})(1 - Pr_k^{j}) + Pr_k^{md}Pr_k^{j}}. \tag{3.16}$$

The conditional probabilities $Pr_{k,1}$ and $Pr_{k,2}$ represent interference due to OOB emissions and mis-detection error respectively. $Pr_{k,3}$ denotes the false-alarm error. $Pr_{k,4}$ represents the accurate sensing level of a cognitive FAP. Therefore, the downlink cross-tier interference $\tilde{I}_{n,u,k}^{MF}$ as a result of OOB emissions and imperfect spectrum sensing on subchannel k based on the above analysis can be expressed as:

$$\tilde{I}_{n,u,k}^{MF} = p_{n,u,k} \underbrace{\left(\sum_{k \in K_o} Pr_{k,1} I_{n,u,k,q}^{MF} + \sum_{k \in K_v} Pr_{k,2} I_{n,u,k,q}^{MF} \right)}_{\tilde{\Gamma}_{n,u,k}^{MF}}. \tag{3.17}$$

Equation (3.17) can be re-written as follows:

$$\tilde{I}_{n,u,k}^{MF} = p_{n,u,k} \tilde{\Gamma}_{n,u,k}^{MF}, \tag{3.18}$$

where $\tilde{\Gamma}^{MF}_{k,u,n}$ can be referred to as channel gain from nth femtocell to a nearby MUE on subchannel k.

Similarly, when two neighbouring femtocells use the same subchannel, there will be co-tier interference. Therefore, the downlink co-tier interference $\tilde{I}^{FF}_{n,u,k}$ can be expressed as:

$$\tilde{I}^{FF}_{n,u,k} = p_{n,u,k} \underbrace{\left(\sum_{k \in K_o} Pr_{k,1} I^{FF}_{n,u,k,q} + \sum_{k \in K_v} Pr_{k,2} I^{FF}_{n,u,k,q} \right)}_{\tilde{\Gamma}^{FF}_{n,u,k}}. \tag{3.19}$$

Equation (3.19) can also be re-written as follows:

$$\tilde{I}^{FF}_{n,u,k} = P_{n,u,k} \tilde{\Gamma}^{FF}_{n,u,k}, \tag{3.20}$$

where $\tilde{\Gamma}^{FF}_{n,u,k}$ is the channel gain between an FAP n and its attached FUE u on subchannel k.

3.4 Problem Formulation

The objective of the work in this chapter is to maximise the throughput of femtocell networks while mitigating the cross-tier and co-tier interference as well as satisfying the QoS requirements of different users with heterogeneous services. Hence, the self-organising radio resource allocation problem is formulated in Equation (3.21) under the constraints C1 - C8 as:

$$\max_{\alpha_{n,u,k} \; p_{n,u,k}} \sum_{n=1}^{N} \sum_{u=1}^{U} \sum_{k=1}^{K} \alpha_{n,u,k} R_{n,u,k} \tag{3.21}$$

$$
\begin{aligned}
s.t.\ C1 &: \sum_{k=1}^{K} \alpha_{n,u,k} p_{n,u,k} \leq P_{\max}\ \forall n, u \\
C2 &: p_{n,u,k} \geq 0\ \forall n, u, k \\
C3 &: \sum_{n=1}^{N} \sum_{k=1}^{K} \alpha_{n,u,k} R_{n,u,k} \geq R_u^{\min}\ \forall u \in \mathcal{U}_{\mathcal{A}} \\
C4 &: \frac{\sum_{n=1}^{N} \sum_{k=1}^{K} \alpha_{n,u,k} R_{n,u,k}}{\sum_{u \in \mathcal{U}_{\mathcal{B}}} R_{n,u,k}} = \phi_u\ \forall u \in \mathcal{U}_{\mathcal{B}} \\
C5 &: \sum_{u=1}^{U} \alpha_{n,u,k} \leq 1\ \forall n, k \\
C6 &: \alpha_{n,u,k} \in \{0, 1\} \\
C7 &: \sum_{n=1}^{N} \sum_{u=1}^{U} \alpha_{n,u,k} p_{n,u,k} \tilde{\Gamma}_{n,u,k}^{MF} \leq I_{th}^{MF}\ \forall k \\
C8 &: \sum_{n=1}^{N} \sum_{u=1}^{U} \alpha_{n,u,k} p_{n,u,k} \tilde{\Gamma}_{n,u,k}^{FF} \leq I_{th}^{FF}\ \forall k.
\end{aligned}
$$

The constraint C1 signifies the limit on the maximum transmit power. The constraint C2 ensures efficient utilisation of power. The constraint C3 is the minimum QoS requirement for every RT FUE in the set $\mathcal{U}_{\mathcal{A}}$. The constraint C4 shows the QoS requirements for NRT and BE FUEs in the set $\mathcal{U}_{\mathcal{B}}$. The QoS requirements of RT FUEs are satisfied first. The remaining radio resources are shared based on a proportional fairness rate ϕ_u among NRT and BE FUEs. The constraint C5 ensures that subchannel k is assigned to at most one FUE at a time. The constraint C6 is a subchannel binary decision indicator. $\alpha_{n,u,k} = 1$, if subchannel k is allocated or $\alpha_{n,u,k} = 0$, otherwise. The constraint C7 and C8 express the maximum cross-tier and co-tier interference limit respectively.

3.5 Problem Solution

The self-organising radio resource allocation problem is formulated in Equation (3.21) subject to the constraints in C1-C8. The computational complexity of the problem is very high to solve due to the variables involved. Therefore, the optimal joint power and subchannel allocation problem is solved using the Lagrangian dual decomposition (LDD) method to get an approximately optimal solution. The method involves three steps which are: formulation of dual decomposition, solution of dual decomposition and updating the dual variables [155], [156].

3.5.1 Formulation of Dual Decomposition

The optimisation problem in Equation (3.21) is complex due to the constraint in C4. The constraint in C4 can be re-written according to [157] as follows:

$$R_1 : R_2 : ... : R_{U_2} = \phi_1 : \phi_2 ... : \phi_{U_2} \ \forall u \in \mathcal{U}_{\mathcal{B}}. \tag{3.22}$$

Equation (3.22) can be substituted into C4 in Equation (3.21). Therefore, the Lagrangian function of Equation (3.21) can be expressed as:

$$\mathcal{L}(\eta,\rho,\xi,\lambda,\theta,\mu)=\left(\sum_{n=1}^{N}\sum_{u=1}^{U}\sum_{k=1}^{K}\alpha_{n,u,k}R_{n,u,k}\right)+\sum_{n=1}^{N}\sum_{u=1}^{U}\eta_{n,u}\left(P_{\max}-\sum_{k=1}^{k}\alpha_{n,u,k}p_{n,u,k}\right)$$
$$+\sum_{n=1}^{N}\sum_{u=1}^{U_1}\rho_{n,u}\left(\sum_{k=1}^{K}\alpha_{n,u,k}R_{n,u,k}-R_u^{min}\right)+\sum_{n=1}^{N}\sum_{u=2}^{U_2}\xi_{n,u}\left(\phi_u\sum_{k=1}^{K}\alpha_{n,u,k}R_{n,u,k}-\sum_{k=1}^{K}R_{n,u,k}\right)$$
$$+\sum_{n=1}^{N}\sum_{k=1}^{K}\lambda_{n,k}\left(1-\sum_{u=1}^{U}\alpha_{n,u,k}\right)+\sum_{k=1}^{K}\theta_k\left(I_{th}^{MF}-\sum_{n=1}^{N}\sum_{u=1}^{U}\alpha_{n,u,k}p_{n,u,k}\tilde{\Gamma}_{n,u,k}^{MF}\right)$$
$$+\sum_{n=1}^{N}\sum_{k=1}^{K}\mu_{n,k}\left(I_{th}^{FF}-\sum_{n=1}^{N}\sum_{u=1}^{U}\alpha_{n,u,k}p_{n,u,k}\tilde{\Gamma}_{n,u,k}^{FF}\right), \tag{3.23}$$

where $\eta,\rho,\xi,\lambda,\theta$, and μ are the Lagrange multiplier vectors associated with C1, C3, C4, C5, C7 and C8 in Equation (3.21) respectively. Applying Karush-Kuhn-Tucker (KKT) conditions according to [138] to the boundary condition in C2 and C6 respectively gives:

$$\left.\frac{\partial\mathcal{L}(\eta,\rho,\xi,\lambda,\theta,\mu)}{\partial p_{n,u,k}}\right|_{p_{n,u,k}=p_{n,u,k}^*}\geq 0 \tag{3.24}$$
$$\left.\frac{\partial\mathcal{L}(\eta,\rho,\xi,\lambda,\theta,\mu)}{\partial \alpha_{n,u,k}}\right|_{\alpha_{n,u,k}=\alpha_{n,u,k}^*}\geq 0 \tag{3.25}$$

where $\alpha_{n,u,k}^*$ is the optimal subchannel allocated to an FUE u in an FAP n on subchannel k, while $p_{n,u,k}^*$ is the corresponding optimal power.

3.5.2 Solution of Dual Decomposition

The dual problem corresponding to the primal problem of Equation (3.23) is expressed as:

$$\min_{\eta,\rho,\xi,\lambda,\theta,\mu\geq 0}\ \max_{\alpha_{n,u,k},\ p_{n,u,k}}\ \mathcal{L}(\alpha_{n,u,k},p_{n,u,k},\eta,\rho,\xi,\lambda,\theta,\mu). \tag{3.26}$$

The dual function corresponding to problem in Equation (3.23) is defined as:

$$\vartheta(\eta,\rho,\xi,\lambda,\theta,\mu) = \max_{\alpha_{n,u,k},p_{n,u,k}} \mathcal{L}(\alpha_{n,u,k},\ p_{n,u,k},\eta,\rho,\xi,\lambda,\theta,\mu). \tag{3.27}$$

The corresponding dual problem to the primal problem is therefore given as:

$$\begin{aligned} &\min_{\rho,\eta,\xi,\lambda,\theta,\mu} \vartheta(\eta,\rho,\xi,\lambda,\theta,\mu), \\ s.t.\ \eta \geq 0,\ \rho \geq 0,\ \xi \geq 0,\ \lambda \geq 0,\ \theta \geq 0,\ \mu \geq 0. \end{aligned} \tag{3.28}$$

The dual problem in Equation (3.26) is decomposed into a slave and a master problems. The inner maximisation in Equation (3.26) consisting of $N \times K$ sub problems is the slave problem as shown in Equation (3.27), which is solved to compute the subchannel and power allocation for the given values of $\eta, \rho, \xi, \lambda, \theta$, and μ. The master problem as shown in Equation (3.28) is the outer minimisation in Equation (3.26), which the Lagrangian multipliers are updated using a sub gradient method. Equation (3.27) can be re-written as:

$$\begin{aligned} \vartheta(\eta,\rho,\xi,\lambda,\theta,\mu) = \max_{\alpha_{n,u,k},\ p_{n,u,k}} \mathcal{L}(\alpha_{n,u,k},p_{n,u,k},\eta,\rho,\xi,\lambda,\theta,\mu) = \\ \max_{\alpha_{n,u,k},p_{n,u,k}} \Bigg[\sum_{n=1}^{N}\sum_{k=1}^{K} \mathcal{L}_{n,k}(\alpha_{n,u,k},p_{n,u,k},\eta,\rho,\xi,\lambda,\theta,\mu) + \sum_{n=1}^{N}\sum_{u=1}^{U} \eta_{n,u} P_{\max} \\ - \sum_{n=1}^{N}\sum_{u=1}^{U_1} \rho_{n,u} R^{min}_{n,u,k} - \sum_{n=1}^{N}\sum_{u=2}^{U_2} \xi_{n,u} R_{n,u,n} + \sum_{n=1}^{N}\sum_{k=1}^{K} \lambda_{n,k} + \sum_{k=1}^{K} \theta_k I^{MF}_{th} + \sum_{n=1}^{N}\sum_{k=1}^{K} \mu_{n,k} I^{FF}_{th} \Bigg]. \end{aligned} \tag{3.29}$$

where

$$\mathcal{L}_{n,k}(\alpha_{n,u,k}, p_{n,u,k}, \eta, \rho, \xi, \lambda, \theta, \mu) = \Bigg[\sum_{u=1}^{U} \alpha_{n,u,k} R_{n,u,k} - \sum_{u=1}^{U} \eta_{n,u} p_{n,u,k} + \sum_{n=1}^{N} \rho_{n,u} \alpha_{n,u,k} R_{n,u,k} + \xi_{u,k} \phi_u \sum_{k=1}^{K} \alpha_{n,u,k} R_{n,u,k} - \sum_{u=1}^{U} \alpha_{n,u,k} - \theta_k \sum_{n=1}^{N} \sum_{u=1}^{U} \alpha_{n,u,k} p_{n,u,k} \tilde{\Gamma}^{MF}_{n,u,k} - \mu_{n,k} \sum_{n=1}^{N} \sum_{u=1}^{U} \alpha_{n,u,k} p_{n,u,k} \tilde{\Gamma}^{FF}_{n,u,k} \Bigg]. \tag{3.30}$$

To obtain $p^*_{n,u,k}$ and $\alpha^*_{n,u,k}$ allocated to an FUE u in an FAP n on subchannel k for $\forall u \in \mathcal{U}_{\mathcal{A}}$ and $\forall u \in \mathcal{U}_{\mathcal{B}}$, the first-order derivatives of Equation (3.27) with respect to $p_{n,u,k}$ is taking, which gives the KKT condition in Equation (3.24). This yields

$$\frac{\partial \vartheta(\eta, \rho, \xi, \lambda, \theta, \mu)}{\partial p_{n,u,k}} = \left(\frac{(1+\rho_{n,u})\alpha_{n,u,k} h^{FF}_{n,u,k} + (1+\xi_{n,u})\alpha_{n,u,k} h^{FF}_{n,u,k}}{\ln 2 (I_M + I_F + W\sigma^2 + p_{n,u,k} h^{FF}_{n,u,k})} \right) - \left(\sum_{z=1, z\neq n}^{N} \mu_{z,k} h^{FF}_{z,u,w,k} - \theta_k \tilde{\Gamma}^{MF}_{n,u,k} \right) - \eta_{n,u} = 0. \tag{3.31}$$

Hence, the optimal power $p^*_{n,u,k}$ allocated to an FUE u in an FAP n is given as:

$$p^*_{n,u,k} = \begin{cases} \left[\frac{(1+\rho_{n,u})+(1+\xi_{n,u})}{\ln 2 \left(\eta_{u,n} + \sum\limits_{z=1, z\neq n}^{N} \mu_{z,k} h^{FF}_{z,u,w,k} + \theta_k \tilde{\Gamma}^{MF}_{n,u,k} \right)} - \frac{I_M + I_F + W\sigma^2}{h^{FF}_{n,u,k}} \right]^+, & \text{if } \alpha^*_{n,u,k} = 1 \\ 0, & \text{otherwise} \end{cases} \tag{3.32}$$

where $[x]^+ = \max[0, x]$. Similarly, to obtain the optimal subchannel $\alpha^*_{n,u,k}$ allocated to an FUE u in an FAP n, the first-order derivatives of Equation (3.27) with respect to $\alpha_{n,u,k}$ is taking, which gives the KKT condition in Equation (3.25). This yields

$$\frac{\partial \vartheta(\eta, \rho, \xi, \lambda, \theta, \mu)}{\partial \alpha_{n,u,k}} = \Big((1+\rho_{n,u}) + (1+\xi_{n,u}) \Big). \log 2 \left(1 + \frac{p^*_{n,u,k} h^{FF}_{n,u,k}}{\ln 2 (I_M + I_F + W\sigma^2)} \right) - \frac{1}{\ln 2} \left(\frac{p^*_{n,u,k} h^{FF}_{n,u,k}}{p^*_{n,u,k} h^{FF}_{n,u,k} + I_M + I_F + W\sigma^2} \right) - \lambda_{n,k} = 0. \tag{3.33}$$

Denote

$$\psi = \Big((1+\rho_{n,u}) + (1+\xi_{n,u})\Big). \\ \log 2\left(1 + \frac{p^*_{n,u,k} h^{FF}_{n,u,k}}{\ln 2 (I_M + I_F + W\sigma^2)}\right) - \frac{1}{\ln 2}\left(\frac{p^*_{n,u,k} h^{FF}_{n,u,k}}{p^*_{n,u,k} h^{FF}_{n,u,k} + I_M + I_F + W\sigma^2}\right) \tag{3.34}$$

Hence, the optimal subchannel $\alpha^*_{n,u,k}$ allocated to an FUE u^* in an FAP n is given as:

$$\alpha^*_{n,u,k} = \begin{cases} 1, & \text{if } (n, u^*, k) = \arg\max \psi \\ 0, & \text{otherwise} \end{cases} \tag{3.35}$$

3.5.3 Updating the Dual Variables

The subgradient method is used to solve the master problem in Equation (3.28) to update the dual variables $\eta, \rho, \xi, \lambda, \theta, \mu$, The subgradient method is used to design a step-size sequence $\Lambda^{(\ell)}$ to update the multipliers in the subgradient direction as:

$$\eta^{(\ell+1)}_{n,u} = \left[\eta^{\ell}_{n,u} - \Lambda^{(\ell)}_1 \left(P_{\max} - \sum_{k=1}^{K} \alpha_{n,u,k} p_{n,u,k})\right)\right]^+, \tag{3.36}$$

$$\rho^{(\ell+1)}_{n,u} = \left[\rho^{(\ell)}_{n,u} - \Lambda^{(\ell)}_2 \left(\alpha_{n,u,k} R_{n,u,k} - R^{\min}_{n,u,k})\right)\right]^+, \tag{3.37}$$

$$\xi^{(\ell+1)}_{n,u} = \left[\xi^{(\ell)}_{n,u} - \Lambda^{(\ell)}_3 \left(\phi_u \sum_{k=1}^{K} \alpha_{n,u,k} R_{n,u,k} - \sum_{k=1}^{K} R_{n,u,n}\right)\right]^+, \tag{3.38}$$

$$\lambda^{(\ell+1)}_{n,k} = \left[\lambda^{(\ell)}_{n,k} - \Lambda^{(\ell)}_4 \left(1 - \sum_{u=1}^{U} \alpha_{n,u,k}\right)\right]^+, \tag{3.39}$$

$$\theta^{(\ell+1)}_{k} = \left[\theta^{(\ell)}_{k} - \Lambda^{(\ell)}_5 \left(I^{MF}_{th} - \sum_{n=1}^{N}\sum_{u=1}^{U} \alpha_{n,u,k} p_{n,u,k} \tilde{\Gamma}^{MF}_{n,u,k}\right)\right]^+, \tag{3.40}$$

$$\mu_{n,k}^{(\ell+1)} = \left[\mu_{n,k}^{(\ell)} - \Lambda_6^{(\ell)}\left(I_{th}^{FF} - \sum_{n=1}^{N}\sum_{u=1}^{U}\alpha_{n,u,k}p_{n,u,k}\tilde{\Gamma}_{n,u,k}^{FF}\right)\right]^{+}, \tag{3.41}$$

where $\Lambda_1^{(\ell)}, \Lambda_2^{(\ell)}, \Lambda_3^{(\ell)}, \Lambda_4^{(\ell)}, \Lambda_5^{(\ell)}$ and $\Lambda_6^{(\ell)}$ are the iteration step sizes. ℓ is the number of iteration. The above Lagrangian multipliers are updated until the convergence is true ($\ell = \ell^{max}$), as long as ℓ is chosen to be sufficiently small. The step sizes are required to satisfy the following conditions:

$$\sum_{\ell=1}^{\infty} s_\ell^{(\ell)} = \infty, \quad \lim_{\ell \longrightarrow \infty} s_\ell^{(\ell)} = 0, \ \forall \ell \in \{1, 2, ...6\}. \tag{3.42}$$

3.6 Proposed Algorithm and its Computational Complexity Analysis

3.6.1 Proposed Algorithm

The procedure of the proposed SORRM algorithm for joint subchannel and power allocation is summarised in Algorithm 1 as follows:

Algorithm 1: **SORRM**

1: **Initialisation**: set $\alpha_{n,u,k}$, η, ρ, ξ, λ, θ, μ, and $p_{n,u,k} = 0$

2: Each FAP measures $h^{FF}_{n,u,k}$ and calculates $\gamma_{n,u,k}$ according to Equation (3.1)

3: Each FAP allocates equal power to each suchannel $\forall n, u, k$

4: Every FAP performs spectrum sensing on each subchannel to determine K_v

5: **while** $\tilde{I}^{MF}_{n,u,k} \leq \tilde{I}^{MF}_{th}$ and $\tilde{I}^{FF}_{n,u,k} \leq \tilde{I}^{FF}_{th}$ **do**

6: (a) find $u^* \in \mathcal{U}_{\mathcal{A}}$ **if** $R_{u^*} \leq R^{min}_{u^*}$ **then**

7: (b) compute $\alpha^*_{n,u^*,k^*} = 1, K = K - k^*$ using Equation (3.35)

8: (c) compute corresponding p^*_{n,u^*,k^*} $\forall u \in \mathcal{U}_{\mathcal{A}}$ using Equation (3.32)

9: **end if**

10: **end while**

11: **while** $K_v \neq \emptyset$ **do**

12: (a) find $u^* \in \mathcal{U}_{\mathcal{B}}$ **if** $\frac{R_{u^*}}{\phi_u} \leq R_{u^*}$ **then**

13: (b) compute $\alpha^*_{n,u^*,k^*} = 1, K = K - k^*$ using Equation (3.35)

14: (c) compute corresponding p^*_{n,u^*,k^*} for $u^* \in \mathcal{U}_{\mathcal{B}}$ using Equation (3.32)

15: **end if**

16: **end while**

17: **for** $k = 1$ to K,

18: Each FAP updates η, ρ, ξ, λ, and μ according to the gradient method

19: **end for**

20: The MBS updates θ and sends the updated value to all FAPs, $\ell = \ell + 1$

22: **Repeat** until convergence ($\ell = \ell^{max}$)

3.6.2 Complexity Analysis

Complexity analysis is an approach to determine the efficiency of algorithms in terms of the number of times some inner loops is executed, the amount of data processed or the amount of memory used. This analysis shows how fast or slow a particular algorithm performs. In complexity analysis, O represents the asymptotic notation, which denotes runtime complexity [158],[159]. The computational complexity of the SORRM algorithm is discussed below:

The SORRM algorithm requires the complexity of $O(NKlog_2U)$ to determine the Lagrange multipliers for different users. Its complexity is $O(\ell^{max})$ in each iteration to find the optimal subchannel α^*_{n,u^*,k^*} and the corresponding optimal power $p^*_{n,u,k}$ in each FAP, where $\ell^{max} = 50$ is the maximum number of iterations for SORRM to converge. The worst-case complexity of finding a suitable subchannel is $O(NUlog_2K)$. Therefore, the overall complexity of SORRM algorithm is $O(NKlog_2U) + O(\ell^{max}) + O(NUlog_2K) = O(NUK\ell^{max}(log_2U + log_2K))$, compared with the exhaustive search, which has the exponential complexity of $O(NU)^K$ as shown in Table 3.3.

Table 3.3: Computational complexity comparison

Algorithm	**Computational Complexity**
Exhaustive Search	$O(NU)^K$
SORRM	$O(NUK\ell^{max}(log_2U + log_2K))$

3.7 Simulation Results and Discussions

3.7.1 Simulation Environment

The simulation parameters are set according to the 3GPP evolved universal terrestrial radio access standard [65]. The radius of the MBS and each FAP are set to 500m and 10m respectively. The path loss model from an FAP PL_{FAP} to FUE/MUE is expressed as [65], [116]:

$$PL_{FAP} = 38.46 + 20log_{10}R + 0.7d + \Xi L_{iw} + 18.3\Im^{(\frac{\Im+2}{\Im+1})-0.46}, \tag{3.43}$$

where d is the distance between the FAP and inside FUE, while R is the distance between the FAP and outside FUE. L_{iw} is the penetration loss in the internal walls of the building, which is 5dB. Ξ and $\Im$ represent the number of penetrated walls and floors respectively. The path loss model from an MBS PL_{MBS} to MUE/FUE is expressed as [65], [116]:

$$PL_{MBS} = 15.3 + 37.6log_{10}R + L_{ow}, \tag{3.44}$$

where R is the distance between the MBS and the MUE/FUE. L_{ow} is the penetration loss in the external walls of the building, which is 10dB.

The standard deviation of log-normal shadowing between MBS and UEs is 8dB, while that between an FAP and UEs is 10dB. The fast fading channel gains are modelled as independent and identically distributed (iid) random variables with unit mean. The probabilities of MUE's occupation, mis-detection and false-alarm are uniformly distributed over [0,1], [0.01, 0.05], and [0.05, 0.1] respectively. It is assumed that K_v and K_o to be $\{1, 3, ..., 99\}$ and $\{2, 4, ..., 100\}$ respectively. The carrier frequency is set to 2.6GHz. The channel bandwidth

is set to 20 MHz and it is divided into 100 subchannels. The thermal noise density is -174dBm/Hz. The maximum transmit power for an MBS is 46dBm. The lower bound and the upper bound on the number of subchannel assignment for all UEs are set to 2 and 20 per femtocell respectively.

3.7.2 Performance Evaluation

The proposed SORRM algorithm is compared with the existing algorithm in [114] termed dynamic spectrum allocation for hybrid access (DSA-HA) in which the spectrum sensing error is not considered and equal power allocation (EPA) algorithm in [116], where the same power is allocated to all subchannels. In the DSA-HA algorithm, the MBS in the network assigns a portion of subchannels to the FAP to serve its associated users while the FAP allocates the subchannels and power to maximise its network utility. The power allocation method (lines 17-20) of the SORRM algorithm is included into the DSA-HA for fair comparison and referred to it as modified DSA-HA (MDSA-HA). In the proposed SORRM algorithm, imperfect spectrum sensing and users with heterogeneous services during the downlink transmission are jointly considered.

In Fig. 3.3, the effect of varying the $P_{\max}$ and the interference thresholds $I_{th} = I_{th}^{MF} = I_{th}^{FF}$ on the femtocell network downlink throughput is investigated. The $R_u^{min} = 8$bits/s/Hz, $P_{\max}$ = 30dBm and $I_{th} = I_{th,k}^{MF} = I_{th}^{FF}$ = 20dBm as the upper benchmark case. It is observed that higher values of interference threshold and transmit power give higher throughput. Moreover, the values of the achievable network throughput are not the same for different $P_{\max}$ and I_{th}. This is due to different channel conditions, the location of users and the requested application

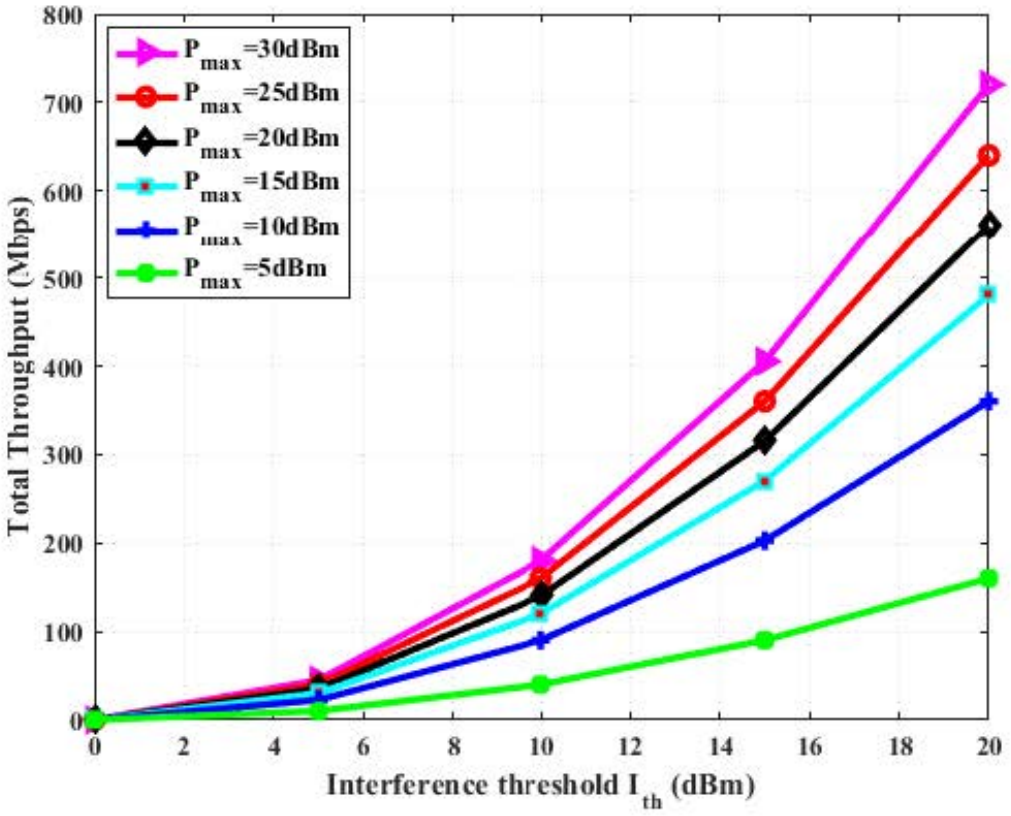

Figure 3.3: Effect of varying the maximum transmit power and interference threshold on the downlink throughput.

of users. Therefore, the values of $P_{\max}$ and I_{th} are carefully selected so that the amount of cross-tier and co-tier interference introduced into a subchannel is limited. It is observed from the figure that the achieved total throughput for $P_{\max} = 5$dBm to 30dBm are marginally close to each other when I_{th} is set to 5dBm and 10dBm. Also, there is an appreciable increase in the overall throughput when $P_{\max}$ is increased from 15dBm to 20dBm as compared to when the values of $P_{\max}$ is increased from 10dBm to 15dB. Also, a steady increase in the total throughput from $P_{\max} = 15$dBm to 30dBm is noticed in the figure. This shows that the proposed algorithm achieves stable power saving for interference mitigation especially in the

event of the ultra-dense deployment of femtocells, which will involve higher total transmit power.

Fig. 3.4 shows the amount of cross-tier interference power introduced into the MUE's subchannel for different values of FAP transmit power from 0dBm to 40dBm with 8 users in each femtocell for SORRM and MDSA-HA. SORRM considers the case of imperfect spectrum

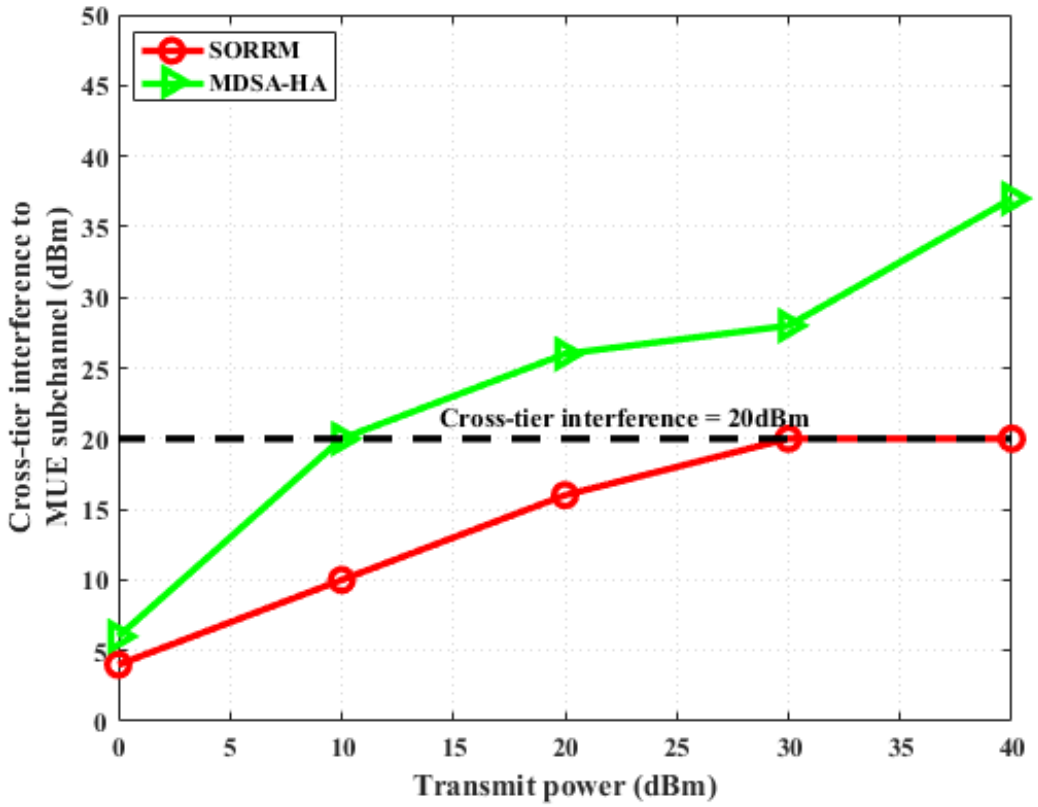

Figure 3.4: The cross-tier interference introduced to each neighbouring MUE on each subchannel against different values of transmit power for SORRM and MDSA-HA.

sensing while MDSA-HA considered perfect spectrum sensing. It is observed from the figure that, for the proposed SORRM algorithm, the cross-tier interference is kept below 20dBm as the transmit power reaches 30dBm. This shows that the cross-tier interference suffered by an MUE in a subchannel can be limited to a particular pre-determined value. Also, this

will enhance the performance of the network and will not cause any throughput degradation whereas, in MDSA-HA, the cross-tier interference for different values of transmit power keeps increasing. This shows that each MUE in a subchannel will experience more interference and this will result in lower achievable throughput.

Fig. 3.5 shows the effect of co-tier interference power to the neighbouring FUEs on each subchannel against different values of FAP's transmit power for SORRM and MDSA-HA. For SORRM, it is observed that the co-tier interference is kept below 20dBm as the transmit

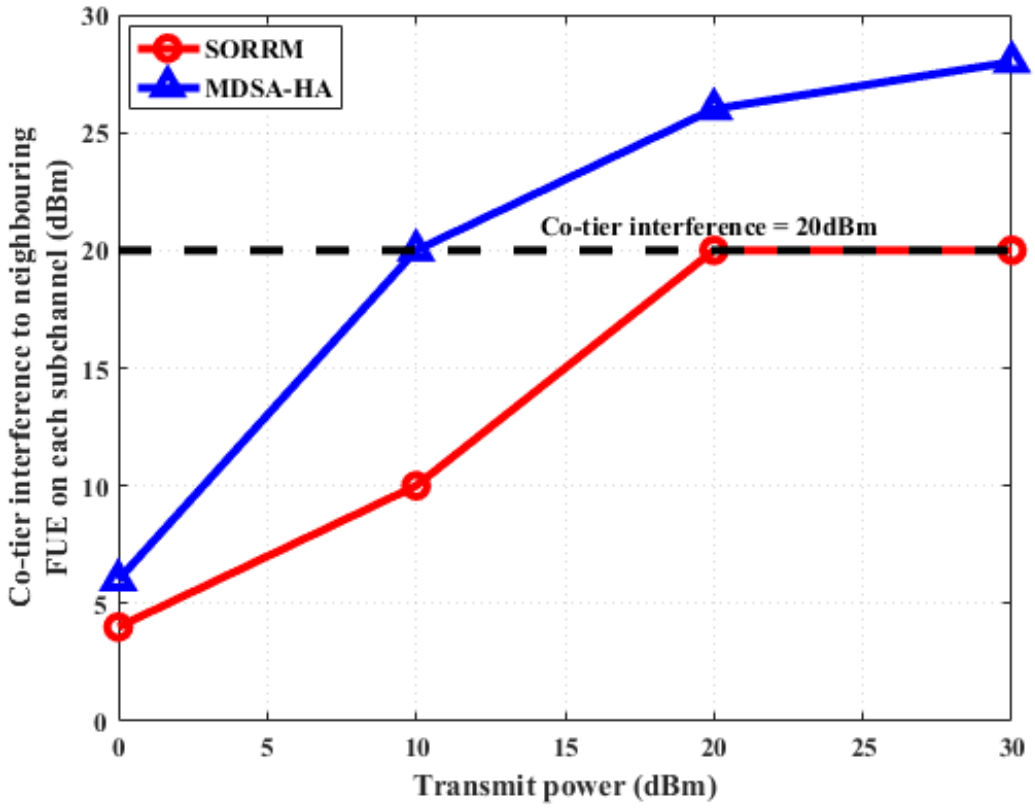

Figure 3.5: The amount of co-tier interference power introduced into the FUE's subchannel versus different values of FAP transmit power for SORRM and MDSA-HA.

power reaches 20dBm, whereas, for MDSA-HA, the interference power keeps increasing. This shows that if the issue of spectrum sensing error is not considered the neighbouring cognitive

femtocell users can experience more co-tier interference from each other and hence, this will result in low throughput performance in the network.

Fig. 3.6 shows the performance of SORRM for different numbers of UEs from 1 to 8 in a femtocell. R_u^{min} is set to 8bits/s/Hz, and the values of $P_{\max}$, I_{th}^{MF}, and I_{th}^{FF} are varied at each iteration. It is observed from the plot that there is an appreciable increase in the total

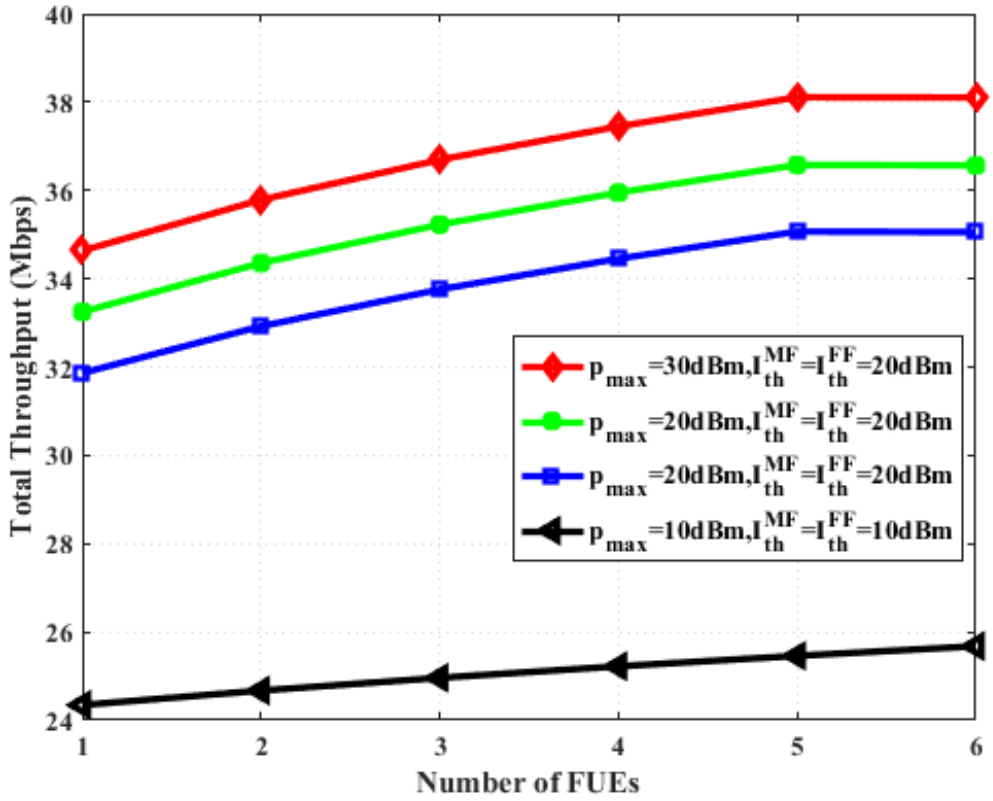

Figure 3.6: Effect of varying the maximum transmit power and interference thresholds on the downlink throughput versus different number of FUEs.

throughput for various values of $P_{\max}$, I_{th}^{MF}, and I_{th}^{FF}. This is because more users in the network increases the total capacity of the network thereby increases the total throughput of the network. Moreover, this indicates that there is a high level of satisfaction for all users

in the network. Also, highest value of throughput is obtained when $P_{\max} = 30$dBm and $I_{th}^{MF} = I_{th}^{FF} = 20$dBm.

Fig. 3.7 shows the performance of SORRM for different numbers of FAPs from 10 to 100 in a femtocell. R_u^{min} is set to 8bits/s/Hz, and the values of $P_{\max}$, $I_{th,k}^{MF}$, and $I_{th,k}^{FF}$ are varied at each iteration. It is observed from the plot that there is a gradual increase in the total throughput. This is because deployment of more FAPs in the network increases the total capacity of the network, thereby, increases the total throughput of users in the network and interference has been limited to a pre-determined value. Moreover, this indicates that the

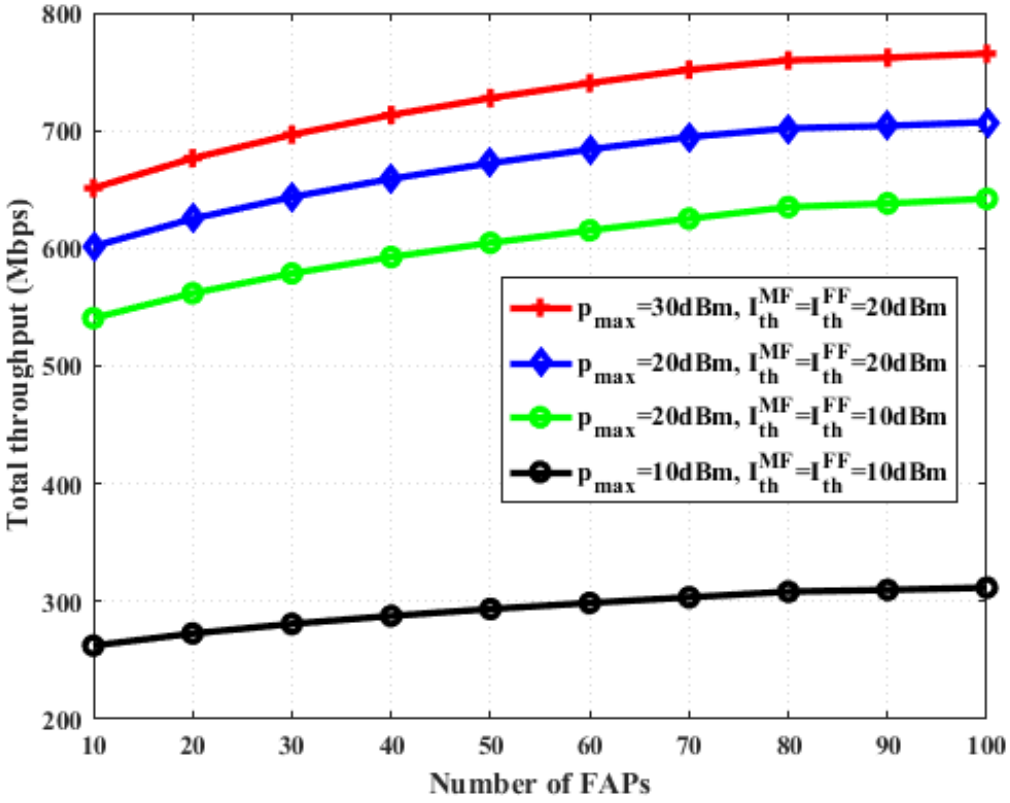

Figure 3.7: Effect of varying the maximum transmit power and interference thresholds on the downlink throughput versus different number of FAPs.

proposed algorithm is effective for the deployment of massive femtocells. From the figure, highest value is obtained when $P_{\max} = 30$dBm and $I_{th}^{MF} = I_{th}^{FF} = 20$dBm.

Fig. 3.8 shows the overall throughput of all the cognitive FAPs when the $P_{\max}$ increases from 5dBm to 25dBm for different ratios of FUEs with heterogeneous services. $I_{th}^{MF} = I_{th}^{FF}$ is set to 20dBm. U_1 and U_2 are set to 5 RT FUEs and 3 NRT and BE FUEs in each FAP respectively. The minimum rates are fixed to 8bits/s/Hz for all RT FUEs. The rate of NRT and BE FUEs is varied between 2bits/s/Hz and 8bits/s/Hz. It is noticed that the overall throughput increases when the ratio of U_1/U_2 increases. This means that the network performance is better with more RT FUEs in the network. Also, it is observed that the overall throughput of all FUEs increases gradually with increase in transmit power from 20dBm to 25dBm. This is because the level of interference is kept below a particular threshold in each subchannel.

Fig. 3.9 shows the achievable average throughput against number of FUEs in the network for different algorithms. $P_{\max} = 20$dBm, $I_{th}^{MF} = I_{th}^{FF} = 30$dBm for all subchannels. It is observed from the figure that the overall throughput for the proposed algorithm is $\sim$ 37Mbps for 1 FUE in the network. Also, the average network throughput keeps increasing as more FUEs are added to the network. This indicates high level of satisfaction for the users in the network. Moreover, the proposed algorithm outperforms the existing algorithm and that of equal power allocation algorithm because the co-tier interference between FUEs has been properly coordinated and the threshold values are carefully selected.

Fig. 3.10 shows the overall throughput versus the number of FAPs for different algorithms. Moreover, different numbers of FAPs from 10 to 100 are considered, where

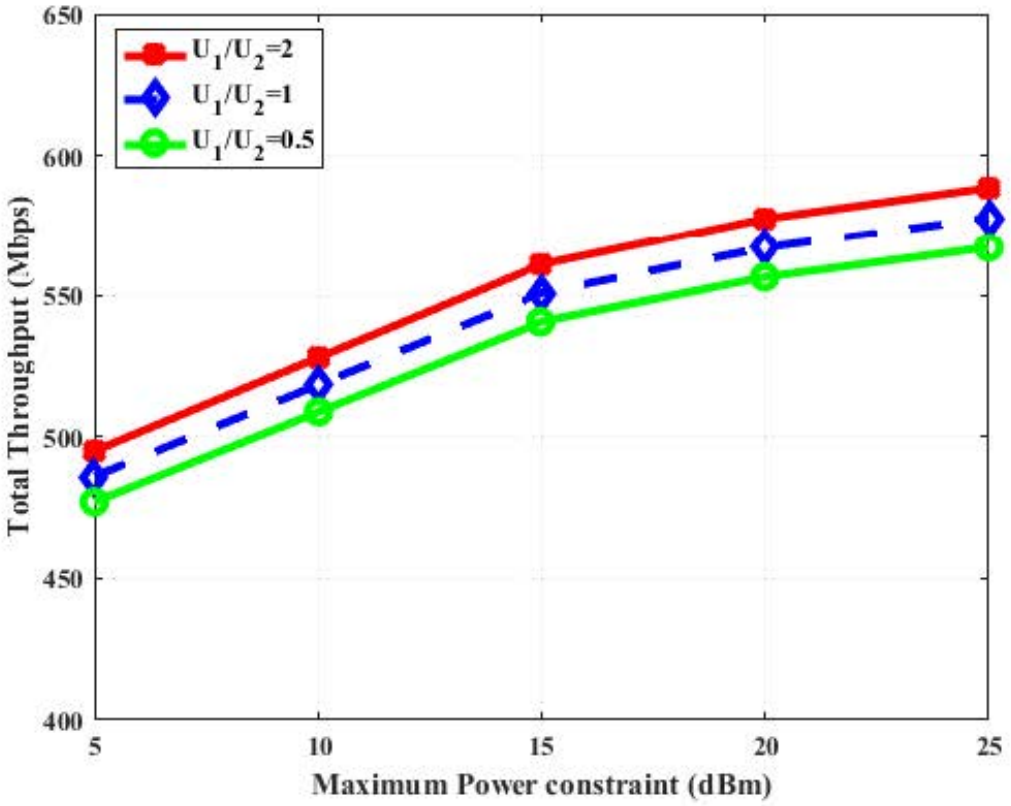

Figure 3.8: Total network throughput versus number of FAPs.

10 FAPs are added in each iteration. The number of RT FUEs is set to 5 while that of NRT and BE FUEs are set to 3. $P_{\max} = 20dBm$ and $I_{th}^{MF} = I_{th}^{FF} = 20dBm$ throughout the simulation. It is observed that the overall throughput is increasing as the number of FAPs increases. This is because the joint optimisation over the FAPs has been able to control the transmit power, cross-tier, and co-tier interference. Also, the proposed algorithm outperforms the existing algorithm and equal power allocation algorithm because the co-tier interference between FAPs has been properly coordinated. This shows that the proposed algorithm is suitable for ultra-dense femtocell networks.

Fig. 3.11 shows the convergence of SORRM and MDSA-HA in terms of average network throughput versus the number of iterations for a minimum of 80 FAPs and maximum of 100

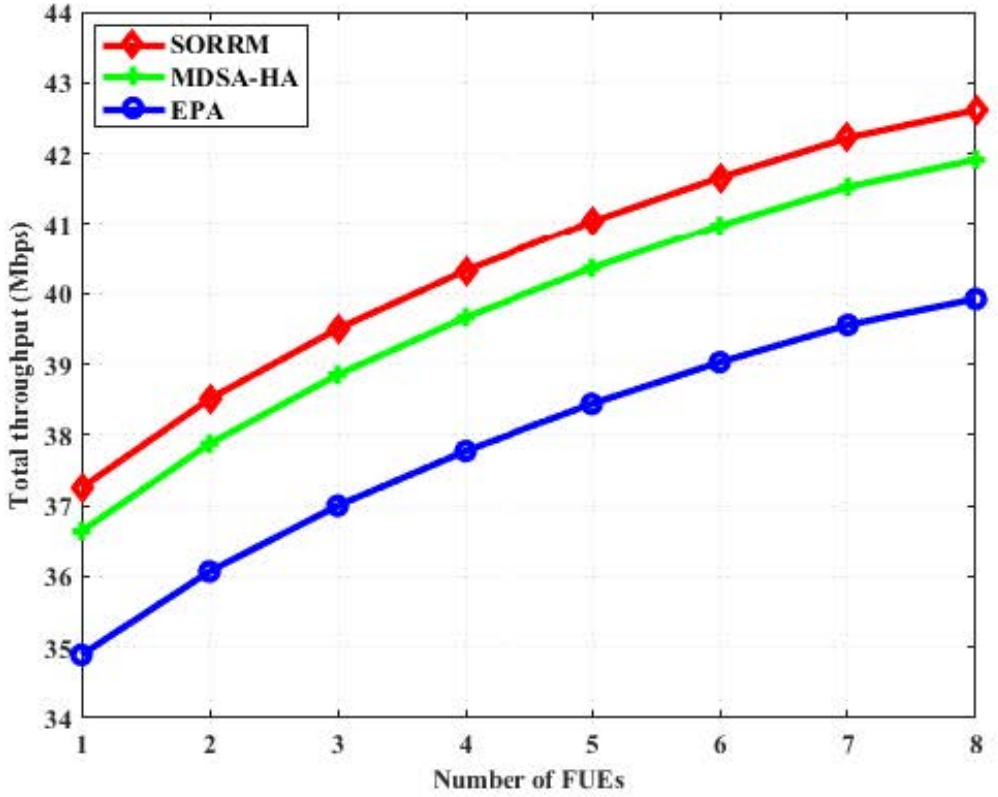

Figure 3.9: Total throughput versus maximum power constraint.

FAPs. R_u^{min} = 8bits/s/Hz for all RT FUEs, $P_{\max}$ = 20dBm, $I_{th}^{MF} = I_{th}^{FF}$ = 20dBm for all subchannels. The locations of the considered 8 UEs per femtocell were kept fixed throughout each simulation.

It is observed from the figure that, the average throughput for 80 FAPs is higher than that of 100 FAPs, this is because co-tier interference increases with the number of femtocells. Additionally, the difference in the performance of the achievable average throughput for 80 and 100 FAPs is not much, this is because co-tier interference has been suppressed to a particular pre-determined value. Also, from the graph, it is observed that the proposed algorithm outperforms the MDSA-HA in terms of the average throughput. This is because the SORRM has taken into consideration the spectrum sensing error and given priority to

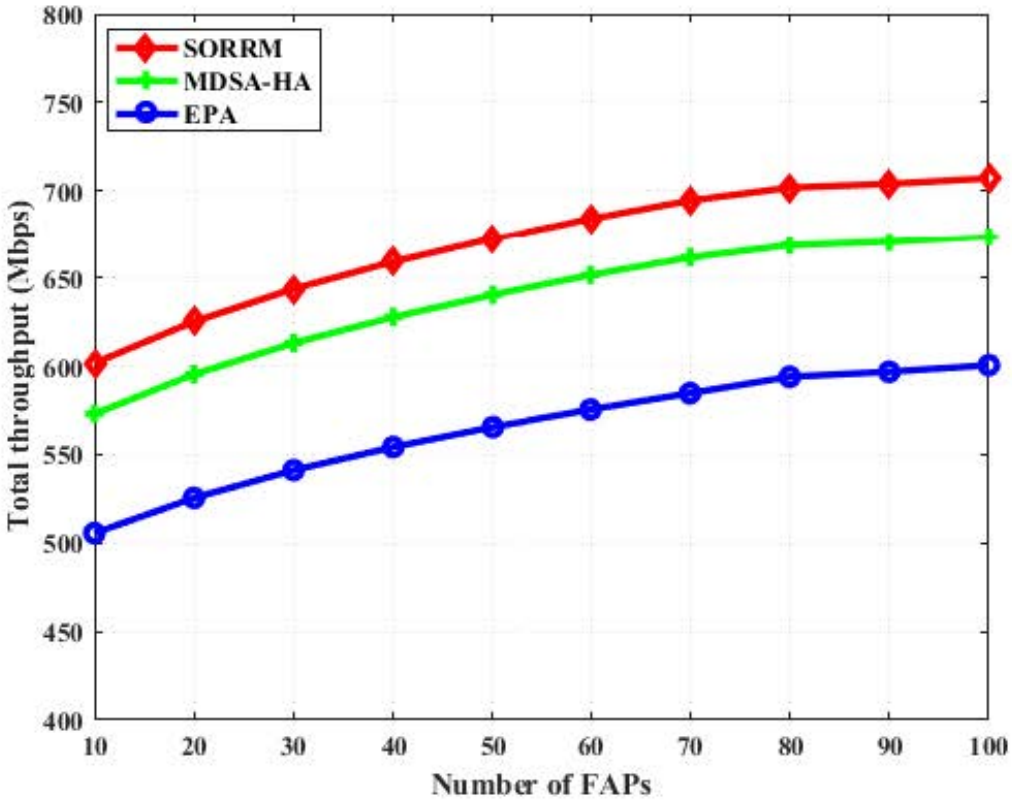

Figure 3.10: Overall network throughput versus number of FAPs

users with real time application. This has improved the network throughput performance. Moreover, SORRM takes only ten iterations to converge to an optimal point. This reveals that the proposed algorithm is appropriate for real implementation of ultra-dense deployment of FAPs.

In Fig. 3.12, the running time of solving the problem of joint subchannel and power allocation using the proposed SORRM, MDSA-HA and exhaustive search method for different number of FAPs from 10 to 100 is shown. The computer used for running the simulations is Intel (R) Core (TM) i7-7500U CPU with 8GB RAM. $R^{\min_u} = 8$bits/s/Hz for all RT FUEs, $P_{\max} = 20$dBm, $I_{th}^{MF} = I_{th}^{FF} = 20$dBm for all subchannels. It is observed that SORRM, MDSA-HA, EPA and the exhaustive method takes 38s, 42s, 44s and 69s

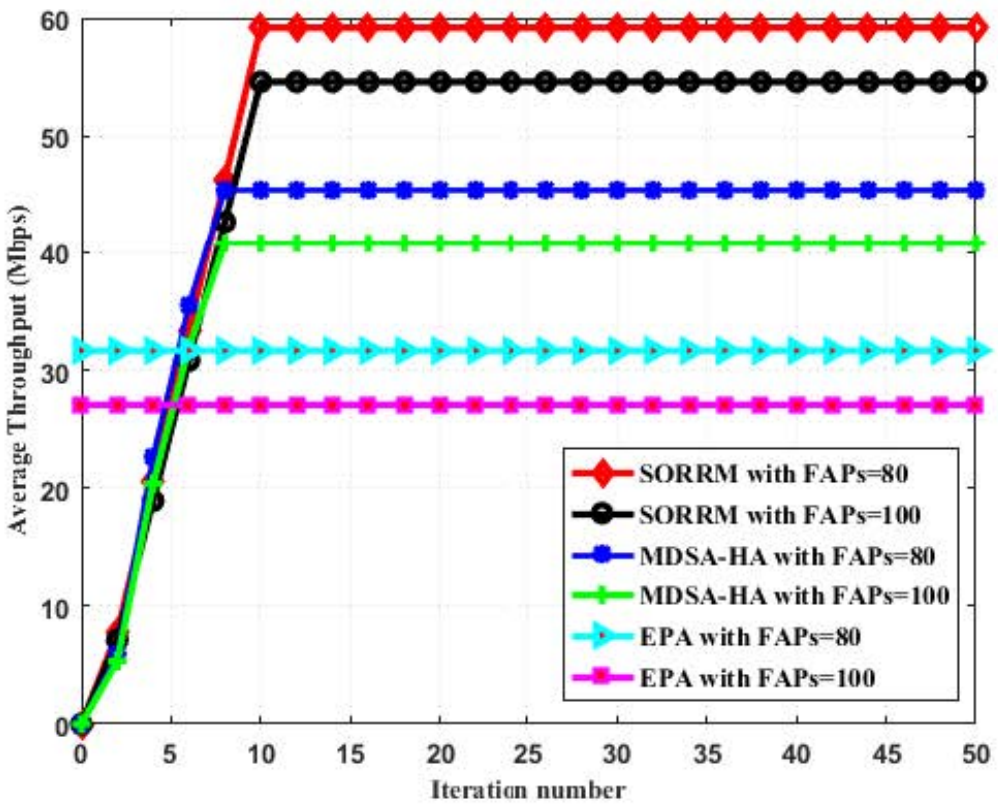

Figure 3.11: Convergence of different algorithms.

respectively to run when 100 FAPs are considered in the simulations. As shown in the figure, the running time of SORRM is very close to that of MDSA-HA and EPA. However, there is a significant reduction in the running time of SORRM as compared with the exhaustive search method.

3.8 Conclusion

In this chapter, a joint subchannel and power problem for throughput maximisation has been formulated as a mixed integer non-linear programming. The formulated optimization problem considers the out-of-band emissions and imperfect spectrum. The problem has been

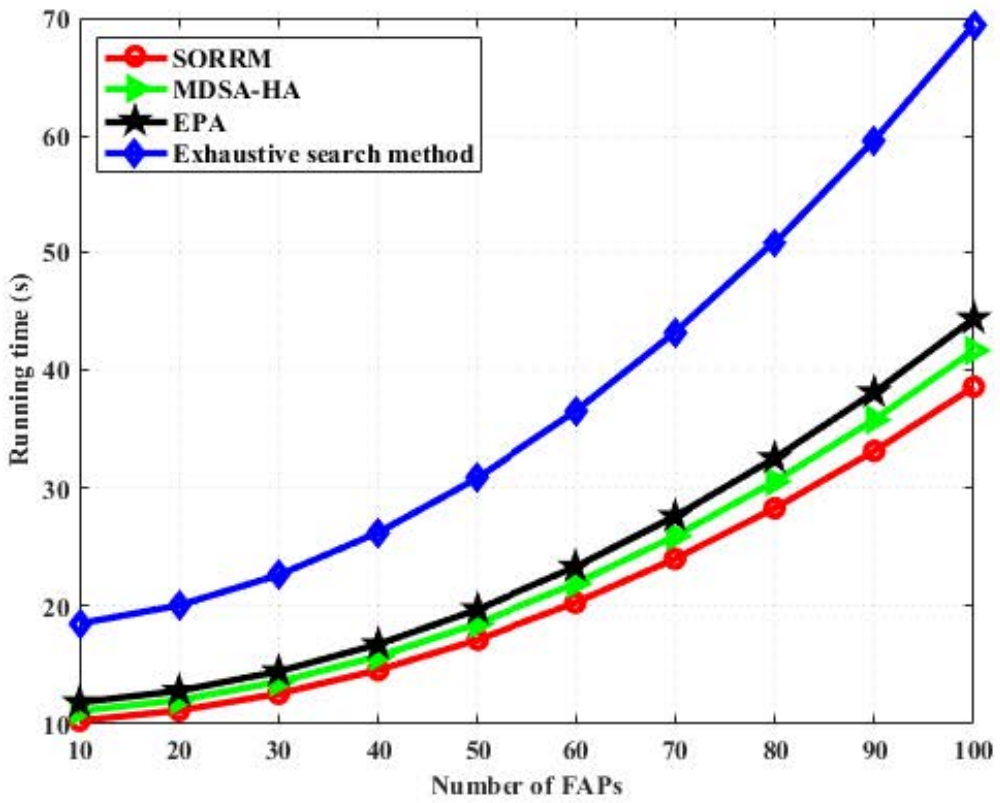

Figure 3.12: The effect of different number of FAPs on the running time for SORRM, MDSA-HA, EPA, and Exhaustive search method.

solved using the method of Lagrangian dual decomposition. Based on the obtained solution, a self-organising radio resource management algorithm has been developed for cognitive femtocell networks to ensure fairness in sharing of radio resources, to minimise cross-tier and co-tier interference and to provide QoS guarantees for different users with heterogeneous services. The computational complexity of the proposed algorithm has been analysed and its performance has been evaluated using MATLAB and compared with the existing algorithms. Simulation results show that the proposed algorithm has a better performance, in terms of interference mitigation and improvement in the overall network throughput. Moreover, extensive simulations demonstrate that the algorithm converges to a near optimal solution.

Finally, the effect of deploying more femtocells on running time has been investigated and there is a significant reduction in the running time of the proposed algorithm as compared with the existing schemes.

Chapter 4

Joint Optimisation of Energy Efficiency and Spectrum Efficiency in 5G Ultra Dense Heterogeneous Networks

4.1 Introduction

The mobile broadband traffic on conventional cellular networks is exploding and the mobile data demand continues to grow in an unprecedented manner due to the advent of smartphones, laptops, tablets and wearable devices with powerful multimedia capabilities and newly introduced applications [33], [59]. Recently, it has been predicted that larger amount of traffic will emanate from indoors in the next few years. Unfortunately, indoor

users suffer reduced received signal strength (RSS) because the transmitted signals from the conventional base stations are weakened by high penetration losses by the time they get to indoor environments.

On the other hand, the explosion of mobile data traffic has led to ever increasing energy consumption and carbon footprint in mobile communication industry. Also, it has been revealed that the escalation of energy consumption in wireless networks results in huge amount of greenhouse gas emission and high operating expenditures (OPEX) [87]. Recently, another report shows that over 80% of the power consumption in mobile telecommunications takes place at the radio access network, more specifically, at the base stations [155]. Hence, the ultra-dense deployment of small cells such as femtocells in the coverage area of the traditional macrocells known as ultra-dense heterogeneous networks (Ultra-dense HetNets) is seen as a cost-efficient solution to address network capacity, indoor coverage and green communications towards sustainable environments in the fifth generation (5G) wireless network. However, the unplanned and ultra-dense deployment of femtocells will lead to increase in total energy consumption, cross-tier and co-tier interference as well as inadequate QoS provisioning. Therefore, there is a need to develop efficient radio resource allocation (RRA) algorithms that will jointly maximise the energy efficiency (EE) and spectrum efficiency (SE).

Moreover, it has been shown in the literature that maximising both the EE and the SE simultaneously is a major challenge in practical wireless network deployments because they conflict with each other, maximising EE results in low performance of SE and vice versa

[126], [155]. Hence, it is very important to make a balanced trade-off between the EE and the SE to achieve the best performance.

4.1.1 Related Work

Most of the previous works on RRA in the literature focused on maximising either the EE or the SE such as the works in [115] and [160]. Interestingly, one of the goals of 5G is to jointly optimise both the EE and the SE [155]. There are very few works on trade-off analysis and joint optimisation of the EE and the SE for downlink orthogonal frequency division multiple access (OFDMA) wireless systems, such as the works in [125], [126] and [161], but cannot be applied directly to ultra-dense HetNets without modification because the works assumed co-tier interference to be negligible, which will not be the case in the networks with the ultra-dense deployment of femtocells. Moreover, these works have not taken the issue of users with different QoS requirements into consideration.

In [126], the authors develop a framework for analysing the SE and the EE trade-off as a Lebesgue measure under different load conditions. The issues of interference and QoS have been considered but the aspect of users' differentiation and fairness, which are also necessary in order to satisfy the QoS requirements of different users have not been addressed. In [161], the authors develop a framework for trade-off analysis as well as joint SE and EE toward green communications but the issue relating to co-tier interference management needs further investigation. Therefore, in the event of ultra-dense deployment of femtocells, the issues relating to cross-tier and co-tier interference, fairness and QoS for the EE and the SE

trade-off analysis needs to be simultaneously considered in order to account for scalability and flexibility in the ultra-dense HetNets.

4.1.2 Contributions and Organisation

In this chapter, three different radio resource allocation algorithms are proposed for the EE maximisation, SE maximisation and joint maximisation of the EE and the SE subject to the constraints of transmit power, QoS, fairness, and interference thresholds for 5G ultra-dense HetNets.

The rest of this chapter is organised as follows: Section 4.2 presents the list of important notations used in this chapter. Section 4.3 discusses the system model such as the achievable rate, signal-to-interference-plus-noise ratio (SINR), overall system throughput and total transmit power. In Section 4.4 and Section 4.5, the issues relating to energy efficiency and spectrum efficiency are discussed respectively. Additionally, the energy-efficient RRA and spectrum-efficient RRA are formulated and solved using the Lagrangian dual decomposition method. Moreover, the energy-efficient and spectrum-efficient RRA algorithms are proposed and the simulation results are discussed. Section 4.6 describes the joint optimisation problem formulation for EE and SE trade-off (EE-SET) for joint power and subchannel allocation. Also, the solution to the formulated optimisation problem, the proposed EE-SET RRA algorithm, and its computational complexity are presented. Moreover, the obtained simulation results are explained and compared with EERRAA and SERRA. Section 4.7 concludes this chapter.

4.2 Notations

The list of important notations used in this chapter is presented in Table 4.1as follows:

Table 4.1: Summary of important symbols II.

Symbol	Description
M	Macro base station
S_n	Set of all femto access points
$\mathcal{U}$	Set of all UEs
S_f	Set of active FUEs
S_m	Set of admitted nearby MUEs
N	Total number of femtocells
U	Total number of all UEs
B	Total Bandwidth of an OFDMA System
K	Total number of subchannels
W	Bandwidth of each subchannel
$\Gamma^{FF}_{n,u,k}$	Channel gain between an FAP n and UE u on subchannel k
$r_{n,u,k}$	Maximum achievable data rate
$\alpha_{n,u,k}$	Subchannel allocation indicator
σ^2	Additive white Gaussian noise (AWGN)
R_T	Overall system throughput.
P_T	Total transmit power
P_c	Sum of circuit power in FAPs
η_{EE}	Energy efficiency
η_{SE}	Spectrum efficiency
λ_{EE}	Normalisation factor associated with energy efficiency
λ_{SE}	Normalisation factor associated with spectrum efficiency

4.3 System Model

In this chapter, the downlink of an OFDMA wireless system comprising one macrocell M also referred to as macro base station (MBS) and a set of femto access points (FAPs) S_n is considered. The MBS serves each associated macro user equipment (MUE) and each FAP n serves its attached femto UEs (FUEs) as illustrated in Fig. 4.1. The hexagon represents the coverage area of an MBS while each circle represents the coverage area of an FAP.

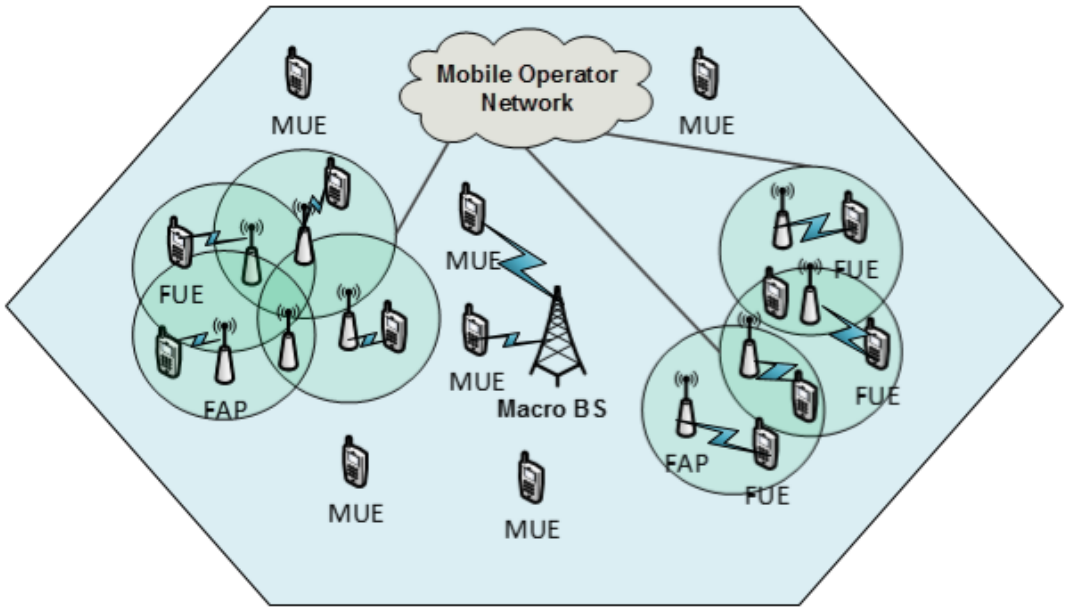

Figure 4.1: The heterogeneous deployment of ultra-dense FAPs overlaying the coverage of an MBS.

Let S_m, and S_f represent the set of admitted nearby MUEs, and the set of active FUEs respectively. Denote N and U as the total number of femtocells and UEs respectively. Therefore, the set of all UEs $\mathcal{U} = S_m \cup S_f$. The total bandwidth B of the OFDMA system is divided into K subchannels. Each subchannel has a bandwidth $W = \frac{B}{K}$.

The maximum achievable data rate (throughput) $r_{n,u,k}$ of UE $u \in \mathcal{U}$ attached to an FAP $n \in S_n$ on subchannel k is given as:

$$r_{n,u,k} = \alpha_{n,u,k} W \log_2 \left(1 + \gamma_{n,u,k}\right) \tag{4.1}$$

where $\alpha_{n,u,k} \in \{0, 1\}$ is the binary index to represent subchannel allocation. $\alpha_{n,u,k} = 1$ denotes that subchannel k is allocated to a UE u; otherwise, $\alpha_{n,u,k} = 0$. $\gamma_{n,u,k}$ is the received signal-to-interference-plus-noise ratio (SINR) at the FAP n from its associated UE u on

subchannel k. It is expressed as:

$$\gamma_{n,u,k} = \frac{p_{n,u,k}\Gamma^{FF}_{n,u,k}}{\sigma^2 + P_{M,j,k}\Gamma^{MF}_{M,j,k} + \sum\limits_{q=1,q\neq n}^{N}\sum\limits_{z=1}^{U} P_{q,z,k}\Gamma^{FF}_{n,u,k}} \tag{4.2}$$

where $p_{n,u,k}$ represents the transmit power used by an FAP $n \in S_n$ to send a signal to a UE u on subchannel k. $\Gamma^{FF}_{n,u,k}$ is the channel gain between an FAP n and UE u on subchannel k. $P_{M,j,k}\Gamma^{MF}_{M,j,k}$ and $\sum\limits_{q=1,q\neq n}^{N}\sum\limits_{z=1}^{U} P_{q,z,k}\Gamma^{FF}_{n,u,k}$ denote the amount of interference which a UE u suffered from other MUE j and other FAP q or FUE z on a subchannel k respectively. σ^2 denotes the additive white Gaussian noise (AWGN) power. Let $\chi_{n,u,k} = \left(\sigma^2 + P_{M,j,k}\Gamma^{MF}_{M,j,k} + \sum\limits_{q=1,q\neq n}^{N}\sum\limits_{z=1}^{U} P_{q,z,k}\Gamma^{FF}_{n,u,k}\right)$, where $\chi_{n,u,k}$ represents interference and noise power.

The overall system throughput R_T and the total transmit power P_T is expressed as in Equation (4.3) and Equation (4.4) respectively:

$$R_T = \sum_{n=1}^{N}\sum_{u=1}^{U}\sum_{k=1}^{K} \alpha_{n,u,k} r_{n,u,k} \tag{4.3}$$

$$P_T = \sum_{n=1}^{N}\sum_{u=1}^{U}\sum_{k=1}^{K} \alpha_{n,u,k} p_{n,u,k} \tag{4.4}$$

4.4 Energy Efficiency (EE)

EE is defined as the ratio of the overall system throughput R_T to the total power consumption $\hat{P}$. It is measured in a number of bits per Joule. Mathematically, it is expressed as:

$$\eta_{EE} = \frac{R_T}{P_T + P_c} = \frac{1}{\hat{P}}\left(\sum_{n=1}^{N}\sum_{u=1}^{U}\sum_{k=1}^{K} \alpha_{n,u,k} r_{n,u,k}\right) \tag{4.5}$$

where P_c is the sum of circuit power in FAPs.

4.4.1 Energy-Efficient Radio Resource Allocation Problem Formulation

Here, the objective is to maximize only the downlink EE of all the FAPs in an HetNet. Moreover, each FUE requires a minimal rate to support its reliable communication, a fair spectrum sharing is also necessary to ensure that an FUE with good channel does not occupy the whole subchannels, while both cross-tier and co-tier interference are kept below their predetermined thresholds. Hence, the energy-efficient radio resource allocation optimization problem is formulated as given in Equation (4.6) under the constraints C1 - C8.

$$\max_{\alpha_{n,u,k}\eta_{EE_{n,u,k}}} \sum_{n=1}^{N}\sum_{u=1}^{U}\sum_{k=1}^{K} \alpha_{n,u,k}\eta_{EE_{n,u,k}} \tag{4.6}$$

$$s.t.\ C1: \sum_{k=1}^{K} \alpha_{n,u,k} \hat{P}_{n,u,k} \leq P_{\max}\ \forall n, u$$

$$C2: \hat{P}_{n,u,k} \geq 0\ \forall n, u, k$$

$$C3: \sum_{k=1}^{K} \alpha_{n,u,k} r_{n,u,k} \geq r_{n,u,k}^{min}\ \forall n, u$$

$$C4: \sum_{u=1}^{U} \alpha_{n,u,k} \leq 1\ \forall n, k$$

$$C5: \alpha_{n,u,k} \in \{0, 1\}$$

$$C6: \beta_{n,u}^{\text{Lower}} \leq \beta_{n,u} \leq \beta_{n,u}^{\text{Upper}}\ \forall n, u, k$$

$$C7: \sum_{n=1}^{N} \sum_{u=1}^{U} \alpha_{n,u,k} \hat{P}_{n,u,k} \tilde{\Gamma}_{n,u,k}^{MF} \leq I_{th}^{MF}\ \forall k$$

$$C8: \sum_{n=1}^{N} \sum_{u=1}^{U} \alpha_{n,u,k} \hat{P}_{n,u,k} \tilde{\Gamma}_{n,u,k}^{FF} \leq I_{th}^{FF}\ \forall k.$$

The constraint C1 denotes the limit on the maximum transmit power. The constraint C2 ensures efficient utilization of power. The constraint C3 is the minimum QoS requirement for every FUE u. The constraint C4 ensures that subchannel k is assigned to at most one user at a time. The constraint C5 can be relaxed in the range of $[0, 1]$, where $\alpha_{n,u,k}$ is the subchannel allocation indicator which is equal to 1 if FUE u occupied a subchannel k, or 0 otherwise. The constraint C6 makes sure that the upper and lower bounds are set on the number of subchannel assigned to each FUE u to ensure fairness in resources sharing. The actual power $\hat{P}_{n,u,k}$ allocated to FUE u in an FAP n can be denoted as $\hat{P}_{n,u,k} = p_{n,u,k} + P_c$. The constraint C7 and C8 express the maximum cross-tier and co-tier interference allowed. $\tilde{\Gamma}_{n,u,k}^{MF}$ and $\tilde{\Gamma}_{n,u,k}^{FF}$ can be obtained from Equations (3.17) and (3.19) respectively.

4.4.2 Solution to the Formulated Energy-Efficient Radio Resource Allocation Problem

The problem in Equation (4.6) can be solved by using the Lagrangian dual decomposition method. The approach has been shown to have lower complexity as compared to other methods such as brute force method [115], [155]. The Lagrangian function of Equation (4.6) is given as:

$$\mathcal{L}^{EE}(\delta,\mu,\varpi,\varrho,\Theta)=\left(\sum_{n=1}^{N}\sum_{u=1}^{U}\sum_{k=1}^{K}\alpha_{n,u,k}\eta_{EE_{n,u,k}}\right)+\sum_{n=1}^{N}\sum_{u=1}^{U}\delta_{n,u}\left(P^{max}-\sum_{k=1}^{K}\alpha_{n,u,k}\hat{P}_{n,u,k}\right)+\sum_{n=1}^{N}\sum_{u=1}^{U}\mu_{n,u}\left(\sum_{k=1}^{K}\alpha_{n,u,k}r_{n,u,k}-r_{n,u}^{min}\right)+\sum_{n=1}^{N}\sum_{k=1}^{K}\varpi_{n,k}\left(1-\sum_{u=1}^{U}\alpha_{n,u,k}\right)+\sum_{k=1}^{K}\varrho_{k}\left(I_{th}^{MF}-\sum_{n=1}^{N}\sum_{u=1}^{U}\alpha_{n,u,k}\hat{P}_{n,u,k}\tilde{\Gamma}_{n,u,k}^{MF}\right)+\sum_{k=1}^{K}\Theta_{k}\left(I_{th}^{FF}-\sum_{n=1}^{N}\sum_{u=1}^{U}\alpha_{n,u,k}\hat{P}_{n,u,k}\tilde{\Gamma}_{n,u,k}^{FF}\right) \tag{4.7}$$

where $\delta,\mu,\varpi,\varrho$, and Θ are the Lagrange multiplier vectors associated with the constraints C1, C3, C4, C7 and C8 respectively. The constraints C2, and C5 are later considered by applying Karush-Kuhn-Tucker (KKT) conditions while constraint C6 is relaxed to an integer. The dual problem corresponding to the primal problem of Equation (4.6) is given by:

$$\min_{\delta,\mu,\varpi,\varrho,\Theta\,\geq\,0}\ \max_{\alpha_{n,u,k},\ \hat{P}_{n,u,k}}\ \mathcal{L}^{EE}(\delta,\mu,\varpi,\varrho,\Theta) \tag{4.8}$$

The Lagrange dual function corresponding to the problem in Equation (4.6) is

$$\vartheta^{EE}(\delta,\mu,\varpi,\varrho,\Theta)=\max_{\alpha_{n,u,k},\ \hat{P}_{n,u,k}}\ \mathcal{L}^{EE}(\delta,\mu,\varpi,\varrho,\Theta) \tag{4.9}$$

The corresponding dual problem to the primal problem of Equation (4.6) is therefore given by

$$\min_{\delta,\mu,\varpi,\varrho,\Theta} \vartheta^{EE}(\delta,\mu,\varpi,\varrho,\Theta)$$
$$s.t.\ \delta \geq 0, \mu \geq 0, \varpi \geq 0, \varrho \geq 0, \Theta \geq 0 \tag{4.10}$$

The dual problem in Equation (4.8) can be decomposed into a slave and a master problems. The slave problem is the inner maximization in Equation (4.8), which is given in Equation (4.9) consisting of Z sub problems solved to compute the subchannel and power allocation for the given values of $\delta, \mu, \varpi, \varrho$, and Θ to obtain energy efficiency maximization. Each FAP solves the slave problem based on the information in each iteration. The outer minimization in Equation (4.8) is given in Equation (4.10) as the master problem in which the Lagrangian multipliers are updated using a sub gradient method (a stochastic process). The MBS in the HetNet solves the master problem.

The optimal power $\hat{P}^*_{n,u,k}$ allocated to an FUE u of an FAP n on a subchannel k to achieve energy efficiency in the network can be obtained by taking the first-order derivatives of Equation (4.7) with respective to $\hat{P}_{n,u,k}$ in constraint C2 of Equation (4.6) as:

$$\frac{\partial \mathcal{L}^{EE}(\delta,\mu,\varpi,\varrho,\Theta)}{\partial \hat{P}^*_{n,u,k}} = A_{n,u,k} - \hbar_{n,u} \geq 0. \tag{4.11}$$

where

$$A_{n,u,k} = \frac{\alpha_{n,u,k}(1+\mu_{n,u})\Gamma^{FF}_{n,u,k}}{\ln 2\left(\alpha_{n,u,k}\chi_{n,u,k} + \hat{P}_{n,u,k}\Gamma^{MF}_{n,u,k}\right)} - \sum_{n=1}^{N} \alpha_{n,u,k}\hat{P}_{n,u,k}\tilde{\Gamma}^{FF}_{n,u,k} - \sum_{n=1}^{N} \alpha_{n,u,k}\hat{P}_{n,u,k}\tilde{\Gamma}^{FF}_{n,u,k}. \tag{4.12}$$

$$\hbar_{n,u}\left(P_{\max} - \sum_{k=1}^{K} \alpha_{n,u,k}\hat{P}_{n,u,k}\right) = 0. \tag{4.13}$$

Therefore, substituting Equation (4.12) and Equation (4.13) into Equation (4.11) yields:

$$\hat{P}^{*}_{n,u,k} = \begin{cases} \left[\dfrac{(1+\mu_{n,u})}{\ln 2 \left(\hbar_{n,u} + \sum\limits_{n=1}^{N} \alpha_{n,u,k} \hat{P}_{n,u,k} \tilde{\Gamma}^{FF}_{n,u,k} + \sum\limits_{n=1}^{N} \alpha_{n,u,k} \hat{P}_{n,u,k} \tilde{\Gamma}^{FF}_{n,u,k} \right)} - \dfrac{\chi_{n,u,k}}{\Gamma^{FF}_{n,u,k}} \right]^{+}, & \text{if } \alpha^{*}_{n,u,k} = 1 \\ 0, & \text{otherwise} \end{cases} \tag{4.14}$$

where $[x]^{+} = \max[0, x]$. Similarly, to obtain the optimal subchannel $\alpha^{*}_{n,u,k}$ allocated to an FUE u in an FAP n, the first-order derivatives of Equation (4.7) is taking with respect to $\alpha_{n,u,k}$. This gives:

$$\frac{\partial \mathcal{L}^{EE}(\delta, \mu, \varpi, \varrho, \Theta)}{\partial \alpha^{*}_{n,u,k}} = D_{n,u,k} - \varpi_{n,k} \geq 0. \tag{4.15}$$

where

$$\begin{aligned} D^{EE}_{n,u,k} &= (1 + \mu_{n,u}). \\ \log 2 \left(\frac{\hat{P}^{*}_{n,u,k} \Gamma^{FF}_{n,u,k}}{\chi_{n,u,k}} \right) - \frac{1}{\ln 2} \left(\frac{\hat{P}^{*}_{n,u,k} \Gamma^{FF}_{n,u,k}}{\hat{P}^{*}_{n,u,k} \Gamma^{FF}_{n,u,k} + \chi_{n,u,k}} \right) &= 0. \end{aligned} \tag{4.16}$$

$$\alpha_{n,u,k} \left(D^{EE}_{n,u,k} - \varpi_{n,k} \right) = 0 \tag{4.17}$$

$$\varpi_{n,k} \left(1 - \sum_{u=1}^{U} \alpha_{n,u,k} \right) = 0 \tag{4.18}$$

Hence, the optimal subchannel $\alpha^{*}_{n,u,k}$ allocated to an FUE u^{*} in an FAP n is obtained by

substituting (4.33)-(4.18) into (4.15). This gives

$$\alpha^*_{n,u,k} = \begin{cases} 1, & \text{if } (n,u^*,k) = \arg\max D^{EE}_{n,u,k} \\ 0, & \text{otherwise} \end{cases} \tag{4.19}$$

The master problem in Equation (4.10) can be solved using a sub gradient method, which iteratively updates in the sub gradient direction until convergence. The update can be performed as:

$$\delta^{(\ell+1)}_{n,u} = \left[\delta^{\ell}_{n,u} - \Lambda^{(\ell)}_1\left(P_{\max} - \sum_{k=1}^{K}\alpha_{n,u,k}\hat{P}_{n,u,k})\right)\right]^+, \ \forall n,h \tag{4.20}$$

$$\mu^{(\ell+1)}_{n,u} = \left[\mu^{(\ell)}_{n,u} - \Lambda^{(\ell)}_2\left(\alpha_{n,u,k}r_{n,u,k} - R^{min}_{n,u})\right)\right]^+ \forall n,u \tag{4.21}$$

$$\varpi^{(\ell+1)}_{n,k} = \left[\varpi^{(\ell)}_{n,k} - \Lambda^{(\ell)}_3\left(1 - \sum_{u=1}^{U}\alpha_{n,u,k}\right)\right]^+ \forall n,k \tag{4.22}$$

$$\varrho^{(\ell+1)}_{k} = \left[\varrho^{(\ell)}_{n,k} - \Lambda^{(\ell)}_4\left(I^{FM}_{th,k} - \sum_{n=1}^{N}\sum_{u=1}^{U}\alpha_{n,u,k}\hat{P}_{n,u,k}\tilde{\Gamma}^{MF}_{n,u,k}\right)\right]^+ \tag{4.23}$$

$$\Theta^{(\ell+1)}_{n,k} = \left[\Theta^{(\ell)}_{n,k} - \Lambda^{(\ell)}_5\left(I^{FF}_{th,k} - \sum_{q=1}^{N}\sum_{w=1}^{U}\alpha_{n,u,k}\hat{P}_{n,u,k}\tilde{\Gamma}^{FF}_{n,u,k}\right)\right]^+ \tag{4.24}$$

where $\Lambda^{(\ell)}_1, \Lambda^{(\ell)}_2, \Lambda^{(\ell)}_3, \Lambda^{(\ell)}_4$ and $\Lambda^{(\ell)}_5$ are the iteration step sizes.

4.4.3 Energy-Efficient Radio Resource Allocation Algorithm

The proposed Energy-Efficient Radio Resource Allocation Algorithm (EERRAA) is defined as follows:

Algorithm 4.1: EERRAA

1: **FAP set**: $(n \in \{1, 2, ..., N\})$,

subchannel set: $(k \in \{1, 2, ..., K\})$

FUE set: $(u \in \{1, 2, ..., U\})$

2: **Initialisation**: set $\alpha_{n,u,k}$, $\hat{P}_{n,u,k}$, δ, μ, ϖ, ϱ, and $\Theta = 0$

3: **For FAP;**

4: **each FAP** measures $\Gamma^{FF}_{n,u,k}$ and calculates $r_{n,u,k}$, $\gamma_{n,u,k}$.

$\tilde{\Gamma}^{MF}_{n,u,k}$, $\tilde{I}^{FF}_{n,u,k}$ according to Equations (3.17), (3.19), (4.1), and (4.2) respectively.

5: **while** $\beta^{\text{Lower}}_{n,u} \leq \beta_{n,u} \leq \beta^{\text{Upper}}_{n,u}$ each FAP

do (a) allocate power equally to each subchannel

(b) computes $\hat{P}^{*}_{n,u,k}$ and $\alpha^{*}_{n,u,k} = 1$

6: **end while**

7: **for** k = 1 to K,

8: **each FAP** $\boldsymbol{n}$ updates δ, μ, ϖ, and ϱ, according to

Equations (4.20), (4.21), (4.22) and (4.24) respectively.

9: **end for**

10: **For the MBS;**

11: MBS estimates Θ, according to (4.23) and sends the updated value

to all FAPs through a common control subchannel.

12: until convergence

4.4.4 Simulation Results and Discussions

In this section, the performance of the proposed EERRAA is analysed through extensive simulations and its performance is compared with the existing algorithm in [160]. The simulation parameters are as shown in Table 4.2.

Table 4.2: Simulation Parameters I

Parameter	**Value**
MBS transmit power	46dBm
FAP transmit power	(0-30dBm)
MBS coverage radius	500m
FAP coverage radius	10m
Carrier frequency	2.6GHz
Carrier bandwidth	20MHz
White noise power density	-174dBm/Hz
Path loss model (indoor-to-indoor)	$38.46+20\log10(R)+0.7d$
Path loss model (outdoor-to-indoor)	$40\log10(R)+20\log10(f)$
Path loss exponent	4
Lognormal shadowing between an MBS and MUEs	8dB
Lognormal shadowing between an FAP and FUEs	10dB

An HetNet with an MBS and a total number of $N = 100$ FAPs is considered. The path loss models for FUEs and MUEs are based on [66]. The total circuit power consumption is set to 20dBm. The cross-tier and co-tier interference are set to 20dBm. The probabilities of mis-detection and false alarm errors are set to [0.01, 0.05], [0.05, 0.1] according to [115] while MUE's occupation is in the range of [0, 1]. The simulated results are obtained using MATLAB.

Fig. 4.2 shows the EE of different RRA algorithms in each subchannel versus the number of various FAP sizes from 10 to 100. The number of FUEs attached to each FAP in this simulation is 6. Equal power allocation has the worst EE because it allocates an equal

maximum transmit power, as the number of FAPs increases, throughput decreases as a result of co-tier interference thus leading to a significant decline in EE of the overall network. Also,

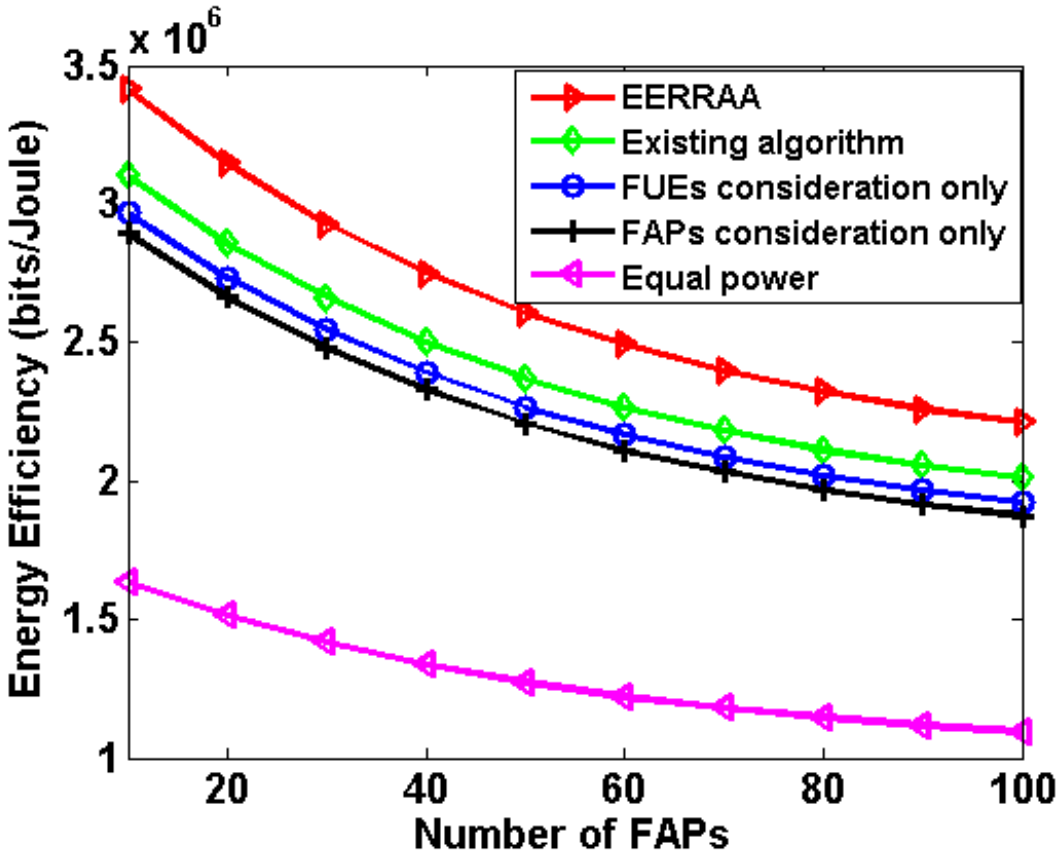

Figure 4.2: EE of different RRA algorithms versus the number of FAPs.

it is observed that EE decreases as only the FUE circuit power consumption is considered, the more the number of FUEs, the greater the circuit power that will be consumed which results in low EE. Considering only the FAPs transmission power also leads to low EE as more FAPs are added to the network. It can be concluded that the proposed EERRAA maximizes the EE in the overall network by 12.9%, 16.67%, 18.64%, and 25.1% as compared to the existing algorithm, FUEs consideration only, FAPs consideration only and equal power allocation respectively.

Fig. 4.3 shows the EE of the network with a different number of MUEs and FUEs. The EE declines with the increasing number of MUEs. The reason is that more MUEs means fewer subchannels will be available to FUEs. FUEs can use the subchannel utilised by other FUEs or MUEs since both the co-tier and cross-tier interference are kept below predetermined thresholds. It is observed that the rate of decrease of the proposed algorithm is gradual with a different number of FUEs and MUEs as compared with the existing algorithm.

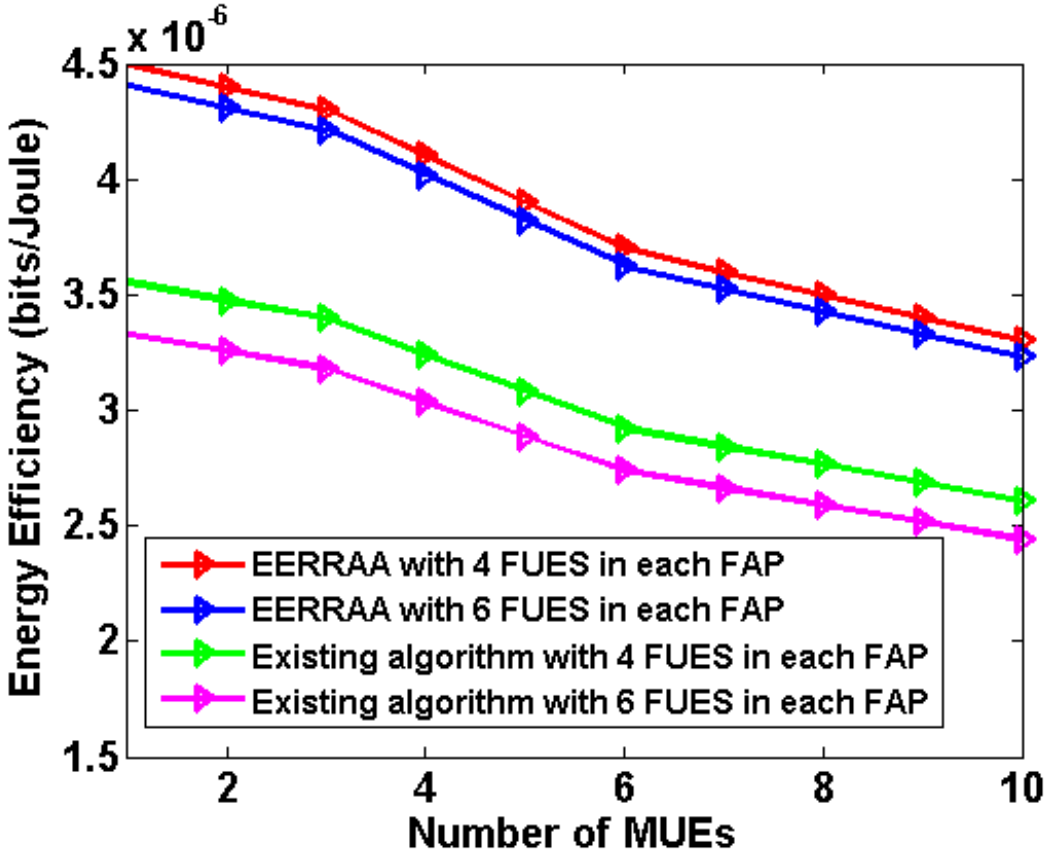

Figure 4.3: EE of the network with a different number of MUEs and FUEs.

Fig. 4.4 shows the convergence performance of the proposed algorithm in terms of EE with the number of iterations for a maximum of 100 FAPs. It is observed that the EE performance of the EERRAA reaches 4.5Mbits/Joule while the EE performance of the existing algorithm reaches 4Mbits/Joule. Also, the algorithms converge to an optimal point

within twenty iterations. It shows that the EERRAA is suitable for implementation of the ultra-densely deployment of FAPs.

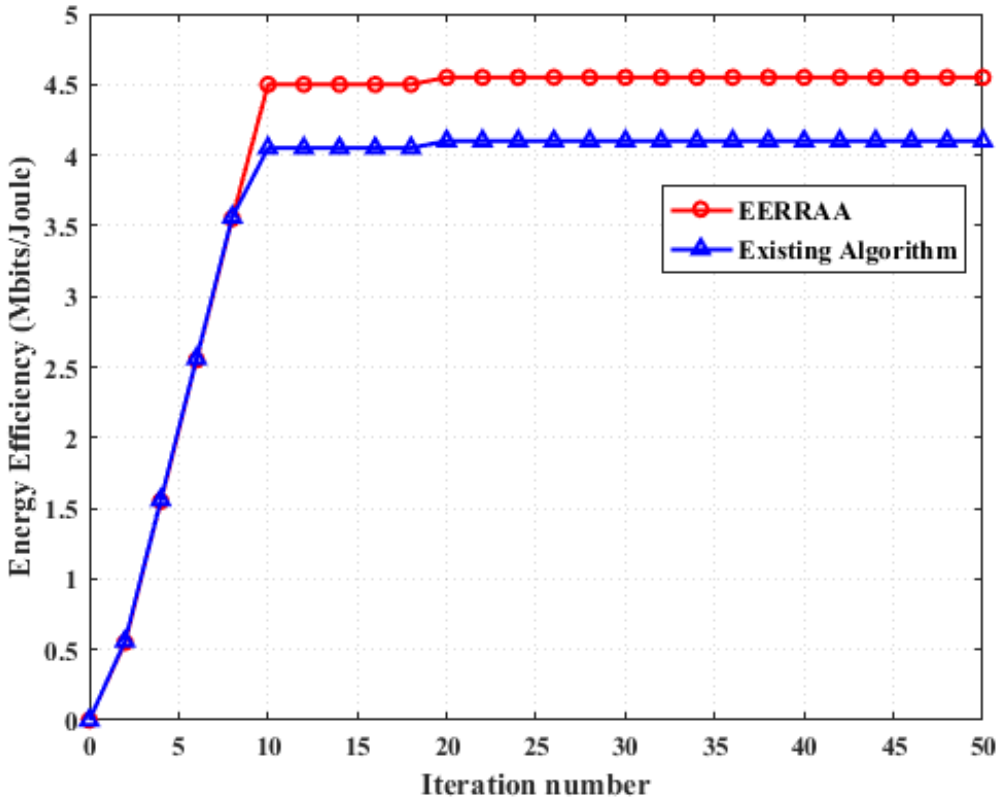

Figure 4.4: Convergence of the EERRAA and existing algorithm in terms of energy efficiency versus the number of iterations.

4.5 Spectrum Efficiency (SE)

SE is a measure of how efficient radio resource is utilised, which is defined as the ratio of the overall system throughput R_T to the bandwidth. It is measured in a number of bits per

seconds per Hertz (bits/s/Hz). Mathematically, it is expressed as:

$$\eta_{SE} = \frac{R_T}{B} = \frac{1}{B}\left(\sum_{n=1}^{N}\sum_{u=1}^{U}\sum_{k=1}^{K}\alpha_{n,u,k}r_{n,u,k}\right) \tag{4.25}$$

4.5.1 Spectrum-Efficient Radio Resource Allocation Problem Formulation and Solution

The objective here is to maximize the downlink SE of all the FAPs in an HetNet subject to constraints C1 to C8 in Equation (4.6). Hence, the spectrum efficient radio resource allocation optimization problem is formulated as in Equation (4.26) under the constraints C1 - C8.

$$\max_{\bar{\alpha}_{n,u,k}\eta_{SE_{n,u,k}}} \sum_{n=1}^{N}\sum_{u=1}^{U}\sum_{k=1}^{K}\bar{\alpha}_{n,u,k}\eta_{SE_{n,u,k}} \tag{4.26}$$

$$s.t.\ C1: \sum_{k=1}^{K}\bar{\alpha}_{n,u,k}\bar{P}_{n,u,k} \leq P_{\max}\ \forall n,u$$

$$C2: \bar{P}_{n,u,k} \geq 0\ \forall n,u,k$$

$$C3: \sum_{k=1}^{K}\bar{\alpha}_{n,u,k}r_{n,u,k} \geq r_{n,u,k}^{min}\ \forall n,u$$

$$C4: \sum_{u=1}^{U}\bar{\alpha}_{n,u,k} \leq 1\ \forall n,k$$

$$C5: \bar{\alpha}_{n,u,k} \in \{0,1\}$$

$$C6: \beta_{n,u}^{\text{Lower}} \leq \beta_{n,u} \leq \beta_{n,u}^{\text{Upper}}\ \forall n,u,k$$

$$C7: \sum_{n=1}^{N}\sum_{u=1}^{U}\bar{\alpha}_{n,u,k}\bar{P}_{n,u,k}\tilde{\Gamma}_{n,u,k}^{MF} \leq I_{th}^{MF}\ \forall k$$

$$C8: \sum_{n=1}^{N}\sum_{u=1}^{U}\bar{\alpha}_{n,u,k}\bar{P}_{n,u,k}\tilde{\Gamma}_{n,u,k}^{FF} \leq I_{th}^{FF}\ \forall k.$$

where $\bar{\alpha}_{n,u,k}$ is the subchannel allocation indicator which is equal to 1 if FUE u occupied a subchannel k, or 0 otherwise. The actual power $\bar{P}_{n,u,k}$ allocated to FUE u in an FAP n can be denoted as $\bar{P}_{n,u,k} = p_{n,u,k} + P_c$. The problem in Equation (4.26) can be solved by using the Lagrangian dual decomposition method. The Lagrangian function of Equation (4.26) is given as:

$$\mathcal{L}^{SE}(\delta,\mu,\varpi,\varrho,\Theta) = \left(\sum_{n=1}^{N}\sum_{u=1}^{U}\sum_{k=1}^{K}\bar{\alpha}_{n,u,k}\eta_{SE_{n,u,k}}\right) + \sum_{n=1}^{N}\sum_{u=1}^{U}\delta_{n,u}\left(P_{\max} - \sum_{k=1}^{K}\bar{\alpha}_{n,u,k}\bar{P}_{n,u,k}\right) + \sum_{n=1}^{N}\sum_{u=1}^{U}\left(\sum_{k=1}^{K}\bar{\alpha}_{n,u,k}r_{n,u,k} - r_{n,u}^{min}\right)\mu_{n,u} + \sum_{n=1}^{N}\sum_{k=1}^{K}\varpi_{n,k}\left(1 - \sum_{u=1}^{U}\bar{\alpha}_{n,u,k}\right) + \sum_{k=1}^{K}\varrho_k\left(I_{th}^{MF} - \sum_{n=1}^{N}\sum_{u=1}^{U}\bar{\alpha}_{n,u,k}\bar{P}_{n,u,k}\tilde{\Gamma}_{n,u,k}^{MF}\right) + \sum_{k=1}^{K}\Theta_k\left(I_{th}^{FF} - \sum_{n=1}^{N}\sum_{u=1}^{U}\bar{\alpha}_{n,u,k}\bar{P}_{n,u,k}\tilde{\Gamma}_{n,u,k}^{FF}\right) \tag{4.27}$$

The dual problem corresponding to the primal problem of Equation (4.26) is given by:

$$\min_{\delta,\mu,\varpi,\varrho,\Theta \,\geq\, 0}\ \max_{\alpha_{n,u,k},\ \hat{P}_{n,u,k}}\ \mathcal{L}^{SE}(\delta,\mu,\varpi,\varrho,\Theta) \tag{4.28}$$

The Lagrange dual function corresponding to the problem in Equation (4.26) is

$$\vartheta^{SE}(\delta,\mu,\varpi,\varrho,\Theta) = \max_{\bar{\alpha}_{n,u,k},\ \hat{P}_{n,u,k}}\ \mathcal{L}^{SE}(\delta,\mu,\varpi,\varrho,\Theta) \tag{4.29}$$

The corresponding dual problem to the primal problem of Equation (4.28) is therefore given by

$$\begin{aligned} &\min_{\delta,\mu,\varpi,\varrho,\Theta}\ \vartheta^{SE}(\delta,\mu,\varpi,\varrho,\Theta) \\ &s.t.\ \delta \geq 0, \mu \geq 0, \varpi \geq 0, \varrho \geq 0, \Theta \geq 0 \end{aligned} \tag{4.30}$$

The dual problem in Equation (4.28) is decomposed into a slave and a master problems. The slave problem is the Equation (4.29), which consists of Z sub problems solved to compute the subchannel and power allocation for the given values of $\delta, \mu, \varpi, \varrho$, and Θ to achieve spectrum efficiency maximization in the network. The master problem is given in Equation (4.30), which the Lagrangian multipliers are updated using a sub gradient method.

The optimal power $\bar{P}^{*}_{n,u,k}$ allocated to an FUE u of an FAP n on a subchannel k to achieve spectrum efficiency maximization can be obtained by taking the first-order derivatives of Equation (4.27) with respective to $\bar{P}_{n,u,k}$. It can be expressed using the same approach as Equations (4.11)-(4.13):

$$\bar{P}^{*}_{n,u,k} = \begin{cases} \left[\frac{(1+\mu_{n,u})}{\ln 2 \left(\hbar_{n,u} + \sum\limits_{n=1}^{N} \bar{\alpha}_{n,u,k} \bar{P}_{n,u,k} \tilde{\Gamma}^{FF}_{n,u,k} + \sum\limits_{n=1}^{N} \bar{\alpha}_{n,u,k} \bar{P}_{n,u,k} \tilde{\Gamma}^{FF}_{n,u,k} \right)} - \frac{\chi_{n,u,k}}{\Gamma^{FF}_{n,u,k}} \right]^{+}, & \text{if } \bar{\alpha}^{*}_{n,u,k} = 1 \\ 0, & \text{otherwise} \end{cases} \tag{4.31}$$

where $[x]^{+} = \max[0, x]$. Similarly, by taking the first-order derivatives of Equation (4.27) with respect to $\bar{\alpha}_{n,u,k}$ this gives the optimal subchannel $\bar{\alpha}^{*}_{n,u,k}$ allocated to an FUE u in an FAP n as

$$\alpha^{*}_{n,u,k} = \begin{cases} 1, & \text{if } (n, u^{*}, k) = \arg\max D^{SE}_{n,u,k} \\ 0, & \text{otherwise} \end{cases} \tag{4.32}$$

where

$$D^{SE}_{n,u,k} = (1+\mu_{n,u}).$$
$$\log 2\left(\frac{\bar{P}^{*}_{n,u,k}\Gamma^{FF}_{n,u,k}}{\chi_{n,u,k}}\right) - \frac{1}{\ln 2}\left(\frac{\bar{P}^{*}_{n,u,k}\Gamma^{FF}_{n,u,k}}{\bar{P}^{*}_{n,u,k}\Gamma^{FF}_{n,u,k}+\chi_{n,u,k}}\right) = 0. \tag{4.33}$$

Also, the master problem in Equation (4.30) can be solved using a sub gradient method, which iteratively update in the sub gradient direction until convergence. The update can be performed as analogous to Equations 4.20-4.24 by replacing $\bar{\alpha}_{n,u,k}$ and $\bar{P}_{n,u,k}$ with $\bar{\alpha}_{n,u,k}$ and $\bar{P}_{n,u,k}$ respectively. This yields:

$$\delta^{(\ell+1)}_{n,u} = \left[\delta^{\ell}_{n,u} - \Lambda^{(\ell)}_{1}\left(P_{\max} - \sum_{k=1}^{K}\bar{\alpha}_{n,u,k}\bar{P}_{n,u,k})\right)\right]^{+}, \ \forall n,u \tag{4.34}$$

$$\mu^{(\ell+1)}_{n,u} = \left[\mu^{(\ell)}_{n,u} - \Lambda^{(\ell)}_{2}\left(\bar{\alpha}_{n,u,k}r_{n,u,k} - R^{min}_{n,u})\right)\right]^{+} \ \forall n,u \tag{4.35}$$

$$\varpi^{(\ell+1)}_{n,k} = \left[\varpi^{(\ell)}_{n,k} - \Lambda^{(\ell)}_{3}\left(1 - \sum_{u=1}^{U}\bar{\alpha}_{n,u,k}\right)\right]^{+} \ \forall n,k \tag{4.36}$$

$$\varrho^{(\ell+1)}_{k} = \left[\varrho^{(\ell)}_{n,k} - \Lambda^{(\ell)}_{4}\left(I^{FM}_{th,k} - \sum_{n=1}^{N}\sum_{u=1}^{U}\bar{\alpha}_{n,u,k}\bar{P}_{n,u,k}\tilde{\Gamma}^{MF}_{n,u,k}\right)\right]^{+} \tag{4.37}$$

$$\Theta^{(\ell+1)}_{n,k} = \left[\Theta^{(\ell)}_{n,k} - \Lambda^{(\ell)}_{5}\left(I^{FF}_{th,k} - \sum_{q=1}^{N}\sum_{w=1}^{U}\bar{\alpha}_{n,u,k}\bar{P}_{n,u,k}\tilde{\Gamma}^{FF}_{n,u,k}\right)\right]^{+} \tag{4.38}$$

where $\Lambda^{(\ell)}_{1}, \Lambda^{(\ell)}_{2}, \Lambda^{(\ell)}_{3}, \Lambda^{(\ell)}_{4}$ and $\Lambda^{(\ell)}_{5}$ are the iteration step sizes.

4.5.2 Spectrum-Efficient Radio Resource Allocation Algorithm

The propose spectrum-efficient radio resource allocation algorithm (SERRAA) is defined as follows:

Algorithm 4.2: SERRAA

1: **FAP set**: $(n \in \{1, 2, ..., N\})$, **subchannel set**: $(k \in \{1, 2, ..., K\})$

FUE set: $(u \in \{1, 2, ..., U\})$

2: **Initialisation**: set $\bar{\alpha}_{n,u,k}$, $\bar{P}_{n,u,k}$, $P^{M}_{n,u,k}$, δ, μ, ϖ, ρ, and $\theta = 0$

3: **For the FAP;**

4: **each FAP** measures $\Gamma^{FF}_{n,u,k}$ and calculates $r_{n,u,k}$, $\gamma_{n,u,k}$, $\tilde{I}^{MF}_{n,u,k}$, and $\tilde{I}^{FF}_{n,u,k}$ according to Equations (3.18), (3.20) (4.1), and (4.2) respectively.

5: **while** $\beta^{L}_{n,u} \leq \beta_{n,u} \leq \beta^{U}_{n,u}$ each FAP

do (a) allocate power equally to each subcarrier

(b) computes $\bar{P}^{*}_{n,u,k}$ and $\bar{\alpha}^{*}_{n,u,k} = 1$

6: **end while**

7: **for** k = 1 to K,

8: **each FAP** $\boldsymbol{n}$ updates δ, μ, ϖ, and ϱ, according to Equations (4.34), (4.35), (4.36) and (4.38) respectively.

9: **end for**

10: **For the MBS;**

11: MBS estimates Θ, according to (4.37) and sends the updated value to all FAPs through a common control subchannel.

12: until convergence

4.5.3 Simulation Results and Discussions

In this section, the performance of the proposed SERRAA in algorithm 4.2 is analysed through extensive simulations and its performance is compared with the existing algorithm in [160]. The simulation parameters are selected as shown in Table 4.2 and Section (4.4.4).

Fig. 4.5 shows the SE of different RRA algorithms versus the number of various FAP sizes from 10 to 100. The number of FUEs attached to each FAP in this simulation is 6. Equal

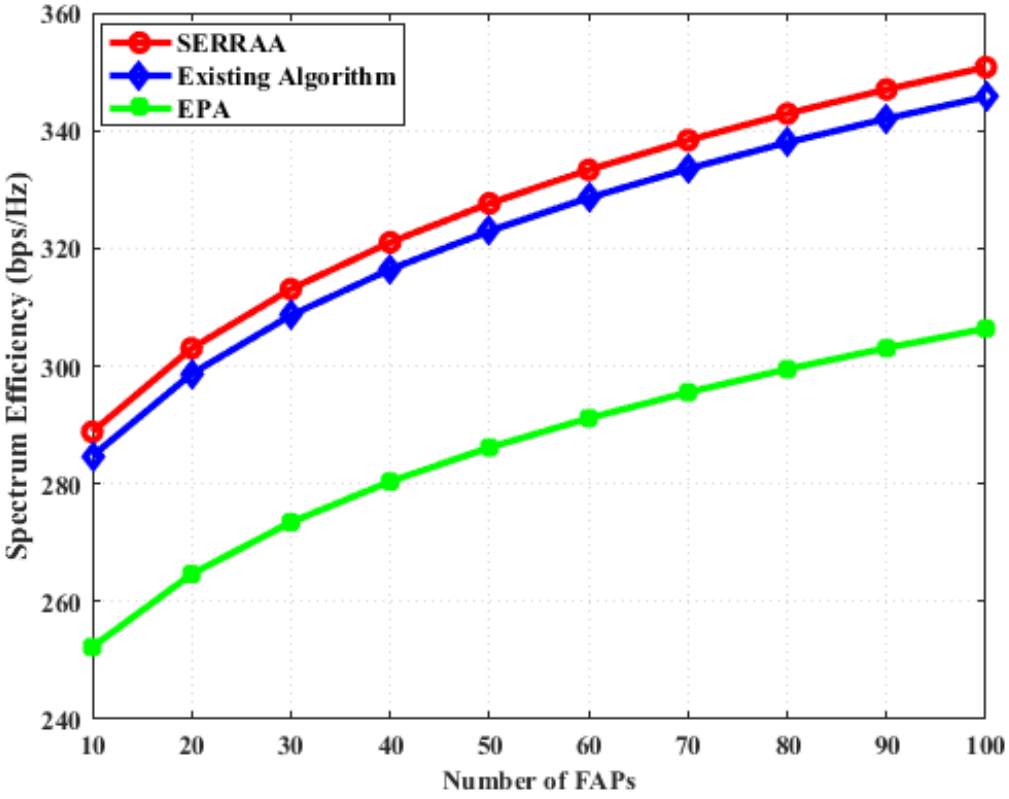

Figure 4.5: SE of different RRA algorithms versus the number of FAPs.

power allocation has the worst SE because it allocates an equal maximum transmit power, as the number of FAPs increases. The throughput increases as a result of more deployment of FAPs in the network thus leading to a significant increase in SE of the overall network.

Also, it is observed that the proposed SERRAA outperforms the existing algorithm and the equal power allocation, this is because cross-tier and co-tier interference that degrades the performance of SE has been limited to a particular pre-determined value. It can be concluded that the proposed algorithm maximises the SE in the overall network by 11.9% and 26.67%, as compared to the existing algorithm, and equal power allocation respectively.

Fig. 4.6 shows the SE of the network with a different number of MUEs and FUEs.

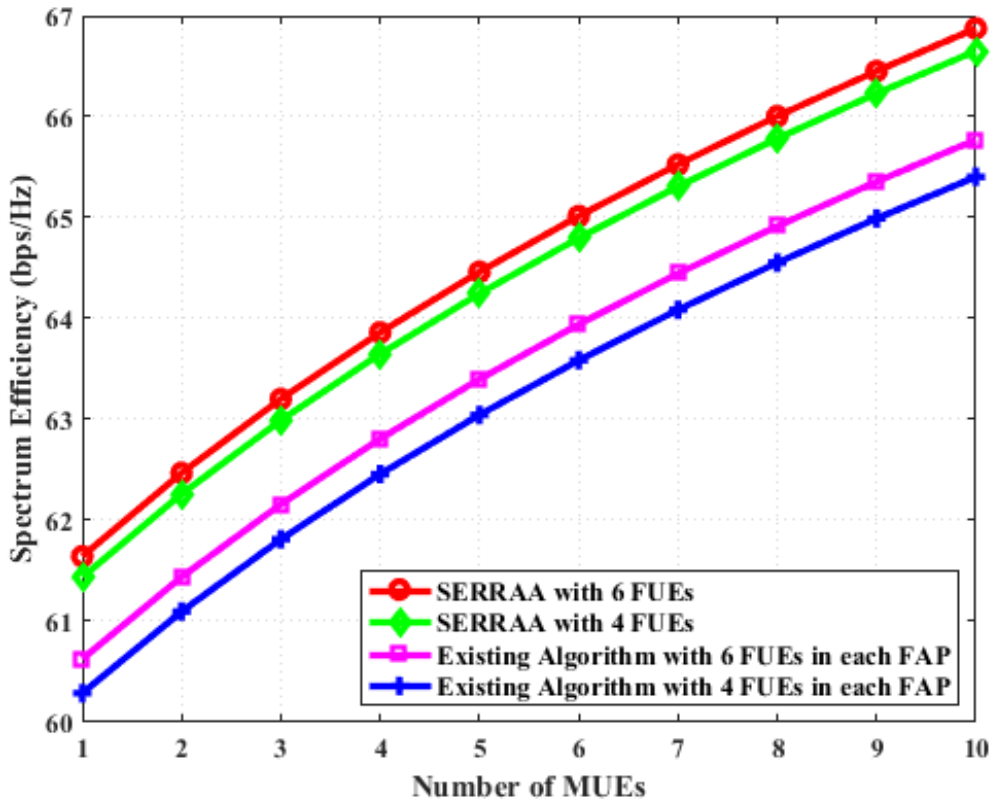

Figure 4.6: SE of the network with a different number of MUEs and FUEs.

The SE increases with more FUEs and MUEs in the network. The reason is that more FUEs in the network means more subchannels will be utilized. FUEs can use the subchannels utilised by other FUEs or MUEs since both the co-tier and cross-tier interference are kept below predetermined thresholds. It is observed that the proposed algorithm outperforms the

existing algorithm with a different number of FUEs and MUEs. This signifies that SERRAA can be utilized with the massive deployment of femtocells to obtain higher SE performance.

Fig. 4.7 shows the convergence performance of the proposed SERRAA in terms of SE with the number of iterations for a maximum of 100 FAPs. The algorithm converges within ten iteration times. It shows that the SERRAA is suitable for implementation of the ultra-densely deployment of FAPs. Also, the obtained SE performance is higher than the existing algorithm after convergence.

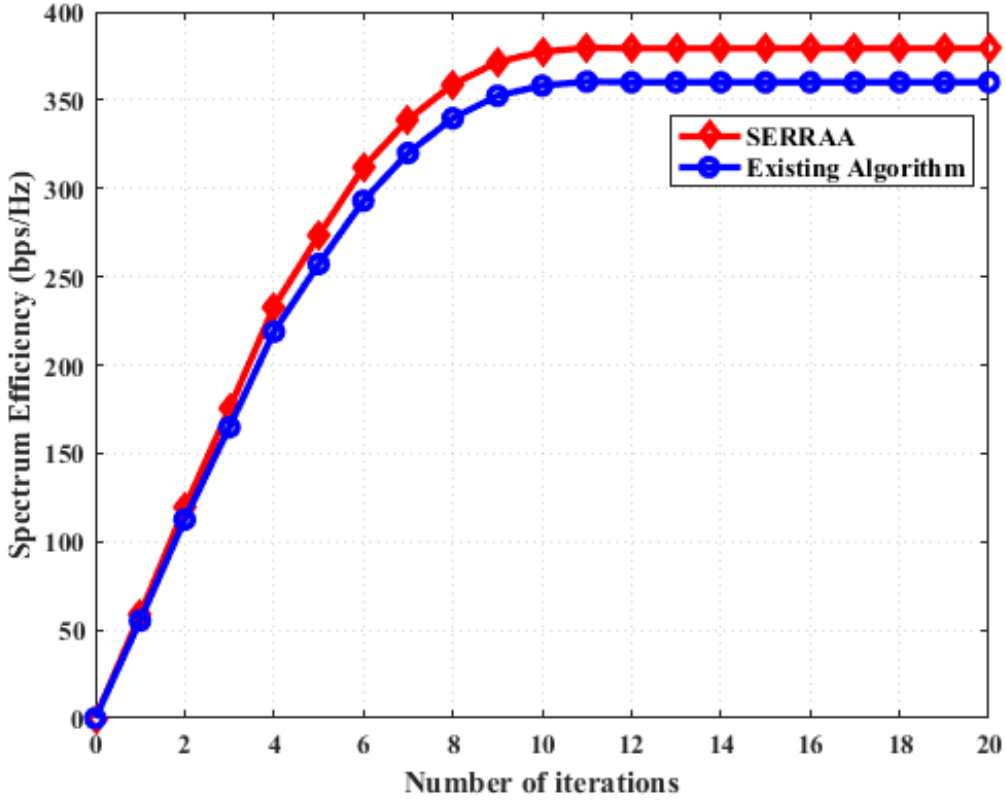

Figure 4.7: Convergence of the proposed SERRAA and the existing algorithm in terms of spectrum efficiency versus the number of iterations.

4.6 Joint Energy Efficiency and Spectrum Efficiency

Here, the objectives are to jointly maximise the EE and SE simultaneously and to achieve an optimal EE and SE (EE-SE) trade-off. The EE and SE trade-off based RRA problem is formulated as a multi-objective optimisation problem (MOP). However, in order to find the Pareto-optimal solution, the problem is converted into a single-objective optimisation problem (SOP) using the weighted sum method. An iterative framework is developed to solve the SOP using the Lagrangian dual decomposition (LDD) method. Based on the obtained solution, an SE-EE trade-off (EE-SET) RRA algorithm is proposed, which achieves an optimal solution with polynomial complexity, compared to an exponential complexity required by direct search methods. The performance of the proposed algorithm is evaluated using MATLAB. Finally, it is demonstrated through extensive simulations that the proposed algorithm converges to an optimal value.

4.6.1 Joint EE and SE Radio Resource Allocation Problem Formulation

The joint EE and SE radio resource allocation problem is formulated as an MOP as:

$$\max_{\alpha_{n,u,k} p_{n,u,k}} \{\eta_{EE}, \eta_{SE}\} \quad s.t.\ P_0 \in \mathbf{P} \tag{4.39}$$

where $\mathbf{P} = P_T | P_{\min} \leq P_T \leq P_{\max}$ is the transmit power constraint. To solve the problem, the concept of Pareto optimality is used as defined in [162], which is stated as:

Definition 1: A point $P_0 \in \mathbf{P}$ is said to be Pareto optimal if and only if there is no other point $P_1 \in \mathbf{P}$, such that $\eta_{EE}(P_1) \geq \eta_{EE}(P_0)$, $\eta_{SE}(P_1) \geq \eta_{SE}(P_0)$ and at least one η_{EE} or η_{SE} has been strictly improved.

The set of all Pareto optimal points indicates an optimal trade-off between η_{EE} and η_{SE} such that it provides the maximum value of η_{EE} for a given η_{SE} or vice versa. In simple words, a point is Pareto optimal if there is no other point that can improve the EE and SE simultaneously. The weighted sum method is capable of providing the set of all Pareto optimal points by solving the MOP in Equation (4.39). Moreover, in order to put both the EE and the SE on the same scale, the normalisation factors λ_{EE} and λ_{SE} associated with EE and SE respectively are introduced. The MOP in Equation (4.39) is then converted into an SOP η using the weighted sum method as shown below:

$$\tilde{\eta} = \max_{\alpha_{n,u,k} n,u,k} \{w\lambda_{EE}\eta_{EE} + (1-w)\lambda_{SE}\eta_{SE}\} \tag{4.40}$$

$$s.t.\ C1: \sum_{k=1}^{K} \alpha_{n,u,k} \tilde{P}_{n,u,k} \leq P_{\max}\ \forall n, u$$

$$C2: \tilde{P}_{n,u,k} \geq 0\ \forall n, u, k$$

$$C3: \sum_{u=1}^{U} \alpha_{n,u,k} \leq 1\ \forall n, u$$

$$C4: 0 \leq \alpha_{n,u,k} \leq 1\ \forall n, u, k$$

$$C5: \sum_{n=1}^{N} \sum_{u=1}^{U} \alpha_{n,u,k} r_{x,u,k} \geq r_{n,u,k}^{min}\ \forall n \in S_f$$

$$C6: \frac{\sum_{n=1}^{N} \sum_{k=1}^{K} \alpha_{n,u,k} r_{n,u,k}}{\sum_{n \in S_n} \sum_{k \in S_k} r_{n,u,k}} = \varphi_{n,u,k}\ \forall u \in S_m$$

$$C7: \sum_{n=1}^{N} \sum_{u=1}^{U} \alpha_{n,u,k} \tilde{P}_{n,u,k} \tilde{\Gamma}_{n,u,k}^{MF} \leq I_{th}^{MF}\ \forall k$$

$$C8: \sum_{n=1}^{N} \sum_{u=1}^{U} \alpha_{n,u,k} \tilde{P}_{n,u,k} \tilde{\Gamma}_{n,u,k}^{FF} \leq I_{th}^{FF}\ \forall k$$

where w represents a scalable and flexible EE-SE trade-off variable such that $0 \leq w \leq 1$. The constraints C1 and C2 keep the transmit power at the FAP n to its attached UE u on subchannel k below the maximum power budget. C3 ensures that a subchannel is assigned to at most one UE u at a time in an FAP n. C4 ensures that $\alpha_{n,u,k} = 1$ if a subchannel k is allocated to a UE u attached to an FAP n or 0 otherwise. C5 guarantees a reliable transmission performance for all UEs in CSG. C6 sets a proportional fairness for all admitted MUEs in the coverage area of a femtocell. C7 enforces a cross-tier interference temperature limit to protect the transmission of a macrocell while C8 imposes a co-tier interference temperature limit to protect neighbouring femtocells from interfering with each other.

For better tractability, the integer variable $\alpha_{n,u,k} \in \{0, 1\}$ is relaxed into a continuous variable $\hat{\alpha}_{n,u,k} \in [0, 1]$. Therefore, the SOP in Equation (4.40), can be re-written as:

$$\eta = \frac{\tilde{\eta}}{\lambda_{EE}} = \max_{\hat{\alpha}_{n,u,k} tilde P_{n,u,k}} \eta_{EE}\left(1 + \beta\left(\frac{\lambda_{SE}\eta_{SE}}{\lambda_{EE}\eta_{EE}}\right)\right) \tag{4.41}$$

$$s.t.\ C1: \sum_{k=1}^{K} \hat{\alpha}_{n,u,k}\tilde{P}_{n,u,k} \leq P_{\max}\ \forall n, u$$

$$C2: \hat{P}_{n,u,k} \geq 0\ \forall n, u, k$$

$$C3: \sum_{u=1}^{U} \hat{\alpha}_{n,u,k} \leq 1\ \forall n, k$$

$$C4: \hat{\alpha}_{n,u,k} \in [0, 1]\ \forall n, u, k$$

$$C5: \sum_{n=1}^{N}\sum_{u=1}^{U} \hat{\alpha}_{n,u,k} r_{x,u,k} \geq r_{n,u,k}^{min}\ \forall n \in S_f$$

$$C6: \frac{\sum_{n=1}^{N}\sum_{k=1}^{K} \hat{\alpha}_{n,u,k} r_{n,u,k}}{\sum_{n\in S_n}\sum_{k\in S_k} r_{n,u,k}} = \varphi_{n,u,k}\ \forall u \in S_m$$

$$C7: \sum_{n=1}^{N}\sum_{u=1}^{U} \hat{\alpha}_{n,u,k}\tilde{P}_{n,u,k}\tilde{\Gamma}_{n,u,k}^{MF} \leq I_{th,k}^{MF}\ \forall k$$

$$C8: \sum_{n=1}^{N}\sum_{u=1}^{U} \hat{\alpha}_{n,u,k}\tilde{P}_{n,u,k}\tilde{\Gamma}_{n,u,k}^{FF} \leq I_{th,k}^{FF}\ \forall k$$

where $\beta \in [0, \infty] = \frac{1-w}{w}$, and it denotes the weighted coefficient. The problem in Equation (4.41) has two properties, which can be stated as follows:

Property 1: The optimal transmit power $\tilde{P}_{n,u,k}^{*}$ to achieve the optimal η^{*} is non-decreasing with β. When $\beta = 0$, the $\tilde{P}_{n,u,k}^{*} = P_{\eta_{EE}}^{*}$, and the problem in Equation (4.41) becomes EE maximisation problem. When $0 < \beta < \infty$, the $p_{n,u,k}^{*}$ strictly increases with β until it approaches the $P_{\max}$. Hence, the $\tilde{P}_{n,u,k}^{*}$ shifts from $P_{\eta_{EE}}^{*}$ towards the $P_{\max}$

Property 2: The η_{EE} and η_{SE} are non-increasing and non-decreasing with the β respectively, if we assume β_1 and β_2 to represent different weighted coefficients such that

$\beta_2 > \beta_1$, then $\tilde{P}^*_{n,u,k}|_{\beta_2} > \tilde{P}^*_{n,u,k}|_{\beta_1}$ Hence, η_{EE} decreases with $\tilde{P}^*_{n,u,k}$ while η_{SE} increases with $\tilde{P}^*_{n,u,k}$ beyond $P^*_{\eta_{EE}}$. The properties have been verified in Fig. 4.8 and 4.9.

The problem in Equation (4.41) is a combinatorial fractional programming problem. It is equivalent to a subtractive form optimisation problem $\mathcal{H}(\eta)$ in Equation (4.42) motivated by [163] to obtain optimal EE-SE trade-off η^* as:

$$\mathcal{H}(\eta) = \max_{\alpha_{\hat{n,u,k}}\tilde{P}_{n,u,k}} \left\{ \sum_{n=1}^{N}\sum_{u=1}^{U}\sum_{k=1}^{K} \alpha_{\hat{n,u,k}} r_{n,u,k}\left(1+\beta\left(\frac{\lambda_{SE}\eta_{SE}}{\lambda_{EE}\eta_{EE}}\right)\right) - \eta^*(\tilde{P})\sum_{n=1}^{N}\sum_{u=1}^{U}\sum_{k=1}^{K}\hat{\alpha}_{n,u,k}\tilde{P}_{n,u,k} \right\} \tag{4.42}$$

$$s.t.\ C1 - C8 \ \text{ in Equation (4.41)}$$

It should be noted that $\mathcal{H}(\eta)$ monotonically decreases when η increases. Therefore, the optimal EE-SE trade-off η^* is obtained by finding the root of $\mathcal{H}(\eta)$.

Lemma 1: $\mathcal{H}(\eta) = 0$ if and only if (iff) $\eta = \eta^*$. The lemma implies that when $\eta \to -\infty$, $\mathcal{H}(\eta) > 0$, on the other hand, when $\eta \to \infty$, $\mathcal{H}(\eta) < 0$. Therefore, $\mathcal{H}(\eta) > 0$, when $\eta \leq 0$ because the first and second terms of Equation (4.42) are positive. Hence, $\mathcal{H}(\eta) = 0$ occurs at $\eta > 0$. As a result, Equation (4.42) is solved for $(\eta) > 0$.

4.6.2 Solution to the Joint SE and EE Radio Resource Allocation Problem Formulation

In this section, an iterative algorithm for solving the subtractive form optimisation problem $\mathcal{H}(\eta)$ in Equation (4.42) is proposed such that the condition stated in lemma 1 is satisfied for power and subchannel allocation based on the Lagrangian dual decomposition method. The

method involves three steps which are: formulation of the dual decomposition, solution of dual decomposition and updating the dual variables using the sub gradient method. The LDD approach is shown in [115] and [155] to have lower computational complexity as compared to the exhaustive search.

4.6.2.1 Formulation of the dual decomposition

In order to apply the LDD method, the Lagrangian function of Equation (4.42) is given as:

$$\begin{aligned}\mathcal{L}(\Phi,\hbar,\Omega,\theta,\rho) = &\left\{\sum_{n=1}^{N}\sum_{u=1}^{U}\sum_{k=1}^{K}\hat{\alpha}_{n,u,k}r_{n,u,k}\left(1+\beta\left(\frac{\lambda_{SE}\eta_{SE}}{\lambda_{EE}\eta_{EE}}\right)\right)-\eta^{*}(\tilde{P})\sum_{n=1}^{N}\sum_{u=1}^{U}\sum_{k=1}^{K}\hat{\alpha}_{n,u,k}\tilde{P}_{n,u,k}\right\}\\ &+\sum_{n=1}^{N}\sum_{u=1}^{U}\Phi_{n,u}\left(P_{\max}-\sum_{k=1}^{K}\hat{\alpha}_{n,u,k}\hat{P}_{n,u,k}\right)+\sum_{n=1}^{N}\sum_{u=1}^{U}\Omega n,u\left(\sum_{k=1}^{K}\hat{\alpha}_{n,u,k}r_{n,u,k}-r_{n,u,k}^{min}\right)\\ &+\sum_{n=1}^{N}\sum_{k=1}^{K}\hbar_{n,k}\left(1-\sum_{u=1}^{U}\hat{\alpha}_{n,u,k}\right)+\sum_{k=1}^{K}\theta_{k}\left(I_{th,k}^{MF}-\sum_{n=1}^{N}\sum_{u=1}^{U}\hat{\alpha}_{n,u,k}\tilde{P}_{n,u,k}\tilde{\Gamma}_{n,u,k}^{MF}\right)\\ &+\sum_{k=1}^{K}\rho_{k}\left(I_{th,k}^{FF}-\sum_{n=1}^{N}\sum_{u=1}^{U}\hat{\alpha}_{n,u,k}\tilde{P}_{n,u,k}\tilde{\Gamma}_{n,u,k}^{FF}\right)\end{aligned} \tag{4.43}$$

where $\Phi,\hbar,\Omega,\theta$, and ρ represent the Lagrangian multipliers associated with C1, C3, C5, C7 and C8 respectively. The Karush-Kuhn-Tucker (KKT) condition is applied to the boundary conditions in C2, C4, and C6, which are equivalent to zero.

4.6.2.2 Solution of the dual decomposition

The dual problem corresponding to the primal problem of Equation (4.43) is given by:

$$\min_{\Phi,\hbar,\Omega,\theta,\rho\,\geq\,0}\ \max_{\Phi,\alpha,}\ \mathcal{L}(\Phi,\hbar,\Omega,\theta,\rho) \tag{4.44}$$

The Equation (4.44) has to be decomposed into a slave and a master problems to solve it. Therefore, the slave problem is the inner maximisation in Equation (4.44) comprising Z sub problems solved to compute the optimal power and subchannel allocation. The optimal power $\tilde{P}^{*}_{n,u,k}$ allocated to UE u on subchannel k and the optimal subchannel $\hat{\alpha}^{*}_{n,u,k}$ assignment to ensure energy efficiency and spectrum efficiency trade-off can be obtained as Equation (4.45) and Equation (4.46) after few mathematical computations respectively:

$$\hat{\alpha}^{*}_{n,u,k} = r_{n,u,k}\left(\beta\left[\frac{\lambda_{SE}\eta_{SE}}{\lambda_{EE}\eta_{EE}}+1\right]\Omega x, n - \hat{P}(\Phi_{n,u}+\theta_k\tilde{I}^{MF}_{th}+\rho_k\tilde{I}^{FF}_{th}\right). \tag{4.45}$$

$$\hat{P}^{*}_{n,u,k} = \left[\frac{W\left(1+\beta\left[\frac{\lambda_{SE}\eta_{SE}}{\lambda_{EE}\eta_{EE}}+\Omega_{x,n}\right]\right)}{ln2\left(\Phi_{n,u}+\sum_{k=1}^{K}\theta_k\tilde{I}^{MF}_{th,k}+\sum_{k=1}^{K}\rho_k\tilde{I}^{FF}_{th,k}\right)}-\frac{1}{\gamma_{n,u,k}}\right]^{+}. \tag{4.46}$$

4.6.2.3 Updating the dual decomposition

The master problem is the outer minimisation in Equation (4.44). The function is differentiable, therefore, it can be solved using a sub gradient method, which iteratively updates the Lagrange multipliers until $\ell = \ell^{max} = 50$ (convergence condition), where ℓ is the number of iteration and ℓ^{max} is the maximum number of iteration. The update is performed as follows:

$$\Phi_{n,u}(\ell+1) = \left[\Phi_{n,u}(\ell) - s_1(\ell)\left(P_{\max}-\sum_{k=1}^{K}\hat{\alpha}_{n,u,k}\tilde{P}_{n,u,k}\right)\right]^{+} \tag{4.47}$$

$$\hbar_{n,k}(\ell+1) = \left[\hbar_{n,k}(\ell) - s_2(\ell)\left(1-\sum_{u=1}^{U}\hat{\alpha}_{n,u,k}\right)\right]^{+} \tag{4.48}$$

$$\Omega_{n,u}(\ell+1) = \left[\Omega_{n,u}(\ell) - s_3(\ell)\left(\sum_{k=1}^{K}\hat{\alpha}_{n,u,k}r_{n,u,k}-r^{min}_{n,u,k}\right)\right]^{+} \tag{4.49}$$

$$\theta_k(\ell+1) = \left[\theta_k(\ell) - s_4(\ell)\left(I_{th,k}^{MF} - \sum_{n=1}^{N}\sum_{u=1}^{U}\hat{\alpha}_{n,u,k}\tilde{P}_{n,u,k}\tilde{\Gamma}_{n,u,k}^{MF}\right)\right]^{+} \tag{4.50}$$

$$\rho_k(\ell+1) = \left[\rho_k(\ell) - s_5(\ell)\left(I_{th,k}^{FF} - \sum_{n=1}^{N}\sum_{u=1}^{U}\hat{\alpha}_{n,u,k}\tilde{P}_{n,u,k}\tilde{\Gamma}_{n,u,k}^{FF}\right)\right]^{+}, \tag{4.51}$$

where $s_1(\ell),\ s_2(\ell),\ s_3(\ell),\ s_4(\ell)$ and $s_5(\ell)$ are the iteration step sizes.

4.6.3 Joint SE and EE Trade-off Radio Resource Allocation Algorithm and its Computational Complexity Analysis

The procedure for the proposed algorithm is shown as follows:

Algorithm 4.3: EE-SE trade-off RRA Algorithm

Step 1: Initialise $\hat{\alpha}_{n,u,k}$, $\tilde{P}_{n,u,k}$, Φ, $\hbar$, Ω, θ and $\rho = 0$

Step 2: For each FAP, calculate $\gamma_{n,u,k}$ using Equation (4.2)

Step 3: For $k = 1 : K$

(a) calculate η^* using Equation (4.42)

(b) computes $\hat{\alpha}^*_{n,u,k}$ and $\tilde{P}^*_{n,u,k}$ according to Equations (4.45) and (4.46)

Step 4: For $k = 1 : K$,

$\ell = \ell + 1$

update $\Phi, \hbar, \Omega$, and ρ using the Equations

(4.47), (4.48), (4.49), and (4.51) respectively.

Step 5: For the MBS, estimate θ, using Equation (4.50) and

sends the updated value to all FAPs

through a common dedicated subchannel.

Step 6: Repeat step 2 to 5 until $\ell = \ell^{max}$.

The proposed algorithm requires the complexity of $O(NKlog_2U)$ to determine the Lagrange multipliers for different users. Its complexity is $O(\ell^{max})$ in each iteration to find the optimal subchannel $\hat{\alpha}^*_{n,u,k}$ and power $\tilde{P}^*_{n,u,k}$ in each FAP, where ℓ^{max} is the maximum number of iterations for the algorithm to converge to an optimal point. The worse-case complexity of finding a suitable subchannel is $O(NUlog_2K)$. Therefore, the overall complexity of the proposed algorithm is $O(NKlog_2U) + O(\ell^{max}) + O(NUlog_2K) = O(NUK\ell^{max}(log_2U + log_2K))$, compared with the exhaustive search, which has an exponential complexity of $O(NU)^K$.

4.6.4 Simulation Results and Discussions

The performance of EE-SE trade-off RRA algorithm is evaluated in MATLAB environment. A two-tier downlink ultra-dense HetNet consisting of 1 MBS and 100 FAPs with 10m each is considered.

4.6.4.1 Simulation Environment

The simulation parameters are set according to [115] and the 3GPP radio access network standard [66]. The path loss is modelled according to [66]. The channel gains are modelled as independent identically distributed (i.i.d.). The carrier frequency and channel bandwith are set to 2GHz. The channel bandwidth is set to 20 MHz and it is divided into 100 subchannels. The thermal noise density is -174dBm/Hz. The maximum transmit power for an MBS is 46dBm. The values of maximum transmit power, cross-tier and co-tier interference thresholds for an FAP are varied at each simulation. The value of circuit power is set to 20dBm. The values of λ_{SE} and λ_{EE} are set to 22dBm and 3×10^4 Hz respectively. The minimum rate requirement is set to 4bits/s/Hz for each user. The upper and lower bound on subchannel assignment for each user are set to 2 and 20 respectively. Table 4.3 summarises some of the parameters used for simulation.

4.6.4.2 Performance Evaluation

Fig. 4.8 shows the relationship between EE and SE trade-off for various values of $P_{\max}$ and $I_{th} = I_{th}^{MF} = I_{th}^{FF} = -90dBm$. The values λ_{SE} and λ_{EE} are set to 22dBm and 3×10^4 such that it achieves highest η_{SE} and η_{EE}. It was observed that as the values of $\beta > 0$, η_{EE}

Table 4.3: Simulation parameters II

Parameter	Value
MBS transmit power	46dBm
FAP transmit power	(0-30dBm)
MBS coverage radius	500m
FAP coverage radius	10m
Number of MBS	1
Number of FAPs	100
Carrier frequency	2.6GHz
Carrier bandwidth	20MHz
White noise power density	-174dBm/Hz
MBS antenna gain	15 dBi
FAP antenna gain	2 dBi
femto UE antenna gain	1 dBi
macro UE antenna gain	1 dBi
Path loss exponent	4
Lognormal shadowing between an MBS and MUEs	8dB
Lognormal shadowing between an FAP and FUEs	10dB

decreases and maximum η_{EE} is achieved when $\beta = 0$. Also, η_{EE} and η_{SE} are non-increasing and non-decreasing respectively. $P^*_{\eta_{EE}}$ is the energy-efficient transmit power at which the optimal η_{EE} can be obtained while $P_{\max}$ is the maximum power at which the optimal η_{SE} is achieved. It is observed from the figure that the values of η_{EE} and η_{SE} are marginally close between 0-18Mbits/J/Hz and 0-6bits/s/Hz. Also, it is noticed that when the values of transmit power is set to 20 dBm, the maximum achievable η_{EE} and η_{SE} are 33 Mbits/J/Hz and 19 bits/s/Hz respectively.

Fig. 4.9 shows the relationship between EE and SE trade-off for various values of $P_{\max}$ and $I_{th} = I^{MF}_{th} = I^{FF}_{th} = 20dBm$. λ_{SE} and λ_{EE} are selected such that it achieves highest η_{SE} and η_{EE}.We also noticed that when the values of transmit power is set to 20 dBm, the

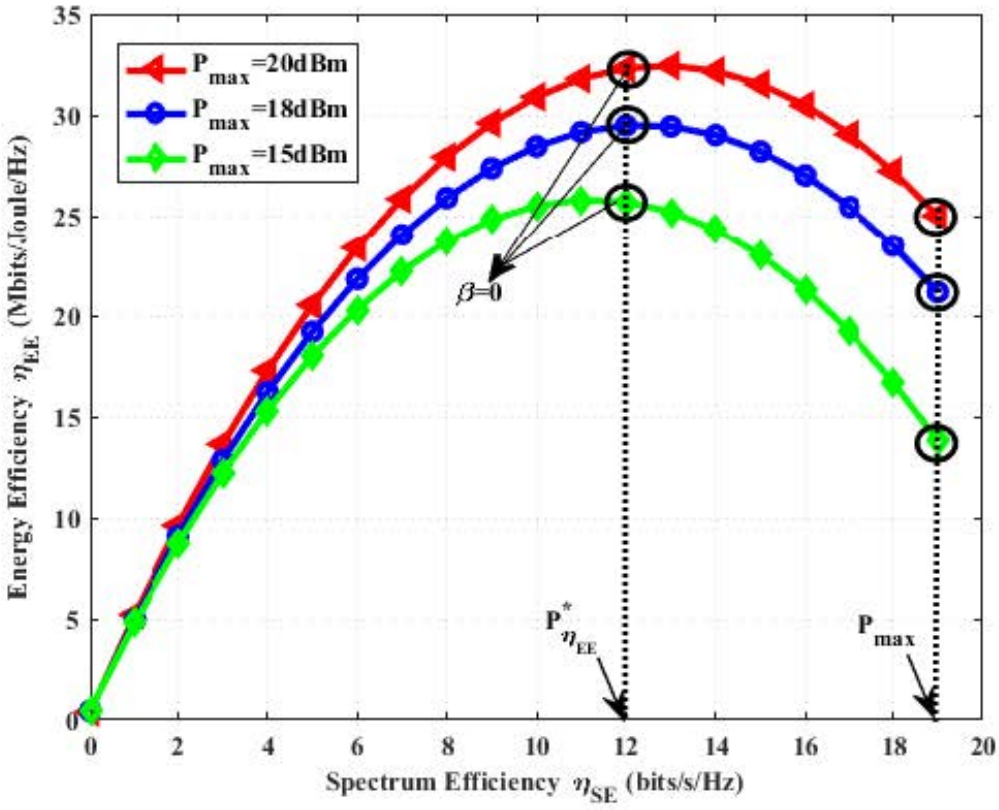

Figure 4.8: SE-EE trade-off for $I_{th} = I_{th}^{MF} = I_{th}^{FF} = -90$dBm

maximum achievable η_{EE} and η_{SE} are 47 Mbits/J/Hz and 22 bits/s/Hz respectively. This shows that the selection of interference thresholds and normalisation factors is critical to the performance results.

Fig. 4.10 depicts the impact of $P_{\max}$ and $I_{th} = I_{th}^{MF} = I_{th}^{FF}$ on the achievable η_{EE} versus trade-off variable w. The figure shows that for $0 \leq w \leq 0.3$, the achieved η_{EE} and η_{SE} are approximately the same. It is also observed that when the $P_{\max}$ = 20dBm and I_{th} = -90dBm, an appreciable value of η_{EE} is obtained as compared to when the $P_{\max}$ = 18dBm, I_{th} = -100dBm and $P_{\max}$ = 15dBm, I_{th} = -110dBm. Moreover, the rate at which η_{EE} is

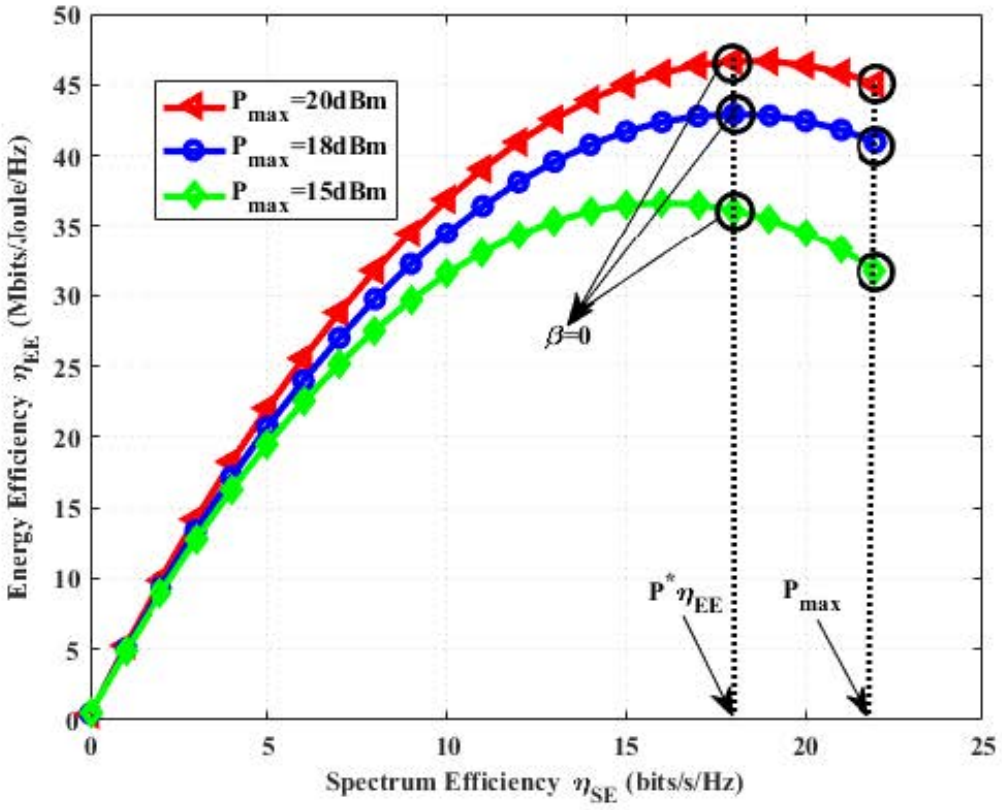

Figure 4.9: SE-EE trade-off for $I_{th} = I_{th}^{MF} = I_{th}^{FF} = 20$dBm

decreasing is gradual for all values of w when $P_{\max} = 20$dBm and I_{th} = -90dBm while rapid decrease is noticed when $P_{\max} = 15$dBm and I_{th} = -110dBm.

Fig. 4.11 depicts the impact of $P_{\max}$ and $I_{th} = I_{th}^{MF} = I_{th}^{FF}$ on the achievable η_{EE} versus trade-off variable w. The figure shows that for $0 \leq w \leq 0.2$, the achieved η_{EE} are approximately the same. It is also observed that when the $P_{\max} = 20$dBm and $I_{th} = 20$dBm, an appreciable value of η_{EE} is obtained. Moreover, the rate at which η_{EE} is decreasing is gradual for all values of w when $P_{\max} = 20$dBm, $I_{th} = 20$dBm and $P_{\max} = 18$dBm, $I_{th} = 20$dBm while rapid decrease is noticed when $P_{\max} = 15$dBm, $I_{th} = 15$dBm and $P_{\max} =$

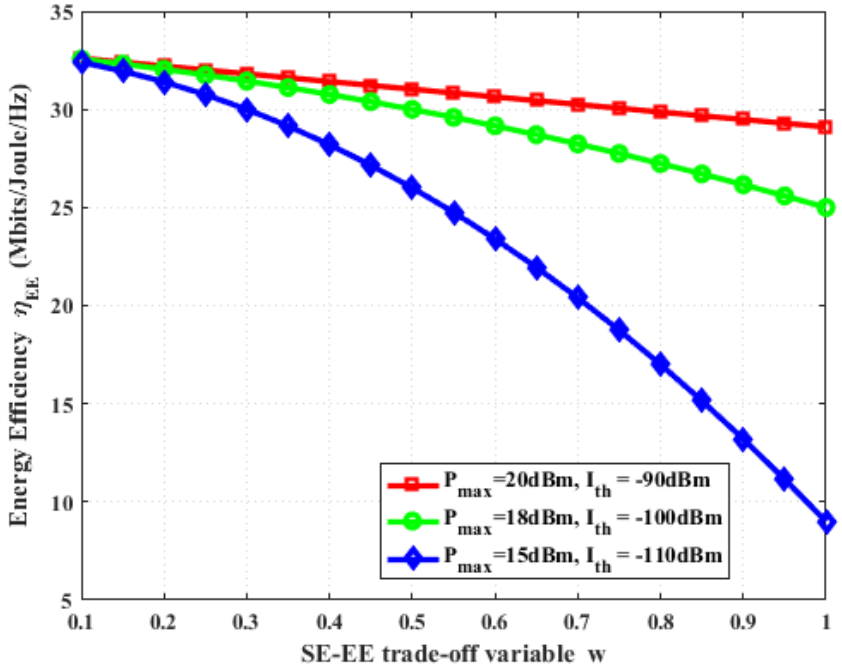

Figure 4.10: EE versus w for various $P_{\max}$, $I_{th} = I_{th}^{MF} = I_{th}^{FF}$.

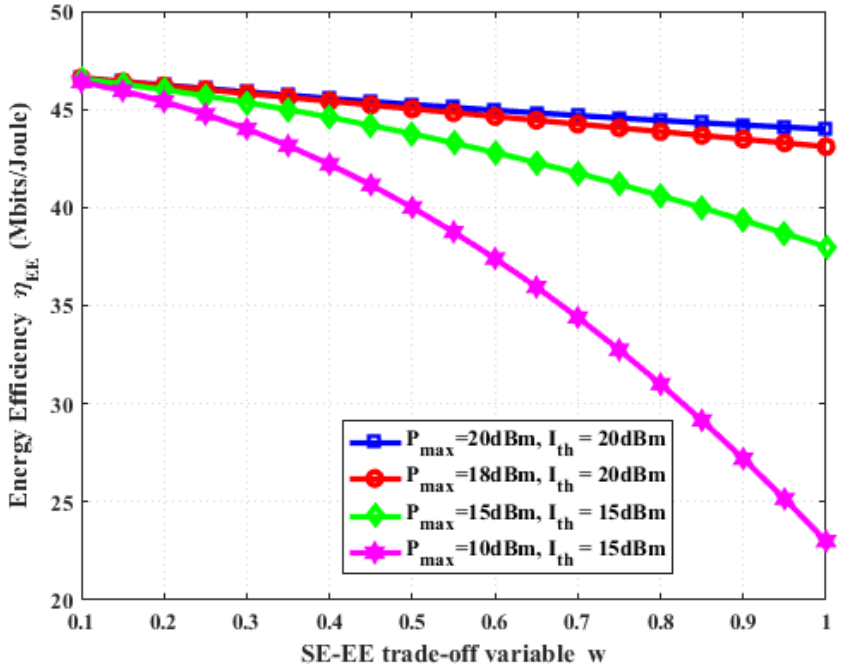

Figure 4.11: EE versus w for various $P_{\max}$, $I_{th} = I_{th}^{MF} = I_{th}^{FF}$

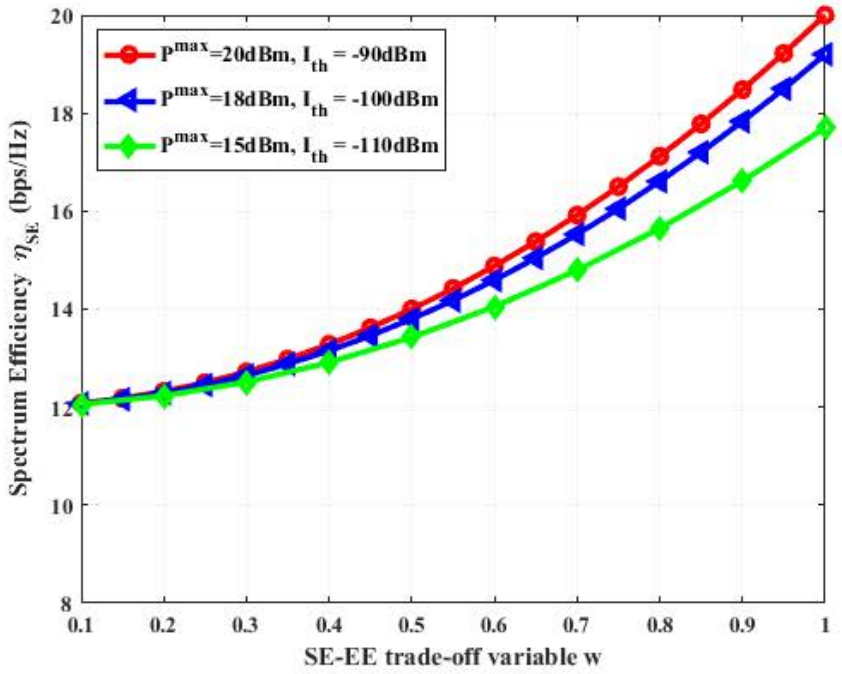

Figure 4.12: SE versus w for various $P_{\max}$, $I_{th} = I_{th}^{MF} = I_{th}^{FF}$

10dBm, I_{th} = 15dBm. This shows that the proposed algorithm will perform better when femtocells are massively deployed, which will involve more power consumption in the network.

Fig. 4.12 depicts the impact of $P_{\max}$ and $I_{th} = I_{th}^{MF} = I_{th}^{FF}$ on the achievable η_{SE} versus trade-off variable w. The figure shows that for $0 \leq w \leq 0.3$, the achieved η_{SE} are approximately the same. It is also observed that when the P_{max} = 20dBm and I_{th} = -90dBm, an appreciable value of η_{EE} is obtained as compared to when the $P_{\max}$ = 18dBm, I_{th} = -100dBm and $P_{\max}$ = 15dBm, I_{th} = -110dBm. Moreover, the rate at which η_{EE} is increasing is steadily for all values of w when $P_{\max}$ = 20dBm and I_{th} = -90dBm.

Fig. 4.13 depicts the impact of $P_{\max}$ and $I_{th} = I_{th}^{MF} = I_{th}^{FF}$ on the achievable η_{SE} versus trade-off variable w. The figure shows that for $0 \leq w \leq 0.2$, the achieved η_{SE} are approximately the same. It is also observed that when the $P_{\max}$ = 20dBm and I_{th} =

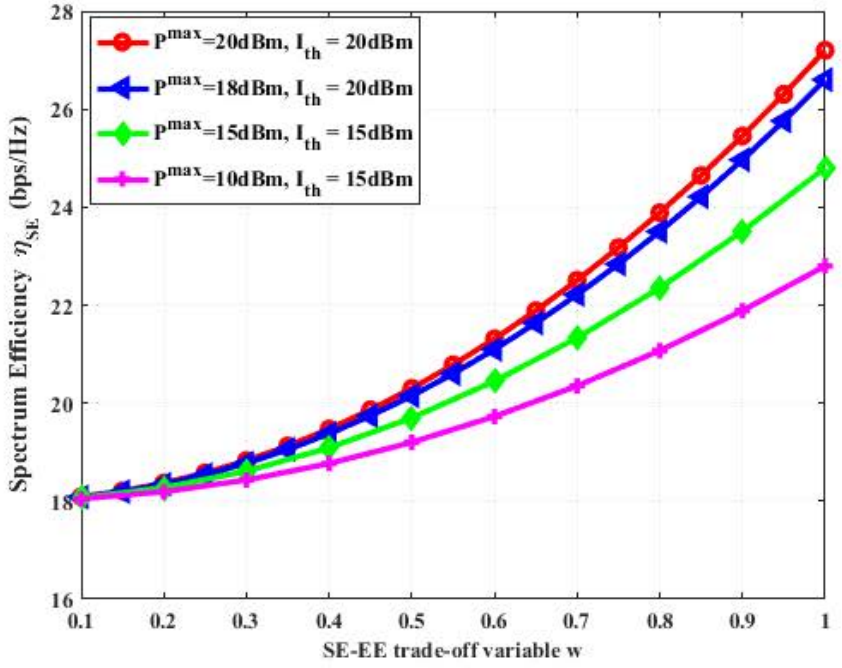

Figure 4.13: SE versus w for various $P_{\max}$, $I_{th} = I_{th}^{MF} = I_{th}^{FF}$

20dBm, an appreciable value of η_{EE} is obtained as compared to when the $P_{\max}$ = 18dBm, I_{th} = 20dBm, $P_{\max}$ = 15dBm, I_{th} = 15dBm and $P_{\max}$ = 10dBm, I_{th} = 15dBm. Moreover, the rate at which η_{EE} is increasing is steadily for all values of w. This shows that the energy efficiency of the network has been greatly maximised.

Fig. 4.14 shows the spectrum efficiency of SERRAA and EE-SE RRA against different number of FAPs. It is observed from the figure that the EE-SET RRA algorithm outperforms the SERRAA. This is because the selection of the trade-off variable with the joint optimization of EE and SE over FAPs has enchanced the performance of the network. Similarly, the energy efficiency of EERRAA and EE-SE RRA against different number of FAPs is demonstrated in Fig. 4.15. It is noticed from the figure that the EE-SET RRA outperforms the EERRAA. In particular, the rate at which the EE is decreasing has been

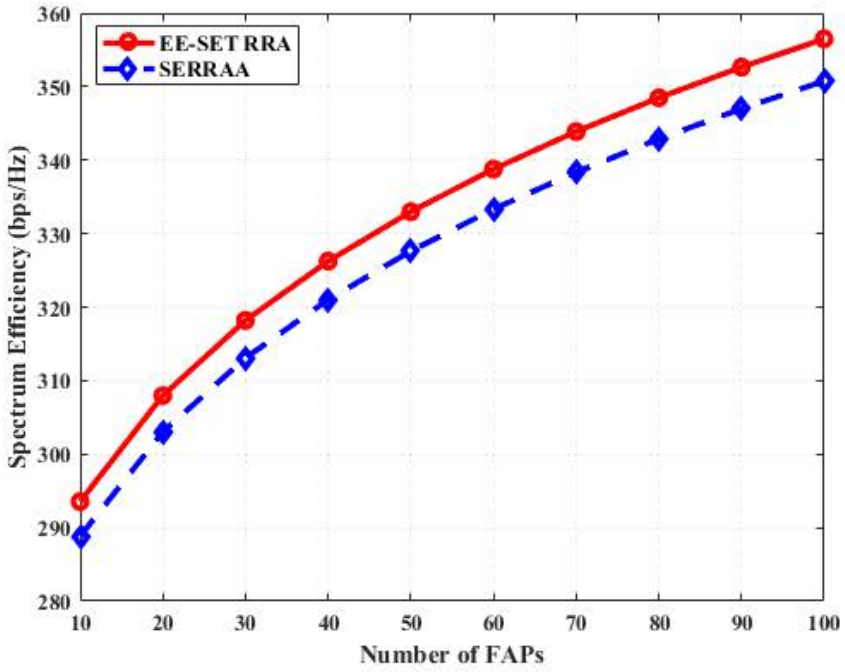

Figure 4.14: SE of SERRAA and EE-SET RRA against different number of FAPs.

greatly reduced. This is due to the careful selection of all the threshold values and the joint optimization of variables over different number of FAPs.

Fig. 4.16 illustrates the average achieved η versus the iteration numbers to study the convergence speed of the proposed EE-SET algorithm for various values of $P_{\max}$. In case I, $I_{th}^{MF} = I_{th}^{FF} = -90dBm$ while the $I_{th}^{MF} = I_{th}^{FF} = 20dBm$ in case II. The achieved η corresponds to the objective function defined in 4.41. It is observed that η increases with $P_{\max}$. This observation shows that the selection of $P_{\max}$ and I_{th} can improve the achieved η_{SE} and η_{EE}. Moreover, the proposed algorithm converges to an optimal value within 10 iterations.

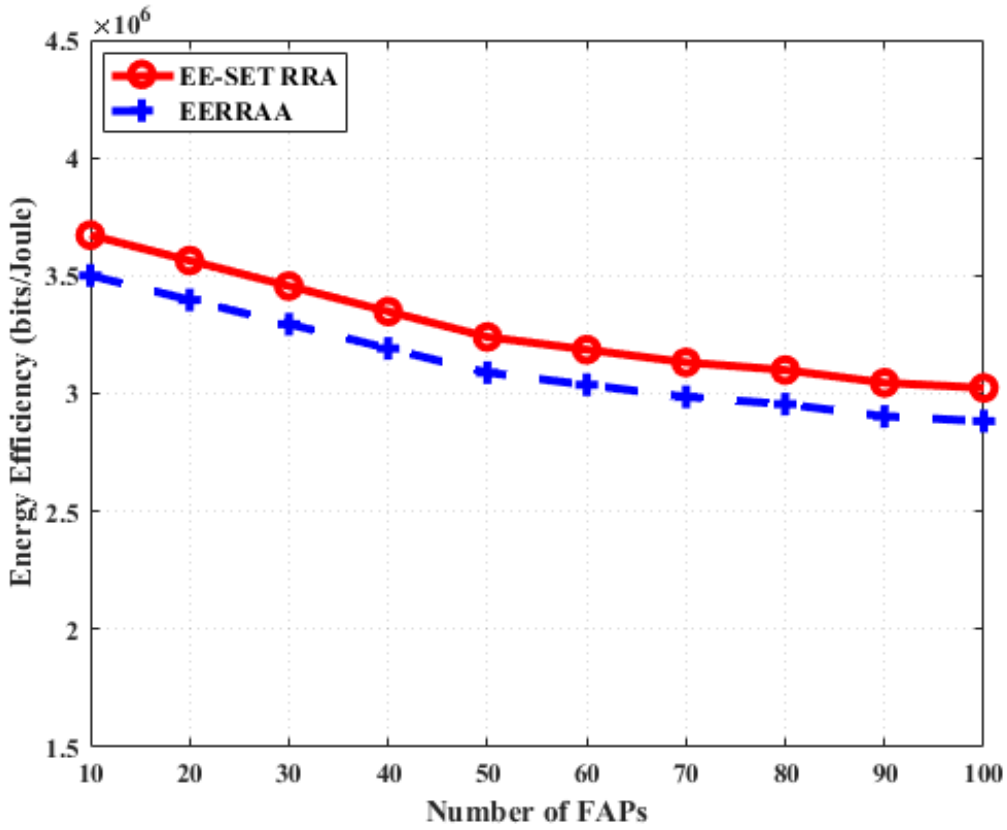

Figure 4.15: EE of EERRAA and EE-SET RRA against different number of FAPs.

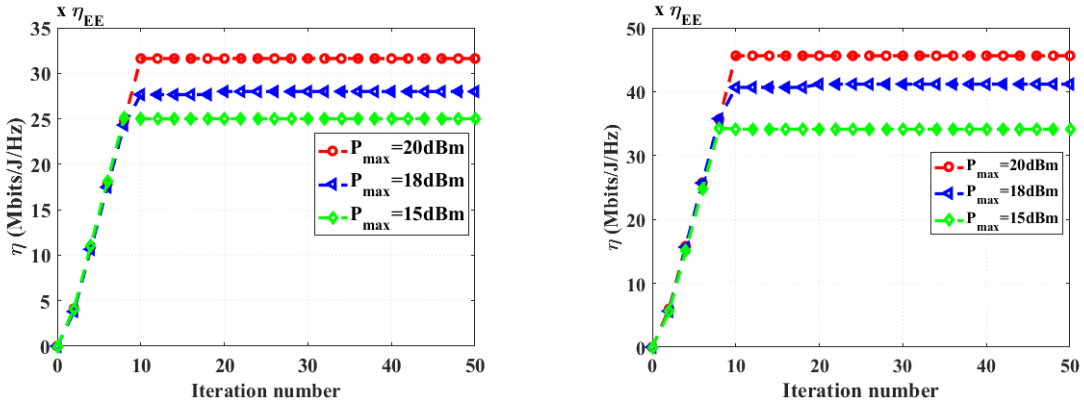

(a) Case I **(b) Case II**

Figure 4.16: Convergence of the Proposed Algorithm.

4.7 Conclusion

In this chapter, three different algorithms have been proposed for power and subchannel allocation in two-tier networks for comparison. First, energy-efficient radio resource allocation has been proposed for energy maximisation in the future 5G ultra-dense HetNets. Second, spectrum-efficient radio resource allocation algorithm has been proposed for efficient utilization of radio resources in 5G ultra-dense HetNets. Lastly, a joint energy efficiency and spectrum efficiency trade-off radio resource allocation algorithm has been proposed for joint optimisation of energy efficiency and spectrum efficiency. The radio resource allocation problems in this chapter have been formulated subject to the constraints of the maximum transmit power, minimum users' QoS requirement, fairness, cross-tier and co-tier interference. The simulation results have shown that the EERRAA and the SERRAA can maximise energy efficiency and spectrum efficiency respectively. Particularly, the EE-SE trade-off RRA algorithm maximises the EE and SE simultaneously, achieves a scalable and flexible SE-EE trade-off with fast convergence and outperforms EERRAA and SERRAA in terms of energy efficiency and spectrum efficiency respectively. The algorithms have a great potential in the 5G ultra-dense heterogeneous network.

Chapter 5

Joint Radio Resource Allocation with Adaptive Modulation and Coding Scheme for Ultra-Dense Heterogeneous Networks

5.1 Introduction

The heterogeneous deployment of femtocells overlaying the traditional macrocells, which is one of the key features of 5G is an effective solution to address the exponential traffic growth, improve indoor coverage, offer high-speed services, increase energy efficiency and spectrum efficiency, and enhance transmission reliability in macrocells as indoor users switch over their traffic from macrocells to femtocells [164]-[167]. However, the unplanned and ultra-dense

deployment of femtocells may result in severe technical issues as mentioned in Section 1.5. Hence, to fully enjoy the benefits of femtocells that adopt the co-channel resource assignment, joint radio resource allocation with adaptive modulation and coding (JRRA-AMC) scheme is another effective approach to ensure green communication, mitigate cross-tier and co-tier interference, and provide an adequate level of quality-of-service (QoS).

5.1.1 Adaptive Modulation and Coding (AMC) Scheme

Adaptive modulation and coding (AMC) is the ability of a network to find the modulation type and the coding rate dynamically based on the current radio frequency (RF) channel conditions conveyed by the UE in measurement reports. The RF digital modulation type usually adopted in the transportation of a piece of information is quadrature phase shift keying (QPSK), 16-quadrature amplitude modulation (16-QAM), 64-QAM, 256-QAM, and 1024-QAM [43], [71]. QPSK is also referred to as 4-QAM. Fig. 5.1 shows the ideal constellations for each modulation, where each dot represents a possible symbol [71]. There are four feasible symbol states in the QPSK modulation type and each symbol carries two bits of information. Also, in 16-QAM, 16 symbol states are possible. Each 16-QAM symbol carries 4 bits. Moreover, in 64-QAM, there are 64 possible symbol states, where each 64-QAM symbol carries 6 bits. The higher-order modulation type is more sensitive to poor channel conditions than the lower-order modulation. The reason is that the detector in the receiver must resolve smaller differences as the constellations become denser [71]. Coding is an error-correction method, which adds extra bits to the data stream that allow error correction. On each resource block (RB), the transmission rate is determined by the selected

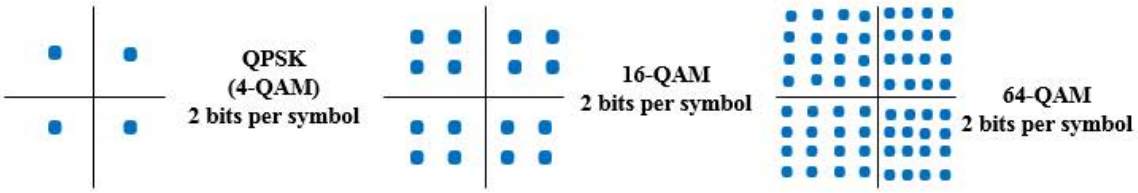

Figure 5.1: 4-QAM, 16-QAM, and 64-QAM [71]

modulation and channel coding combination. Therefore, AMC scheme is a technique that is basically used to determine the capacity of a wireless connections based on the received signal quality [103]. It allows an OFDMA-based system to select the most appropriate modulation and coding scheme (MCS) depending on the channel quality.

5.1.2 Related Work

The research on ultra-dense heterogeneous networks consisting of traditional macrocells and small cells is gaining more attentions from telecommunication industry and research community. However, the issue of interference management and radio resource allocation (RRA) in such networks is critical [34], [168], [169]. In the literature, several algorithms have been proposed on the issue of RRA but the majority of the algorithms have considered only cross-tier interference, while the issue of co-tier interference, which will be one of the major issues in the ultra-dense deployment scenario of femtocells has not been thoroughly investigated [116], [131]. In [131], the authors propose an optimal power and subchannel allocation scheme to minimise the received signal-to-interference-plus-noise ratio (SINR) of each femtocell user and the number of subchannels required to maintain reliable QoS. Meanwhile, cross-tier interference is limited to a pre-determined value but the issues relating

to co-tier interference and QoS have not been addressed. In all the aforementioned works, radio resource allocation (RRA) and cross-tier interference management have been widely investigated but the aspects of co-tier interference and QoS provisioning need further investigation and improvement to fully satisfy users' QoS requirements. Moreover, some works have not considered the aspect of users' differentiation, which is also necessary in order to satisfy the QoS requirements of different users with diverse service types [103], [170]. Service types include real-time (RT), non-real-time (NRT) and best effort (BE) services. In [103], the authors consider RRA with AMC scheme, they introduce a simple self-organisation rule to minimise cell transmit power and taking realistic resource allocation constraints into account. The radio resource allocation problem is formulated as an integer linear programming (ILP) subject to the constraint of QoS requirements. The formulated problem is solved by using the network simplex algorithm implemented in the LEMON library. However, the proposed algorithm needs modification before it can be applied to ultra-dense heterogeneous small cells scenario. The authors in [170] consider joint RRA with AMC scheme with consideration for QoS differentiation for downlink OFDMA-based LTE system, using clustering method, but the aspect of self-organisation capabilities has not been introduced in the work. In more recent works such as in [171], [172], various issues based on radio resource management such as spectral efficiency and energy efficiency enhancement, interference mitigation and QoS provisioning have been considered but the feature of self-organisation capabilities has not been considered.

In [171], the authors study the problem of power control for interference management in ultra-dense small cell networks by proposing a game with dynamic pricing. The RRA

problem is formulated to maximise the sum-rate of all the small cells while keeping tolerable interference to the macrocell users. Similarly, the authors in [172] propose a hierarchical radio resource allocation framework based on joint power control and subchannel allocation for interference mitigation in extremely dense small cell networks, which is formulated as a combinatorial optimisation problem but the issues relating to users' differentiation as well as self-organisation capabilities need to be addressed.

5.1.3 Contributions and Organisation

In contrast to the existing works and conventional methods, in this chapter, the focus is on the issue of joint power control and resource blocks allocation with AMC scheme for CR-enabled femtocells during the downlink transmission based on the LTE-A standards. Here, the objective is to minimise the total downlink transmit power across femtocells to facilitate green communication by considering the location and the service requirement of each user in the network. The contributions of this chapter can be summarised as follows:

(i) The power minimisation for joint RRA (RB and power) in the downlink of OFDMA ultra-dense HetNets problem is formulated as an optimisation problem subject to the constraints of the maximum transmit power, QoS requirements, fairness, cross-tier and co-tier interference.

(ii) The formulated optimisation problem belongs to the class of mixed integer non-linear programming (MINLP), which is NP-hard. However, in order to find the optimal solution, a reformation-linearisation technique (RLT) based on a branch and bound

approach is introduced to simplify the aforementioned MINLP. Therefore, the problem is reduced to a mixed-integer linear programming (MILP).

(iii) A framework is developed to solve the reduced MILP using the IBM ILOG CPLEX [30], which achieves an approximation solution to the optimal solution with polynomial complexity, compared to an exponential complexity required by direct search methods. Based on the obtained solution, an RRM algorithm termed joint radio resource allocation with adaptive modulation and coding scheme (JRRA-AMC) is proposed. The algorithm has the potential of mitigating the cross-tier and co-tier interference and providing adequate QoS to femtocell users in terms of throughput and fairness in sharing radio resource in the 5G wireless networks.

(iv) It is demonstrated through extensive simulations that the proposed algorithm converges to a near optimal value.

The rest of this chapter is organised as follows: The summary of notations used in this chapter is presented in Section 5.2. Section 5.3 discusses the system model such as signal-interference-plus-noise ratio (SINR) and achievable rate. Section 5.4 describes the optimisation problem formulation for power minimisation. Section 5.5 presents the proposed joint radio resource allocation with adaptive modulation and coding (JRRA-AMC) scheme and its computational complexity. Section 5.6 explains the obtained simulation results. Section 5.7 concludes this chapter.

5.2 Notations

The summary of notations used in this chapter is presented in Table 5.1

Table 5.1: Summary of important symbols III.

Symbol	Description
N	Total number of cognitive FAPs
M	Macro base station
H	total number of FUEs
J	total number of MUEs
S_m	Set of admitted nearby MUEs
S_f	Set of active FUEs
$\mathcal{K}$	Set of RBs
$\mathcal{K}_v$	Set of vacant RBs
$\mathcal{K}_o$	Set of occupied RBs
$\mathcal{S}_l$	Set of MCSs
$\gamma_{n,u,k,l}$	SINR of UE u in an FAP n that uses MCS l in RB k
$P_{n,u,k,l}$	Transmit power applied by an FAP n that uses MCS l in RB k
$G^{FAP}_{n,u,k}$	Transmitting antenna gain of an FAP n communicating with u in RB k
$G^{UE}_{n,u,k}$	Receiving antenna gain of a UE u in an FAP n in RB k
$\lambda_{n,u}$	Shadow fading between an FAP n and its associated UE u
σ^2	Additive white Gaussian noise (AWGN)
$R_{n,u,k,l}$	Data rate for UE u in an FAP n that uses MCS l in RB k
N_{sc}	Number of data subcarriers
T_s	Frame duration
η_l	Efficiency of the selected MCS l
N_{sy}	Number of symbols in an RB k

5.3 System Model

In this chapter, a downlink communication of an HetNet is considered, consisting of a macro base station (MBS) termed M, which provides an umbrella coverage for the overall network and a total number of N cognitive radio enabled FAPs, which are ultra-densely deployed in a random manner in the coverage area of the MBS. The two-tier network adopts a co-channel assignment, where the femtocell users share the same resource blocks with the users of the

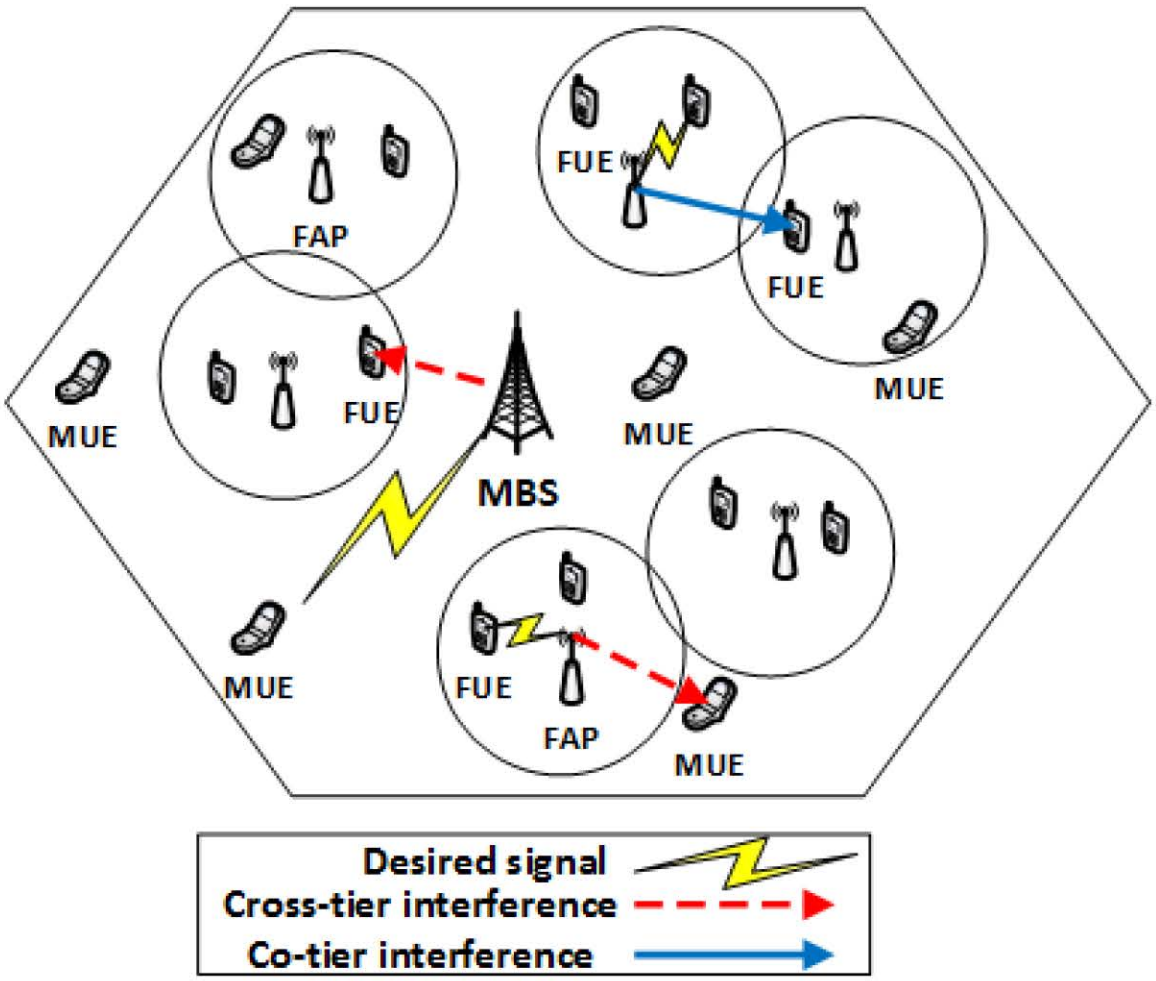

Figure 5.2: The heterogeneous deployment of ultra-dense FAPs overlaying the coverage of an MBS.

macrocell. This is illustrated in Fig. 5.2. The FUEs are able to opportunistically access the spectrum bands from MUEs through a CR-enabled femtocells.

A scenario where both the MBS and the cognitive FAPs belong to the same wireless system such as OFDMA-based long term evolution-advanced (LTE-A) is considered, where the frame structures of the MBS and the cognitive femtocells are the same. The OFDMA-based systems allocate the basic element of radio resource called a resource block in order to reduce the complexity of RRA [14].

Let $S_n = \{1, 2, ..., N\}$ and $\mathcal{U} = \{1, 2, ..., U\}$ denote the set of cognitive femtocells and UEs respectively in the network. The UEs are divided into two classes, S_f and S_m. S_f represents the set of all high priority FUEs $\{1, 2, ..., H\}$, which are UEs of users in the CSG, and S_m denotes the set of all nearby MUEs $\{1, 2, ..., J\}$, which are UEs of macrocell users in the coverage area of a cognitive FAP. Therefore, the total number of $U = S_f \cup S_m$. The demands of registered FUEs are met first, then the remaining RBs are shared among the nearby MUEs based on a proportional rate. The available frequency bandwidth B of the OFDMA system is divided into K RBs. The set of RBs $\mathcal{K}$ is represented by $\{1, 2, ..., K\}$. The set of vacant and occupied RBs is denoted by $\mathcal{K}_v$ and $\mathcal{K}_o$ respectively. The smallest number of RBs that can be allocated to a UE u corresponds to 0.5ms with the frequency band of 180 kHz [14], [15].

In this study, the modulation types considered are QPSK, 16-QAM, and 64-QAM, which transmit bit *(b)* = 2, 4 and 6 bits per OFDMA symbol respectively as shown in Table 5.2 [14], [103]. The purpose of using MCS is to reduce the rate at which communication links are broken and ensure QoS for all admitted users. The set of MCSs $\mathcal{S}_l$ is denoted by $\{1, 2, ..., L\}$, where L represents the total number of MCS levels. In this chapter, six MCS levels are considered. Therefore, $L = 6$. The channel coding employed in LTE-A systems is the turbo coding, which is a form of iterative coding. According to a target block error rate (BLER) suffered by an RB k, a minimum signal-to-interference-plus-noise ratio (SINR) threshold is set to achieve the desired MCS based on the channel quality indicator (CQI) feedback through a common control channel (CCC) [103]. A BLER is defined as the ratio of the number of erroneous blocks received to the total number of blocks sent [15]. The target

Table 5.2: Modulation and Coding Schemes (MCS) [103]

MCS	Modulation type	Transmit bits	Coding rate	Efficiency (bits/sym)	SINR level(dB)
1	QPSK	2	$\frac{1}{2}$	1	9.4
2	QPSK	2	$\frac{3}{4}$	1.5	11.2
3	16-QAM	4	$\frac{1}{2}$	2	16.4
4	16-QAM	4	$\frac{3}{4}$	3	18.2
5	64-QAM	6	$\frac{1}{2}$	4	22.7
6	64-QAM	6	$\frac{3}{4}$	4.5	24.4

BLER, which accounts for the service type chosen for different MCS are assumed to be zero, but generally, this may take a positive value depending on the requested service type [14]. User's CQIs show the level of the received signal strength of the interference suffered by the user in all RBs. The different MCS and the corresponding SINR levels are summarised in Table 5.2. The transmission rate on each RB k depends on the selected modulation and coding scheme.

5.3.1 Signal Quality and Transmit Power Modelling

The required SINR $\gamma_{n,u,k,l}$ of UE u belonging to a cognitive FAP n that uses MCS l in RB k is given as:

$$\gamma_{n,u,k,l} = \frac{P_{n,u,k,l}\Gamma^{FF}_{n,u,k}}{\underbrace{\sum_{q=1,q\neq n}^{N}\sum_{w=1}^{U} P_{q,w,k,l}\Gamma^{FF}_{n,w,k}}_{I_F} + \underbrace{P_{m,j,k,l}\Gamma^{MF}_{m,j,u,k}}_{I_M} + \sigma^2}, \tag{5.1}$$

where $P_{n,u,k,l}$ is the transmit power applied by a cognitive FAP n to its attached UE u that uses MCS l in an RB k. $\Gamma^{FF}_{n,u,k}$ is the channel gain on an RB k from a cognitive FAP n to its

associated UE u. $I_M = P_{m,j,k,l}\Gamma^{MF}_{m,j,u,k}$ and $I_F = \sum_{q=1,q\neq n}^{N} \sum_{w=1}^{U} P_{q,w,k,l}\Gamma^{FF}_{n,w,k}$ are the interference caused by the MBS and the FAPs respectively. $P_{q,w,k,l}$ is the unwanted transmit power applied by another FAP $q \neq n$ to a nearby UE $w \neq u$ that uses MCS l on an RB k. $\Gamma^{FF}_{n,w,k}$ is the channel gain from a cognitive FAP n to a nearby UE $w \neq u$ on an RB k. $P_{m,j,k,l}$ is the transmit power of an MBS M servicing an MUE j that uses MCS l on an RB k. $\Gamma^{MF}_{M,j,u,k}$ is the channel gain between an MBS M and its attached MUE j to a nearby UE w on an RB k. σ^2 denotes the Additive White Gaussian Noise (AWGN) power.

The channel gain $\Gamma_{n,u,k}$ can be calculated as [131]:

$$\Gamma_{n,u,k} = \frac{G^{FAP}_{n,u,k} G^{UE}_{n,u,k}}{\lambda_{n,u} PL_{FAP}} \tag{5.2}$$

where $G^{FAP}_{n,u,k}$ and $G^{UE}_{n,u,k}$ are the transmitting-antenna gain of the cognitive FAP n and the receiving-antenna gain of its attached UE u on the RB k respectively. $\lambda_{n,u}$ is the shadow fading between an FAP n and its associated UE u. PL_{FAP} is the path loss model from an FAP n to an FUE/MUE. In this chapter, the path loss is obtained according to the 3GPP standards and it is expressed as [15]:

$$PL_{FAP} = 38.46 + 20log_{10}d_o + 0.7d_i + \Xi L_{iw} + 18.3\Psi^{(\frac{\Psi+2}{\Psi+1})-0.46}, \tag{5.3}$$

where d_i is the distance between an FAP and inside UE, while d_o is the distance between an FAP and outside UE. L_{iw} is the penetration loss in the internal walls of the building, which is 5dB. Ξ and Ψ represent the number of penetrated walls and floors respectively. The path loss model from an MBS PL_{MBS} to an MUE/FUE is expressed as [15]:

$$PL_{MBS} = 15.3 + 37.6log_{10}d + L_{ow}, \tag{5.4}$$

where d is the distance between the MBS and the MUE/FUE. L_{ow} is the penetration loss in the external walls of the building, which is 10dB.

The SINR threshold $\gamma^{th}_{n,u,k,l}$ of a selected MCS l is expressed as:

$$\gamma^{th}_{n,u,k,l} = \max_{\alpha_{n,u,k,l}\gamma_{n,u,k,l}} \sum_{l=1}^{L} \alpha_{n,u,k,l}\gamma_{n,u,k,l} \tag{5.5}$$

where $\alpha_{n,u,k,l}$ is a decision binary variable that is equal to 1 if a UE $u \in S_f \cup S_m$ in cognitive FAP n makes use of an MCS l on an RB k, or 0 otherwise. It is worth mentioning that $\sum_{l=1}^{L} \alpha_{n,u,k,l} = \beta_{n,u,l}$, where $\beta_{n,u,l}$ is a decision binary variable that is equal to 1 if a UE $u \in S_f \cup S_m$ in a cognitive FAP k uses an MCS l, or 0 otherwise. It is compulsory for a UE u on an RB k to select at least an MCS l.

The transmit power that a cognitive FAP n will allocate to each RB k in order to achieve the SINR threshold $\gamma^{th}_{n,u,k,l}$ for the selected MCS l according to Equation (5.1) is given as:

$$P_{k,u,n,l} = \frac{\gamma^{th}_{k,u,n,l}(I_M + I_F + \sigma^2)}{\Gamma^{FF}_{n,u,k}}. \tag{5.6}$$

5.3.2 QoS Requirements

The data rate for a UE u in a cognitive femtocell n using an MCS l on each RB k is given as:

$$R_{n,u,k,l} = \Phi\eta_l = \frac{N_{sc}N_{sy}\eta_l}{T_s}, \tag{5.7}$$

where $\Phi = \frac{N_{sc}N_{sy}\eta_l}{T_s}$ is a fixed parameter, which depends on the network configuration; N_{sc} and N_{sy} are the number of data subcarriers (frequency) and symbols (time) in an RB k respectively, T_s is the frame duration, η_l is the efficiency of the selected MCS l. According to [14], [15], $N_{sc} = 12$, $N_{sy} = 7$ and $T_s = 0.5$ms.

The maximum achievable transmission rate (throughput) $\tau_{n,u,k,l}$ for a UE u in femtocell n to use an MCS l on an RB k is given as:

$$\tau_{n,u,k,l} = \sum_{n=1}^{N}\sum_{u=1}^{U}\sum_{k=1}^{K}\sum_{l=1}^{L}\alpha_{n,u,k,l}R_{n,u,k,l}. \tag{5.8}$$

The OFDMA system is assumed to support three service types which are real-time (RT), non-real-time (NRT) and best effort (BE). The RT service is further divided into voice RT and video RT. Each service type has different QoS requirements. For RT UE u, the QoS requirements are the bit-error-rate (BER), the maximum packet delay tolerance and the maximum packet dropping ratio. For NRT UE u, the QoS requirements are BER and the minimum transmission rate. For BE UE u, the QoS requirements have only the BER [154]. Therefore, a user selects an MCS that corresponds to the predetermined SINR threshold in order to satisfy these QoS requirements.

5.4 Problem Formulation and Solution

A joint RRA with AMC scheme is considered for cognitive femtocell downlink transmission that adopts co-channel assignment and therefore, there will be interference. The objective is to minimise the total transmit power with respect to the appropriate SINR threshold

corresponding to the selected MCS l on an RB k by each UE u in a cognitive femtocell n, in order to satisfy the QoS requirements of users in terms of throughput. The power minimization optimisation problem is formulated as an MINLP, which is very difficult to solve. Hence, the problem is transformed into an MILP form using a linear reformulated technique based on a branch and bound approach. In order to solve the resultant MILP, the IBM ILOG CPLEX software is used.

5.4.1 Problem Formulation

The joint RRA with AMC scheme that aims at minimising the total transmit power is formulated as follows:

$$\min_{\alpha_{n,u,k,l} P_{n,u,k,l}} \sum_{n=1}^{N} \sum_{u=1}^{U} \sum_{k=1}^{K} \sum_{l=1}^{L} \alpha_{n,u,k,l} P_{n,u,k,l}. \tag{5.9}$$

Equation 5.9 represents the objective function, while the constraints in the proposed optimisation problem can be expressed as follows:

First, the total transmit power by a femtocell that can be assigned to its associated UEs cannot exceed a maximum value which is the total transmit power limit. Thus, it can be expressed as:

$$\sum_{u=1}^{U} \sum_{k=1}^{K} \alpha_{n,u,k,l} P_{n,u,k,l} \leq P_{max} \ \forall n, \ \forall l \tag{5.10}$$

where $P_{n,u,k,l}$ is the power transmitted from a cognitive FAP n to its attached UE u that uses MCS l on an RB k. $P_{min} < P_{n,u,k,l} \leq P_{max}$ if an RB k is assigned to a UE u or $P_{n,u,k,l} = 0$ otherwise. P_{min} is the antenna power sensitivity, while P_{max} is the upper bound on the downlink transmit power applied by each femtocell to its associated UE u on the RB k.

Second, the QoS requirement of each UE u associated with a cognitive femtocell n in terms of SINR should be guaranteed to maintain reliable communications. Hence, the QoS requirement is given as:

$$\sum_{n=1}^{N}\sum_{l=1}^{L}\alpha_{n,u,k,l}R_{n,u,k,l} \geq \tau_{n,u,k,l}^{min}\ \forall k,\ \forall u \in S_f \tag{5.11}$$

where $\tau_{n,u,k,l}^{min}$ is the minimum QoS requirement for UE $u \in S_f$ in cognitive femtocell n.

Third, the remaining resources are shared among the admitted nearby MUEs in S_m based on a proportional rate φ_k after the demands of FUEs in CSG have been fully met. Therefore, it can be expressed as:

$$\frac{\sum\limits_{n=1}^{N}\sum\limits_{l=1}^{L}\alpha_{n,u,k,l}R_{n,u,k,l}}{\sum\limits_{n\in S_m}R_{n,u,k,l}} = \varphi_k\ \forall k,\ \forall u \in S_m. \tag{5.12}$$

Fourth, in order to protect the transmission of the macrocell network, an upper bound $\tilde{I}_{th}^{MF}$ is introduced to constrain the cross-tier interference from the cognitive femtocell on an RB k to the macrocell as:

$$\sum_{n=1}^{N}\sum_{u=1}^{U}\alpha_{k,u,n,l}P_{k,u,n,l}\tilde{\Gamma}_{n,u,k}^{MF} \leq \tilde{I}_{th}^{MF}\ \forall k,\ \forall l \tag{5.13}$$

Fifth, to protect the transmission of neighbouring femtocell networks, an upper bound $\tilde{I}_{th}^{FF}$ is introduced to constrain the co-tier interference from the neighbouring femtocells on an RB k as:

$$\sum_{q=1,q\neq n}^{N}\sum_{w=1}^{U}\alpha_{k,u,n,l}P_{q,w,n,l}\tilde{\Gamma}_{n,w,k}^{FF} \leq \tilde{I}_{th}^{FF}\ \forall k,\ \forall l \tag{5.14}$$

Sixth, an RB k is assigned to at most one UE u that uses an MCS l at a time in a cognitive FAP n. Therefore, the RB assignment can be done based on:

$$\sum_{u=1}^{U}\sum_{l=1}^{L}\alpha_{n,u,k,l} \leq 1 \ \forall n, \ \forall k. \tag{5.15}$$

Seventh, an MCS l must be used by at most one UE u at a time in a cognitive FAP k. Therefore, the MCS assignment can be done based on:

$$\sum_{l=1}^{L}\beta_{n,u,l} \leq 1 \ \forall n, \ \forall u \in S_f \cup S_m. \tag{5.16}$$

Eight, if an RB k is assigned to a user u in cognitive femtocell n, then one of the MCSs is compulsorily used. Therefore, the corresponding $\alpha_{n,u,k,l} = 1$. This can be expressed as:

$$\sum_{l=1}^{L}\alpha_{n,u,k,l} = \beta_{n,u,l} \ \forall n, \ \forall u \in S_f \cup S_m, \ \forall k \tag{5.17}$$

Ninth, the $\alpha_{n,u,k,l} \in \{0,1\}$ is a decision binary variable that is equal to 1 if a UE $u \in S_f \cup S_m$ makes use of MCS l on an RB k, or 0 otherwise. Thus it is expressed as:

$$\alpha_{n,u,k,l} = \begin{cases} 1, & \text{RB } k \text{ is allocated} \\ 0, & \text{otherwise} \end{cases} \tag{5.18}$$

Finally, $\beta_{n,u,l} \in \{0,1\}$ is a decision binary variable that is equal to 1 if UE u uses MCS l, or 0 otherwise. This can be written as:

$$\beta_{n,u,l} = \begin{cases} 1, & \text{MCS } l \text{ is selected} \\ 0, & \text{otherwise} \end{cases} \tag{5.19}$$

Consequently, the complete optimisation problem aiming at power minimization is formulated as follows:

$$\min_{\alpha_{n,u,k,l} P_{n,u,k,l}} \sum_{n=1}^{N} \sum_{u=1}^{U} \sum_{k=1}^{K} \sum_{l=1}^{L} \alpha_{n,u,k,l} P_{n,u,k,l} \tag{5.20}$$

$$\begin{aligned}
s.t.\ C1 &: \sum_{u=1}^{U} \sum_{k=1}^{K} \alpha_{n,u,k,l} P_{n,u,k,l} \leq P_{max}\ \forall n,\ \forall l \\
C2 &: \sum_{n=1}^{N} \sum_{l=1}^{L} \alpha_{n,u,k,l} R_{n,u,k,l} \geq \tau_{n,u,k,l}^{min}\ \forall k,\ \forall u \in S_f \\
C3 &: \frac{\sum_{n=1}^{N} \sum_{l=1}^{L} \alpha_{n,u,k,l} R_{n,u,k,l}}{\sum_{u \in J} R_{n,u,k,l}} = \varphi_k\ \forall k,\ \forall u \in S_m \\
C4 &: \sum_{n=1}^{N} \sum_{u=1}^{U} \alpha_{n,u,k,l} P_{n,u,k,l} \tilde{\Gamma}_{n,u,k}^{MF} \leq \tilde{I}_{th}^{MF}\ \forall k,\ \forall l \\
C5 &: \sum_{q=1, q \neq n}^{N} \sum_{w=1}^{U} \alpha_{n,u,k,l} P_{q,w,k,l} \tilde{\Gamma}_{n,w,k}^{FF} \leq \tilde{I}_{th}^{FF}\ \forall k,\ \forall l \\
. \ C6 &: \sum_{u=1}^{U} \sum_{l=1}^{L} \alpha_{n,u,k,l} \leq 1\ \forall n,\ \forall k \\
C7 &: \sum_{l=1}^{L} \beta_{n,u,l} \leq 1\ \forall n,\ \forall u \in S_f \cup S_m \\
C8 &: \sum_{l=1}^{L} \alpha_{n,u,k,l} = \beta_{n,u,l}\ \forall n,\ \forall u \in S_f \cup S_m,\ \forall k \\
C9 &: \alpha_{n,u,k,l} \in \{0,1\}\ \forall n,\ \forall u \in S_f \cup S_m,\ \forall k,\ \forall l \\
C10 &: \beta_{n,u,l} \in \{0,1\}\ \forall n,\ \forall u \in S_f \cup S_m,\ \forall l
\end{aligned}$$

where constraint C1 represents the limit on the maximum transmit power allowed at the FAP n. The constraint in C2 is the minimum QoS requirement for every FUE $u \in S_f$ according to the service throughput demand. The constraint C3 makes sure that the remaining resources

are shared among nearby MUEs in S_m based on a proportional rate φ_k. C4 and C5 enforce the maximum cross-tier interference tolerable at the MUEs and the maximum co-tier interference allowed in each RB k respectively. $\alpha_{n,u,n,l}$ and $\beta_{k,u,l}$ in C6 and C7 are the RB and MCS allocation indicators, that must be assigned to at most one UE u at a time respectively. The constraint in C8 ensures that one of the MCSs is selected. $\alpha_{n,u,k,l} = 1$ and $\beta_{n,u,l} = 1$ in C9 and C10 show that an RB k and MCS l are allocated to UE u respectively or 0 otherwise.

5.4.2 Reformulation Linearisation Technique

The basic idea of RLT is to introduce auxiliary variables to replace the inherent polynomial terms in the original optimisation problem and add the linear constraints that are associated with the new variables. Hence, the problem will be easy to solve using a linear problem solver. Let $\mathbb{P}_{n,u,k,l} = \alpha_{n,u,k,l} P_{n,u,k,l}$ be the actual power allocated to UE u attached to a cognitive femtocell n on an RB k, while $\mathbb{R}_{n,u,k,l} = \alpha_{n,u,k,l} R_{n,u,k,l}$ denotes the lower bound of the data rate for a UE u in a cognitive femtocell n using an MCS l on an RB k.

In this case, the optimisation problem in Equation (5.20) can be rewritten as:

$$\min_{\alpha_{n,u,k,l}\mathbb{P}_{n,u,k,l}} \sum_{n=1}^{N} \sum_{u=1}^{U} \sum_{k=1}^{K} \sum_{l=1}^{L} \mathbb{P}_{n,u,k,l} \tag{5.21}$$

$$
\begin{aligned}
s.t.\ C1 &: \sum_{u=1}^{U}\sum_{k=1}^{K}\mathbb{P}_{n,u,k,l} \leq P_{max}\ \forall n,\ \forall l \\
C2 &: \sum_{n=1}^{N}\sum_{l=1}^{L}\alpha_{n,u,k,l}\mathbb{R}_{n,u,k,l} \geq \tau_{n,u,k,l}^{min}\ \forall k,\ \forall u \in S_f \\
C3 &: \frac{\sum_{k=1}^{K}\sum_{l=1}^{L}\alpha_{n,u,k,l}\mathbb{R}_{n,u,k,l}}{\sum_{u\in S_m} R_{n,u,k,l}} = \varphi_k\ \forall n,\ \forall u \in S_m \\
C4 &: \sum_{n=1}^{N}\sum_{u=1}^{U}\mathbb{P}_{n,u,k,l}\tilde{\Gamma}_{n,u,k}^{MF} \leq \tilde{I}_{th}^{MF}\ \forall k,\ \forall l \\
C5 &: \sum_{q=1,q\neq n}^{N}\sum_{w=1}^{U}\mathbb{P}_{n,u,k,l}\tilde{\Gamma}_{n,w,k}^{FF} \leq \tilde{I}_{th}^{FF}\ \forall k\ \forall l \\
&C6 - C10.
\end{aligned}
$$

Therefore, the optimal power $\mathbb{P}^*_{n,u,k,l}$ and the optimal RB allocation $\alpha^*_{n,u,k,l}$, for a selected MCS l^* that corresponds to the predefined SINR threshold $\gamma^{th}_{n,u,k,l}$ is obtained by solving Equation (5.21) using CPLEX.

5.5 The Proposed Algorithm and its Computational Complexity Analysis

5.5.1 Proposed Algorithm

In the proposed algorithm, the major radio resources to be allocated are power and RBs with an appropriate MCS selection. The optimisation problem involves power minimisation approach, which allows an easier reuse of the same radio resources with less transmit power to select the appropriate MCS that corresponds to the predetermined SINR threshold. The

proposed algorithm enables each FAP to perform spectrum sensing so as to identify the potential RBs in $\mathcal{K}_v$ that can be shared among the attached UEs. Following the spectrum sensing step, each FAP determines the set of high priority FUEs in S_f and nearby MUEs in S_m in its coverage. Then, it calculates the $\tilde{\Gamma}^{MF}_{n,u,k}$ and $\tilde{\Gamma}^{FF}_{n,u,k}$ using Equations (3.17) and Equation (3.19) respectively. Also, each FAP solves the problem in Equation (5.21) to obtain the optimal power $\mathbb{P}^*_{n,u,k,l}$, RB k^* and MCS l^*. The two major factors that are very important to the resource allocation are the location and the demand of each UE. All UEs that are closer to an FAP $\leq$ 5m are allocated less power so that neighbouring FAPs can reuse the same RB, however, this is subject to the cross-tier and co-tier interference constraints already specified in the constraints C4 and C5 of Equation (5.21). Thus, each FAP calculates the channel quality based on Equation (5.1). The pseudo codes of the proposed JRRA-AMC scheme are summarised as follows:

Algorithm 5.1: JRRA-AMC

1: **Cognitive FAP set**: $S_n = \{1, 2, ..., N\}$, **UE set**: $\mathcal{U} = \{1, 2, ..., U\}$,

RB set: $\mathcal{K}_v = \{1, 2, ..., K\}$, **MCS set**: $S_l = \{1, 2, ..., L\}$,

2: Initialise $\alpha_{n,u,k,l}$, $\beta_{n,u,l}$, $\mathbb{P}_{n,u,k,l} = 0$

3: **For each FAP** $n \in S_n$ **do**

4: (a) perform spectrum sensing to determine the vacant RBs in $\mathcal{K}_v$,

5: (b) determine the UEs in S_f and S_m and calculate $\tilde{\Gamma}^{MF}_{n,u,k}$, and $\tilde{\Gamma}^{FF}_{n,u,k}$

7: (c) calculates $\gamma_{n,u,k,l}$ according to Equation (5.1)

8: **end for**

9: **while** $\gamma_{n,u,k,l} \leq \gamma^{th}_{n,u,k,l}$ **do** $\forall u \in S_f$

10: (a) solve Equation (5.21) to compute $\mathbb{P}^*_{n,u,k,l}$ and $\alpha^*_{n,u,k,l}$ for k^* and l^*.

12: **if** $u^* \in S_f$, **then**

13: Each FAP allocate $\mathbb{P}^*_{n,u,k,l}$, $\alpha^*_{n,u,k,l} = 1$ and $\beta_{n,u,l} = 1$

14: **end if**

15: **end while**

16: **while** $\gamma_{n,u,k,l} \leq \gamma^{th}_{n,u,k,l}$

17: each FAP update and allocate $\mathbb{P}^*_{n,u,k,l}$ and $\alpha^*_{n,u,k,l}$ $\forall u^* \in S_m$,

18: **if** $S_f = \emptyset$ **then**

19: Each FAP update and allocate $\mathbb{P}^*_{n,u,k,l}$, $\alpha^*_{n,u,k,l} = 1$ and $\beta_{n,u,l} = 1$

20: **end if**

21: **end while**

22: Repeat until $\mathcal{K}_v = \emptyset$

5.5.2 Computational complexity Analysis

The computational complexity of the JRRA-AMC algorithm is discussed below:

The JRRA-AMC scheme requires the complexity of $O(U)$ to determine the high priority FUEs in CSG and nearby MUEs. Its complexity is $O(NUK)$ in each iteration to determine the optimal RB allocation $\alpha^*_{n,u,k,l}$ and power $\mathbb{P}^*_{n,u,k,l}$ in each FAP. The worse-case complexity of finding a suitable MCS l^* that corresponds to the predefined SINR is $O(NULK^2)$. Therefore, the overall complexity of the JRRA-AMC algorithm is $O(U) + O(NULK^2) = O(NULK^2)$, compared with the exhaustive search, which has an exponential complexity of $O(NUL)^K$. The JRRA-AMC has a lower complexity, particularly for a large number of K.

5.6 Simulation Results and Discussions

5.6.1 Simulation Environment

The performance of the proposed JRRA-AMC scheme is evaluated using the system parameters according to the 3GPP LTE-A standard [15]. The minimum data rate for all FUEs is set to 9 bits/s/Hz. The lower bound and the upper bound on the number of RBs assignment for all FUEs are set to 2 and 20 per femtocell respectively. The total number of K is 100 RBs. The values of maximum transmit power, and interference constraint are varied at each iteration. The cross-tier interference is set to be equal to the co-tier interference according to [115]. The MUEs and FUEs are distributed uniformly. 5 FUEs and 3 MUEs are considered in each FAP. Fig. 5.3 shows the cellular network topology and the locations of 100 FAPs randomly deployed in the coverage area of an MBS (randomly generated). The

radius of the MBS and each FAP are set to 500m and 10m respectively. The path loss model for an FAP is obtained according to the Equation (5.3) while the path loss model for an MBS is modelled according to Equation (5.4). The signal losses due to window and wall are set to 10dB and 5dB respectively. The probability of mis-detection Pr_n^{md}, false-alarm Pr_n^{fa} and primary MUE Pr_n^j are set to [0.05,0.1], [0.01,0.05], [0,1]. $\mathcal{K}_v = \{1, 3, ..., 99\}$ and $\mathcal{K}_v = \{2, 4, ..., 100\}$. The simulation parameters are summarised in Table 5.3.

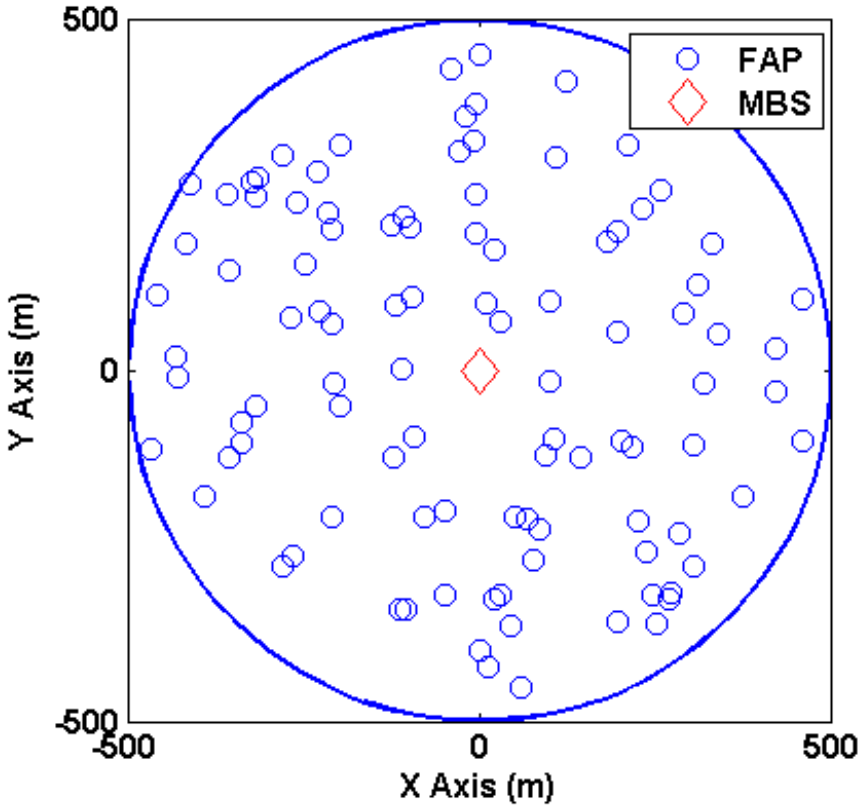

Figure 5.3: Cellular network topology and FAPs' locations in an arbitrary scenario.

Table 5.3: Simulation parameters III

Parameter	Value
MBS transmit power	46dBm
FAP transmit power	(0-23dBm)
MBS coverage radius	500m
FAP coverage radius	10m
Carrier frequency	2.6GHz
Carrier bandwidth	20MHz
White noise power density	-174dBm/Hz
MBS antenna gain	15 dBi
FAP antenna gain	2 dBi
femto UE antenna gain	1 dBi
macro UE antenna gain	1 dBi
Path loss exponent	4
Lognormal shadowing between an MBS and MUEs	8dB
Lognormal shadowing between an FAP and FUEs	10dB

5.6.2 Performance Evaluation

The proposed JRRA-AMC algorithm is compared with the existing algorithm in [170] and equal power allocation (EPA). The algorithm in [170] considers joint RRA with AMC scheme with consideration for QoS differentiation for users, which is based on clustering method. The algorithm is named adaptive modulation and coding-QoS resource allocation proposal (AMC-QRAP) but the aspect of spectrum sensing and co-tier interference has not been considered. Moreover, in equal power allocation, the same power is allocated to every RB irrespective of the location of the UE as well as the requested service. In the proposed JRRA-AMC algorithm, the focus is on the issue of joint power control and resource blocks allocation with AMC scheme for CR-enabled femtocells during the downlink transmission using a reformulated-linearisation technique that is based on BnB optimization tool.

Fig. 5.4 presents the BER against SINR for 4-QAM (QPSK), 16-QAM and 64-QAM. It can be seen from the figure that for 4-QAM, 16-QAM, and 64-QAM, the SINR level can reach 12.6dB, 17.8dB, and 22dB for BER of 10^{-6}. Moreover, 64-QAM gives the best SINR performance. This shows that higher order modulation and coding schemes should be selected first to ensure higher throughput for reliable communications.

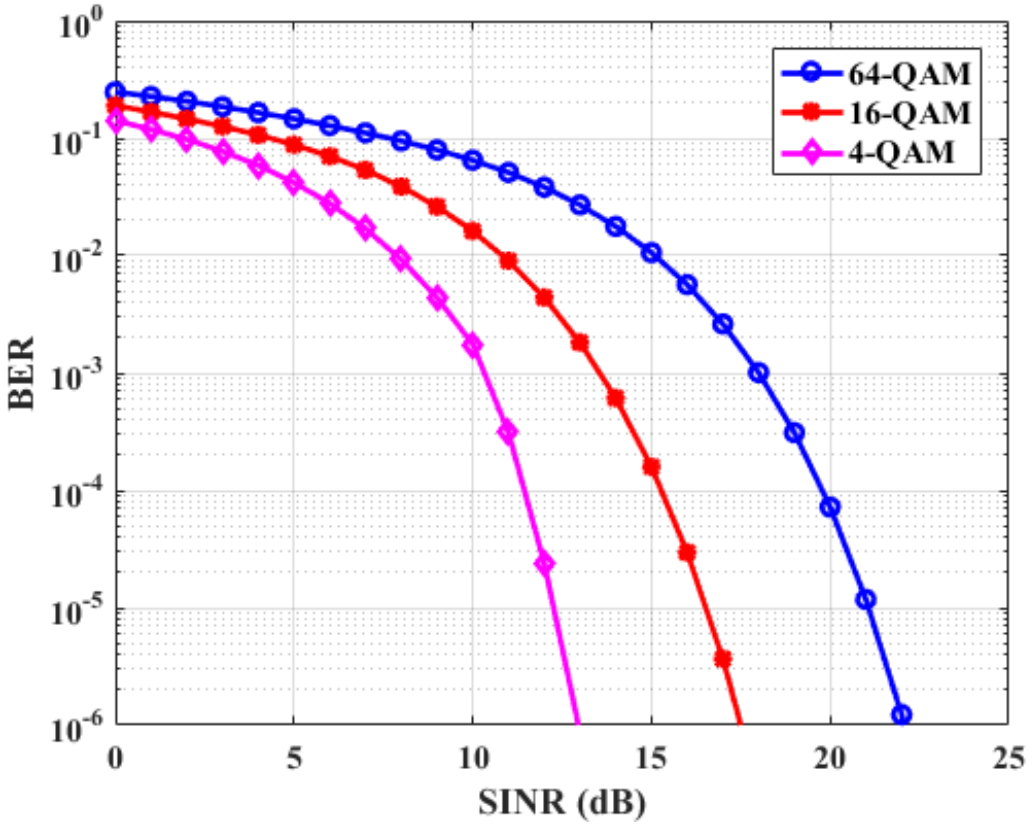

Figure 5.4: BER versus SINR for 4-QAM, 16-QAM, and 64QAM.

Fig. 5.5 shows the effect of cross-tier and co-tier interference thresholds on each RB with the maximum transmit power ranging from 5dBm to 25dBm. It is observed from the figure that for considering imperfect spectrum sensing, the interference is kept below -90dBm on each RB as the maximum transmit power reaches 20dBm. Also, it is observed that when

perfect spectrum sensing is considered, the interference keeps increasing. This shows that to ensure better network performance, interference must be suppressed to a predetermined value and there should be a consideration for spectrum sensing error to avoid network performance degradation.

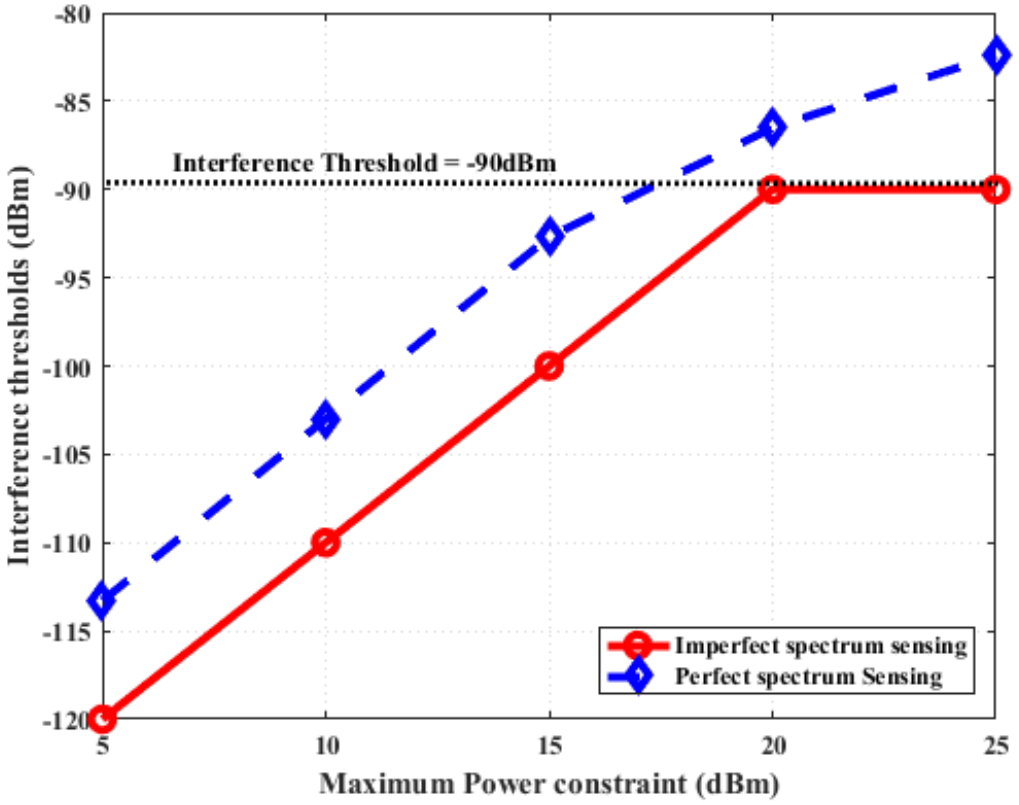

Figure 5.5: Interference thresholds versus maximum power constraints

Fig. 5.6 presents the average power allocation versus the number of RBs per UE. The number of RBs allocation is based on the available RBs from the spectrum sensing results and the requested service type. The potential spectrum sensing error has been considered in order to mitigate interference in the optimization problem. It is observed that as the allocated power per UE increases for different values of interference thresholds, the number

of RBs per UE also increases, which is necessary to support the higher order MCS and requested service type. The higher order MCS are assigned first to achieve higher spectral efficiency. It is also observed that the interference is minimised as the transmit power also is minimised for proper spatial reuse. This improves the performance of the network as the received interference level is kept below a certain threshold. The SINR threshold is set to 30dB.

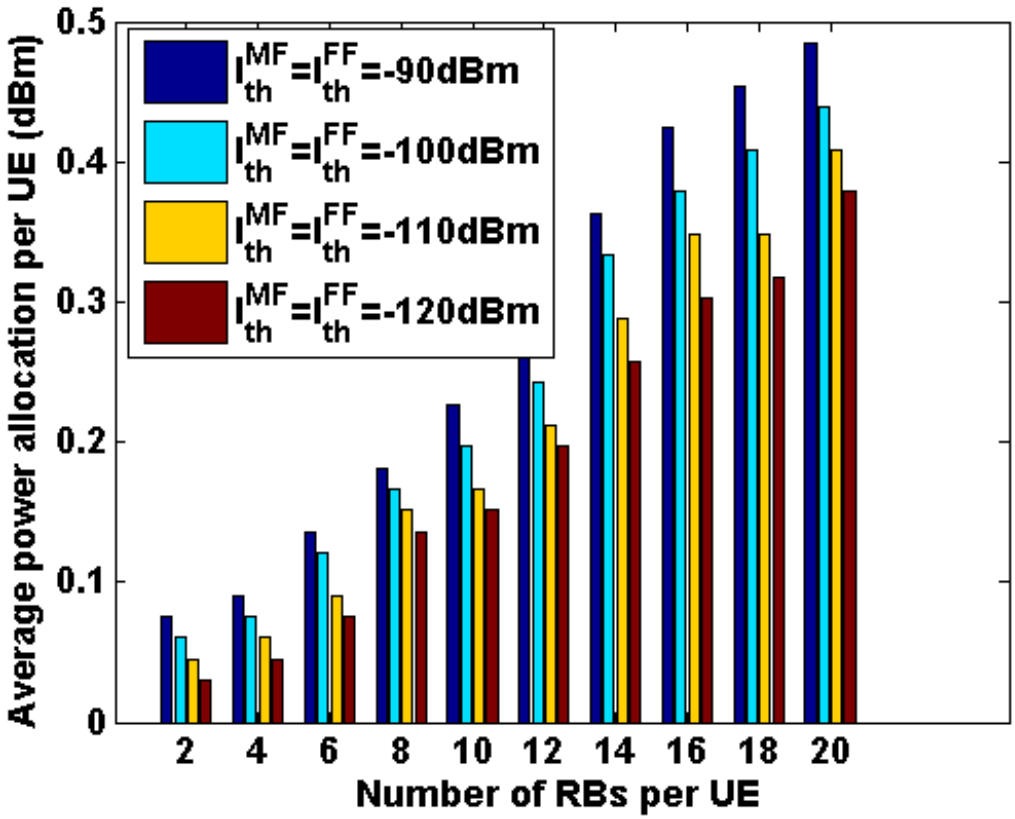

Figure 5.6: Average power allocation per UE versus the number of RBs per UE for SINR threshold = 30dBm.

Fig. 5.7 shows the average throughput of JRRA-AMC scheme achieved for different values of transmit power constraint. It is clear from the figure that the interference is minimised as the transmit power is minimised. This happens because UEs with smaller throughput

is allocated with less power, also based on the position of the UEs. On the other hand, if the throughput demand is higher, optimal power is assigned to support the request but subject to the maximum transmit power constraint. Also, the demand of the UEs in CSG is satisfied first while the remaining RBs are shared among the nearby macrocell UEs. The transmit power and the interference levels are kept below certain thresholds. Moreover, a higher value of throughput is noticed when the transmit power and interference thresholds are set to 25dBm and -90dBm respectively.

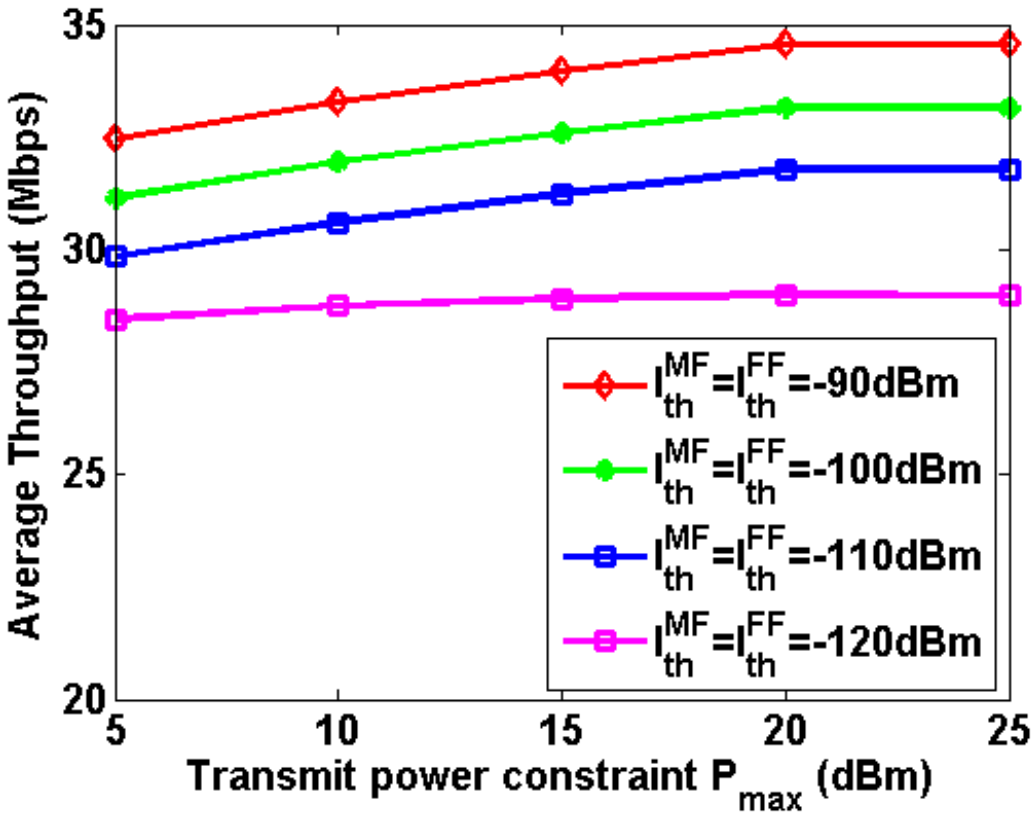

Figure 5.7: Effect of transmit power constraint and interference thresholds on the average throughput achieved.

Fig. 5.8 shows the average throughput of the proposed JRRA-AMC, AMC-QRAP and EPA. The maximum transmit power is set to 25dBm. Different sizes of FAPs are added from

10 to 100 in the network and the SINR threshold is set to 30dBm. $\tilde{I}_{th,k}^{MF} = \tilde{I}_{th,k}^{FF}$ = -90dBm for all RBs. From the figure, it is observed that the JRRA-AMC scheme outperforms the AMC-QRAP and EPA in terms of average throughput. This is because JRRA-AMC ensures that enough resources are available to satisfy the QoS requirements of high priority FUEs before the admission of nearby MUEs into the network. This enhances the achieved average throughput by 16.7% and 22.4% as compared with AMC-QRAP and EPA respectively. It is also noticed that there is an insignificant decrease in the average throughput as more FAPs are added to the network, which shows a high level of satisfaction for UEs in the network. This also indicates that the proposed algorithm can be implemented in the ultra-dense heterogeneous networks.

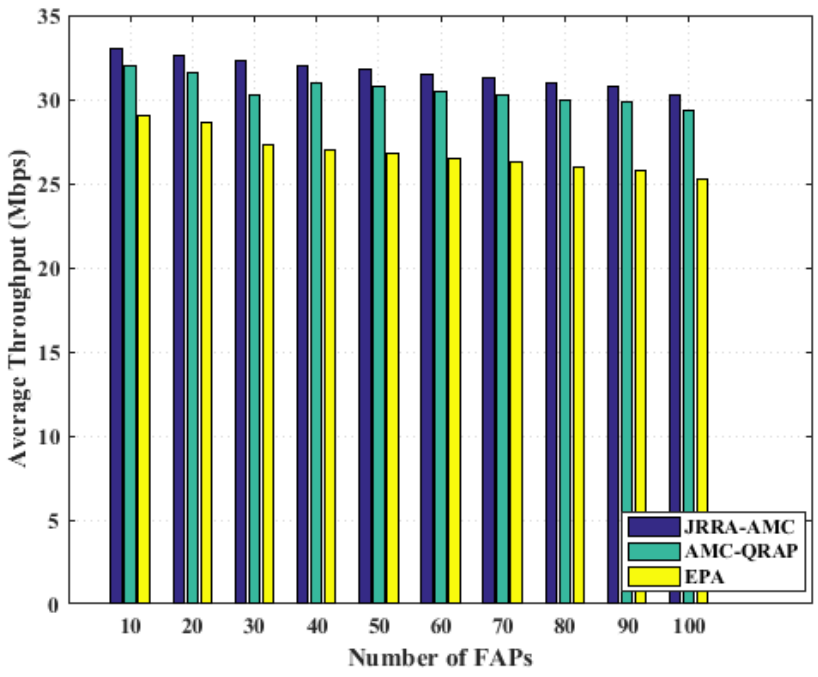

Figure 5.8: Average throughput versus number of FAPs.

Fig. 5.9 shows the convergence of the JRRA-AMC algorithm with P_{max} = 20dBm, P_{max} = 15dBm, AMC-QRAP and EPA in terms of the average network throughput versus the number of iterations. $\tilde{I}_{th}^{MF} = \tilde{I}_{th}^{FF}$ = -90dBm for all RBs, SINR threshold is set to 30dBm. The locations of the considered 8 UEs per femtocell were kept fixed throughout each simulation. From the graph, it is observed that the proposed algorithm takes only 12 iterations to converge to an optimal point. This shows that it is suitable for real implementation of ultra-dense deployment of FAPs.

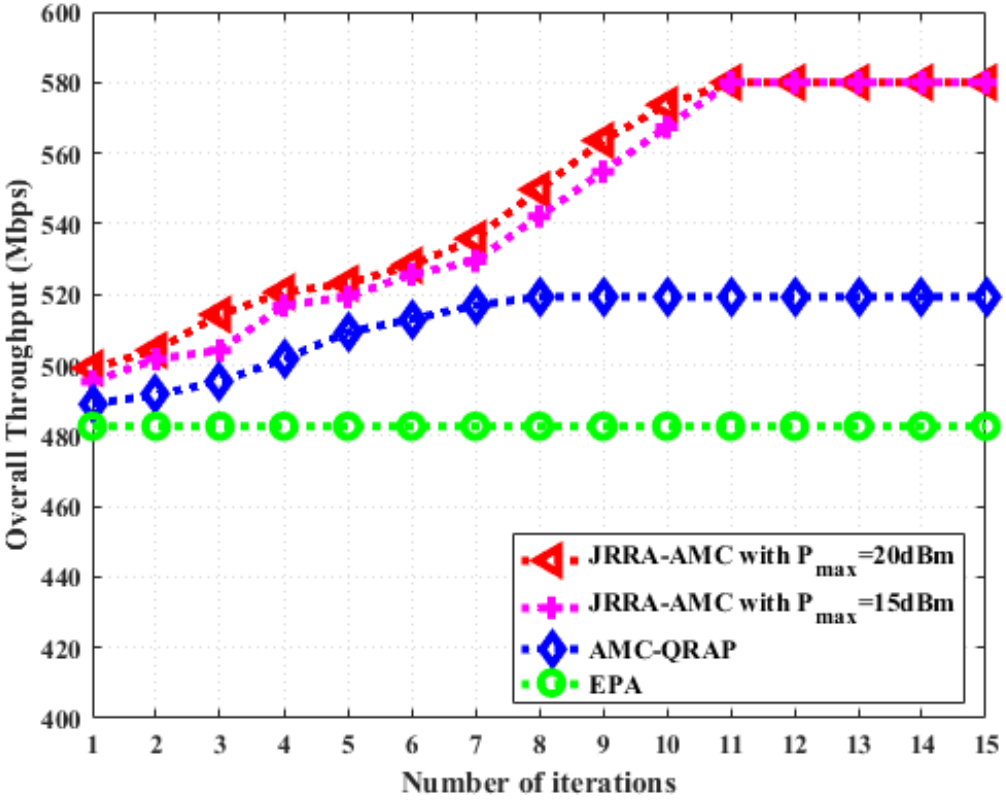

Figure 5.9: Convergence of different algorithms.

5.7 Conclusion

In this chapter, a joint radio resource allocation with adaptive modulation and coding algorithm for 5G ultra-dense networks has been proposed. The proposed algorithm is capable of mitigating cross-tier and co-tier interference by spectrum sensing and minimising the transmit power, with respect to the appropriate SINR threshold corresponding to a particular MCS level, to satisfy the QoS requirements of users in terms of throughput of all the registered FUEs and maximise the throughput of admitted nearby MUEs as much as possible. The performance of the proposed algorithm has been evaluated and compared with that of AMC-QRAP and EPA. Simulation results show that the proposed algorithm fulfils QoS requirements of the two classes of UEs considered and outperforms the other two existing algorithms in terms of the average network throughput with fast convergence.

Chapter 6

Conclusion and Future Works

In this thesis, efficient radio resource management (RRM) algorithms for the downlink transmission of a cognitive femtocell in the fifth generation (5G) networks using orthogonal frequency division multiple access (OFDMA) have been proposed. Also, various RRM problems have been presented using optimisation-based formulations comprising an objective function and some network constraints. The consideration of different objective functions yields definite radio resource allocation (RRA) strategies, one for each optimisation aim. Some of these optimisation aims bring about conflicting issues between them, such as the case of the joint maximisation of energy efficiency and spectrum efficiency. In this thesis, the interest is to design efficient RRM algorithms that will address the technical challenges, which may arise in HetNets due to the unplanned and ultra-dense deployment of femtocells in the coverage area of conventional macrocells. RRM algorithms aiming at the throughput maximisation, energy efficiency maximisation, joint energy efficiency and spectrum efficiency maximization and power minimisation have been proposed.

This thesis takes a step further and develops different RRM schemes that are able to jointly address the technical challenges such as severe interference, a significant increase in total energy consumption, unfairness in radio resource sharing and inadequate quality-of-service (QoS) provisioning that may arise in ultra-dense heterogeneous networks. These RRM strategies consist of distinct RRA algorithms, such as subchannel assignment and power allocation, whose functionalities have been found using different optimisation tools. Eventually, these algorithms are evaluated using system-level simulations, interesting and significant conclusions have been taken. Sections 6.1, 6.2, and 6.3 summarise the major conclusions, some perspectives of future work and concluding remarks respectively.

6.1 Summary of Contributions

The need to provide efficient and cost-effective solutions that can meet the predicted traffic explosion and improve the quality-of-service of mobile users is the primary goal of the network and service providers. With the ever-increasing demand for mobile services and the availability of smart mobile devices, the traditional cellular networks need to optimise the limited radio resources to meet the numerous users' service demands due to its limited capacity. A novel solution to this capacity limitation is the deployment of heterogeneous networks. This solution, which has a great potential to provide the mobile users with an adequate level of QoS, also brings about some technical problems. Hence, the focus of this thesis is to provide effective radio resource management algorithms that have capabilities to mitigate interference, ensure fairness in radio resource sharing and provide an adequate level of QoS to users.

In this thesis, various factors such as imperfect spectrum sensing, users' location, maximum transmit power and QoS requirements have been considered in the design of the new RRM algorithms for heterogeneous networks. Specifically, the thesis has focused on providing efficient RRM algorithms for ultra-dense and unplanned deployment of femtocells. In all the considered cases, performance evaluations have been carried out and comparative performance of the existing solutions with the proposed solutions have also been carried out under different performance metrics. A precise summary of this thesis is outlined below:

- An extensive survey of recent advances in radio resource management for future generation heterogeneous wireless has been presented in **chapter 2**. In particular, a detailed explanation of the requirements of 5G systems with the advanced cellular technologies in 5G wireless networks has been provided. Also, the technical issues, which may arise as a result of the unplanned and ultra-dense deployment of femtocells in the coverage area of macrocells have been described. Moreover, existing RRM algorithms for the heterogeneous networks that offer the visions of 5G wireless networks have been explored to provide insight into the design of the new RRM algorithms proposed in this thesis. Furthermore, a brief description of some common optimisation tools for solving RRM problems has been presented.

- In **chapter 3**, a new self organising radio resource management (SORRM) algorithm has been proposed for managing the operation of a cognitive femtocell autonomously. The characteristics of SORRM algorithm include spectrum sensing, spectrum decision and joint allocation of subchannel and power in heterogeneous networks. The performance of SORRM algorithm has been evaluated against the existing dynamic spectrum

allocation for hybrid access (DSA-HA) scheme, and equal power allocation (EPA) method using different performance indicators such as throughput and convergence speed. The DSA-HA has been modified for a fair comparison. The simulation results show that SORRM method provides outstanding performance and improvement over the existing solutions. The proposed algorithm is less complex and reduces interference, ensures fairness and provides an adequate level of QoS in terms of throughput in a heterogeneous wireless network with fast convergence.

- A new energy-efficient radio resource allocation algorithm (EERRAA), a spectrum-efficient radio resource allocation algorithm (SERRAA) and a joint energy efficiency and spectrum efficiency trade-off radio resource allocation algorithm (EE-SET RRA) for 5G ultra-dense heterogeneous networks have been proposed in **chapter 4**. The algorithms involve maximisation of energy efficiency, maximisation of spectrum efficiency and simultaneous maximisation of energy efficiency and spectrum efficiency respectively. Also, the EE-SE trade-off has been determined by the normalisation factors that put both the EE and SE on a similar scale. The performance of the proposed algorithms has been evaluated against existing schemes using different performance indicators such as throughput, energy efficiency and spectrum efficiency based on long term evolution-advanced (LTE-A) standards. Also, the simulation results show that the proposed EE-SET RRA algorithm outperform the proposed EERRAA and SERRAA in terms of energy efficiency and spectrum efficiency respectively. Also, the EE-SET algorithm reduces interference, and provides an adequate level of QoS in terms of throughput, energy efficiency, spectrum efficiency and a flexible and scalable

trade-off between energy efficiency and spectrum efficiency in the heterogeneous wireless network.

- In **chapter 5**, a novel joint radio resource allocation with adaptive modulation and coding scheme has been developed for 5G ultra-dense heterogeneous networks. The characteristics of the proposed algorithm include power control, power update, joint radio resource allocation as well as modulation and coding selection. The performance of the proposed algorithm has been compared with related existing algorithms. The simulation results show that the proposed scheme outperforms the existing algorithms. Moreover, the algorithm reduces interference, ensure fairness in resource sharing and provide an adequate level of QoS in terms of throughput in the heterogeneous wireless network with fast convergence.

6.2 Future Work

This thesis presents efficient RRM algorithms for future generation heterogeneous wireless networks. The proposed solutions for radio resource allocation are based on downlink transmission. Also, half-duplex transmission mode such as frequency division multiplexing, which means a user can transmit or receive on any frequency channel at different time slots has been considered. However, there are more open issues that require further investigations, which will provide an improvement to the outcome of this thesis. Some research challenges that require further work are outlined below:

- **Consideration of uplink interference Scenarios:** The work carried out in this thesis has not explored the impact of cross-tier and co-tier uplink interference. In the future work, cross-tier uplink interference scenario and co-tier uplink interference scenario will be considered in the design of radio resource allocation, which can be implemented in a femto user equipment.

- **Integrating full-duplexing capability into cognitive femtocell network:** Recently, full duplex (FD) communication, has been referred to as a promising technology that has the capability to enable attainment of double spectral efficiency in 5G [173], [174]. FD capability can simultaneously serve a pair of users on the same channel at the same time. However, FD communication brings in the acute self-interference (SI) between the simultaneous transmission and reception paths at each small cell, which arises due to the signal leakage and imperfect isolation between transmit and receive antennas. Hence, self-interference management is a key challenge in realising the FD communications at the cognitive femtocells. In addition, another major issue for the FD cellular networks is the uplink-downlink interference between the concurrent uplink and downlink transmissions taking place within a single cell or multiple neighbouring cells (i.e user-to-user interference). For example, for any two users scheduled to use the same channel, the uplink signal (signal coming from the user equipment) of one user may cause serious interference to the downlink signal (signal coming from the serving base station) of the other user. Hence, there is a need for the development of advanced interference management to address all these types of interference. FD networking has more complicated interference environments. However, new scheduling algorithms and

advanced interference cancellation techniques are necessary, to maximise the capacity gain and energy efficiency in a full-duplex cognitive femtocell system.

6.3 Concluding Remarks

This thesis proposes efficient radio resource management algorithms and provides suggestions for future works. Therefore, this thesis has contributed to the existing solutions and will help the mobile operators to provide efficient and cost-effective services for indoor users in the future wireless networks.

References

[1] V. Chandrasekhar, J. Andrews, and A. Gatherer, "Femtocell Networks: A survey," *IEEE Comms. Mag.,* vol. 46, no. 9, pp. 59-67, Sept. 2008.

[2] N. Saquib, E. Hossain, L. Le and D. Kim, "Interference management in OFDMA femtocell networks: Issues and approaches," *IEEE Wireless Comm.,* vol. 19, no. 3, pp. 86-95, Jun. 2012.

[3] A. Galindo-Serrano and L. Giupponi, "Self-organized femtocells: a Fuzzy Q-learning approach," *Wireless Netw.,* DOI: 10.1007/s11276-013-0609-6, pp. 441-455, Jul. 2013.

[4] Cisco Visual Networking Index: Global Mobile Data Traffic Forecast Update, 2016-2021, white paper, San Jose, CA, USA, Feb. 2017.

[5] S. Chen and J. Zhao, "The requirements, challenges, and technologies for 5G of terrestrial mobile telecommunication," *IEEE Commun. Mag.,* vol. 52, no. 5, pp. 3643, May 2014.

[6] T. Olwal, K. Djouani, and Anish M. Kurien, "A survey of resource management toward 5G radio access networks," *IEEE Commun. Surv. and Tut.,* vol. 18, no. 3, pp. 154-180,

3rd Quart., Aug. 2016.

[7] M. Agiwa, A. Roy, and N. Saxena, "Next Generation 5G wireless Networks: A comprehensive Survey," *IEEE Commun. Surv. and Tut.,* vol. 18, no. 3, pp. 1617-1655, Sept. 2016.

[8] A. Ghosh *et al.*, "Heterogeneous cellular networks: From theory to practice," *IEEE Commun. Mag.,* vol. 50, no 6, pp. 54-64, June 2012.

[9] M. Kamel, W. Hamouda, and A. Youssef, "Ultra-dense Networks: A survey," *IEEE commun. surv. and tut.,* vol. 18, no. 4, pp. 2522-2545, Dec. 2016.

[10] Z. Yan, W. Zhou, S. Chen, and H. Liu, "Modeling and Analysis of Two-Tier HetNets With Cognitive Small Cells," *IEEE Access,* vol. 5, pp. 2904-2012, Mar. 2017. DOI 10.1109/ACCESS.2016.2628910

[11] M. Peng, C. Wang, J. Li, H. Xiang, and V. Lau, "Recent advances in underlay heterogeneous networks: Interference control, resource allocation, and self-organization," *IEEE Commun. Surv. and Tut.,* vol. 17, no. 3, pp. 700-729, Jun. 2015.

[12] Y. Lee, T. Chuah, J. Loo, and A. Vinel, "Recent advances in radio resource management for heterogeneous LTE/LTE-A Networks," *IEEE Commun. Surv. and Tut.,* vol. 16, no. 4, pp. 2142-2180, Dec. 2014.

[13] T. Zahir, K. Arshad, A. Nakata, and K. Moessner CTAN, "Interference Management in Femtocells," *IEEE Comm. Surveys and Tut.,* vol. 15, no. 1, pp. 293-311, Feb. 2013.

[14] A. Hatoum, R. Langar, N. Aitsaadi, R. Boutaba, and G. Pujolle, "Cluster-Based Resource Management in OFDMA Femtocell Networks with QoS guarantees," *IEEE Trans. Veh. Tech,* vol. 63, no. 5, pp. 2378-2391, Jun. 2014.

[15] "Technical Specification Group Radio Access Network; Evolved Universal Terrestrial Radio Access (E-UTRA); Further advancements for E-UTRA physical layer aspects," Sophia-Antipolis, France, TR 36.814, Mar. 2010. [Online]. Available: http://www.3gpp.org/DynaReport/36.814.htm

[16] A. Abrol, and R. Kumar,"Power Optimization in 5G Networks: A Step Towards GrEEn Communication," *IEEE Access.,* vol. 4, pp. 1355-1374, Apr. 2016. Digital Object Identifier 10.1109/ACCESS.2016.2549641

[17] R. Balakrishnan and B. Canberk, "Traffic-Aware QoS Provisioning and Admission Control in OFDMA Hybrid Small Cells," *IEEE Trans. on Veh. Tech,* vol. 63, no. 2, pp. 802-810, Feb. 2014.

[18] H. Elmaghraby, and Z. Ding,"Scheduling and Power Allocation for Hybrid Access Cognitive Femtocells," *IEEE Trans. Wirel. Commun.,* pp. 2520-2533 Apr. 2017.

[19] A. Valcarce, D. Lopez-Perez, G. De La Roche, and J. Zhang,"Limited access to OFDMA femtocells," *in Proc. IEEE 20th Int. Symp. Pers., Indoor Mobile Radio Commun.,* Sept. 2009, pp. 1-5.

[20] A. Damnjanovic *et al.*, "A survey on 3GPP heterogeneous networks," *IEEE Wireless Commun.,* vol. 18, no. 3, pp. 10-21, Jun. 2011.

[21] L. Huang, G. Zhu, and X. Du, "Cognitive Femtocell Networks: An opportunistic spectrum access for future indoor wireless coverage," *IEEE Wireless Commun.,* vol. 20, no. 2, pp. 44-51, Apr. 2013.

[22] S. Al-Rubaye,"Radio Network Management in Cognitive LTE-Femtocell Systems," *PhD thesis, School of Engineering and Design, Brunel University, U.K.,* Jan., 2013.

[23] H. Kpojime, and G. Safdar, "Interference mitigation in cognitive-radio-based femtocells," *IEEE Commun. Surv. and Tut.,* vol. 17, no. 3, pp. 1511-1534, Sept. 2015.

[24] I. Akyildiz, W. Lee, M. Vuran, and S. Mohanty,"A survey on spectrum management in cognitive Radio Networks," *IEEE Comms. Mag.,* vol 46, no. 4, pp.40-48, Apr. 2008.

[25] A. Zakaria, R. Saeed, "A review in Interference Analysis and Management between Hierarchical and Flat Architectures Communications," *International Conference on Computing, Electrical and Electronic Engineering (ICCEEE),* vol. 16., no. 1 , pp. 153-159, Mar. 2013.

[26] I. F. Akyildiz, W.-Y. Lee, M. C. Vuran, and S. Mohanty, "NeXt generation/dynamic spectrum access/cognitive radio wireless networks: A survey," *Comput. Netw.,* vol. 50, no. 13, pp. 2127-2159, Sep. 2006.

[27] S. Haykin, "Cognitive radio: Brain-empowered wireless communications," *IEEE J. Sel. Areas Commun.,* vol. 23, no. 2, pp. 201-220, Feb. 2005.

[28] J. W. Huang and V. Krishnamurthy, "Cognitive base stations in LTE/ 3GPP Femtocells: A correlated equilibrium game-theoretic approach," *IEEE Trans. Commun.,* vol. 59, no. 12, pp. 3485-3493, Dec. 2011.

[29] 3GPP, Technical report 36.921 (v13.0.0), "Home eNode B (HeNB) Radio Frequency Requirements Analysis," Release 13, Jan. 2016.

[30] http://www-01.ibm.com.com/software/integration/optimization/cplex-optimizer/.

[31] S. Khwandah, J. Cosmas, I. Glover, P. Lazaridis, G. Araniti, and Z. Zaharis,"An Enhanced Cognitive Femtocell Approach for Co-Channel Downlink Interference Avoidance," *IEEE Wirel. Commun.,* vol. 23, no. 6, pp. 132-139, Dec. 2016.

[32] J. Xu *et al.*,"Cooperative distributed optimization for the Hyper-Dense Small Cell Deployment," *IEEE Comms. Mag.,* vol. 52, no. 5, pp. 61-67, May. 2014.

[33] I. Hwang, B. Song, and S. S. Soliman, "A holistic view on hyper-dense heterogeneous and small cell networks," *IEEE Commun. Mag.,* vol. 51, no. 6, pp. 20-27, Jun. 2013.

[34] A. Ebrahim, and E. Alsusa,"Interference and Resource Management Through Sleep Mode Selection in Heterogeneous Networks," *IEEE Trans. Commun.,* vol. 65, no. 1, pp. 257-269, Jan. 2017.

[35] Z.S. Bojkovic, M. R. Bakmaz, B. M. Bakmaz, "Research Challenges for 5G Cellular Architecture," *TELSIKS 2015,* pp. 215-222, Oct. 2015.

[36] J. Andrews *et al.*,"What will 5G be?," *IEEE J. Sel. Areas Comm.,* vol. 32, no. 6, pp. 1065-1082, Jun. 2014.

[37] A. Gupta, and R. Kumar,"A Survey of 5G Network: Architecture and Emerging Technologies," *IEEE Access.,* vol. 3, pp. 1206-1232, Aug. 2015. Digital Object Identifier 10.1109/ACCESS.2015.2461602

[38] M. Fallgren *et al.*, "Scenarios, Requirements, and KPIs for 5G Mobile and Wireless System," *document ICT-317669-METIS/D1.1,* Apr. 2013.

[39] A. Osseiran *et al.*, "Scenarios for 5G mobile and wireless communication: The vision of the METIS project," *IEEE Comms. Mag.,* vol. 52, no. 5, pp. 26-35, May. 2014.

[40] GSMA Intelligence, "Understanding 5G: Perspectives on future technological advancements in mobile," *White paper*, 2014.

[41] M. Mushtaq, A. Mellouk, B. Augustin, and S. Fowler, "QoE Power-Efficient Multimedia Delivery Method for LTE-A," *IEEE Commun. Mag.,* vol. 10, no. 2, pp. 749-760, Jun. 2016.

[42] N. Bhushan *et al.*, "Network densification: The dominant theme for wireless evolution into 5G," *IEEE Commun. Mag.,* vol. 52, no. 2, pp. 82-89, Feb. 2014.

[43] D. Lopez-Perez, M. Ding, H. Claussen, and A. Jafari "Towards 1 Gbps/UE in cellular systems: Understanding ultra-dense small cell deployments," *IEEE Commun. Surv and Tut.,* vol. 17, no. 4, pp. 2078-2101, 1st Quart. 2015.

[44] A. Goldsmith, "Wireless Communications," *Cambridge University Press.,* 2005.

[45] C-X. Wang, *et al.*, "Cellular Architecture and Key Technologies for 5G Wireless Communication Networks," *IEEE Communications Magazine,* vol. 52, no. 2, pp. 122-130, 2014.

[46] L. Wang, H. Ngo, M. Elkashlan, T. Duong, and K. Wong, "Massive MIMO in Spectrum Sharing Networks: Achievable Rate and Power Efficiency," *IEEE Syst. Journ.,* vol. 11, no. 1, pp. 20-31, Mar. 2017.

[47] L. Lu *et al.*, "An Overview of Massive MIMO: Benefits and Challenges," *IEEE Journal of Selected Topics in Signal Processing,* vol. 8, no. 5, pp. 742-758, 2014.

[48] K. Prasad, E. Hossain, and V. K. Bhargava, "Energy Efficiency in Massive MIMO-Based 5G Networks: Opportunities and Challenges," *IEEE Commun. Mag.,* vol. 52, no. 2, pp. 86-94, Jun. 2017.

[49] E. Larsson, *et al.*, "Massive MIMO for Next Generation Wireless Systems," *IEEE Communications Magazine,* vol. 52, no. 2, pp. 186-195, 2014.

[50] H. Q. Ngo, E. G. Larsson, T. L. Marzetta, "Energy and Spectral Efficiency of Very Large Multiuser MIMO Systems," *IEEE Transactions on Communications,* vol. 61, no. 4, pp. 1436-1449, 2013.

[51] W. H. Chin, Z. Fan, R. Haines, "Emerging Technologies and Research Challenges for 5G Wireless Networks," *IEEE Wireless Communications,* vol. 21, no. 2, pp. 106-112, 2014.

[52] J. Choi, D. J. Love, U. Madhow, "Limited Feedback in Massive MIMO Systems: Exploiting Channel Correlations via Noncoherent Trellis-Coded Quantization," *Proc. 47th CISS,* Baltimore, MD, pp. 1-6, 2013.

[53] Z. Pi, F. Khan, "An Introduction to Millimeter-Wave Mobile Broadband Systems" *IEEE Communs. Mag.,* vol. 49, no. 6, pp. 101-107, 2011.

[54] Z. Cao, X. Zhao, and F. M. Soares, N. Tessema, and A. M. J. Koonen, "38-GHz Millimeter Wave Beam Steered Fiber Wireless Systems for 5G Indoor Coverage: Architectures, Devices, and Links" *IEEE Jour. Quant. Elect.,* vol. 53, no. 2, pp. 1-9, Feb. 2017.

[55] T. S. Rappaport, *et al.*, "Millimeter Wave Mobile Communications for 5G Cellular: It Will Work!" *IEEE Access,* vol. 1, pp. 335-349, 2013.

[56] R. Taori, A. Sridharan, "Point-to-Multipoint In-Band mmwave Backhaul for 5G Networks" *IEEE Communications Magazine,* vol. 53, no. 1, pp. 195-201, 2015.

[57] ArrayComm, and William Webb, Ofcom, London, U.K., 2007.

[58] 3rd Generation Partnership Project,"Feasibility study on licensed assisted access to unlicensed spectrum," *Sophia Antipolis, France, Tech. Rep. 3GPP TR 36.889,* 2014.

[59] Enabling hyper-dense small sell deployments with ultraSON, Qualcomm Research, San Diego, CA, USA, pp. 1-21, Feb. 2014.

[60] D. Lopez-Perez *et al.*, "Enhanced intercell interference coordination challenges in heterogeneous networks," *IEEE Wireless Commun.,* vol. 18, no. 3, pp. 22-30, Jun. 2011.

[61] H. ElSawy, E. Hossain, and D. I. Kim, "HetNets with cognitive small cells: User offloading and distributed channel allocation techniques," *IEEE Commun. Mag.,* vol. 51, no. 6, pp. 28-36, Jun. 2013.

[62] D. Cavalcanti, D. P. Agrawal, C. Cordeiro, B. Xie, and A. Kumar, "Issues in integrating cellular networks, WLANs, and MANETs: A futuristic heterogeneous wireless network," *IEEE Wireless Commun.,* vol. 12, no. 3, pp. 30-41, June 2005.

[63] M. Peng, D. Liang, Y. Wei, and J. Li, H. Chen, "Self-Configuration and Self-Optimization in LTE-Advanced Heterogeneous Networks," *IEEE Commun. Mag.,* vol. 51, no. 5, pp. 36-45, May. 2013.

[64] J. Lee, Y. Kim, Y. Kwak, J. Zhang, A. Papasakellariou, T. Novlan, C. Sun, and Y. Li, "LTE-Advanced in 3GPP Rel-13/14: An Evolution Toward 5G," *IEEE Commun. Mag.,* vol. 53, no. 7, pp. 36-42, Mar. 2016.

[65] 3GPP, "Evolved universal terrestrial radio access (E-UTRA) and evolved universal terrestrial radio access (E-UTRAN); overall description; stage 2," *Tech. Rep. TS 36.300 v10.3.0, Release 10,* 3rd. Generation Partnership Project (3GPP), 2011.

[66] 3GPP, "Evolved universal terrestrial radio access (E-UTRA); FDD home enode B (HeNB) radio frequency (RF) requirements analysis," *Tech. Rep. TR 25.921 v9.0.0, Release 9*, 3rd. Generation Partnership Project (3GPP), 2010.

[67] 3GPP, "UTRAN architecture for 3G home node b (HNB); stage 2," *Tech. Rep. TS 25.467 v10.1.0, Release 10*, 3rd. Generation Partnership Project (3GPP), 2011.

[68] "Technical Specication Group Radio Access Network; Evolved Universal Terrestrial Radio Access (E-UTRA); Physical channels and modulation," Sophia-Antipolis, France, TS 36.211, Sep. 2012. [Online]. Available: http://www.3gpp.org/DynaReport/36.211.htm

[69] W. Forum, "Network architecture: Architecture, detailed protocols, and procedures - femtocells core specification," *Tech. Rep. WMF-T33-118-R016v01*, WiMAX Forum, 2010

[70] IEEE, "IEEE standard for local and metropolitan area networks - part 16: Air interface for broadband wireless access systems - advanced air interface," *Tech. Rep. IEEE Std 802.16m*, Institute of Electrical and Electronics Engineers (IEEE), 2011.

[71] "LTE Resource Guide; Anritsu Testing the Future," 2009. [Online]. Available: http://www.us.anritsu.com/

[72] F. Capozzi, G. Piro, L.A. Grieco, G. Boggia, and P. Camarda,"Downlink packet scheduling in LTE cellular networks: Key design issues and a survey," *IEEE Commun. Surveys Tuts.,* vol. 15, no. 2, pp. 678700, May 2013.

[73] E. Rodrigues,"Adaptive Radio Resource management for OFDMA-Based Macro- and Femtocell Networks," *PhD thesis, Universitat Politecnica de Catalunya* May, 2011.

[74] S. Parkvall, A. Furuskar, and E. Dahlman, "Evolution of LTE toward IMT-advanced," *IEEE Communications Magazine*, vol. 49, pp. 84-91, Feb. 2011.

[75] H. Elsawy, E. Hossain, and M. Haenggi, "Stochastic geometry for modeling, analysis, and design of multi-tier and cognitive cellular wireless networks: A survey," *IEEE Commun. Surveys Tuts.,* vol. 13, no. 3, pp. 996-1019, Sep. 2013.

[76] "Self-Organizing Networks (SON); Concepts and requirements," *3rd Generation Partnership Project, Sophia Antipolis Cedex, France,* 3GPP TS 32.500 v11.1.0, Oct. 2011.

[77] "Self-configuring and Self-Optimizing Network (SON) use cases and solutions," *3rd Generation Partnership Project, Sophia Antipolis Cedex, France,* 3GPP TR 36.902 v9.3.1, Mar. 2011.

[78] D. Muirhead, M. Imran, and K. Arshad,"A Survey of the Challenges, Opportunities, and Use of Multiple Antennas in Current and Future 5G Small Cell Base Stations," *IEEE Access.,* vol. 4, pp. 2952-2964, Jul. 2016. Digital Object Identifier 10.1109/ACCESS.2016.2569483

[79] Z. Liu, P. Zhang, X. Guan, X. Li, H. Yang,"Robust power control for femtocell networks with imperfect channel state information," *IET Commun.,* vol. 10, no. 8, pp. 882-890, Jan. 2016.

[80] H. Wang and Z. Ding,"Macrocell-queue-stabilization-based power control of femtocell networks," *IEEE Trans. Wireless Commun.* vol. 13, no. 9, pp. 5223-5236, Sep. 2014.

[81] K. Senel, and M. Akar, "A Distributed Coverage Adjustment Algorithm for Femtocell Networks," *IEEE Trans. Veh. Techn.,* vol. 66, no. 2, pp. 1739-1747, Feb. 2017.

[82] M. Ndong and T. Fujii, "Handling Cross-Tier Interference in Underlay Macrocell System for Future Small Cell Networks," *Journ. Commun. and Netw.,* vol. 19, no. 1, pp. 23-31, Feb. 2017.

[83] T. M. Nguyen, Y. Jeong, T. Quek, W. P. Tay, and H. Shin,"Interference alignment in a Poisson eld of MIMO femtocells," *IEEE Trans. Wireless Commun.,* vol. 12, no. 6, pp. 2633-2645, Jun. 2013.

[84] W. C. Cheung, T. Quek, and M. Kountouris, "Throughput optimization, spectrum allocation, and access control in two-tier femtocell networks," *IEEE J. Sel. Areas Commun.,* vol. 30, no. 3, pp. 561-574, Apr. 2012.

[85] H. Zhang *et al.*, "Resource allocation in spectrum-sharing OFDMA femtocells with heterogeneous services," *IEEE Trans. Commun.,* vol. 62, no. 7, pp. 2366-2377, Jul. 2014.

[86] C. Niu, Y. Li, R. Hu, and F. Ye, "Femtocell-enhanced multi-target spectrum allocation strategy in LTE-A HetNets," *IET Commun.,* vol. 11, no. 6, pp. 887-896, Mar. 2017.

[87] Y. Cohen, S. Zhang, S Xu, and G. Li, "Fundamental Trade-offs on Wireless Networks," *IEEE Comms Mag.,* vol. 49, no. 6, pp. 30-37, Jun. 2011.

[88] T. Mao, G. Feng, L. Liang, S. Qin, and B. Wu, Member, "Distributed Energy-Efficient Power Control for MacroFemto Networks," *IEEE Trans. Veh. Tech.,* vol. 65, no. 2, pp. 718-731, Feb. 2016.

[89] H. Ghazzai,M. Farooq, A. Alsharoa,E. Yaacoub, A. Kadri, and M-S. Alouini, "Green Networking in Cellular HetNets: A Unified Radio Resource Management Framework with Base Station ON/OFF Switching," *IEEE Veh. Tech.,* vol. PP, no. 99, pp. 1-15, 2016. DOI 10.1109/TVT.2016.2636455

[90] H. Shi, R. Prasad, E. Onur, and I. Niemegeers, "Fairness in wireless networks: Issues, measures, and challenges," *IEEE Commun. Surv. and Tut.,* vol. 16, no. 1, pp. 5-24, Mar. 2014.

[91] H. B. Jung, and D. K. Kim, "Power Control of Femtocells Based on Max-Min Fairness in Heterogeneous Networks," *IEEE Communications Letters,* vol. 17, no. 7, pp. 1372-1375, July 2013.

[92] Y. Lee, J. Loo, T. Chuah, and A. El-Saleh, "Fair Resource Allocation With Interference Mitigation and Resource Reuse for LTE/LTE-A Femtocell Networks," in *IEEE Trans. on Veh. Tech.,* vol. 65, no. 10, pp. 8203-8217, Oct. 2016.

[93] J. Zhu, and H-C. Yang, "Low-Complexity QoS-Aware Coordinated Scheduling for Heterogeneous Networks," in *IEEE Trans. on Veh. Tech.,* vol. PP, no. 99, pp. 1-6, 2016. DOI 10.1109/TVT.2016.2628387.

[94] C. Wang, S. Fang, H-C. Wu, S. Chiou, W. Kuo, and P. Lin, "Novel User-Placement Ushering Mechanism to Improve Quality-of-Service for Femtocell Networks," in *IEEE Trans. on Veh. Tech.,* vol. PP, no. 99, pp. 1-12, 2016.

[95] A. Shifat, M. Chowdhury, and Y. Jang, "Game-Based Approach for QoS Provisioning and Interference Management in Heterogeneous Networks," in *IEEE Access,* vol. PP, no. 99, pp. 1-12, 2017. DOI 10.1109/ACCESS.2017.2704094

[96] R. Cavalcante, S. Stanczak, J. Zhang and H. Zhuang "Low Complexity Iterative Algorithms for power estimation in Ultra-Dense Load Coupled Networks," in *IEEE Trans. on signal processing,* vol. 64, no. 22, pp. 6058-6070, Nov. 2016.

[97] M. Salem, A. Adinoyi, M. Rahman, H. Yanikomeroglu, D. Falconer, Y. Kim, E. Kim, and Y, Cheong, "An overview of radio resource management in relay-enhanced OFDMA-based networks," *IEEE Commun. Surv. and Tut.,* vol. 12, no. 3, pp. 422-438, Apr. 2010.

[98] T. Lotfollahzadeh, S. Kabiri, H. Kalbkhani, M. Shayesteh, "Femtocell base station clustering and logistic smooth transition autoregressive-based predicted signal-to-interference-plus-noise ratio for performance improvement of two-tier macro/femtocell networks," *IET Signal Process.,* vol. 10, pp. 1-11, 2016.

[99] A. Abdelnasser, E. Hossain, and D. Kim, "Clustering and Resource Allocation for Dense Femtocells in a Two-Tier Cellular OFDMA Network," *IEEE Trans. on Wireless Commun.,* vol. 13, no. 3, pp. 1628-1641, Mar. 2014.

[100] I-S. Cho and S. Baek, "Distributed Power Allocation for Femtocell Networks Subject to Macrocell SINR Balancing," *IEEE Commun. Lett.,* vol. 20, no. 11, pp. 2296-2299, Nov. 2016.

[101] O. Falowo and A. Chan, "Joint Call Admission Control Algorithm for Fair Radio Resource Allocation in Heterogeneous Wireless Networks Supporting Heterogeneous Mobile Terminals," *IEEE CCNC*, pp. 1-5, 2010.

[102] A. Asadi, and V. Mancuso, "A Survey on Opportunistic Scheduling in Wireless Communications," *IEEE Commun. Surv. and Tut.,* vol. 15, no. 4, pp. 1671-1688, Dec. 2013.

[103] D. Lopez-Perez, X. Chu, A. Vasilakos, and H. Claussen, "Power Minimization Based Resource Allocation for Interference Mitigation in OFDMA Femtocell Networks," *IEEE Jour. On select. Areas in comm.,* vol. 32, no. 2, pp. 333-344, Feb. 2014.

[104] R. Fantacci, D. Marabissi, D. Tarchi, and I. Habib, "Adaptive modulation and coding techniques for OFDMA systems," *IEEE Transactions on Wireless Communications,* vol. 8, pp. 4876-4883, Sep. 2009

[105] M. Lin, N. Bartolini, and T. Porta, "Power Adjustment and Scheduling in OFDMA Femtocell Networks," *IEEE INFOCOM 2016,* pp. 1-9, April. 2016

[106] K. Ahuja, Y. Xiao, and M. van der Schaar, "Efficient Interference Management Policies for Femtocell Networks," *IEEE Trans. Wirel. Commun.,* vol. 12, no. 10, pp. 4879-4893, Sept. 2015.

[107] G. Huang and J. Li, "Interference Mitigation for Femtocell Networks Via Adaptive Frequency Reuse," *IEEE Trans. On Veh. Tech.,* vol. 65, no. 4, pp. 2814-2823, Apr. 2016.

[108] Y. Zheng, S. Sun, B. Rong, M. Kadoch, Y. Yamao, "Traffic Aware Power Allocation and Frequency Reuse for Green LTE-A Heterogeneous Networks," *IEEE ICC 2015,* pp. 1-6, June. 2015.

[109] B. Ma, M. Cheung, V. Wong, and J. Huang, "Hybrid Overlay/Underlay Cognitive Femtocell Networks: A Game Theoretic Approach," *IEEE Trans. On Wirel. Commun.,* vol. 14, no. 6, pp. 3259-3270, June. 2015.

[110] H. Zhang, D. Jiang, F. Li, K. Liu, and H. Song, "Cluster-Based Resource Allocation for Spectrum-Sharing Femtocell Networks," *IEEE Access,* vol. 4, pp. 8643-8356, Jan. 2017.

[111] G. Alnwaimi, S. Vahid, and K. Moessner, "Dynamic Heterogeneous Learning Games for Opportunistic Access in LTE-Based Macro/Femtocell Deployments," *IEEE Trans. Wirel. Commun,* vol. 14, no. 4 pp. 2294-2308, Apr. 2015.

[112] Z. Gao, B. Wen, L. Huang, C. Chen, and Z. Su, "Q-Learning-Based Power Control for LTE Enterprise Femtocell Networks," *IEEE Syst. Journ.,* vol. PP, no. 99 pp. 1-9, Jan. 2016. DOI: 10.1109/JSYST.2016.2535461

[113] O. Aliu, A. Imran, M. Imram and B. Evans,"A survey of self-organisation in Future cellular networks," *IEEE Commun Surv. and Tut.,* vol. 15, no. 1, 1st Quart. pp. 336-361, Mar. 2013.

[114] L. Zhang, T. Jiang, and K. Luo, "Dynamic Spectrum Allocation for the Downlink of OFDMA-Based Hybrid-Access Cognitive Femtocell Networks," *IEEE Trans. On Veh. Tech.,* vol. 65, no. 3, pp. 1761-1771, Mar. 2016.

[115] H. Zhang, C. Jiang, X. Mao and H. Chen, "Interference-Limited Resource Optimization in Cognitive Femtocells with Fairness and Imperfect Spectrum Sensing," *IEEE Trans. On Veh. Tech.,* vol. 65, no. 3, pp. 1761-1771, Mar. 2016.

[116] Y. Zhang, and S. Wang, "Resource Allocation for Cognitive Radio-Enabled Femtocell Networks with Imperfect Spectrum Sensing and Channel Uncertainty" *IEEE Trans. on veh. Tech.,* vol. 65, no. 9 pp. 7719-7728, Sept. 2016.

[117] T. LeAnh, N. Tran, S. Lee, E-N. Huh, Z. Han, and C. Hong, "Distributed Power and Channel Allocation for Cognitive Femtocell Network Using a Coalitional Game in Partition-Form Approach," *IEEE Trans. Veh. Tech.,* vol. 66, no. 4, pp. 3475-3490, Apr. 2017.

[118] T. LeAnh, N. Tran, W. Saad, L. Le, D. Niyato, T. Ho, and C. Hong, "Matching Theory for Distributed User Association and Resource Allocation in Cognitive Femtocell Networks," *IEEE Trans. Veh. Tech.,* pp. 1-16, Mar. 2017. DOI 10.1109/TVT.2017.2689795

[119] W. Lee, J. Kang, and J. Kang, "Joint Resource Allocation for Throughput Enhancement in Cognitive Radio Femtocell Networks," *IEEE Commun. Lett.,* vol. 4, no. 2, pp. 181-184, Jun. 2015.

[120] S. Al-Rubaye, A. Al-Dulaimi, and J. Cosmas, "Cognitive femtocell," *IEEE Veh. Technol. Mag.,* vol. 6, no. 1, pp. 44-51, Mar. 2011.

[121] G. Gur, S. Bayhan, and F. Alagoz, "Cognitive femtocell networks: An overlay architecture for localized dynamic spectrum access," *IEEE Wireless Commun.,* vol. 17, no. 4, pp. 62-70, Aug. 2010.

[122] W. Wang, G. Yu, and A. Huang, "Cognitive radio enhanced interference coordination for femtocell networks," *IEEE Commun. Mag.,* vol. 51, no. 6, pp. 37-43, Jun. 2013.

[123] M. Masoudi, H. Zaefarani, A. Mohammadi, and C. Cavdar, "Energy and Spectrum Efficient Resource Allocation in Two-Tier Networks: A Multiobjective Approach," *IEEE WCNC,* pp. 1-6, Mar. 2017.

[124] C. Yang, J. Li, and M. Guizani, "Cooperation for spectral and energy efficiency in ultra-dense small cell networks," *IEEE Wireless Commun.,* vol. 22, no. 2, pp. 64-71, Feb. 2016.

[125] X. Ge *et al.*, "Spectrum and energy efficiency evaluation of two-tier femtocell networks with partially open channels," *IEEE Trans. Veh. Technol.,* vol. 63, no. 3, pp. 1306-1319, Mar. 2014.

[126] J. Rao, and A. Fapojuwo "An analytical framework for evaluating spectrum/energy efficiency of heterogeneous cellular networks," *IEEE Trans. on Veh. Tech.,* vol. 65, no. 5, pp. 3568-3584, May. 2016.

[127] W. Godoy, A. Barton and B. Perera, "A Procedure for formulation of Multi-objective Optimization Problems in Complex Water Resources Systems," *19th Intl. Congress on Modelling as Simulation, Perth, Australia*, pp. 12-16 Dec, 2011.

[128] M. Mili, K. Hamdi, F. Marvasti, and M. Bennis,"Joint Optimization for Optimal Power Allocation in OFDMA Femtocell Networks," *IEEE Commun. Lett.,* vol. 20, no. 1, pp. 133-136, Jan. 2016.

[129] E. Tsiropoulou, P. Vamvakas and S. Papavassiliou, "Supermodular Game-Based Distributed Joint Uplink Power and Rate Allocation in Two-Tier Femtocell Networks," *IEEE Trans. on Mob. Comp.,* vol. 66, no. 4, pp. 1-14, 2016. DOI 10.1109/TMC.2016.2622263

[130] C. Xu, M. Sheng, X. Wang, C-X Wang and J. Li, "Distributed Subchannel Allocation for Interference Mitigation in OFDMA Femtocells: A Utility-Based Learning Approach," *IEEE Trans. Veh. Tech.,* vol. 64, no. 6, pp. 2463-2475, Jun. 2015.

[131] L. Guo, H. Wu, Y. Wu, and X. Liu, "Optimal total-downlink transmitting-power and subchannel allocation for green cellular networks," *IEEE ICC.,* 2015, pp. 1471-1476.

[132] A. Saeed, E. Katranaras, M. Dianati, and M. Imran,"Dynamic femtocell resource allocation for managing inter-tier interference in downlink of heterogeneous networks," *IET Commun.,* vol. 10, no. 6, pp. 641-650, Nov. 2016.

[133] R. Hernandez-Aquino, S. Zaidi, M. Ghogho, D. McLernon, and A. Swami, "Stochastic Geometric Modeling and Analysis of Non-Uniform Two-Tier Networks: A Stienens

Model-Based Approach," *IEEE Trans. Wirel. Commun.,* vol. 16, no. 6, pp. 3476-3491, Jun. 2017.

[134] J. Ding *et al.*, "Stochastic Topology Cognition in Heterogeneous Networks," *IEEE Access,* DOI: 10.1109 pp. 1-13, 2016.

[135] N. Sharma, D. Badheka, and A. Anpalagan,"Multiobjective Subchannel and Power Allocation in Interference-Limited Two-Tier OFDMA Femtocell Networks," *IEEE Sys. Journ.,* vol. 10, no. 2, pp. 544-555, Jun. 2016.

[136] H. W. Kuhn, "The Hungarian method for the assignment problem," *Naval Res. Logistics Quart.*, vol. 2, no. 12, pp. 83-97, 1955.

[137] G. Cao, D. Yang, X. Ye, X. Zhang, "A Downlink Joint Power Control and Resource Allocation Scheme for Co-Channel MacrocellFemtocell Networks," *IEEE WCNC,* 2011, pp. 211-286.

[138] S. Boyd and L. Vandenberghe, Convex Optimization. Cambridge, U.K.: Cambridge Univ. Press, 2004.

[139] L. Liang, W. Wang, Y. Jia and S. Fu, "A Cluster-based energy-efficient resource management scheme for ultra-dense networks," *IEEE Access,* vol. 4, pp. 6823-6832, Nov. 2016.

[140] X. Ge, S. Tu, G. Mao, C. Wang, and T. Han, "5G Ultra-dense cellular networks," *IEEE Commun. Mag.,* vol. 23, no. 1, pp. 72-79, Feb. 2016.

[141] D. Wu, Q. Wu, Y. Xu and Y. Liang, "QoE and energy aware resource allocation in small cell networks with power selection, load management and channel allocation" *IEEE Trans. Veh. Tech.,* vol. PP, no 99 doi:10.1109/TVT.2017.2650949.

[142] Z. Wang, B. Hu, X. Wang and S. Chen, "Interference pricing in 5G ultra-dense small cell networks: A Stackelberg game approach," *IET Commun.,* vol. 10, no. 15, pp. 1865-1872, Aug. 2016.

[143] J. Xu *et al.*, "Cooperative distributed optimization for the hyper-dense small cell deployment," *IEEE Commun. Mag.,* vol. 52, no. 5, pp. 61-67, May 2014.

[144] H. Klessig *et al.*, "From immune cells to self-organizing ultra-dense small cell networks," *IEEE J. Sel. Areas Commun.,* vol. 34, no. 4, pp. 800-811, Apr. 2016.

[145] W. Nasrin, and J. Xie, "Effect of Heterogeneous Frequency changes in cognitive radio femtocell networks," *IEEE GLOBECOM, 2016,* pp. 1-6.

[146] T. Ho, N. Tran, S. Kazmi, D. Kim and C. Hong, "Distributed resource allocation for interference management and QoS Guarantee in Underlay cognitive femtocell networks," *IEEE GLOBECOM, 2016,* pp. 1-6.

[147] A. Al-Dulaimi, A. Anpalagan, S. Al-Rubaye, and Q. Ni, "Adaptive management of cognitive radio networks employing femtocells," *IEEE Sys. Jour.,* vol. PP, no. 99, pp. 1-12, DOI: 10.1109/JSYST.2016.

[148] G. Alnwaimi, S. Vahid, and K. Moessner, "Dynamic Heterogeneous Learning games for opportunistic access in LTE-based macro/femtocell deployments," *IEEE Trans. Wireless. Commun.,* vol. 14, no. 4, pp. 2294-2308, Apr. 2015.

[149] T. LeAnh, N. Tran, S. Lee, E. Huh, Z. Han and C. Hong, "Distributed power and channel allocation for cognitive femtocell network using a coalitional game in partition form approach" *IEEE Trans. Veh. Tech.,* vol. PP, no 99 doi:10.1109/TVT.2016.2536759.

[150] N. Zhang, S. Zhang, J. Zheng, X. Fang, Jon W. Mark, and X. Shen "User satisfaction-aware radio resource management in ultra-dense small cell networks," *IEEE ICC, 2016,* pp. 1-5.

[151] D. Qu, Y. Zhou, L. Tian, and J. Shi, "User-centric QoS-aware interference coordination for ultra dense cellular networks," *IEEE GLOBECOM, 2016,* pp. 1-6.

[152] O. Anjum, O. Yilman, C. Wijting, M. Uusitalo, "Traffic-aware resource sharing in ultra-dense small cell networks," *IEEE EuCNC, 2015,* pp. 195-199.

[153] W. Lee, and J. Kang, "Joint Resource Allocation for Throughput Enhancement in cognitive radio femtocell networks" *IEEE Commun. Letter.,* vol. 4, no. 2 pp. 181-184, Apr. 2015.

[154] W. Chung, C. Chang, and C. Ye, "A Cognitive Priority-based Resource Management Scheme for Cognitive Femtocells in LTE Syatems," *IEEE ICC, 2013,* pp. 6220-6224.

[155] H. Pervaiz, L. Musavian, Q. Ni, and Z. Ding, "Energy and Spectrum Transmission Techniques Under QoS Constraints Toward Green Heterogeneous Networks," *IEEE Access,* vol. 3, pp. 1655-1671, Oct. 2015.

[156] W. Yu, and R. Lui, "Dual methods for nonconvex spectrum optimization of multicarrier systems" *IEEE Trans. on comms.,* vol. 54, no. 7 pp. 1310-1322, Jul. 2006.

[157] R. Xie, F. Richard, and H. Ji, "Dynamic Resource Allocation for Heterogeneous Cognitive Radio Networks with Imperfect Spectrum Sensing" *IEEE Trans. on Veh. Tech.,* vol. 61, no. 2 pp. 770-780, Feb. 2012.

[158] V. Adamchik, "Complexity of Algorithm" *Carnegie Mellon School of Computer Science* pp. 1-7. https://www.cs.cmu.edu/ adamchik/15-122/lectures/complexity/complexity.pdf

[159] H. Wilf, "Algorithms and Complexity" *University of Pennsylvania Philadelphia,* PA 19104-6395 pp.1-139. https://www.math.upenn.edu/ wilf/AlgoComp.pdf

[160] L. Chen, X. Li, and H. Ji, "An Interference-Mitigation Channel Allocation Algorithm for Energy-Efficient Femtocell Networks," *IEEE WCNC,* 2014, pp. 2318-2323.

[161] W. Yu, L. Musavian, and Q. Ni, "Tradeoff Analysis and Joint Optimization of Link-Layer Energy Efficiency and Effective Capacity Toward Green Communications," *IEEE Trans. on Wireless. comms.,* vol. 15, no. 5, pp. 3339-3353, May 2016.

[162] M. Emmerich and A. Deutz., "Multicriteria optimization and decision making," *Leiden Univ. Leiden Tech. Rep.,* pp.1-102, 2006.

[163] W. Dinkelbach, "On nonlinear fractional programming," *Management Science*, vol. 13, pp. 492498, Mar. 1967. Available: http://www.jstor. org/stable/2627691

[164] S. Samarakoon, M. Bennis, W. Saad, M. Debbah, and M. Latva-Aho, "Ultra dense small cell networks: Turning density into energy efficiency," *IEEE Jour. Sel. Areas Commun.,* vol. 34, no. 5, pp. 1267-1280, May 2016.

[165] T. Zhang, J. Zhao, L. An, and D. Liu, "Energy efficiency of base station deployment in ultra dense HetNets: A stochastic geometry analysis" *IEEE Wireless Commun. Lett.,* vol. 5, no. 2 pp. 184-187, Apr. 2016.

[166] C. Yang, J. Li, Q. Ni, A. Anpalagan, M. Guizani, "Interference-aware energy efficiency maximization in 5G ultra-dense networks," *IEEE Trans. Commun.,* vol. PP, doi:10.1109/tcomm.2016.2638906.

[167] J. Xu *et al.*, "Cooperative distributed optimization for the hyper-dense small cell deployment," *IEEE Commun. Mag.,* vol. 52, no. 5, pp. 61-67, May 2014.

[168] B. Soret, K. I. Pedersen, N. T. K. Jrgensen, and V. Fernandez-Lopez, "Interference coordination for dense wireless networks," *IEEE Commun. Mag.,* vol. 53, no. 1, pp. 102-109, Jan. 2015.

[169] A. Asadi, V. Sciancalepore, and V. Mancuso, "On the efficient utilization of radio resources in extremely dense wireless networks," *IEEE Commun. Mag.,* vol. 53, no. 1, pp. 126-132, Jan. 2015.

[170] R. Hatoum, Abbas Hatoum, AlaaGhaith, and G.Pujolle, "Adaptive modulation and coding for QoS-based Femtocell Resource Allocation with Power Control," *Globecom, 2014,* pp. 4543-4549.

[171] J. Zheng, Y. Wu, N. Zhang, H. Zhou, Y. Cai, and X. Shen, "Optimal power control in Ultra-dense small cell network: A game-theoretic approach" *IEEE Trans. Wireless. Commun.,* vol. PP, doi:10.1109/twc/2016.2646346.

[172] J. Qiu, G. Ding, Q. Wu, Z. Q, T. Tsiftsis, Z. Du, and Y. Sun, "Hierarchical resource allocation framework for hyper-dense small cell networks," *IEEE Access.* vol. 4, no. 2, pp. 8657-8669, Jan. 2017.

[173] R. Li, Y. Chen, G. Ye Li, and G. Liu, "Full duplex in cellular networks," *IEEE Comm. Mag.,* vol. 55, no. 4, pp. 184-191, Apr. 2017.

[174] I. Randrianaatenaina, H. Dahrouj, H. Elsawy, and M. Alouini, "Interference Management in Full-Duplex Cellular Networks with Partial Spectrum Overlap", IEEE ACCESS, vol. 5, pp. 7567-7583, June. 2017